UNIVERSITÀ
DEGLI STUDI
DI PADOVA

Head Office: Università degli Studi di Padova

Department of Chemical Sciences (DiSC)

Ph.D. COURSE IN: Molecular Sciences

CURRICULUM: Chemical Sciences

CYCLE: 38th

Study of gold-catalyzed hydroarylations in unconventional media

Coordinator: Prof. Stefano Corni

Supervisor: Prof. Andrea Biffis

Co-Supervisor: Prof. Cristina Tubaro

Host-Supervisor: Dr. Didier Bourissou

Ph.D. student : Francesco Ravera

Abstract and Aim of the thesis

The following manuscript collect the scientific effort of the last three years of research that the author spent in the laboratory of Prof. Andrea Biffis. The general topic is related to cationic Au-catalysis and, in particular, how cationic gold complexes can be involved in the electrophilic activation of unsaturated substrate to fabricate new C-C bonds. After an introductory chapter on the general aspects of gold-chemistry and an overview on alkyne hydrofunctionalization reactions (**Chapter 1**), we report a new methodology for the direct synthesis of coumarins by hydroarylation of the analogous aryl-alkynoates (**Chapter 2.1**). The element of novelty is about the use of ionic liquids (ILs) as reaction media, which led to enhanced catalytic activity and a significant reduction in the amount of gold complex required (0.01-0.5mol%). In the following section (**Chapter 2.2**), the same reaction was tackled by an intermolecular approach, hence starting from alkynoate derivatives and phenols as coupling reagents. Building on the previous MSc theses of Dr. Sara Bonfante and Pietro Bax in our group, we carried out a systematic investigation to identify suitable conditions to favor the desired transformation over competing side reactions, with selectivity emerging as the main challenge. Ultimately, we developed an efficient protocol to obtain coumarin derivatives from both simple propiolates and more elaborate alkynoates, while also demonstrating the recyclability of the system. Nonetheless, certain limitations remain: deactivated aromatic rings and monosubstituted phenols often display poor reactivity or lead to competing pathways, reducing overall efficiency. Motivated by these observations, we were interested in evaluating the effect of more polarizing Au(III)-complexes for the activation of electron-poor rings (**Chapter 3**). The project was developed in collaboration to the group of Dr. Didier Bourissou, which in 2018 reported well-defined cyclometalated gold(III) complexes bearing a phosphino-naphthyl backbone capable of promoting hydroarylation of alkynes with activated arenes. The complexes were recorded to be unactive contextually to the direct activation of aryl-propiolates with activated phenols. Nevertheless, we conducted complementary studies to understand the behavior of (P,C)Au^{2+} complexes in ionic liquids, addressing in detail the role of the counter-anion and of the acidic additive to enhance the reactivity and/or specific selectivity Although these complexes were inactive for the direct activation of aryl propiolates with activated phenols, we performed complementary studies to probe the behavior of (P,C)Au(III) complexes in ionic liquids, paying particular attention to the influence of the counterion and acidic additives on reactivity and selectivity. Stoichiometric test put under evidence the reasons why only the intramolecular version of the reaction is effective in yielding the desired product. Finally, **Chapter 4** presents a novel Au-catalyzed methodology for the direct amidation of heteroaromatic substrates. We demonstrate that organic isocyanates can act as electrophilic partners in a hydroarylation-type process. In analogy to the corresponding alkyne reactions, we carried out a mechanistic study to confirm the outer-sphere

pathway, supported by Hammett analysis of substituted aryl isocyanates and kinetic isotope effect measurements with deuterated nucleophiles. Furthermore, we isolated and characterized a family of Au(I)–(isocyanate) adducts, which displayed distinct NMR signatures upon metal coordination. The addition of N-methylpyrrole enabled the formation of a new π-complex that, in the presence of isocyanates, delivered the amidation products, confirming its role as a key resting state in the catalytic cycle.

List of publications

1. P. Bax[§], F. Ravera[§] ([§]equal contribution), S. Bonfante, F. Floreani, A. Biffis "Direct Coumarin Synthesis by Gold Catalyzed Hydroarylation of Alkynoic Acids/Esters" *ChemCatChem*, **2025**, e00465. doi.org/10.1002/cctc.202500465
2. F. Ravera, M.S.M. Holmsen, P. Sgarbossa, D. Bourissou, A. Biffis, "Gold(III) Catalysis in Ionic Liquids: The Case Study of Coumarin Synthesis" *Adv. Synth. Catal.* **2025**, *367*, e202400706. doi.org/10.1002/adsc.202400706
3. F. Ravera, F. Floreani, C. Tubaro, M. Roverso, R. Pedrazzani, M. Bandini, A. Biffis, "An Improved Gold(I) Catalytic System for the Preparationof Coumarins via Intramolecular Cyclization" *Chem Asian J.* **2025**, *20*, e202400725. doi.org/10.1002/asia.202400725
4. F. Ravera, A. Bortoli, J. J. Gamboa-Carballo, S. Mallet-Ladeira, K. Miqueu, D. Bourissou, Andrea Biffis, "Activation of Isocyanates at Gold: Towards Au-Catalyzed C–H Amidation of Pyrroles" (*manuscript submitted for revision*).

Table of Contents

1. Gold, chemical properties, reactivity and technologic relevance

1.1. Introduction on gold and its general properties

Gold is a metal that along the human history was often associated to richness and prestige. Due to its natural yellow color and resistance to oxidation, from which its attribute of “noble metal”, its use was made extensive for the production of beauty items and coinage: together with copper and silver, they are typically addressed with the name “coinage metals”. Metallic gold can be as well subjected to mechanical transformations with ease, and it is often used in combination with other metallic elements to reduce the price and increase the robustness of the final item.[1] Gold covers also important applications in electronics industry for the manufacture of circuit boards presenting high robustness to corrosion and excellent conductivity ($\rho[20°C]=2.35\mu\Omega\cdot cm$).[1] This is made possible by the modern technologies for the extraction and refinement of this element: gold-enriched minerals are treated with dilute cyanide solutions in the presence of air, allowing to dissolve it as $[NaAu(CN)_2]$, which is then reduced by activated carbon or zinc dust and further refined electrochemically (Wohlwill process) to yield up to 99.99% purities.[1–3]

From a chemical point of view, gold (namely Au) is a metallic element of the late transition-metal series (atomic number 79), presenting only one stable isotope and electronic configuration $[Xe]4f^{14}5d^{10}6s^1$. The valence shell can indeed explain the good electric and thermal conductivities of this element and, in a broader sense, the physical properties of the 11th group metals. The characteristic golden color of the gold arises as well from this particular configuration and is explained by the band theory. The presence of a filled d-band near in energy to the nearest unfilled s-p band enables the absorption of a small portion of the UV- and blue-spectra, resulting in the observed yellow color.[3] On the other hand, formation of nanostructured Au(0) dispersions by exposing chloroauric acid to different reductants allows to obtain red, blue and intermediate violet colors due to the plasmonic resonance arising from the nanoconfinement of the surface electrons of the material.[4,5] This feature of colloids has attracted large interest in the scientific community and it is now employed in the construction of optical sensors as well in electrochemical applications.[6–8] To further comment on the electronic aspects of this metal and its analogues in electronic configuration (Ag, Cu), their chemical reactivity is traditionally compared to the one of alkali-metals (ns^1 configuration). Their chemical similarities are however limited to some

stoichiometric aspects of species at the +1 oxidation state. Conversely, the less effective shielding of the valence d-orbitales increases substantially the reduction potential of the redox couple Au(+1)/Au(0) (1.691V vs -3.045 – -2.714V of alkali metals). This results also in a smaller ionic-radius of Au(I) with respect to cesium (Cs, configuration $[Xe]6s^1$), with direct consequences on the physical properties of gold (gold is more dense and presents a higher melting point) and a higher covalent character of its compounds.[3] Metallic gold can be also solubilized in liquid ammonia, gaining one electron to complete the 6s-shell and originating a formal Au(-1) species whose stoichiometry is not well-defined.[3] Alternatively, zerovalent gold can be dissolved in concentrated HCl in the presence of a strong oxidant, such as HNO_3. The last process allows to take directly bulk gold to chloroauric acid, in which Au assumes a +3 oxidation state. The enhanced stability of these two oxidation states are mainly attributed to relativistic effects[9] operating on s- and p-electrons which will be described in the next paragraphs. In other words, the stabilization of the Au(-1) state could be addressed looking to the electronegativity value of 2.4, which is the highest value found for a metal in the periodic table, while the high crystal field stabilization energy (CFSE) of Au(III)-d_8 square-planar complexes is an important thermodynamic contribute to the stability of the latter species. The speciation of chemical compounds containing gold includes Au(+5) species, though in limited examples, such as the hexafluoroaurate anion $[AuF_6]^-$ and the dimeric neutral $[Au_2(\mu^2\text{-}F)_2F_{10}]$ complex.[10,11] On the other hand Au(+2) species displaying a Au-Au bond are often found as products of 1+1 e^- oxidations over di-nuclear Au(+1) complexes,[12,13] while mononuclear species are rarely found[10,14,15] or only postulated.[16] Mononuclear Au(0) complexes exist but they lack in stability, from which the choice of bulky-porphyrin-like ligands with π-accepting groups over the backbone.[17] Alternatively, di-nuclear species have been reported with an Au-Au which enhances the stability.[18,19]

1.2. π-acidic properties and elementary-steps at Au(I/III) complexes

The renewed interest in gold chemistry and catalysis arises from the ability of cationic Au(I) and Au(III) complexes to act as π-acidic species when coordinated to unsaturated π-systems, as first demonstrated by the pioneering work of Teles and Tanaka on the direct hydration of alkynes mediated by Au(I) species.[20,21] Both the soft character of the metal center and the presence of a net positive charge in the complex play key roles in these transformations. The bonding situation in such π-complexes is well rationalized by the Dewar–Chatt–Duncanson (DCD) model.[22] In this

framework, the frontier molecular orbitals of the ligand overlap with the metal d orbitals to form a stable adduct, reinforced by synergistic σ-donation and π back-donation (**Figure 1.1**). For the specific examples of Au(I) and Pd(II) metal centers the first two reported interactions are of negligible apport in energy; the latter for symmetry restrains.[23] On the other hand, the d_{z2} orbital at the metal center is occupied and the σ-backdonation may occur from the orbital $\pi_{//}$ of the alkyne to an hybrid *spd*.

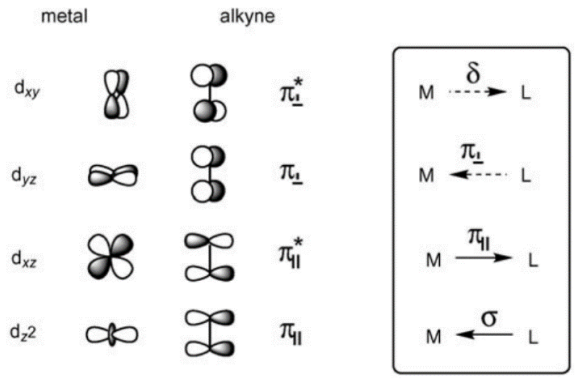

Figure 1.1 *– Qualitative description of the orbital interactions between a TM and an alkyne ligand.*[23]

As an example, the Au(I)–(η^2-acetylene) π-bond has been studied computationally, showing that the dominant contribution to orbital overlap arises from ligand-to-metal σ-donation (~65%), compared to metal-to-ligand π back-donation (~27%).[24] Acetylene can therefore be classified as a two-electron donor (L-type ligand) with low propensity for π back-donation. This result has been experimentally validated by Campos and co-workers, who reported the first example of a phosphine–Au–(π-acetylene) complex.[25] In particular, the adduct is stabilized by confinement of acetylene within a pocket formed by the ligand side-arms. Similar conclusions apply to ethylene, which behaves as an even slightly better donor than acetylene.[26] For both ligands, a shorter C-C bond distance is recorded after coordination, as previously observed for Cu and Ag analogues.[27,28] This phenomenon is due to torsional vibration at the ligand.

The oxidation state of the metal center can drastically influence the balance between σ-donation and π back-donation in the coordination bond. For instance, in a Pt(0) complex, the electron-rich metal center is more prone to back-donate electron density into the alkyne's antibonding orbital. In this case, the DCD model may be less appropriate than a metallacyclopropene model, which accounts for distortions in the ligand structure and the loss of planarity. Choosing the correct

bonding model is not straightforward, as it depends on the nature, charge, and geometry of both the metal center and the π-ligand. At the opposite extreme, Münz and co-workers reported an analogous π-basic interaction by coupling electron-poor π-systems with electron-rich Pd(0) complexes bearing a CAAC-type ligand with an embedded imine fragment (σ symmetric M→L donation).[29]

Independently of these considerations, we define a π-acid as any species capable of redistributing the electron density of an unsaturated C-X π-system (with X = C, O, N, S). The result is partial electron withdrawal, generating a site susceptible to nucleophilic attack. A simplified representation of this mechanism is shown in **Figure 1.2**, which depicts the classic carbophilic activation of acetylene toward functionalization by a generic protic nucleophile (HNu). The final product results from the trans addition of H^+ and Nu^- across the former alkyne. In the absence of available protons, any suitable electrophile may complete the reaction by effecting terminal demetallation.

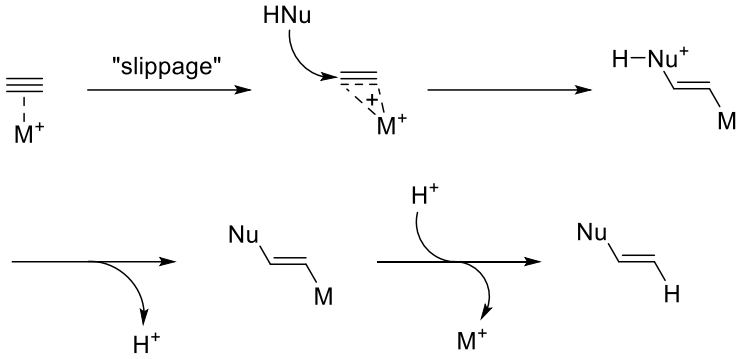

Figure 1.2 *– General mechanism for the addition of a nucleophile HNu to alkynes by carbophilic activation of the triple bond.*

This is not the only possible pathway. An inner-sphere mechanism is also feasible, in which the nucleophile first coordinates to the metal center and then migrates to the activated alkyne via a concerted process. Evidence for this has been observed in alkyne hydroarylation, where metalated arenes and/or *syn*-addition products were detected.[30] Another important avenue is the activation of alkynes toward nucleophilic attack by olefins. This reactivity leads to the formation of reactive Au–carbene intermediates that can undergo C–H insertion into arenes, structural rearrangements, or further nucleophilic attack.[31,32] Echavarren has reviewed this chemistry comprehensively, exposing in particular its application to the synthesis of strained small rings.[33] Fürstner and co-

workers, who pioneered some of these synthetic strategies, also proposed a unified mechanism to rationalize these transformations.[34,35]

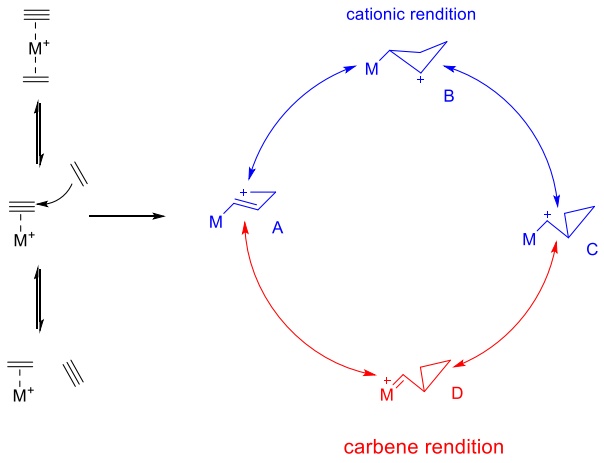

Figure 1.3 *– Carbene-carbocation hypothesis on ene-yne cycloisomerization reactions*[34,35]

In this mechanism (**Figure 1.3**), once the olefin binds to the activated metal–alkyne complex through slippage of the metal fragment, a set of resonance structures stabilizes the evolving carbocation–carbenoid intermediate. The prevalence of one structure over another depends on the substrate and the possibility of forming stable products. Importantly, the attack occurs selectively from the alkene to the alkyne, and not vice versa. This selectivity can be explained on kinetic grounds: as noted earlier, ethylene can act as a better donor than acetylene,[24] favoring this direction of reactivity. By contrast, simultaneous coordination of both molecules often results in an unreactive species, since excess electron donation to the metal increases back-donation to the alkyne and suppresses carbophilic activation.

In conclusion, activation of π-systems toward nucleophilic attack by soft electrophilic centers offers a powerful tool for constructing complex molecular architectures. However, the mechanistic variables are numerous, making prediction of reaction outcomes challenging.

1.3. Relativistic effects at gold: the influence on electronic properties

Although the carbene–carbocation hypothesis was not initially supported by clear experimental evidence, it is now widely accepted by the scientific community. In particular, this model successfully predicted the affinity of soft and hardly oxidizable late transition metal cations toward

unsaturated C–C bonds. It also accounts for the effects of charge and coordination number, anticipating that cationic, monocoordinated $LAu(I)^+$ complexes provide the most effective scaffold for alkyne coordination and activation.

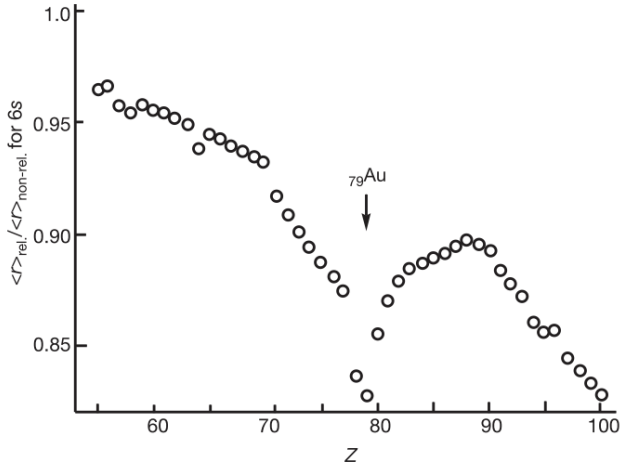

Figure 1.4 *– 6s orbitals relative contraction in function of the atomic number Z.*[36]

These features are rationalized by the relativistic contraction of the 6s orbital (**Figure 1.4**), which increases the energy of the 5d orbitals and enhances their diffuse character due to increased shielding.[37,38] This phenomenon is experimentally reflected in the high energy of the L–Au(I) coordinative interaction, with L representing a phosphine or carbene ancillary ligand. It also contributes to the large first ionization potential of gold (9.22 eV vs. 7.57 eV for silver) and explains the formation of unique Au–Au interactions[39,40] with energies comparable to hydrogen bonds.[36]

Computational analyses of coordination numbers and geometries in d^{10} metals highlight the tendency of Au(I) to form dicoordinated complexes with linear geometry. This behavior arises from the high deformation energy required to bend such linear species in order to free another coordination site. By contrast, the interaction energy gained in tricoordinated complexes is insufficient to account for differences in the behavior of group 11 metals. Indeed, when considering the same ligand set (with identical charges), the calculated association energies are similar for all monovalent cations of this group.[41]

These insights have key implications for gold(I) catalysis. They rule out the formation of tricoordinated Au(I) species as the initial step in catalytic cycles. Instead, the liberation of a coordination site—often by halide removal—is required to achieve carbophilic activation. Once a site becomes available, the catalyst is highly reactive; potential deactivation by binding additional alkene or alkyne moieties is disfavored.

In summary, Au(I) centers represent highly efficient electrophilic scaffolds due to their softness and limited back-donation to alkyne antibonding orbitals. Their resistance to oxidative addition, coupled with their soft character, allows Au(I) complexes to tolerate a wide range of functional groups and thus broadens the scope of applicable substrates.

1.4. Hydrofunctionalizations of alkynes

As outlined in the former sections, gold complexes constitute an extremely valuable choice as catalysts for a broad range of applications.[42–45] Regardless its high price, the high stability of Au species and their broad range in terms of electronic properties contributed in taking gold at the center of a large number of studies in the last two decades. Since costs in the chemical industry are a non-negligible aspect to be considered, a solid methodology and prevision of the system behavior is needed before going to proper applications. The unique alkynophilicity of Au(I) complexes could indeed be a powerful tool for the activation of such compounds toward nucleophilic attacks. but the interpretation of the mechanistic-path that leads to products is not often clear or experimentally supported. The carbocation-carbenoid formalism could give some hint for the interpretation of the following reactions.

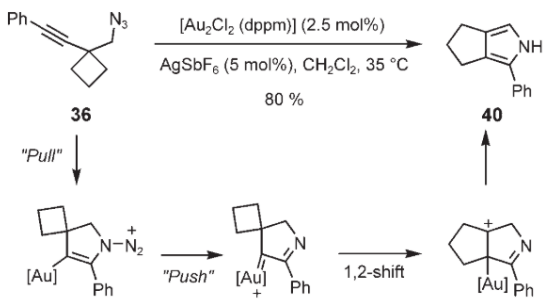

Figure 1.5 *– Pull and Push mechanism in Schmidt reaction for pyrrole synthesis*[46]

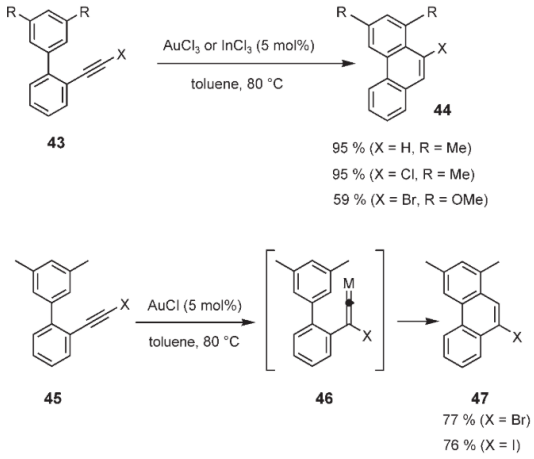

Figure 1.6 *– Change of selectivity by vinylidene intermediate formation in phenanthrenes synthesis*[47]

The first example reports an acetylenic-adapted Schmidt reaction, catalyzed by a binuclear Au(I) complex (**Figure 1.5**).[46] The alkyne electron density is pulled by the metal center, according to the

carbophilic activation mechanism, favoring the nitrogen nucleophilic attack and the slippage of gold along the triple-bond axis. On this particular framework, the carbenoid rendition suites perfectly in order to explain the role of the metal back-donation in the electrophilic cleavage. After nitrogen liberation, the carbocation can be regenerated by 1,2-shift and isomerization to achieve the desired product. In the case of **Figure 1.6** it is reported a curious change in selectivity varying the catalyst. In order to explain the halogen shift during the cyclization, the Au(I) alkyne complex may pass through a vinylidene intermediate formation. Also in the case of $AuCl_3$ we have some possibility for the vinylidene intermediate formation, which leads to the 5-exo-isomer formation.[48] The two former examples are merely illustrative. The important concept that has to pass through is that the reactivity of those systems is extremely various and deeply linked to the specific nature of the substrates. The lack of prevision and the difficulties on mechanism interpretations are still now the main concerns that limit their synthetic applications. Moreover, such processes find robust applications when limited to their intramolecular version, while intermolecular reactions suffer of low predictability, difficulties in optimization and/or limited generality in scope. Keeping the focus on intermolecular alkyne functionalization by protic nucleophiles HNu, the reaction mechanism can be typically reduced to the one reported in **Figure 1.7a**.[49] The alkyne first approaches the metal center generating a formal Au-(η^2-alkyne) π-adduct (**A**). This species is amenable to undergo a nucleophilic attack with formal reduction of the double bond to produce an Au-vinyl intermediate with a positive charge delocalized onto the organic fragment (**B**). The latter intermediate can eventually lose a proton to form the corresponding neutral Au-(alkenyl) species, where the Au atom and the nucleophilic residue lay opposite, in an *anti*-geometry. A proton source from the solvent may act as H^+ donor to cleave the Au-C bond and regenerate the active species. This cycle resembles the one proposed by Fujiwara and co-workers for the hydroarylation of alkynes catalyzed by Pd(II)$(OAc^F)_2$ (**Figure 1.7b**).[30,50] On the other hand, an inner-sphere mechanism is also possible in this case, with the electrophilic metalation of the aromatic nucleophile preceding the coordination of the alkyne. However, this mechanism is operating to lower extents than the outer-sphere one. Specifically, the most controversial step is represented by the *trans*-addition of the aryl group to the olefin (**D**). It is known that the 1,2-migratory insertion of the aryl-residue onto the alkyne moiety should result in a *cis* addition and consequently lead to the *E*-product. On this basis, Alper *et al*. proposed a kinetically driven isomerization of the vinylic complex, passing through a dipolar intermediate.[51] Finally, isotopic experiments confirmed the protic demetallation upon performing the reaction in TFA-d_1. In this conditions the *trans* deuterium addition is almost

completely selective. On the other hand, hydroarylation of deuterated benzene in normal TFA (reaction **II**) yields only a negligible amount of deuterated product.[30]

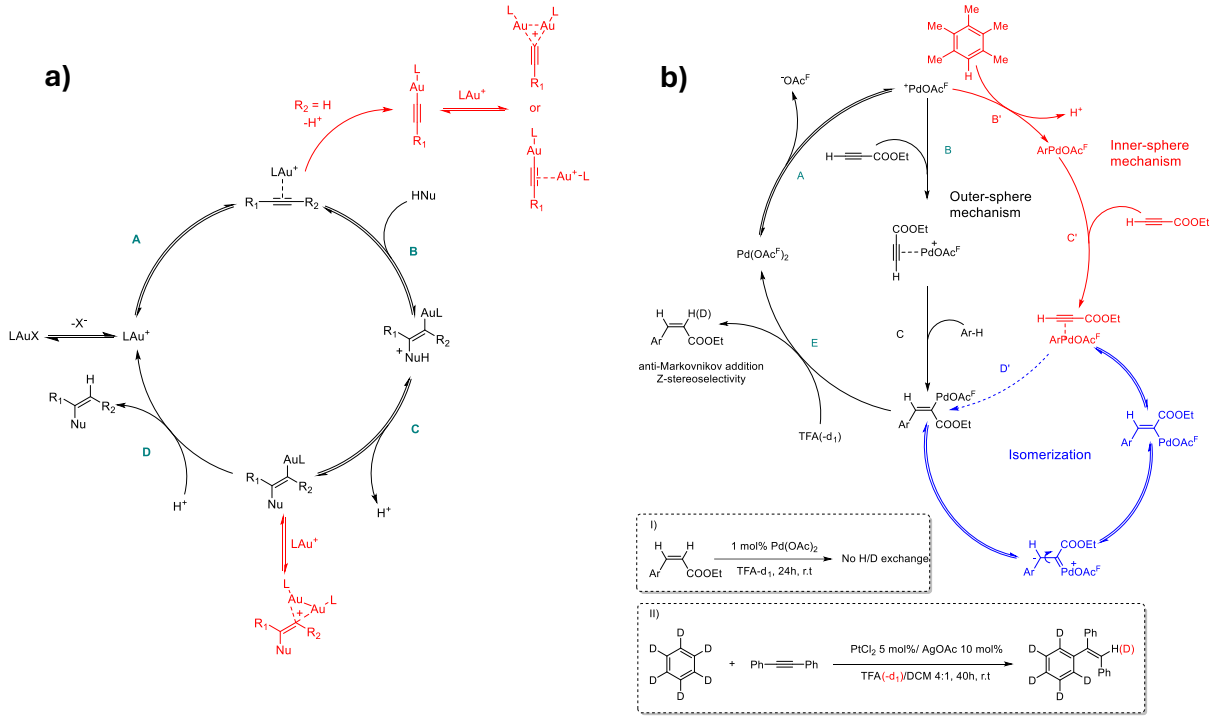

Figure 1.7 *– **a)** General mechanism for cationic gold(I)-catalyzed alkynes hydrofunctionalization and **b)** mechanism of the Fujiwara's hydroarylation of alkynes.*

The ability of gold to insert within aromatic Ar-H bonds is rather limited and often limited to Au(III) metal centers subjected to harsh conditions and/or exposed to activated rings. In addition, isolation and characterization of geminal alkynyl and vinyl complexes as unreactive off-cycle products further corroborate an outer-sphere mechanism as the most probable.[52,53] The nature of the nucleophile could be different (heteroatom-based or carbon-based nucleophiles) with obvious implications on the activation parameters in the catalytic cycle, while the regiochemistry of the reaction is often defined by the substituents at the alkyne.[49] Keeping the focus on alkynes hydroarylation reactions, it is not possible to unambiguously define the *r.d.s,* of the process. Initial studies conducted by Reetz confirmed the general selectivity trends reported for the Pd-catalyzed process.[54] The hydroarylation of ethyl propiolate with mesitylene in nitromethane was addressed with a broad variety of catalysts. As result of this screening, gold(I) complexes show to be more effective than simple salts such as AuCl or $AuCl_3$, regarding both activity and product selectivity.

The process does not request the presence of an acid co-catalyst but an increase of the equivalents of arenes is needed in order to achieve high yields. In general, the most favorable conditions for this reaction see the activation of electron-poor alkynes toward electron-rich arenes. The right choice of the ligand is fundamental in order to modulate the catalytic performance of the process. Strong electron-donating ligands support the protonolysis step and improve the complex stability.[55] On the other hand, increasing the electron density on the gold center enhances the π back-donation to the alkyne, with possible issues on the substrate activation. The activation of electron rich olefins by Au(I) catalysis is as well possible using poorly-donating cationic ligands, as reported by Alcarazo with its cationic pyridinophosphine ligands.

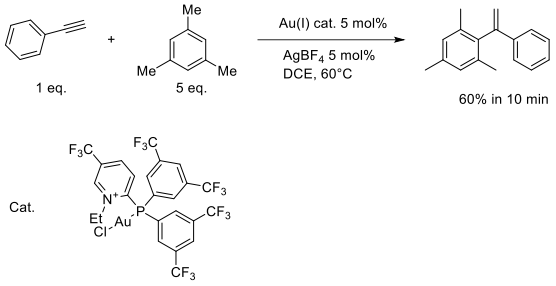

Figure 1.8 *– Hydroarylation of phenyl acetylene with mesitylene catalyzed by Alcarazo catalyst.*[56]

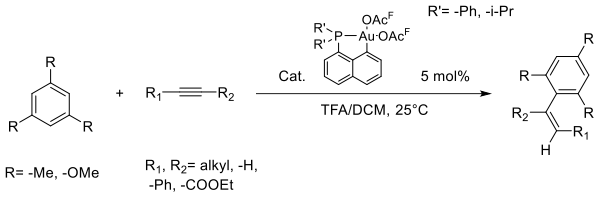

Figure 1.9 *– Gold(III) cyclometalated (P,C) complexes as catalyst for electron rich alkynes activation.*[57]

The catalyst reported in ***Figure 1.8*** is also able to perform hydroarylation of phenylacetylene with mesitylene in DCE under mild conditions. Indeed, even the gold oxidation state plays a role on the activation of such challenging substrates. Simple salt $AuCl_3$, suitably activated by exchange of the chloride with a non-coordinating anion, was already known to be able to perform hydroarylations of alkynes, also in absence of acid conditions.[54,58] Recently, Bourissou and co-workers reported cyclometallated (P,C)Au(III) complexes with excellent results on their application in catalysis (**Figure 1.9**).[57] The hydroarylation of electron-rich phenyl- and diphenyl-acetylene with 1,3,5-tri-methoxybenzene (TMB) and mesitylene leads to almost complete conversion in short reaction times at 5 mol% catalyst loading and Fujiwara-type conditions. For this system, the presence of ^{F}AcOH is necessary in order to unlock reactivity. A follow-up work on this system disclosed the mechanism of this transformation, which is operating in complete agreement with the previously reported outer-sphere mechanism for Pd(II) and Au(I) complexes. In particular, the Au(III)-(η^2-

alkyne) adduct could be generated in the gas phase and identified by mass spectrometry and CID techniques.[59]

1.5. Role of the counter anion and the "silver effect"

As it was anticipated in the previous sections, the cleavage of one coordinative bond at the gold(I) center is fundamental for generating the monocoordinated, cationic active species. This concept is common for all electrophilic gold catalysts and it is already reported in the literature.[61–63] However, in the process optimization the role of the counter ion is often considered marginal with respect to other parameters (nature of the ligand, temperature, solvent, etc). In **Figure 1.10** is reported a pie chart collecting the data on experimental studies on gold catalysis published in 2017. It is evident that the study of the counter anion effect are limited only to 14% of the studies that have been undertaken. Under this framework, the screening study conducted by Hashmi and co-workers aims to furnish a solid procedure for the counter-ion selection.[60] As overall result, the authors outlined that the pattern of reactivity on a benchmark reaction by changing counter anion is similar for different complexes. Thus, the counter-ion screening should precede the selection of the ligand for a target reaction. The species that allows to reach the highest reactivity are typically noncoordinating and rigid anions such as NTf_2^- or SbF_6^-.

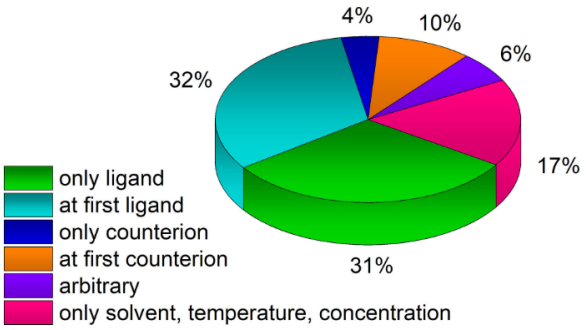

Figure 1.10 *– Catalytic process optimization basing on the procedures in 2017 (116 publications at 16.11.2017, Scifinder, keyword: gold catalyzed)* [60]

Classically, the more convenient method to afford the anion exchange is the substitution of a halido ligand (often a chloride) by reaction with a silver salt. This method is easy and effective, even though it leads to some disadvantages. First of all, the catalyst could undergo only partial activation, regardless the anion exchange is assisted by precipitation of AgCl. As second and more important drawback, silver species cannot be considered as innocent. The presence of silver in solution could involve the gold complex in formation of bimetallic species with detrimental or even advantageous effects in catalysis. The formation of silver-vinyl gold complexes has been reported by Zdhanko and Maier, and the silver effect has been tested in hydroalkoxylation reactions.[64]

Before them, in 2009, mechanistic studies on these species were carried out in the context of the intramolecular hydroarylation of allenes.[65] To make an example, it is evident the case of diphenylacetylene hydration catalyzed by IPrAuCl/$AgSbF_6$ (**Table 1.1**).[64] In absence of the silver salt precipitate, the cationic gold complex cannot yield the desired ketone. A control test excludes either the possibility of $AgSbF_6$ to perform the addition of water at the triple bond.

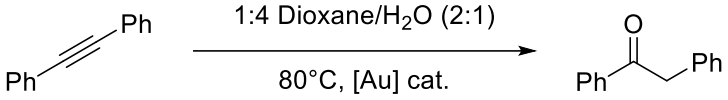

entry	catalyst	Time (h)	Yield (%)
1	IPrAuCl/$AgSbF_6$ 2mol%, no filtration	2	97
2	5mol% IPrAuSbF_6	24	0
3	5mol% $AgSbF_6$	24	0
4	2mol% IPrAuSbF_6 + 2mol% $AgSbF_6$	12	95
5	2mol% IPrAuSbF_6 + 1mol% $AgSbF_6$	24	88
6	2mol% IPrAuSbF_6 + 0.5mol% $AgSbF_6$	24	67

Table 1.1 *– Bimetallic Au/Ag catalysis for the diphenylacetylene hydration*[66]

This reaction is a clear case of Au/Ag bimetallic catalysis, that, together with the purely gold catalyzed processes, represents the extremes of a broad number of cases. Most commonly it is observed a simple silver-assisted catalysis, where either the gold complex, the silver salt or their mixture can perform the same reaction (examples are reported in **Figure 1.11**).

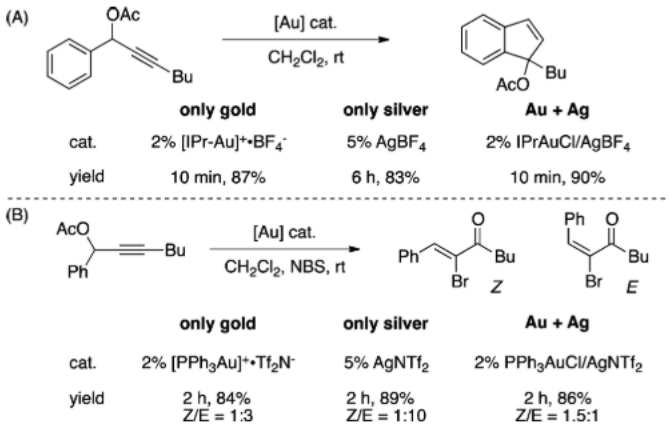

Figure 1.11 *– Ag-assisted gold catalysis of an electron-rich alkyne* ***A)*** *intramolecular hydroarylation and propargyl-rearrangement and* ***B)*** *propargyl acetate-rearrangement.*[66]

In order to evaluate the performance of the gold complex upon a selected reaction, it is indeed needed to ensure that the silver salt does not participate. The easier method is by filtration of the solid precipitate after activation or even by substituting silver with another Lewis acid as chloride extractor, such as BF_3·Et_2O.[64,67] Other silver-free methods involve the use of protic polar solvents (water or alcohols) or Deep Eutectic Solvents (DES, mixtures of a halide salt and an hydrogen bond-donor) as reaction media. Under these conditions, the chloride anion can liberate the active site to perform carbophilic activation at the gold center. Tailored ligands presenting a modified side-arm which can be involved in H-bond interactions with the halido-ligand are used to weaken the coordinative bond to gold, favoring the displacement of the halide for the reagent.[68,69]

1.6. Ionic Liquids as reaction media for cationic gold-catalysis

Since before the beginning of this century ionic liquids, or molten salts, were described as fluids that are completely comprised of ions.[70] By this definition, any ionic compound above its melting point could have been included in this category. Nowadays the term “ionic liquids” is referred only to salts with melting temperature under 100°C. They can be liquid even at room temperature, colorless and poorly viscous. The chemical nature of these species is quite broad and the cation or anion moiety can be changed independently. In ***Figure 1.12*** are reported examples of ionic liquids and a table reporting the melting points of some imidazolium-based salts.[71]

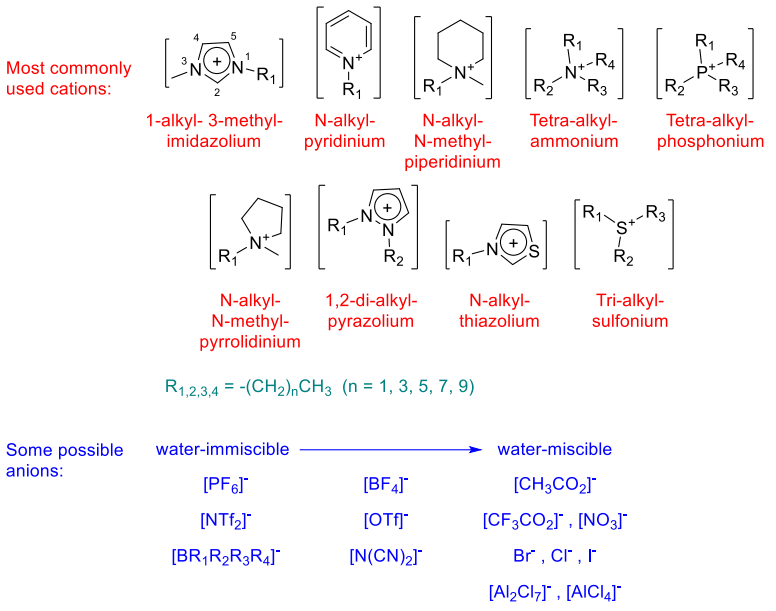

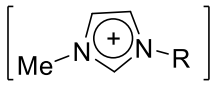

R	X	mp/°C
Me	Cl	125
Et	Cl	87
n-Bu	Cl	65
Et	NO_3	38
Et	$AlCl_4$	7
Et	BF_4	6
Et	CF_3SO_3	-9
Et	$(CF_3SO_3)_2N$	-3
Et	CF_3CO_2	-14
n-Bu	CF_3SO_3	16

Figure 1.12 *– Chemical nature of cations and anions in ionic liquids and melting points of some imidazolium-based salt.*[71]

The principle behind their physical state has to be allocated to the scarce intermolecular interactions between the oppositely charged ions. The cation is typically an asymmetric and hindered organic molecule, with low ability as H-bond donor. The anion could be either a halide or, as it is often the case for room temperature ionic liquids, a noncoordinating fluorinated anion.[71] In the last two decades, the interest in these fluids as sustainable reaction media has increased, in substitution to classic organic solvents. The wide range of chemical, physical and electrochemical-stability, together with the lower polarity with respect to water, makes these species extremely appealing for the immobilization of homogeneous catalysts. Moreover, their polarity and other physical properties, such as the relative solubility of organic substrates or gases, can be finely modulated by selection of the cation and anion moieties. The application of ILs media for homogeneous or, more often, biphasic catalysis has been already reported in the literature for a broad variety of reactions and methodologies for catalyst recovery and recycling have been developed.[71–73] From a mechanistic point of view, it is hard to determine if the catalytic process occurs in the IL phase, in the organic one or even in both of them. However, since organic solvents are generally not capable to extract the complex, it is more probable that the product forms in the

ionic medium through a similar mechanism observed in classic solvents. All these concepts can generally be applied also to gold catalysis. The cationic active species formation is indeed favored by charge stabilization and weak intermolecular interaction. As appointed by Chauvin's work on alkene hydroformylation, hydrogenation and isomerization catalyzed by phosphine rhodium complexes, the cationic active species are not solvated by ionic liquids.[74] The catalytically active species reported in ***Figure 1.13*** is supposed to be in equilibrium with the monohydride neutral complex after deprotonation.

$$[RhH_2(PPh_3)_2(Solv.)_n]^+ \overset{-H^+}{\rightleftharpoons} [RhH(PPh_3)_2(Solv.)_n]$$

Figure 1.13 – *Protonation equilibrium of the catalytic active species for catalytic hydrogenations*[74]

Dissolving the complex in BMIM SbF_6 only one signal has been observed by ^{31}P NMR, indicating the presence of only one symmetric species: probably the di-hydride complex with two free coordinating sites. This feature could explain why, in some cases, the IL environment leads to improvements in terms of catalytic activity and even selectivity. This effect has been recorded also by Biffis and co-workers in the case of the hydroarylation of ethyl propiolate with mesitylene catalyzed by IPrAuCl/$AgNTf_2$ (***Table 1.2***).[75]

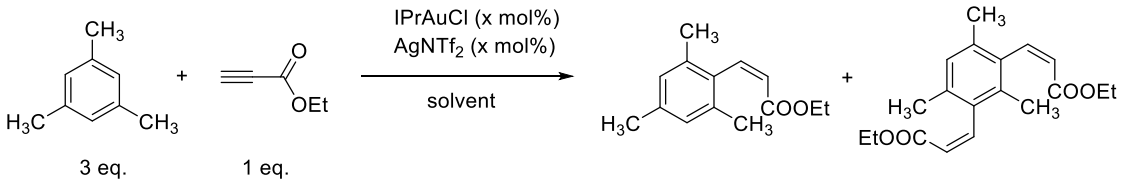

Conditions	Alkyne conversion	Mono-/Di-hydroarylation products molar ratio
BMIM NTf_2, 0.5 mol% cat. , 3h	> 90 %	5 : 1
$(CH_2)_2Cl_2$, 60°C , 5 mol% cat. , 4h	> 90 %	2 : 1

Table 1.2 – *Effect of the IL media on propiolic acid hydroarylation with mesitylene*

The same reaction is reported to be much more efficient in BMIM NTf_2, achieving more than 90% of alkyne conversion and improved selectivity toward the single adduct formation. In order to have a

comparable result in solvent DCE, the catalyst loading has to be increased from 0.5 to 5 mol% and the reaction performed for longer times at higher temperature. As shown in the reaction mechanism reported in ***Figure 1.14***, the different cationic species involved in the catalytic cycle can benefit from the stabilization by the IL medium. Both substitution of the halide with a less-coordinating anion, formation of the π-adduct (**A**) and nucleophilic attack (**B**) are exposed to stabilizing interactions by the presence of low coordinating, H-bond accepting anions.[76] Regarding the latter property, the ability of the ionic environment to get involved in the proton-shuttling may have a strong influence on the efficiency of both generating the neutral Au-vinyl species (**C**) after nucleophilic attack and at the same time lowering the energy barrier to overcome the protonolysis and afford the hydroarylation product.[76] Since the r.d.s. of the reaction cannot always be clarified, the multiple effects of employing ionic liquids in this specific transformation may be of great use to improve the catalytic performance.

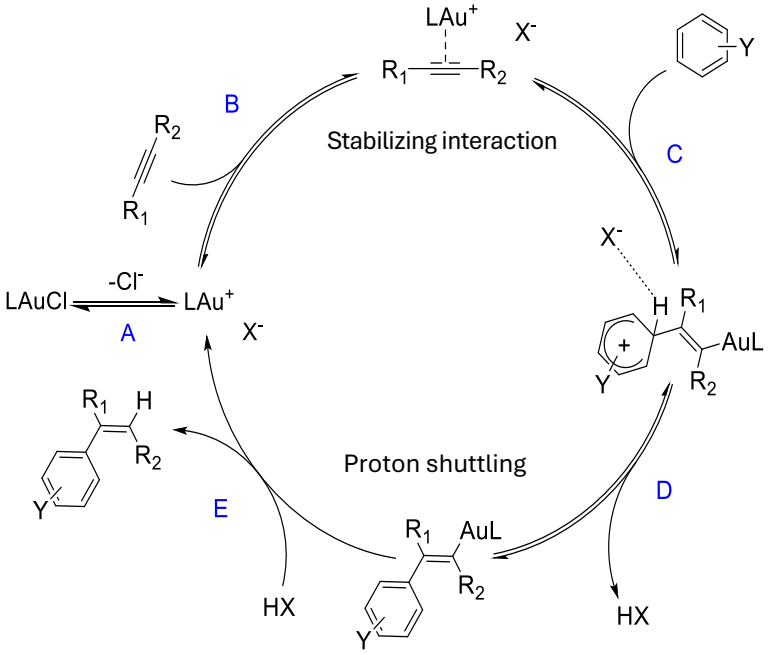

Figure 1.14 *– Revised mechanism for the intermolecular hydroarylation of alkynes by a Au/IL system.*

1.6. References

[1] H. Renner, G. Schlamp, D. Hollmann, H. M. Lüschow, P. Tews, J. Rothaut, K. Dermann, A. Knödler, C. Hecht, M. Schlott, R. Drieselmann, C. Peter, R. Schiele in *Ullmann's Encyclopedia of Industrial Chemistry*, John Wiley & Sons, Ltd, **2000**.

[2] E. Gail, S. Gos, R. Kulzer, J. Lorösch, A. Rubo, M. Sauer, R. Kellens, J. Reddy, N. Steier, W. Hasenpusch in *Ullmann's Encyclopedia of Industrial Chemistry*, John Wiley & Sons, Ltd, **2011**.

[3] N. N. Greenwood, A. Earnshaw, Eds. in *Chemistry of the Elements (Second Edition)*, Butterworth-Heinemann, Oxford, **1997**, pp. 1173–1200.

[4] J. Turkevich, P. C. Stevenson, J. Hillier, "A study of the nucleation and growth processes in the synthesis of colloidal gold" *Discuss. Faraday Soc.* **1951**, *11*, 55–75.

[5] K. L. Kelly, E. Coronado, L. L. Zhao, G. C. Schatz, "The Optical Properties of Metal Nanoparticles: The Influence of Size, Shape, and Dielectric Environment" *J. Phys. Chem. B* **2003**, *107*, 668–677.

[6] J. Homola, S. S. Yee, G. Gauglitz, "Surface plasmon resonance sensors: review" *Sensors and Actuators B: Chemical* **1999**, *54*, 3–15.

[7] E. Hutter, J. H. Fendler, "Exploitation of Localized Surface Plasmon Resonance" *Advanced Materials* **2004**, *16*, 1685–1706.

[8] N. Nath, A. Chilkoti, "A Colorimetric Gold Nanoparticle Sensor To Interrogate Biomolecular Interactions in Real Time on a Surface" *Anal. Chem.* **2002**, *74*, 504–509.

[9] P. Pyykko, J. P. Desclaux, "Relativity and the periodic system of elements" *Acc. Chem. Res.* **1979**, *12*, 276–281.

[10] I.-C. Hwang, K. Seppelt, "Gold Pentafluoride: Structure and Fluoride Ion Affinity" *Angewandte Chemie International Edition* **2001**, *40*, 3690–3693.

[11] S. Riedel, M. Kaupp, "Has AuF_7 Been Made?" *Inorg. Chem.* **2006**, *45*, 1228–1234.

[12] H. Schmidbaur, "Inorganic chemistry with ylides" *Acc. Chem. Res.* **1975**, *8*, 62–70.

[13] C. Tubaro, M. Baron, M. Costante, M. Basato, A. Biffis, A. Gennaro, A. A. Isse, C. Graiff, G. Accorsi, "Dinuclear gold(i) complexes with propylene bridged N-heterocyclic dicarbene ligands: synthesis, structures, and trends in reactivities and properties" *Dalton Trans.* **2013**, *42*, 10952.

[14] A. J. Blake, J. A. Greig, A. J. Holder, T. I. Hyde, A. Taylor, M. Schröder, "Bis(1,4,7-trithiacyclononane)gold Dication: A Paramagnetic, Mononuclear AuII Complex" *Angewandte Chemie International Edition in English* **1990**, *29*, 197–198.

[15] S. Preiß, C. Förster, S. Otto, M. Bauer, P. Müller, D. Hinderberger, H. Hashemi Haeri, L. Carella, K. Heinze, "Structure and reactivity of a mononuclear gold(II) complex" *Nature Chem* **2017**, *9*, 1249–1255.

[16] J. C. Pérez-Sánchez, R. P. Herrera, M. Concepción Gimeno, "Unlocking the catalytic potential of gold(II) complexes: a comprehensive reassessment" *Dalton Trans.* **2024**, *53*, 382–393.

[17] N. Mézailles, N. Avarvari, N. Maigrot, L. Ricard, F. Mathey, P. Le Floch, L. Cataldo, T. Berclaz, M. Geoffroy, "Gold(I) and Gold(0) Complexes of Phosphinine-Based Macrocycles" *Angewandte Chemie International Edition* **1999**, *38*, 3194–3197.

[18] D. S. Weinberger, M. Melaimi, C. E. Moore, A. L. Rheingold, G. Frenking, P. Jerabek, G. Bertrand, "Isolation of Neutral Mono- and Dinuclear Gold Complexes of Cyclic (Alkyl)(amino)carbenes" *Angewandte Chemie International Edition* **2013**, *52*, 8964–8967.

[19] Y. Li, T. Xu, X. Ji, J. Zeng, J. Xie, J. Ma, C. Zhu, Q. Zhu, "Dinuclear Au(0) Complex Supported by Tridentate P–Mg–P Ligands" *Angewandte Chemie International Edition* **2025**, *64*, e202509553.

[20] J. H. Teles, S. Brode, M. Chabanas, "Cationic Gold(I) Complexes: Highly Efficient Catalysts for the Addition of Alcohols to Alkynes" *Angewandte Chemie International Edition* **1998**, *37*, 1415–1418.

[21] E. Mizushima, K. Sato, T. Hayashi, M. Tanaka, "Highly Efficient AuI-Catalyzed Hydration of Alkynes" *Angewandte Chemie International Edition* **2002**, *41*, 4563–4565.

[22] J. Chatt, L. A. Duncanson, "Olefin co-ordination compounds. Part III. Infra-red spectra and structure: Attempted preparation of acetylene complexes" *Journal of the Chemical Society (Resumed)* **1953**, 2939–2947.

[23] A. Fürstner, P. W. Davies, "Catalytic Carbophilic Activation: Catalysis by Platinum and Gold π Acids" *Angew Chem Int Ed* **2007**, *46*, 3410–3449.

[24] M. S. Nechaev, V. M. Rayón, G. Frenking, "Energy Partitioning Analysis of the Bonding in Ethylene and Acetylene Complexes of Group 6, 8, and 11 Metals: (CO)5TM−C2Hx and Cl4TM−C2Hx (TM = Cr, Mo, W), (CO)4TM−C2Hx (TM = Fe, Ru, Os), and TM+−C2Hx (TM = Cu, Ag, Au),," *J. Phys. Chem. A* **2004**, *108*, 3134–3142.

[25] C. L. Johnson, D. J. Storm, M. A. Sajjad, M. R. Gyton, S. B. Duckett, S. A. Macgregor, A. S. Weller, M. Navarro, J. Campos, "A Gold(I)–Acetylene Complex Synthesised using Single-Crystal Reactivity" *Angewandte Chemie International Edition* **2024**, *63*, e202404264.

[26] R. H. Hertwig, W. Koch, D. Schröder, H. Schwarz, J. Hrušák, P. Schwerdtfeger, "A Comparative Computational Study of Cationic Coinage Metal−Ethylene Complexes (C2H4)M+ (M = Cu, Ag, and Au)" *J. Phys. Chem.* **1996**, *100*, 12253–12260.

[27] A. Reisinger, N. Trapp, I. Krossing, S. Altmannshofer, V. Herz, M. Presnitz, W. Scherer, "Homoleptic Silver(I) Acetylene Complexes" *Angewandte Chemie International Edition* **2007**, *46*, 8295–8298.

[28] A. Noonikara-Poyil, S. G. Ridlen, I. Fernández, H. V. R. Dias, "Isolable acetylene complexes of copper and silver" *Chem. Sci.* **2022**, *13*, 7190–7203.

[29] A. Mondal, K. Breitwieser, S. Danés, A. Grünwald, F. W. Heinemann, B. Morgenstern, F. Müller, M. Haumann, M. Schütze, D. Kass, K. Ray, D. Munz, "π-Lewis Base Activation of Carbonyls and Hexafluorobenzene" *Angewandte Chemie International Edition* **2025**, *64*, e202418738.

[30] C. Jia, W. Lu, J. Oyamada, T. Kitamura, K. Matsuda, M. Irie, Y. Fujiwara, "Novel Pd(II)- and Pt(II)-Catalyzed Regio- and Stereoselective *trans* -Hydroarylation of Alkynes by Simple Arenes" *J. Am. Chem. Soc.* **2000**, *122*, 7252–7263.

[31] A. M. Echavarren, C. Nevado, "Non-stabilized transition metal carbenes as intermediates in intramolecular reactions of alkynes with alkenes" *Chem. Soc. Rev.* **2004**, *33*, 431–436.

[32] C. Bruneau, "Electrophilic Activation and Cycloisomerization of Enynes: A New Route to Functional Cyclopropanes" *Angewandte Chemie International Edition* **2005**, *44*, 2328–2334.

[33] M. Mato, A. Franchino, C. García-Morales, A. M. Echavarren, "Gold-Catalyzed Synthesis of Small Rings" *Chemical Reviews* **2020**, DOI 10.1021/acs.chemrev.0c00697.
[34] A. Fürstner, "Gold and platinum catalysis—a convenient tool for generating molecular complexity" *Chem. Soc. Rev.* **2009**, *38*, 3208–3221.
[35] A. Fürstner, "From Understanding to Prediction: Gold- and Platinum-Based π-Acid Catalysis for Target Oriented Synthesis" *Acc. Chem. Res.* **2014**, *47*, 925–938.
[36] D. J. Gorin, F. D. Toste, "Relativistic effects in homogeneous gold catalysis" *Nature* **2007**, *446*, 395–403.
[37] P. Pyykko, "Relativistic effects in structural chemistry" *Chem. Rev.* **1988**, *88*, 563–594.
[38] P. Pyykkö, "Theoretical Chemistry of Gold" *Angew Chem Int Ed* **2004**, *43*, 4412–4456.
[39] P. Pyykkö, "Strong closed-shell interactions in inorganic chemistry" *Chemical Reviews* **1997**, *97*, 597–636.
[40] H. Schmidbaur, A. Schier, "Aurophilic interactions as a subject of current research: an up-date" *Chem. Soc. Rev.* **2012**, *41*, 370–412.
[41] M. A. Carvajal, J. J. Novoa, S. Alvarez, "Choice of Coordination Number in d^{10} Complexes of Group 11 Metals" *J. Am. Chem. Soc.* **2004**, *126*, 1465–1477.
[42] A. S. K. Hashmi, "Gold-Catalyzed Organic Reactions" *Chem. Rev.* **2007**, *107*, 3180–3211.
[43] A. S. K. Hashmi, M. Rudolph, "Gold catalysis in total synthesis" *Chem. Soc. Rev.* **2008**, *37*, 1766.
[44] M. Rudolph, A. S. K. Hashmi, "Gold catalysis in total synthesis—an update" *Chem. Soc. Rev.* **2012**, *41*, 2448–2462.
[45] A. S. K. Hashmi, "Introduction: Gold Chemistry" *Chemical Reviews* **2021**, DOI 10.1021/acs.chemrev.1c00393.
[46] D. J. Gorin, N. R. Davis, F. D. Toste, "Gold(I)-Catalyzed Intramolecular Acetylenic Schmidt Reaction" *J. Am. Chem. Soc.* **2005**, *127*, 11260–11261.
[47] V. Mamane, P. Hannen, A. Fürstner, "Synthesis of Phenanthrenes and Polycyclic Heteroarenes by Transition-Metal Catalyzed Cycloisomerization Reactions" **n.d.**, DOI 10.1002/chem.200400220.
[48] A. Fürstner, V. Mamane, "Flexible Synthesis of Phenanthrenes by a $PtCl_2$ -Catalyzed Cycloisomerization Reaction" *J. Org. Chem.* **2002**, *67*, 6264–6267.
[49] C. H. Leung, M. Baron, A. Biffis, "Gold-Catalyzed Intermolecular Alkyne Hydrofunctionalizations—Mechanistic Insights" *Catalysts* **2020**, *10*, 1210.
[50] C. Jia, D. Piao, J. Oyamada, W. Lu, T. Kitamura, Y. Fujiwara, "Efficient Activation of Aromatic C-H Bonds for Addition to C-C Multiple Bonds" *Science* **2000**, *287*, 1992–1995.
[51] D. Zargarian, H. Alper, "Palladium-catalyzed hydrocarboxylation of alkynes with formic acid" *Organometallics* **1993**, *12*, 712–724.
[52] D. Weber, M. A. Tarselli, M. R. Gagné, "Mechanistic Surprises in the Gold(I)-Catalyzed Intramolecular Hydroarylation of Allenes" *Angew. Chem. Int. Ed.* **2009**, *48*, 5733–5736.
[53] D. Weber, M. R. Gagné, "σ–π-Diauration as an alternative binding mode for digold intermediates in gold(ı) catalysis" *Chem. Sci.* **2013**, *4*, 335–338.
[54] M. T. Reetz, S. Sommer, "Gold-Catalyzed Hydroarylation of Alkynes" *Eur. J. Org. Chem.* **2003**, 3485–3496.

[55] W. Wang, G. B. Hammond, B. Xu, "Ligand Effects and Ligand Design in Homogeneous Gold(I) Catalysis" *J. Am. Chem. Soc.* **2012**, *134*, 5697–5705.

[56] H. Tinnermann, C. Wille, M. Alcarazo, "Synthesis, Structure, and Applications of Pyridiniophosphines" *Angewandte Chemie International Edition* **2014**, *53*, 8732–8736.

[57] C. Blons, S. Mallet-Ladeira, A. Amgoune, D. Bourissou, "(P,C) Cyclometalated Gold(III) Complexes: Highly Active Catalysts for the Hydroarylation of Alkynes" *Angew. Chem. Int. Ed.* **2018**, *57*, 11732–11736.

[58] Z. Shi, C. He, "Efficient Functionalization of Aromatic C−H Bonds Catalyzed by Gold(III) under Mild and Solvent-Free Conditions" *J. Org. Chem.* **2004**, *69*, 3669–3671.

[59] M. S. M. Holmsen, C. Blons, A. Amgoune, M. Regnacq, D. Lesage, E. D. Sosa Carrizo, P. Lavedan, Y. Gimbert, K. Miqueu, D. Bourissou, "Mechanism of Alkyne Hydroarylation Catalyzed by (P,C)-Cyclometalated Au(III) Complexes" *J. Am. Chem. Soc.* **2022**, *144*, 22722–22733.

[60] J. Schießl, J. Schulmeister, A. Doppiu, E. Wörner, M. Rudolph, R. Karch, A. S. K. Hashmi, "An Industrial Perspective on Counter Anions in Gold Catalysis: Underestimated with Respect to 'Ligand Effects'" *Advanced Synthesis and Catalysis* **2018**, *360*, 2493–2502.

[61] P. W. Davies, N. Martin, "Counterion Effects in a Gold-Catalyzed Synthesis of Pyrroles from Alkynyl Aziridines" *Org. Lett.* **2009**, *11*, 2293–2296.

[62] A. Homs, C. Obradors, D. Lebœuf, A. M. Echavarren, "Dissecting Anion Effects in Gold(I)-Catalyzed Intermolecular Cycloadditions" *Advanced Synthesis & Catalysis* **2014**, *356*, 221–228.

[63] M. Jia, M. Bandini, "Counterion Effects in Homogeneous Gold Catalysis" *ACS Catal.* **2015**, *5*, 1638–1652.

[64] A. Zhdanko, M. E. Maier, "Explanation of 'Silver Effects' in Gold(I)-Catalyzed Hydroalkoxylation of Alkynes" *ACS Catal.* **2015**, *5*, 5994–6004.

[65] D. Weber, M. R. Gagné, "Dinuclear Gold−Silver Resting States May Explain Silver Effects in Gold(I)-Catalysis" *Org. Lett.* **2009**, *11*, 4962–4965.

[66] D. Wang, R. Cai, S. Sharma, J. Jirak, S. K. Thummanapelli, N. G. Akhmedov, H. Zhang, X. Liu, J. L. Petersen, X. Shi, "'Silver Effect' in Gold(I) Catalysis: An Overlooked Important Factor" *J. Am. Chem. Soc.* **2012**, *134*, 9012–9019.

[67] W. Fang, M. Presset, A. Guérinot, C. Bour, S. Bezzenine-Lafollée, V. Gandon, "Silver-Free Two-Component Approach in Gold Catalysis: Activation of [LAuCl] Complexes with Derivatives of Copper, Zinc, Indium, Bismuth, and Other Lewis Acids" *Chemistry – A European Journal* **2014**, *20*, 5439–5446.

[68] S. Sen, F. P. Gabbaï, "An ambiphilic phosphine/H-bond donor ligand and its application to the gold mediated cyclization of propargylamides" *Chem. Commun.* **2017**, *53*, 13356–13358.

[69] A. Franchino, M. Montesinos-Magraner, A. M. Echavarren, "Silver-Free Catalysis with Gold(I) Chloride Complexes#" *Bulletin of the Chemical Society of Japan* **2021**, *94*, 1099–1117.

[70] K. R. Seddon, "Ionic Liquids for Clean Technology" *Journal of Chemical Technology & Biotechnology* **1997**, *68*, 351–356.

[71] N. V. Plechkova, K. R. Seddon, "Applications of ionic liquids in the chemical industry" *Chem. Soc. Rev.* **2008**, *37*, 123–150.

[72] R. Sheldon, “Catalytic reactions in ionic liquids” *Chem. Commun.* **2001**, 2399–2407.
[73] J. Dupont, R. F. De Souza, P. A. Z. Suarez, “Ionic Liquid (Molten Salt) Phase Organometallic Catalysis” *Chem. Rev.* **2002**, *102*, 3667–3692.
[74] Y. Chauvin, L. Mussmann, H. Olivier, “A novel class of versatile solvents for two-phase catalysis: Hydrogenation, isomerization, and hydroformylation of alkenes catalyzed by rhodium complexes in liquid 1,3-dialkylimidazolium salts” *Angewandte Chemie (International Edition in English)* **1996**, *34*, 2698–2700.
[75] A. Biffis, C. Tubaro, M. Baron, “Advances in Transition-Metal-Catalysed Alkyne Hydroarylations” *The Chemical Record* **2016**, *16*, 1742–1760.
[76] S. Bonfante, P. Bax, M. Baron, A. Biffis, “Gold(I)-Catalyzed Direct Alkyne Hydroarylation in Ionic Liquids: Mechanistic Insights” *Catalysts* **2023**, *13*, 822.

2.1. An improved gold(I)–based catalytic system for the intramolecular synthesis of coumarins

2.1.1. Introduction

Coumarins are heterocyclic molecules defined by a common chromen–2–one motif which is often found in numerous natural products (***Figure 2.1***).[1–6] Many of these heterocycles display notable biological (anticancer,[7] anti–inflammatory,[8,9] antifungal,[10] etc) properties, as well as luminescence properties for photoelectronic applications.[11–13] Interestingly, with a proper design of the bicyclic scaffold, these features can be conveniently tuned, thereupon enhancing the most relevant property for the target application.[7,14,15]

A wide range of stoichiometric organic transformations has been developed over the years to construct and modify the coumarin framework, enabling faster investigation of the diverse properties of this heterocyclic family. Classical methods, such as the Pechmann condensation or the Perkin synthesis, generally require harsh reaction conditions and often suffer from low yields and poor atom economy. In contrast, more recent synthetic strategies rely on π–acidic transition metal catalysts to activate double or triple bonds in phenol–derived acrylates or propiolates, thereby promoting cyclization with the aromatic ring.[16–20]

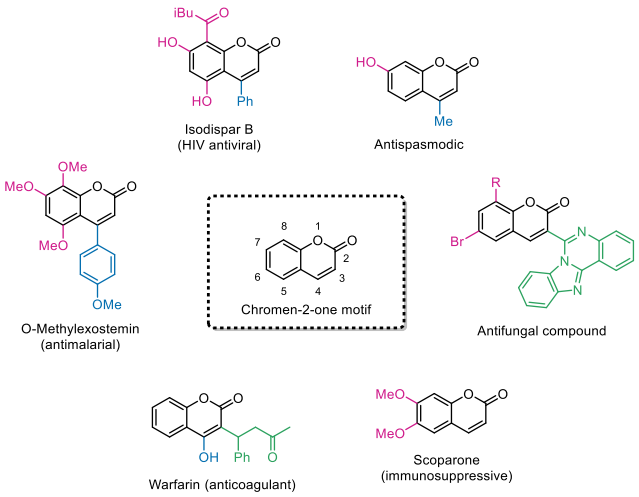

Figure 2.1 – *Selection of bioactive compounds based on the coumarin core*

Gold(I)–based complexes have emerged as promising precatalysts for this task,[21,22] enabling a simple two steps synthesis of coumarins. A first step consists in a pre–esterification of a phenol

with a propiolic acid, usually mediated by a di–substituted carbodiimide, followed by an intramolecular hydroarylation process triggered by electrophilic induction at the alkyne after coordination to gold (***Figure* 2.2**).[23–35]

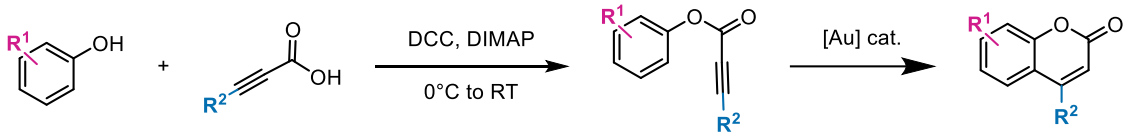

Figure 2.2 *– Synthetic strategy to build coumarin scaffolds*

In this respect, a former report by Banwell et al. showcases the main trends and limitations of gold(I) precatalysts in the cyclization of aryl propiolate derivatives.[36] The appropriate activation of the aromatic ring toward electrophilic substitution by derivatization with electron donating functional groups appears to be crucial yielding good catalytic efficiencies. On the other hand, moderately high catalyst loadings are required (3–5 mol%), which represents a major drawback regarding gold catalysis.[37,38] This limitation is particularly evident when compared to other gold–mediated processes, such as alkyne hydration, hydroamination, and hydroalkoxylation, which are often reported to proceed efficiently under remarkably low catalyst loadings, in some cases well below 0.1 mol%.[39] In contrast, only a few examples of hydroarylation reactions performed with such low gold contents have been documented so far.[40]

These considerations emphasize the urgency for new catalytic systems to be developed. The new method should be capable of combining a broader substrate tolerance with reduced catalyst loadings, thus enhancing both the catalytic efficiency and the substrate tolerance of gold–catalyzed hydroarylation reactions. Our longstanding experience in the study of late transition metal catalysts for direct alkyne hydroarylation reactions led us recently to develop a system based on gold(I) complexes in ionic liquids (ILs) as catalysts featuring high activity in the hydroarylation of alkynoic acids and esters with electron rich arenes and heteroarenes under mild conditions.[41,42] We then set out to apply this reaction to the development of a synthetic protocol for the preparation of functionalized coumarins via intramolecular hydroarylation of phenol derived propiolic esters.

2.1.2. Results and Discussion

Our investigation started with the preparation of the alkynoate ester **1a** to screen the best conditions to perform the intramolecular hydroarylation reaction. The commercial complex $IPrAuNTf_2$ (IPr= N,N'–(2,6–diisorpopylphenyl)imidazole–2–ylidene, NTf_2^-= bis(trifluoromethylsulfonyl)imide) was chosen as catalyst, since it was already proved competent in our previous investigations on the intermolecular alkyne hydroarylation with arenes.[42] In this case, no silver–mediated activation was necessary due to the presence of the weakly coordinating anion NTf_2^- tethered to gold, which can be conveniently displaced in presence of the substrate under catalytic conditions.

Prompted by our recent findings on the synergistic role of gold catalysis and ILs in intermolecular hydroarylation reactions, we addressed our initial efforts towards a screening of ILs as reaction media. Interestingly, through the combined use of NTf_2^- anion and BMIM (1–butyl–2–methylimidazolium) as cation, almost quantitative yields of **2a** could be reached within 30 minutes at 0.5 mol% gold catalyst (**Table 2.1**, entry 1). The perfluorinated anion BF_4^- also gave a system with appreciable catalytic activity (**Table 2.1**, entry 4) which was unexpected if compared again with the intermolecular reaction. It must be said that only freshly supplied ILs must be used when the counteranion is a perfluorocomplex in order to ensure good reproducibility. These counteranions slowly decompose, likely through a hydrolytic pathway, and the resulting impurities can negatively impact catalytic performance.[29] Interestingly, the nature of the cation had also some effect on the overall catalytic performance, which was most evident with the anions providing lower activity. Indeed, little differences were observed with NTf_2^- as the anion (entries 11, 12 and 13); only with the cation BMPyrr the activity was significantly lower, though still high (entry 13). On the contrary, use of the BMMIM cation instead of BMIM caused an impressive activation of the catalytic system when OTf^- was used as anion (**Table 2.1**, entry 10). An opposite trend was observed for BF_4^- (**Table 2.1**, entries 4 and 5), whereas the system with PF_6^- as anion remained inactive, probably due to its higher tendency to hydrolyze. We tend to attribute this effect to the fact that in comparison with BMIM the BMMIM cation lacks the capacity to act as a hydrogen bond donor.[43] This capacity may give rise to strong interionic interactions, when the cation is coupled with anions exhibiting strong hydrogen bond basicity, with the consequent formation of microheterogeneities in the ionic liquid phase.[44]

Table 2.1 – *Effect of the ionic liquid on the reaction performance*

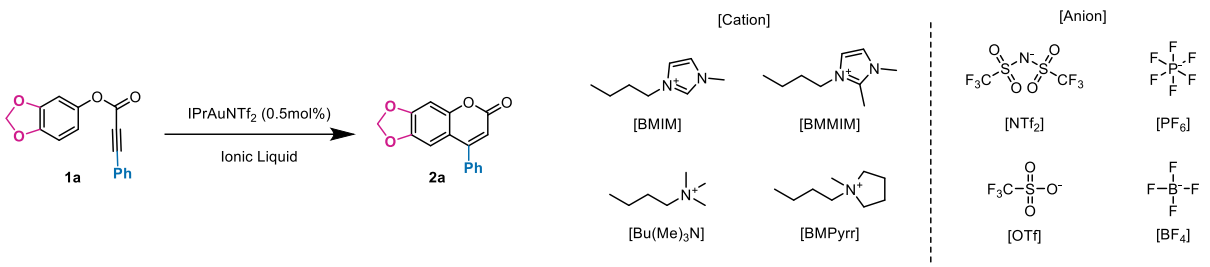

Entry	[Cation]	[Anion]	T (°C)	Time (h)	Yield (%)[a]
1	[BMIM]	[NTf_2]	40	0.5	97
2	[BMIM]	[OTf]	40	4	NR[b]
3	[BMIM]	[PF_6]	40	4	NR[b]
4	[BMIM]	[BF_4]	40	1	52
				2	97
5	[BMMIM]	[BF_4]	40	6	15
				24	48
6	[BMMIM]	[BF_4]	50	6	31
				24	95
7	[BMIM]	[PF_6]	50	3	NR[b]
8	[BMMIM]	[PF_6]	50	3	NR[b]
9	[BMIM]	[OTf]	50	24	NR[b]
10	[BMMIM]	[OTf]	50	6	38
				24	>99
11	[BMMIM]	[NTf_2]	40	0.5	>99
12	[$Bu(Me)_3N$]	[NTf_2]	40	0.5	93
				1	>99
13	[BMPyrr]	[NTf_2]	40	1	85
				2	>99

[a] Yields were determined by ^{1}H NMR spectroscopy with dimethylsulfone or 1,2–dimethoxyethane as internal standards; [b] NR: no reaction.

In the absence of such strong interionic interactions, (*i.e.* when the anion has low hydrogen bond basicity, as in the case of NTf_2^-), the effect of the cation vanishes and can present itself again only when the change in the physico–chemical properties is so large to alter the solubility of the substrate or of the catalyst in the ionic liquid.

Once the optimal ionic liquid had been selected, we turned our attention to the minimization of the gold content in order to obtain efficient catalysis (**Table 2.2**).

Table 2.2 *– Effect of acid addition on the reaction performance*

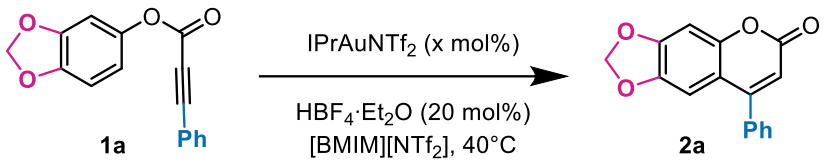

Entry	[Au] (mol%)	HBF_4 (mol%)	Time (h)	Yield (%)[a]
1	0.5	–	0.5	97
2	0.5	20	0.5	>99
3	0.1	–	24	NR[b]
4	0.1	20	1	79
			1.5	98
5	0.05	20	1	30
			3	93
6	0.01	20	3	35
			5	61
			24	>99
7	–	20	24	NR[b]

[a] Yields were determined by ^{1}H NMR spectroscopy with dimethylsulfone or 1,2–dimethoxyethane as internal standards; [b] NR: no reaction.

As mentioned above, using our system it was possible to lower the gold content down to 0.5 mol% without compromising the catalytic performance. Moreover, by adding 20 mol% of a Brønsted acid (in our case $HBF_4 \cdot Et_2O$) as co–catalyst, it was possible to further lower the gold content to 0.01 mol% without significant erosion of the chemical outcome (99% yield; **Table 2.2**, entry 6).

The possible roles of the acid additive are to assist the protic cleavage of the Au-C bond, which may be the rate determining step of the reaction, and to keep the catalyst active when lower amounts of gold(I) complex are employed.[37] In the latter context, the acid cocatalyst is supposed to restore the active monomeric gold complex by attacking off–cycle intermediates such as *gem*–diaurated species.[45,46] The effect of the acid additive is evident when 0.1 mol% of gold(I) complex

was employed: the system is completely static/poisoned under neutral conditions (**Table 2.2**, entry 3). On the other hand, as soon as $HBF_4 \cdot Et_2O$ is added the complete restoration of the catalytic activity occurs (**Table 2.2**, entry 4). In presence of the acidic co-catalyst, the hydroarylation reaction could be promoted using only 0.01 mol% of $IPrAuNTf_2$, and still a quantitative yield was obtained after 1 day reaction (**Table 2.2**, entry 6). To our knowledge, it is the first time that gold(I)–catalysts were employed in such low amounts in the framework of C–H bond functionalization reactions. At this point, a selected sample of 15 substrates was taken into consideration to test the synthetic application and the generality of the method (***Figure* 2.3**).

Figure 2.3 *– Reaction scope* [a]

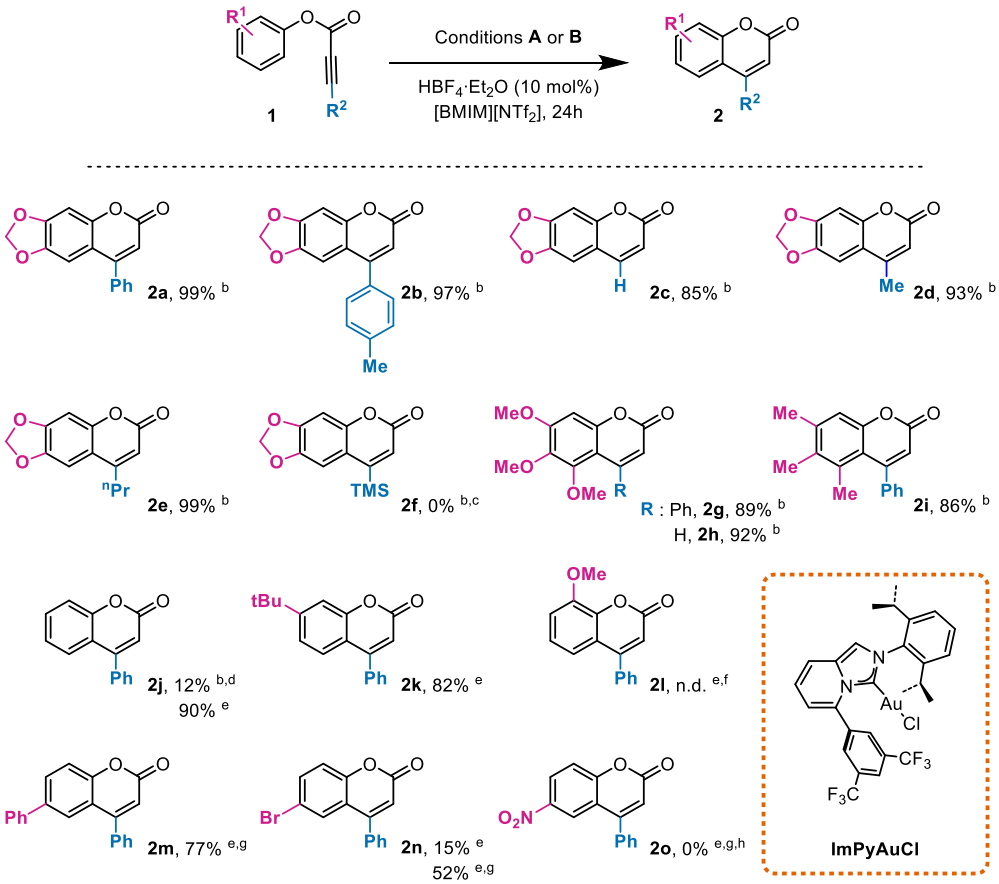

[a] *Isolated yields are reported;* [b] *Conditions* ***A****: [**1**] = 0.67 M, 0.05 mol% $IPrAuNTf_2$ at 40 °C;* [c] *No reaction observed;* [d] *84% of* ***1j*** *was recovered;* [e] *Conditions* ***B****: [**1**] = 0.67 M, 0.5 mol% $IPrAuNTf_2$ at 80 °C;* [f] ***2l*** *was detected by ^1H NMR spectroscopy, however purification by column chromatography was impractical due to the presence of multiple by–products;* [g] *The complex ImPyAuCl was employed instead of $IPrAuNTf_2$ with 1 equiv. $AgSbF_6$ as activator;* [h] *extensive hydrolysis of* ***1o*** *was detected by ^1H NMR spectroscopy;*

By reducing the acid additive loading at 10 mol% and fixing arbitrarily the reaction time at 24 h, we could still obtain quantitative conversion of **1a** to yield the corresponding coumarin **2a** at low amount of $IPrAuNTf_2$ (conditions **A**). The presence of more donating group at the alkyne moiety, such as *p*–tolyl (**1b**) or alkyl chains with different lengths (**1d** or **1e**) showed a low influence on the catalytic performance allowing to achieve quantitative conversion of the alkynoates and isolated yields above 90%. On the other hand, an even more electron–rich alkyne, such as **1f,** resulted completely inactive toward the employed conditions. However, a higher steric hindrance near the electrophilic center cannot be excluded from the causes of this lack in activity. The effect of substituents at the *meta* positions of the aryl ring was also tested. 3,4,5–Trisubstituted–phenol derivatives **1g** and **1i** were employed achieving good yields. Comparable efficiencies are found as well when a terminal alkyne moiety is employed (**1c** and **1h**).

Poor yields were obtained with substrate **1j** bearing an unsubstituted phenyl ring, (12% yield). However, by just increasing the amount of catalyst (0.5 mol%) and reaction temperature (80 °C, conditions **B**) **2j** could be conveniently isolated in 90% yield. Substrate **1k** was as well included in the scope, with 82% isolated yield and complete selectivity toward the reported isomer **2k**. it is indeed reasonable that the carbon atom enclosed in between the tBu and the ester group would be less available due to steric shielding. Surprisingly, moving to substrate **1l** we encountered unexpected selectivity issues which made unpracticable the purification of **2l** by column chromatography.

Finally, we tackled the suitability of more deactivated substrates, bearing different electron withdrawing groups at the *para* position of the aryl moiety. A first attempt was conducted employing conditions **B** and **1n** as substrate but only 15% yield was achieved after 24 h. Structural modification at the NHC ligand proved to be an efficient strategy to overcome this issue. In particular, the electrophilic character of the gold metal center could be enhanced by a Buchwald–type pendant installed on the pyridine–derived NHC ligand (ImPy). In fact, the group of Prof. Marco Bandini at the University of Bologna has recently reported on the beneficial effect of CF_3–containing ligands on electrophilic gold–catalyzed processes.[47,48] This modification (catalyst ImPyAuCl) resulted in an impressive enhancement of the catalytic performance, achieving **2n** in 52% yield. Activation of the 4–phenyl derivative **1m** was as well accomplished, achieving 77% yield of **2m**, while the more deactivated nitro compound **1o** showed no conversion to hydroarylation products. Analysis of the reaction crude by ^1H NMR spectroscopy consistently showed hydrolysis of the ester

group as the only reaction taking place, with a rate increasing with higher gold complex loading: neither **1o** nor **2o** were detected after one day of reaction when 2 mol% ImPyAuCl were employed.

2.1.3. Conclusion and perspectives

A new ionic liquid–based system was reported, showing enhanced catalytic performance in the gold–catalyzed intramolecular hydroarylation of aryl alkynoates. Extremely low catalyst loadings could be employed in the case of activated substrates with a good tolerance toward the alkyne substituent, allowing to access a broad variety of 4–substituted coumarins. Different aromatic rings could be incorporated in the reaction scope using harsher conditions and a higher amount of gold catalyst, although such amount was still lower than what is generally employed in the literature in the context of hydroarylation processes. Finally, tuning the electronic properties of the metal center by means of the reported ImPy–NHC ligand, we could access coumarins **2m** and **2n** with analogous results to the ones obtained by Shi and He with 5 mol% $AuCl_3$/3AgOTf catalyst,[23] which have been up to now the best result reported in gold catalysis for those substrates.

2.1.4. Experimental section

Synthesis of aryl alkynoates

Aryl alkynoates were prepared according to a previously reported procedure:[49]

In a round–bottom flask, a stirred solution of the phenol (3.0 mmol, 1.0 eq.) in DCM (12 ml) was cooled to 0°C and the propiolic acid* derivative (3.3 mmol, 1.1 eq.) was added. Subsequently, a mixture of dicyclohexylcarbodiimide (DCC, 873.0 mg, 4.4 mmol, 1.5 eq.) and 4–dimethylaminopyridine (DMAP, 36.0 mg, 0.3 mmol, 0.1 eq.) in DCM (6 mL) was added dropwise to the round–bottom flask. The resulting mixture was allowed to warm up and stirred at room temperature for 12 hours. Then the mixture was filtered and the solid residue on the filter was washed with DCM (15 mL). The combined organic phases were concentrated under reduced pressure and the obtained residue purified by flash chromatography over silica gel. The desired product was isolated upon evaporation of the relevant fractions.

* Propiolic acid, phenylpropiolic acid, 3–(trimethylsilyl)–2–propynoic acid, 2–butynoic acid and 2–hexynoic acid were directly purchased and used without further purification, while the derivative 3–(4'–methyl–phenyl)–2–propynic acid was synthesized according to the following procedure:[49] 4–iodotoluene (1.323 g, 6.0 mmol, 1.0 eq.), 1,8–diazabicyclo(5.4.0)undec–7–ene (DBU, 2.01 g, 13.2 mmol, 2.2 eq.), and $Pd(PPh_3)_4$ (347.1 mg, 0.3 mmol, 5 mol %) were taken in a flame dried, round bottom flask with a magnetic stirrer. The reaction tube was purged with argon and then dry DMSO (15 mL) was added via a syringe. Propiolic acid (0.40 ml, 6.6 mmol, 1.1 eq.) was added into the flask and then the mixture was stirred at room temperature for 12 h. After completion of the reaction (TLC monitored), EtOAc (10 mL) was added into the reaction mixture. The reaction mixture was extracted with saturated aqueous $NaHCO_3$. The aqueous layer was separated, acidified by addition of cold HCl (1 M) and extracted with DCM. The combined organic layers were dried with anhydrous Na_2SO_4 and filtered, and the solvent was removed under reduced pressure. The resulting crude product was purified by column chromatography on silica gel (MeOH/DCM/AcOH 8:90:2 as eluent). The product was identified by ^1H NMR spectroscopy and was subsequently employed for the synthesis of the corresponding aryl alkynoate.

3',4'–Methylendioxy–phenyl 3–phenyl–2–propynoate – 1a

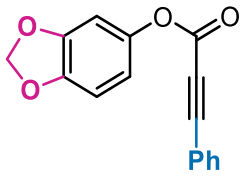

Synthesized employing sesamol and 3–phenyl–2–propynoic acid as starting materials. The corresponding alkynoate was isolated by flash chromatography (eluent EtOAc/Hex 1:10) to obtain 593 mg of product as a white solid (2.22 mmol, 74% yield). Spectroscopic data were in agreement with previously reported ones. [50]

^{1}H NMR (300 MHz, $CDCl_3$): δ 7.66–7.60 (m, 2H), 7.53–7.45 (m, 1H), 7.44–7.36 (m, 2H), 6.80 (d, 1H, *J* = 8.4 Hz), 6.71 (d, 1H, *J* = 2.4 Hz), 6.64 (dd, 1H, *J*= 8.4 Hz, *J* = 2.4 Hz,), 5.99(s, 2H) ppm.

3',4'–Methylendioxy–phenyl 3–(4'–methylphenyl)–2–propynoate – 1b

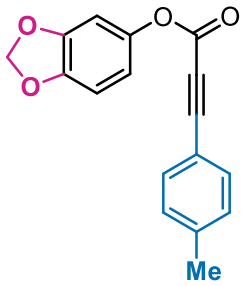

Synthesized employing sesamol and 3–(4'–methylphenyl)–2–propynoic acid as starting materials. The corresponding alkynoate was isolated by flash chromatography (eluent EtOAc/Hex 1:10) to obtain 52.6 mg of product as a pale yellow solid (0.188 mmol, 3% overall yield from 4–iodotoluene and propiolic acid*).

^{1}H NMR (300MHz, $CDCl_3$): δ 7.57–7.48 (m, *J* = 7.8 Hz, 2H), 7.26–7.16 (m, *J* = 7.8 Hz, 2H), 6.80 (d, *J* = 8.3 Hz, 1H), 6.70 (brs, 1H), 6.64 (d, *J* = 8.3 Hz, 1H), 5.99 (s, 2H), 2.40 (s, 3H) ppm; **^{13}C{^{1}H} NMR (75.5 MHz, $CDCl_3$):** δ 152.9, 148.2, 145.9, 144.5, 142.0, 133.3, 129.6, 116.2, 114.1, 108.2, 103.7, 101.9, 89.5, 80.0, 21.9 ppm; **HRMS (ESI+):** calcd for $[M+H]^+ = C_{17}H_{13}O_4^+$: 281.0808 m/z. Found: 281.0890 m/z.

* the low yield is mainly due to the inefficiency of the Sonoghashira coupling of 4–iodotoluene with propiolic acid.

3',4'–Methylendioxy–phenyl–2–propynoate – 1c

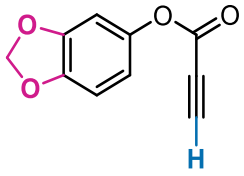

Synthesized employing sesamol and propiolic acid as starting materials. The corresponding alkynoate was isolated by flash chromatography (eluent EtOAc/Hex 1:10) to obtain 356 mg of product as a white solid (1.87 mmol, 62% yield). Spectroscopic data were in

agreement with previously reported ones.[36]

^{1}H NMR (300 MHz, $CDCl_3$): δ 6.79 (d, *J* = 8.4 Hz, 1H), 6.66 (d, *J* = 2.4 Hz, 1H), 6.59 (dd, *J* = 8.4, 2.4 Hz, 1H), 5.99 (s, 2H), 3.07 (s, 1H) ppm.

3',4'–Methylendioxy–phenyl–2–butynoate – 1d

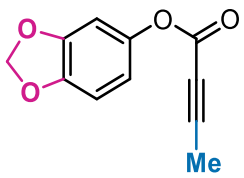

Synthesized employing sesamol (scaled–up procedure to 6 mmol) and 2–butynoic acid as starting materials. The corresponding alkynoate was isolated by flash chromatography (eluent EtOAc/Hex 1:10) to obtain 846 mg of product as a white solid (4.14 mmol, 69% yield).

^{1}H NMR (300 MHz, $CDCl_3$): δ 6.74 (d, *J* = 8.4 Hz, 1H), 6.63 (d, *J* = 2.3 Hz, 1H), 6.55 (dd, *J* = 8.4, 2.3 Hz, 1H), 5.94 (s, 2H), 2.01 (s, 3H) ppm; **^{13}C{^{1}H} NMR (75.5 MHz, $CDCl_3$):** δ 152.3, 148.2, 145.8, 144.4, 114.0, 108.1, 103.6, 101.9, 88.4, 72.1, 3.9 ppm; **HRMS (ESI+):** calcd for $[M+H]^+ = C_{11}H_9O_4^+$: 205.0495. Found: 205.0546.

3',4'–Methylendioxy–phenyl–2–hexynoate – 1e

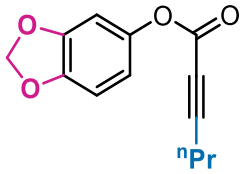

Synthesized employing sesamol and 2–hexynoic acid as starting materials. The corresponding alkynoate was isolated by flash chromatography (eluent EtOAc/Hex 1:10) to obtain 395 mg of product as a white solid (1.70 mmol, 57% yield).

^{1}H NMR (300 MHz, $CDCl_3$): δ 6.77 (d, 1H, *J* = 8.4 Hz), 6.64 (d, 1H, *J* = 2.4 Hz), 6.57 (dd, 1H, *J* = 8.4, 2.4 Hz), 5.98 (s, 2H), 2.37 (t, 2H, *J* = 7.1 Hz), 1.65 (ses, 2H, *J* = 7.2 Hz), 1.04 (t, 3H, *J* = 7.4 Hz) ppm; **^{13}C{^{1}H} NMR (75.5 MHz, $CDCl_3$):** δ 152.5, 148.2, 145.8, 144.5, 114.0, 108.1, 103.7, 101.9, 92.4, 72.9, 21.1, 20.9, 13.6 ppm; **HRMS (ESI+):** calcd for $[M+H]^+ = C_{13}H_{13}O_4^+$: 233.0808 m/z. Found: 233.0844 m/z.

3',4'–Methylendioxy–phenyl–3–trimethylsilyl–2–propynoate – 1f

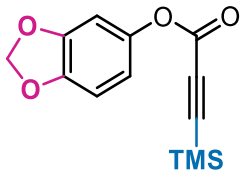

Synthesized employing sesamol (scaled–up procedure to 6 mmol) and 3–trimethyl–silyl–2–propynoic acid as starting materials. The corresponding alkynoate was isolated by flash chromatography (eluent EtOAc/Hex 1:10) to obtain 393 mg of product as a colorless oil (1.50 mmol, 25 % yield).

^{1}H NMR (300MHz, $CDCl_3$): δ 6.76 (d, *J* = 8.4 Hz, 1H), 6.64 (d, *J* = 2.4 Hz, 1H), 6.57 (dd, *J* = 8.4, 2.4 Hz, 1H), 5.97 (s, 2H), 0.28 (s, 9H) ppm; **^{13}C{^{1}H} NMR (75.5 MHz, $CDCl_3$):** δ 151.6, 148.2, 145.9, 144.2, 113.9, 108.1, 103.6, 101.9, 96.9, 94.0, –0.8 ppm; **HRMS (ESI+):** calcd for $[M+H]^+ = C_{13}H_{15}O_4Si^+$: 263.0734 m/z. Found: 263.0772 m/z.

3',4',5'–Trimethoxy–phenyl–3–phenyl–2–propynoate – 1g

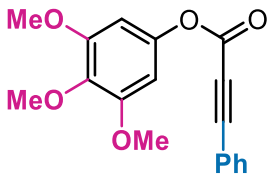

Synthesized employing 3,4,5–trimethoxyphenol and 3–phenyl–2–propynoic acid as starting materials. The corresponding alkynoate was isolated by flash chromatography (eluent EtOAc/Hex 1:5) to obtain 561 mg of product as a yellow solid (1.80 mmol, 60% yield). Spectroscopic data were in agreement with previously reported ones.[16]

^{1}H NMR (300 MHz, $CDCl_3$): δ 7.67–7.58 (m, 2H), 7.54–7.46 (m, 1H), 7.45–7.36 (m, 2H), 6.44 (s, 2H), 3.85 (s, 6H), 3.84 (s, 3H) ppm.

3',4',5'–Tri–methoxy–phenyl–3–phenyl–2–propynoate – 1h

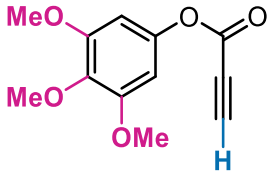

Synthesized employing 3,4,5–trimethoxy–phenol and propiolic acid as starting materials. The corresponding alkynoate was isolated by flash chromatography (eluent EtOAc/Hex 1:5) to obtain 309 mg of product as an orangish solid (1.31 mmol, 44% yield).

^{1}H NMR (300 MHz, $CDCl_3$): δ 6.38 (s, 2H), 3.83 (s, 6H), 3.82 (s, 3H), 3.09 (s, 1H) ppm; **^{13}C{^{1}H} NMR (75.5 MHz, $CDCl_3$):** δ 153.7, 151.1, 145.9, 136.4, 98.9, 77.1, 74.3, 61.0, 56.3 ppm; **HRMS (ESI+):** calcd for

$[M+H]^+ = C_{12}H_{13}O_5^+$: 237.0757 m/z. Found: 237.0785 m/z.

3',4',5'–Trimetyl–phenyl–3–phenyl–2–propynoate – 1i

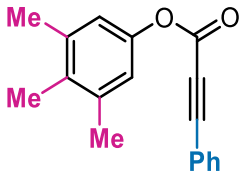

Synthesized employing 3,4,5–tri–methyl–phenol and 3–phenyl–2–propynoic acid as starting materials. The corresponding alkynoate was isolated by flash chromatography (eluent EtOAc/Hex 1:10) to obtain 384 mg of product as a white solid (1.45 mmol, 48% yield).

^{1}H NMR (300 MHz, $CDCl_3$): δ 7.69–7.61 (m, *J* = 7.8 Hz, 2H), 7.54–7.46 (m, 1H), 7.45–7.37 (m, 2H), 6.85 (s, 2H), 2.31 (s, 6H), 2.16 (s, 3H) ppm; **^{13}C{^{1}H} NMR (75.5 MHz, $CDCl_3$):** δ 153.0, 147.3, 138.0, 133.5, 133.2, 131.0, 128.7, 120.2, 119.4, 88.3, 80.5, 20.8, 15.1 ppm; **HRMS (ESI+):** calcd for $[M+H]^+ = C_{18}H_{17}O_2^+$: 265.1223 m/z. Found: 265.1256 m/z.

Phenyl–3–phenyl–2–propynoate – 1j

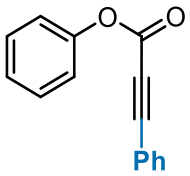

Synthesized employing phenol and 3–phenyl–2–propynoic acid as starting materials. The corresponding alkynoate was isolated by flash chromatography (eluent EtOAc/Hex 1:20) to obtain 415 mg of product as a white solid (1.87 mmol, 62% yield). Spectroscopic data were in agreement with previously reported ones.[50]

^{1}H NMR (300 MHz, $CDCl_3$): δ 7.66–7.61 (m, 2H), 7.53–7.37 (m, 5H), 7.32–7.27 (m, 1H), 7.23–7.17 (m, 2H) ppm.

3'–Tert–butyl–phenyl–3–phenyl–2–propynoate – 1k

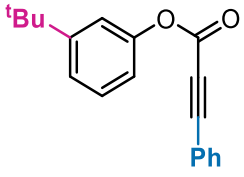

Synthesized employing 3–tert–butyl–phenol and 3–phenyl–2–propynoic acid as starting materials. The corresponding alkynoate was isolated by flash chromatography (eluent EtOAc/Hex 1:20) to obtain 366 mg of product as a greenish oil (1.31 mmol, 44% yield). Spectroscopic data were in agreement with previously reported ones.

^{1}H NMR (300 MHz, $CDCl_3$): δ 7.66–7.60 (m, 2H), 7.53–7.45 (m, 1H), 7.44–7.37 (m, 2H), 7.34 (d, *J* = 7.6 Hz, 1H), 7.31 (dt, *J* = 7.8, 1.6 Hz,

1H), 7.19 (t, *J* = 1.9 Hz, 1H), 7.03 (dt, *J* = 7.5, 1.9 Hz, 1H), 1.34 (s, 9H) ppm; **$^{13}C\{^{1}H\}$ NMR (75.5 MHz, $CDCl_3$):** δ 153.5, 152.6, 150.2, 133.3, 131.1, 129.2, 128.8, 123.6, 119.5, 118.6, 88.7, 80.5, 35.0, 31.4 ppm; **HRMS (ESI+):** calcd for $[M+H]^+$ = $C_{19}H_{19}O_2^+$: 279.1380 m/z. Found: 279.1408 m/z.

2'–Methoxy–phenyl 3–phenyl–2–propynoate – 1l

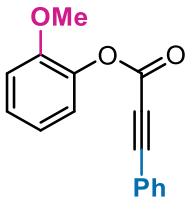

Synthesized employing guaiacol and 3–phenyl–2–propynoic acid as starting materials. The corresponding alkynoate was isolated by flash chromatography (eluent EtOAc/Hex 1:5) to obtain 401 mg of product as a pale yellow solid (1.59 mmol, 53% yield). Spectroscopic data were in agreement with previously reported ones. [51]

^{1}H NMR (300MHz, $CDCl_3$): δ 7.66–7.58 (m, 2H), 7.52–7.44 (m, 1H), 7.43–7.35 (m, 2H), 7.30–7–22 (m, 1H), 7.20–7.13 (m, 1H), 7.05–6.95 (m, 2H), 3.85 (s, 3H) ppm.

Biphenyl–4'–yl–3–phenyl–2–propynoate – 1m

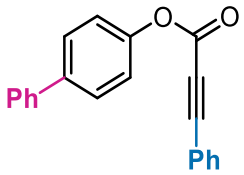

Synthesized employing 4–phenyl–phenol and 3–phenyl–2–propynic acid as starting materials. The corresponding alkynoate was isolated by flash chromatography (eluent Toluene/Hex 1:1) to obtain 608 mg of product as a white solid (2.04 mmol, 68% yield). Spectroscopic data were in agreement with previously reported ones.[52]

^{1}H NMR (300 MHz, $CDCl_3$): δ 7.68–7.60 (m, 5H), 7.60–7.55 (m, 2H), 7.55–7.33 (m, 6H), 7.31–7.24 (m, 2H) ppm.

4'–Bromo–phenyl–3–phenyl–2–propynoate – 1n

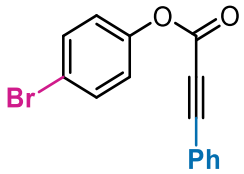

Synthesized employing 4–bromo–phenol and 3–phenyl–2–propynoic acid as starting materials. The corresponding alkynoate was isolated by flash chromatography (eluent EtOAc/Hex 1:10) to obtain 738 mg of product as a white solid (2.45 mmol, 82% yield). Spectroscopic data were in agreement with previously reported ones.[52]

^{1}H NMR (300 MHz, $CDCl_3$): δ 7.67–7.60 (m, 2H), 7.57–7.51 (m, *J* = 8.8 Hz, 2H), 7.51–7.46 (m, 1H), 7.46–7.37 (m, 2H), 7.14–7.06 (m, *J* = 8.8 Hz, 2H) ppm.

4'–Nitro–phenyl–3–phenyl–2–propynoate – 1o

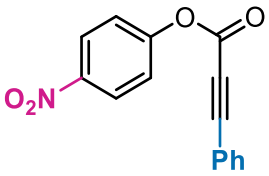

Synthesized employing 4–bromo–phenol and 3–phenyl–2–propynoic acid as starting materials. The corresponding alkynoate was isolated by flash chromatography (eluent EtOAc/Hex 1:10) to obtain 571 mg of product as a pale yellow solid (2.14 mmol, 71% yield). Spectroscopic data were in agreement with previously reported ones.[51]

^{1}H NMR (400 MHz, $CDCl_3$): δ 8.34–8.29 (m, *J* = 9.2 Hz, 2H), 7.68–7.64 (m, 2H), 7.56–7.50 (m, 1H), 7.47–7.38 (m, 4H) ppm.

Synthesis of the catalyst ImPyAuCl

The synthesis has been accomplished according to a reported literature procedure.[47] In a flame–dried two–necked round bottom flask filled with argon the imidazolium salt ImPy·HCl (52.2 mg, 0.10 mmol, 1 eq.) was dissolved in 1 mL of anhydrous DCM and then Ag_2O (25.6 mg, 0.11 mmol, 1.1 eq.) was added: aluminum foils were used to protect the reaction mixture from light. The reaction mixture was stirred at room temperature overnight. TLC monitoring using EtOAc/^{c}Hex 1:2 was performed to identify formation of the respective NHC–Ag complex. The reaction was filtered through a Celite® pad followed by DCM to rinse the filter. The organic phase was then evaporated, taken up in 1 mL of anhydrous DCM and transferred inside a two–necked round–bottom flask under inert atmosphere (aluminum foils were employed also in this step). [$AuCl(SMe_2)$] (29.6 mg, 0.10 mmol, 1 eq.) was then added and the solution was stirred at room temperature for 5 h. After the silver precursor was completely consumed, the reaction crude was filtered through a Celite® pad, the filter was rinsed with DCM and all volatiles were removed in *vacuo*. The resulting yellowish solid was recrystallized by layering n–hexane over a concentrated solution of DCM, to afford 49.1 mg of the desired ImPyAuCl complex (0.068 mmol, 68% yield). The collected spectroscopic data were in accordance with previously reported ones.[47]

ImPyAuCl

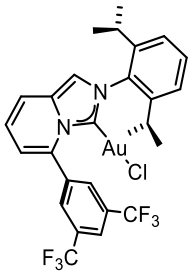

^{1}H NMR (300 MHz, $CDCl_3$): δ = 8.11 – 7.97 (m, 3H), 7.57 (dd, *J* = 9.3, 0.9 Hz, 1H), 7.47 (t, *J* = 7.8 Hz, 1H), 7.41 (s, 1H), 7.26 – 7.21 (m, 2H), 7.12 (dd, *J* = 9.3, 6.7 Hz, 1H), 6.73 (dd, *J* = 6.7, 0.9 Hz, 1H), 2.16 (hept, *J* = 6.6 Hz, 2H), 1.25 (d, *J* = 6.8 Hz, 6H), 1.13 (d, *J* = 6.6 Hz, 6H) ppm; **^{19}F NMR (188 MHz, $CDCl_3$):** δ –62.92 ppm.

General procedure for catalytic test of Table 2.1

The substrate **1a** (133.1, 0.5 mmol) was placed in a flame–dried Schlenk tube under argon atmosphere. The gold catalyst IPrAuNTf$_2$ (2.2 mg, 0.0025 mmol) was added to the flask along with 0.75 ml of a suitable ionic liquid. The internal standard, dimethylsulfone or 1,2–dimethoxyethane, (0.25 mmol) was then added to the same flask and the mixture was stirred at room temperature for five minutes. At this point a ^{1}H NMR check was taken, and the Schlenk tube was then moved in a thermostatic bath at 40 or 50 °C. The reaction kinetic was followed by sampling aliquots of the reaction crude at different times and analyzing them by ^{1}H NMR.

General procedure for catalytic test of Table 2.2

Different amounts of IPrAuNTf$_2$ catalyst (0.1, 0.05 or 0.01 mol% with respect to **1a**) were deposit through a titled solution of the complex in DCM.* The same procedure as for **Table 2.1** was used: in particular, [BMIM][NTf$_2$] was employed as ionic liquid. The acidic additive $HBF_4 \cdot Et_2O$ (14 µl, 0.1 mmol) was added to the reaction mixture as the first ^{1}H NMR check was collected. The Schlenk tube was then placed in a thermostatic bath at 40°C and the reaction kinetic was monitored as above.

*DCM was previously treated with basic alumina in order to remove acid traces.

General procedures for hydroarylation reactions

- Conditions **A**:

The substrate (0.5 mmol) was placed in a flame–dried Schlenk tube under argon atmosphere. A freshly prepared solution of the gold catalyst IPrAuNTf$_2$ (4.3 mg, 0.005 mmol) in [BMIM][NTf$_2$] (50 µl) was added to the flask (50 µl, 0.25 µmol, 0.05 mol% [Au] loading), along with 0.7 ml of [BMIM][NTf$_2$]

and the mixture was stirred for 5 min at room temperature. The acid co–catalyst $HBF_4 \cdot Et_2O$ (7 µl, 0.05 mmol) was then added to the mixture and the flask was placed in a thermostatic bath at 40 °C for 24 h. A ^1H NMR check was then taken to confirm the presence of products. The reaction crude was then subjected to column chromatography purification without any pre–treatment to afford the spectroscopically pure coumarin upon collection of the relevant fractions.

- Conditions **B**:

The substrate (0.5 mmol) and the gold catalyst $IPrAuNTf_2$ or ImPyAuCl (0.0025 mmol) were placed in a flame–dried Schlenk tube under argon atmosphere. The ionic liquid [BMIM][NTf_2] (0.75 ml) was added to the flask and the mixture was stirred for 5 min at room temperature.* The acid co–catalyst $HBF_4 \cdot Et_2O$ (7 µl, 0.05 mmol) was then added to the mixture and the flask was placed in a thermostatic bath at 80 °C for 24 h. A ^1H NMR check was then taken to confirm the presence of products. The reaction crude was then subjected to column chromatography purification without any pre–treatment to afford the spectroscopically pure coumarin upon collection of the relevant fractions.

* When ImPyAuCl was employed, 0.1 ml of $AgSbF_6$ solution in [BMIM][NTf_2] (8.6 mg $AgSbF_6$, 0.025 mmol, in 1 ml of ionic liquid) was added to remove the chloride ligand. The mixture volume was then diluted to 0.75 ml with fresh [BMIM][NTf_2].

6,7–Methylendioxy–4–phenyl–2H–chromen–2–one – 2a

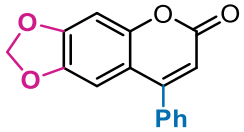

Compound **2a** was synthesized from **1a** according to general conditions **A** and purified by column chromatography (eluent EtOAc/Hex 1:4) to afford 131.3 mg of the corresponding coumarin as a white solid (0.49 mmol , 99% yield). Spectroscopic data were in agreement with previously reported ones.[53]

^1H NMR (300 MHz, $CDCl_3$): δ 7.52–7.50 (m, 3H), 7.45–7.39 (m, 2H), 6.88 (s, 1H), 6.82 (s, 1H), 6.23 (s, 1H), 6.05 (s, 2H) ppm; **$^{13}C\{^1H\}$ NMR (75.5 MHz, $CDCl_3$):** δ 161.3, 156.0, 151.5, 151.3, 144.9, 135.8, 129.7, 129.0, 128.3, 113.0, 112.3, 104.5, 102.5, 98.7 ppm.

6,7–Methylendioxy–4–(4'–methylphenyl)–2H–chromen–2–one – 2b

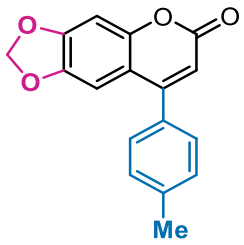

Compound **2b** was synthesized in lower scale from **1b** (0.1mmol), according to general conditions **A** and purified by column chromatography to afford 27.1 mg of the corresponding coumarin as a white solid (0.097 mmol, 97% yield).

^{1}H NMR (300MHz, $CDCl_3$): δ 7.35–7.27 (m, 4H), 6.88 (s, 1H), 6.86 (s, 1H), 6.21 (s, 2H), 6.04 (s, 2H), 2.44 (s, 3H) ppm; **$^{13}C\{^1H\}$ NMR (75.5 MHz, $CDCl_3$):** δ 161.4, 156.1, 151.5, 151.2, 144.9, 139.9, 132.9, 129.7, 128.3, 113.1, 112.1, 104.6, 102.5, 98.7, 21.5 ppm; **HRMS (ESI+):** calcd for $[M+H]^+ = C_{17}H_{13}O_4^+$: 281.0808 m/z. Found: 281.0878 m/z.

6,7–Methylendioxy–2H–chromen–2–one – 2c

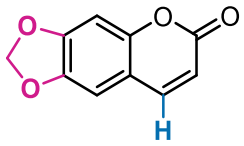

Compound **2c** was synthesized from **1c** according to general conditions **A** and purified by column chromatography (eluent DCM) to afford 80.6 mg of the corresponding coumarin as a white solid (0.42 mmol, 85% yield). Spectroscopic data were in agreement with previously reported ones.[36]

^{1}H NMR (300 MHz, $CDCl_3$): δ 7.58 (d, *J* = 9.5 Hz, 1H), 6.83 (s, 2H), 6.28 (d, *J* = 9.5 Hz, 1H), 6.07 (s, 2H) ppm; **$^{13}C\{^1H\}$ NMR (75.5 MHz, $CDCl_3$):** δ 161.3, 151.4, 151.4, 145.0, 143.6, 113.5, 112.8, 105.1, 102.4, 98.5 ppm.

6,7–Methylendioxy–4–methyl–2H–chromen–2–one – 2d

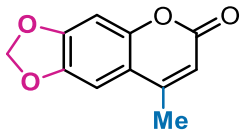

Compound **2d** was synthesized from **1d** according to general conditions **A** and purified by column chromatography (eluent DCM) to afford 95.3 mg of the corresponding coumarin as a white solid (0.47 mmol, 93% yield).

^{1}H NMR (400 MHz, $CDCl_3$): δ 6.92 (s, 1H), 6.77 (s, 1H), 6.12 (d, *J* = 0.8 Hz, 1H), 6.05 (s, 2H), 2.34 (d, *J* = 0.8 Hz, 3H) ppm; **$^{13}C\{^1H\}$ NMR (100.6**

MHz, $CDCl_3$): δ 161.3, 152.5, 151.0, 150.6, 145.0, 113.9, 112.3, 102.4, 102.2, 98.4, 19.2 ppm; **HRMS (ESI+):** calcd for $[M+H]^+$ = $C_{11}H_9O_4^+$: 205.0495 m/z. Found: 205.0538 m/z.

6,7–Methylendioxy–4–n–propyl–2H–chromen–2–one – 2e

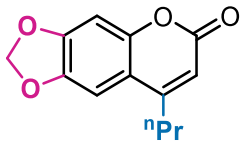

Compound **2e** was synthesized from **1e** according to general conditions **A** and purified by column chromatography (eluent EtOAc/Hex 1:4) to afford 115.2 mg of the corresponding coumarin as a brownish solid (0.5 mmol, 99% yield). Spectroscopic data were in agreement with previously reported ones.[54]

^{1}H NMR (300 MHz, $CDCl_3$): δ 6.97 (s, 1H), 6.81 (s, 1H), 6.13 (t, *J* = 0.8 Hz, 1H), 6.05 (s, 2H), 2,64 (td, *J* = 7.6, 0.8 Hz, 2H), 1.70 (ses, *J* = 7.6 Hz, 2H), 1.03 (t, *J* = 7.4 Hz, 3H) ppm; **^{13}C{^{1}H} NMR (75.5 MHz, $CDCl_3$):** δ 161.7, 156.4, 151.0, 151.0, 145.1, 113.3, 111.3, 102.4, 102.0, 98.7, 34.4, 21.5, 14.0 ppm.

5,6,7–Trimethoxy–4–phenyl–2H–chromen–2–one – 2g

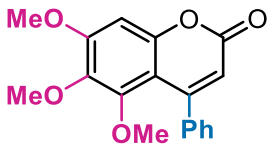

Compound **2g** was synthesized from **1g** according to general conditions **A** and purified by column chromatography (gradient EtOAc/Hex 1:5 to 1:2) to afford 139.2 mg of the corresponding coumarin as a yellow solid (0.45 mmol, 89% yield). Spectroscopic data were in agreement with previously reported ones.[16]

^{1}H NMR (300 MHz, $CDCl_3$): δ 7.49–7.36 (m, 3H),7.36–7.27 (m, 2H), 6.72 (s, 1H), 6.05 (s, 1H), 3.93 (s, 3H), 3.78 (s, 3H), 3.25 (s, 3H) ppm; **^{13}C{^{1}H} NMR (75.5 MHz, $CDCl_3$):** δ 160.7, 157.0, 155.5, 151.8, 151.2, 139.6, 139.1, 128.1, 127.6, 127.3, 114.2, 107.4, 96.4, 61.2, 61.0, 56.4 ppm.

5,6,7–Trimethoxy–2H–chromen–2–one – 2h

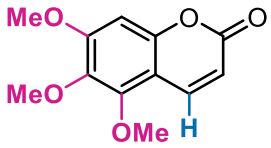

Compound **2h** was synthesized from **1h** according to general conditions **A** and purified by column chromatography (gradient EtOAc/Hex 1:5 to 1:2) to afford 108.6 mg of the corresponding coumarin as a yellow solid (0.46 mmol, 92% yield). Spectroscopic data were in agreement with previously reported ones.[55]

^{1}H NMR (300 MHz, $CDCl_3$): δ 7.92 (d, *J* = 9.6 Hz, 1H), 6.61 (s, 1H), 6.22 (d, *J* = 9.6Hz, 1H), 4.02 (s, 3H), 3.92 (s, 3H), 3.85 (s, 3H) ppm; **^{13}C{^{1}H} NMR (75.5 MHz, $CDCl_3$):** δ 161.4, 157.3, 151.6, 149.4, 139.0, 138.3, 112.6, 107.3, 95.7, 61.9, 61.4, 56.5 ppm.

5,6,7–Trimethyl–4–phenyl–2H–chromen–2–one – 2i

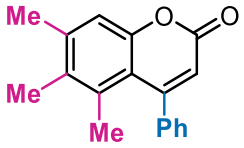

Compound **2i** was synthesized from **1i** according to general conditions **A** and purified by column chromatography (eluent EtOAc/Hex 1:4) to afford 113.3 mg of the corresponding coumarin as a dark yellow solid (0.43 mmol, 86% yield).

^{1}H NMR (300 MHz, $CDCl_3$): δ 7.48–7.41 (m, 3H), 7.34–7.27 (m, 2H), 7.11 (s, 1H), 6.21 (s, 1H), 2.39 (s, 3H), 2.15 (s, 3H), 1.76 (s, 3H) ppm; **^{13}C{^{1}H} NMR (75.5 MHz, $CDCl_3$):** δ 160.9, 156.9, 153.2, 141.5, 140.6, 135.3, 133.3, 128.9, 128.9, 127.3, 116.8, 116.6, 116.2, 21.5, 20.7, 15.9 ppm; **HRMS (ESI+):** calcd for $[M+H]^+ = C_{18}H_{17}O_2^+$: 265.1223 m/z. Found: 265.1249 m/z.

4–Phenyl–2H–chromen–2–one – 2j

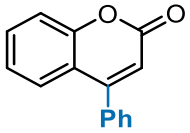

Compound **2j** was synthesized from **1j** according to general conditions **B** ($IPrAuNTf_2$ was employed as the catalyst) and purified by column chromatography (eluent EtOAc/Hex 1:8) to afford 100.3 mg of the corresponding coumarin as a white solid (0.45 mmol, 90% yield). Spectroscopic data were in agreement with previously reported ones.[23]

^{1}H NMR (300 MHz, $CDCl_3$): δ 7.58–7.40 (m, 8H), 7.26–7.21 (m, 1H), 6.37 (s, 1H) ppm; **$^{13}C\{^1H\}$ NMR (75.5 MHz, $CDCl_3$):** δ 160.8, 155.8, 154.3, 135.3, 132.0, 129.8, 129.0, 128.5, 127.1, 124.3, 119.1, 117.4, 115.3 ppm.

7–Tert–butyl–4–phenyl–2H–chromen–2–one – 2k

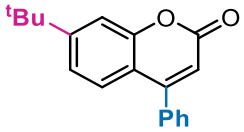

Compound **2k** was synthesized from **1k** according to general conditions **B** ($IPrAuNTf_2$ was employed as the catalyst) and purified by column chromatography (eluent EtOAc/Hex 1:8) to afford 113.9 mg of the corresponding coumarin as a viscous whitish oil (0.41 mmol, 82% yield). Spectroscopic data were in agreement with previously reported ones.[53]

^{1}H NMR (400 MHz, $CDCl_3$): δ 7.54–7.49 (m, 3H), 7.44–7.40 (m, 4H), 7.28–7.25 (m, 1H), 6.32 (s, 1H), 1.35 (s, 9H) ppm; **$^{13}C\{^1H\}$ NMR (100.6 MHz, $CDCl_3$):** δ 161.3, 156.6, 155.6, 154.4, 135.5, 129.7, 128.9, 128.5, 126.6, 121.8, 116.6, 114.3, 114.2, 35.3, 31.1 ppm.

4,6–Di–phenyl–2H–chromen–2–one – 2m

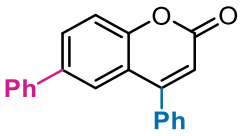

Compound **2m** was synthesized from **1m** according to general conditions **B** (ImPyAuCl was employed as the catalyst) and purified by column chromatography (eluent EtOAc/Hex 1:5) to afford 115.4 mg of the corresponding coumarin as a white solid (0.39 mmol, 77% yield). Spectroscopic data were in agreement with previously reported ones.[56]

^{1}H NMR (300 MHz, $CDCl_3$): δ 7.75 (dd, *J* = 8.6, 2.2 Hz, 1H), 7.66 (d, *J* = 2.2 Hz, 1H), 7.58–7.58 (m, 3H), 7.58–7.45 (m, 5H), 7.45–7.39 (m, 2H), 7.39–7.31 (m, 1H), 6.40 (s, 1H) ppm; **$^{13}C\{^1H\}$ NMR (75.5 MHz, $CDCl_3$):** δ 160.8, 155.8, 153.8, 139.8, 137.7, 135.3, 131.0, 129.9, 129.1, 129.1, 128.6, 127.8, 127.2, 125.4, 119.3, 117.9, 115.7 ppm.

6–Bromo–4–phenyl–2H–chromen–2–one – 2n

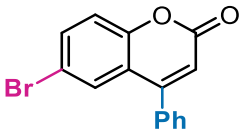

Compound **2n** was synthesized from **1n** according to general conditions **B** (ImPyAuCl was employed as the catalyst) and purified by column chromatography (eluent EtOAc/Hex 1:10) to afford 77.9 mg of the corresponding coumarin as a white solid (0.26 mmol, 52% yield). Spectroscopic data were in agreement with previously reported ones.[23]

^{1}H NMR (300 MHz, $CDCl_3$): δ 7.59–7.66 (m, 2H), 7.55–7.57 (m, 3H), 7.43–7.45 (m, 2H), 7.30 (d, *J* = 8.8 Hz, 1H), 6.41 (s, 1H) ppm; **$^{13}C\{^1H\}$ NMR (75.5 MHz, $CDCl_3$):** δ 160.0, 154.6, 153.2, 134.8, 134.6, 130.1, 129.5, 129.2, 128.4, 120.8, 119.2, 117.1, 116.2 ppm.

2.1.5. References

[1] J. R. S. Hoult, M. Payá, "Pharmacological and biochemical actions of simple coumarins: Natural products with therapeutic potential" *General Pharmacology: The Vascular System* **1996**, *27*, 713–722.

[2] K. Fylaktakidou, D. Hadjipavlou-Litina, K. Litinas, D. Nicolaides, "Natural and Synthetic Coumarin Derivatives with Anti-Inflammatory / Antioxidant Activities" *CPD* **2004**, *10*, 3813–3833.

[3] K. Kaur, M. Jain, T. Kaur, R. Jain, "Antimalarials from nature" *Bioorganic & Medicinal Chemistry* **2009**, *17*, 3229–3256.

[4] K. N. Venugopala, V. Rashmi, B. Odhav, "Review on Natural Coumarin Lead Compounds for Their Pharmacological Activity" *BioMed Research International* **2013**, *2013*, 1–14.

[5] E. Paenurk, K. Kaupmees, D. Himmel, A. Kütt, I. Kaljurand, I. A. Koppel, I. Krossing, I. Leito, "A unified view to Brønsted acidity scales: do we need solvated protons?" *Chem. Sci.* **2017**, *8*, 6964–6973.

[6] S. C. Heghes, O. Vostinaru, C. Mogosan, D. Miere, C. A. Iuga, L. Filip, "Safety Profile of Nutraceuticals Rich in Coumarins: An Update" *Front. Pharmacol.* **2022**, *13*, 803338.

[7] A. Thakur, R. Singla, V. Jaitak, "Coumarins as anticancer agents: A review on synthetic strategies, mechanism of action and SAR studies" *European Journal of Medicinal Chemistry* **2015**, *101*, 476–495.

[8] W. Pu, Y. Lin, J. Zhang, F. Wang, C. Wang, G. Zhang, "3-Arylcoumarins: Synthesis and potent anti-inflammatory activity" *Bioorganic & Medicinal Chemistry Letters* **2014**, *24*, 5432–5434.

[9] J. Grover, S. M. Jachak, "Coumarins as privileged scaffold for anti-inflammatory drug development" *RSC Adv.* **2015**, *5*, 38892–38905.

[10] M. K. Kathiravan, A. B. Salake, A. S. Chothe, P. B. Dudhe, R. P. Watode, M. S. Mukta, S. Gadhwe, "The biology and chemistry of antifungal agents: A review" *Bioorganic & Medicinal Chemistry* **2012**, *20*, 5678–5698.

[11] B. Wagner, "The Use of Coumarins as Environmentally-Sensitive Fluorescent Probes of Heterogeneous Inclusion Systems" *Molecules* **2009**, *14*, 210–237.

[12] X. Liu, J. M. Cole, P. G. Waddell, T.-C. Lin, S. McKechnie, "Molecular Origins of Optoelectronic Properties in Coumarins 343, 314T, 445, and 522B" *J. Phys. Chem. C* **2013**, *117*, 14130–14141.

[13] C. Hua, K. Zhang, M. Xin, T. Ying, J. Gao, J. Jia, Y. Li, "High quantum yield and pH sensitive fluorescence dyes based on coumarin derivatives: fluorescence characteristics and theoretical study" *RSC Adv.* **2016**, *6*, 49221–49227.

[14] A. Kumar, R. Baccoli, A. Fais, A. Cincotti, L. Pilia, G. Gatto, "Substitution Effects on the Optoelectronic Properties of Coumarin Derivatives" *Applied Sciences* **2020**, *10*, 144.

[15] K. Szwaczko, "Coumarins Synthesis and Transformation via C–H Bond Activation—A Review" *Inorganics* **2022**, *10*, 23.

[16] C. Jia, D. Piao, T. Kitamura, Y. Fujiwara, "New Method for Preparation of Coumarins and Quinolinones via Pd-Catalyzed Intramolecular Hydroarylation of C−C Triple Bonds" *J. Org. Chem.* **2000**, *65*, 7516–7522.

[17] R. Li, S. R. Wang, W. Lu, "$FeCl_3$ -Catalyzed Alkenylation of Simple Arenes with Aryl-Substituted Alkynes" *Org. Lett.* **2007**, *9*, 2219–2222.

[18] A. Carral-Menoyo, A. Misol, M. Gómez-Redondo, N. Sotomayor, E. Lete, "Palladium(II)-Catalyzed Intramolecular C–H Alkenylation for the Synthesis of Chromanes" *J. Org. Chem.* **2019**, *84*, 2048–2060.

[19] O. Zaitceva, V. Bénéteau, D. S. Ryabukhin, I. I. Eliseev, M. A. Kinzhalov, B. Louis, A. V. Vasilyev, P. Pale, "Cyclization of aryl 3-aryl propynoates into 4-arylcoumarins catalyzed by cyclometalated Platinum(II) complexes" *Tetrahedron* **2020**, *76*, 131029.

[20] V. Ortiz-de-Elguea, A. Carral-Menoyo, L. Simón-Vidal, M. Martinez-Nunes, I. Barbolla, M. G. Lete, N. Sotomayor, E. Lete, "Pd(II)-Catalyzed Fujiwara–Moritani Reactions for the Synthesis and Functionalization of Substituted Coumarins" *ACS Omega* **2021**, *6*, 29483–29494.

[21] C. C. Chintawar, A. K. Yadav, A. Kumar, S. P. Sancheti, N. T. Patil, "Divergent Gold Catalysis: Unlocking Molecular Diversity through Catalyst Control" *Chem. Rev.* **2021**, *121*, 8478–8558.

[22] D. Campeau, D. F. León Rayo, A. Mansour, K. Muratov, F. Gagosz, "Gold-Catalyzed Reactions of Specially Activated Alkynes, Allenes, and Alkenes" *Chem. Rev.* **2021**, *121*, 8756–8867.

[23] Z. Shi, C. He, "Efficient Functionalization of Aromatic C−H Bonds Catalyzed by Gold(III) under Mild and Solvent-Free Conditions" *J. Org. Chem.* **2004**, *69*, 3669–3671.

[24] H. A. Wegner, S. Ahles, M. Neuburger, "A New Gold-Catalyzed Domino Cyclization and Oxidative Coupling Reaction" *Chemistry A European J* **2008**, *14*, 11310–11313.

[25] X. Huo, X. Ren, Y. Xu, X. Li, X. She, X. Pan, "Enantioselective total synthesis of hydramicromelin B" *Tetrahedron: Asymmetry* **2008**, *19*, 343–347.

[26] R. S. Menon, A. D. Findlay, A. C. Bissember, M. G. Banwell, "The Au(I)-Catalyzed Intramolecular Hydroarylation of Terminal Alkynes Under Mild Conditions: Application to the Synthesis of 2*H*-Chromenes, Coumarins, Benzofurans, and Dihydroquinolines" *J. Org. Chem.* **2009**, *74*, 8901–8903.

[27] J. H. Do, H. N. Kim, J. Yoon, J. S. Kim, H.-J. Kim, "A Rationally Designed Fluorescence Turn-On Probe for the Gold(III) Ion" *Org. Lett.* **2010**, *12*, 932–934.

[28] T. Shibuya, K. Nakamura, K. Tanaka, "Cationic gold(I) axially chiral biaryl bisphosphine complex-catalyzed atropselective synthesis of heterobiaryls" *Beilstein J. Org. Chem.* **2011**, *7*, 944–950.

[29] P. A. Vadola, D. Sames, "Catalytic Coupling of Arene C–H Bonds and Alkynes for the Synthesis of Coumarins: Substrate Scope and Application to the Development of Neuroimaging Agents" *J. Org. Chem.* **2012**, *77*, 7804–7814.

[30] A. C. Shaikh, S. Shalini, R. Vaidhyanathan, M. V. Mane, A. K. Barui, C. R. Patra, Y. Venkatesh, P. R. Bangal, N. T. Patil, "Identifying Solid Luminogens through Gold-Catalysed Intramolecular Hydroarylation of Alkynes" *Eur J Org Chem* **2015**, *2015*, 4860–4867.

[31] K. Usui, K. Yamamoto, Y. Ueno, K. Igawa, R. Hagihara, T. Masuda, A. Ojida, S. Karasawa, K. Tomooka, G. Hirai, H. Suemune, "Internal-Edge-Substituted Coumarin-Fused [6]Helicenes:

Asymmetric Synthesis, Structural Features, and Control of Self-Assembly" *Chemistry A European J* **2018**, *24*, 14617–14621.

[32] M.-L. Delcourt, C. Reynaud, S. Turcaud, L. Favereau, J. Crassous, L. Micouin, E. Benedetti, "3D Coumarin Systems Based on [2.2]Paracyclophane: Synthesis, Spectroscopic Characterization, and Chiroptical Properties" *J. Org. Chem.* **2019**, *84*, 888–899.

[33] X. Zhu, G. Xu, L. Chamoreau, Y. Zhang, V. Mouriès-Mansuy, L. Fensterbank, O. Bistri-Aslanoff, S. Roland, M. Sollogoub, "Permethylated NHC-Capped α- and β-Cyclodextrins (ICyD ^{Me}) Regioselective and Enantioselective Gold-Catalysis in Pure Water" *Chemistry A European J* **2020**, *26*, 15901–15909.

[34] C. C. James, D. Wu, E. O. Bobylev, A. Kros, B. De Bruin, J. N. H. Reek, "Protection of a Gold Catalyst by a Supramolecular Cage Improves Bioorthogonality" *ChemCatChem* **2022**, *14*, e202200942.

[35] J. Brom, A. Maruani, S. Turcaud, S. Lajnef, F. Peyrot, L. Micouin, E. Benedetti, "[2.2]Paracyclophane-based coumarins: effective organo-photocatalysts for light-induced desulfonylation processes" *Org. Biomol. Chem.* **2024**, *22*, 59–64.

[36] A. Cervi, Y. Vo, C. L. L. Chai, M. G. Banwell, P. Lan, A. C. Willis, "Gold(I)-Catalyzed Intramolecular Hydroarylation of Phenol-Derived Propiolates and Certain Related Ethers as a Route to Selectively Functionalized Coumarins and 2 *H* -Chromenes" *J. Org. Chem.* **2021**, *86*, 178–198.

[37] M. Kumar, G. B. Hammond, B. Xu, "Cationic Gold Catalyst Poisoning and Reactivation" *Org. Lett.* **2014**, *16*, 3452–3455.

[38] Z. Lu, T. Li, S. R. Mudshinge, B. Xu, G. B. Hammond, "Optimization of Catalysts and Conditions in Gold(I) Catalysis—Counterion and Additive Effects" *Chem. Rev.* **2021**, *121*, 8452–8477.

[39] A. Kumar, N. T. Patil, "Ligand-Enabled Sustainable Gold Catalysis" *ACS Sustainable Chem. Eng.* **2022**, *10*, 6900–6918.

[40] D. Malhotra, M. S. Mashuta, G. B. Hammond, B. Xu, "A Highly Efficient and Broadly Applicable Cationic Gold Catalyst" *Angew Chem Int Ed* **2014**, *53*, 4456–4459.

[41] C. Tubaro, M. Baron, A. Biffis, M. Basato, "Alkyne hydroarylation with Au N-heterocyclic carbene catalysts" *Beilstein J. Org. Chem.* **2013**, *9*, 246–253.

[42] M. Baron, A. Biffis, "Gold(I) Complexes in Ionic Liquids: An Efficient Catalytic System for the C-H Functionalization of Arenes and Heteroarenes under Mild Conditions" *Eur. J. Org. Chem.* **2019**, *2019*, 3687–3693.

[43] S. J. Pike, J. J. Hutchinson, C. A. Hunter, "H-Bond Acceptor Parameters for Anions" *J. Am. Chem. Soc.* **2017**, *139*, 6700–6706.

[44] D. Yalcin, I. D. Welsh, E. L. Matthewman, S. P. Jun, M. Mckeever-Willis, I. Gritcan, T. L. Greaves, C. C. Weber, "Structural investigations of molecular solutes within nanostructured ionic liquids" *Phys. Chem. Chem. Phys.* **2020**, *22*, 11593–11608.

[45] D. Weber, M. A. Tarselli, M. R. Gagné, "Mechanistic Surprises in the Gold(I)-Catalyzed Intramolecular Hydroarylation of Allenes" *Angew. Chem. Int. Ed.* **2009**, *48*, 5733–5736.

[46] D. Weber, M. R. Gagné, "σ–π-Diauration as an alternative binding mode for digold intermediates in gold(ı) catalysis" *Chem. Sci.* **2013**, *4*, 335–338.

[47] R. Pedrazzani, A. Pintus, R. De Ventura, M. Marchini, P. Ceroni, C. Silva López, M. Monari, M. Bandini, "Boosting Gold(I) Catalysis via Weak Interactions: New Fine-Tunable Impy Ligands" *ACS Org. Inorg. Au* **2022**, *2*, 229–235.

[48] R. Pedrazzani, S. Kiriakidi, M. Monari, I. Lazzarini, G. Bertuzzi, C. S. López, M. Bandini, "Fluorinated Biphenyl Phosphine Ligands for Accelerated [Au(I)]-Catalysis" *ACS Catal.* **2024**, *14*, 6128–6136.

[49] H. Li, S. Liu, Y. Huang, X.-H. Xu, F.-L. Qing, "Tandem trifluoromethylthiolation/aryl migration of aryl alkynoates to trifluoromethylthiolated alkenes" *Chem. Commun.* **2017**, *53*, 10136–10139.

[50] A. Mathuri, B. Pal, M. Pramanik, P. Mal, "Chemodivergent Chalcogenation of Aryl Alkynoates or *N* -Arylpropynamides Using 9-Mesityl-10-Methylacridinium Perchlorate Photocatalyst" *J. Org. Chem.* **2023**, *88*, 10096–10110.

[51] M. Roy, R. Jamatia, A. Samanta, K. Mohar, D. Srimani, "Change in the Product Selectivity in the Visible Light-Induced Selenium Radical-Mediated 1,4-Aryl Migration Process" *Org. Lett.* **2022**, *24*, 8180–8185.

[52] S. Sau, P. Mal, "3-Nitro-coumarin synthesis *via* nitrative cyclization of aryl alkynoates using *tert* -butyl nitrite" *Chem. Commun.* **2021**, *57*, 9228–9231.

[53] Z. Wang, X. Li, L. Wang, P. Li, "Photoinduced cyclization of alkynoates to coumarins with N-Iodosuccinimide as a free-radical initiator under ambient and metal-free conditions" *Tetrahedron* **2019**, *75*, 1044–1051.

[54] M. D. P. Olaya, N. E. Vergel, J. L. López, D. Viña, M. F. Guerrero, "8-Propyl-6H-[1,3]dioxolo[4,5-g]chromen-6-one: A new coumarin with monoamine oxidase B inhibitory activity and possible anti-parkinsonian effects" *Braz. J. Pharm. Sci.* **2020**, *56*, e17609.

[55] C. Schultze, B. Schmidt, "Prenylcoumarins in One or Two Steps by a Microwave-Promoted Tandem Claisen Rearrangement/Wittig Olefination/Cyclization Sequence" *J. Org. Chem.* **2018**, *83*, 5210–5224.

[56] D. Kim, M. Min, S. Hong, "One-pot catalysis of dehydrogenation of cyclohexanones to phenols and oxidative Heck coupling: expedient synthesis of coumarins" *Chem. Commun.* **2013**, *49*, 4021.

2.2. Toward an intermolecular approach: the intermolecular synthesis of coumarins

2.2.1. Introduction

Coumarins have already been presented in the previous chapter as a synthetic target of interest for the properties imparted by their precise chromen–2–one structure,[1] such as luminescence (fluorescent labels/probes)[2,3] and bioactivity (active pharmaceutical ingredients/pesticides).[4–7] A gold(I)–mediated intramolecular approach was presented as an effective and easy–to–use strategy to yield these molecules at low tenors of gold. However, a pre–esterification step was necessary in order to produce the aryl alkynoates that were successfully employed in the cyclization reaction. A direct approach to enclose both the aromatic ring and the alkyne would be even more suited in terms of simplicity and economic advantages (only one purification is needed).

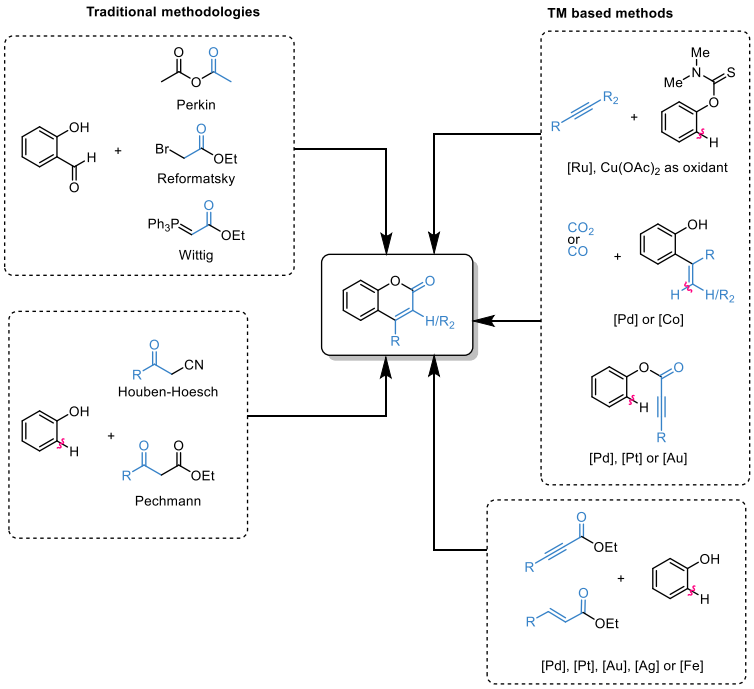

Figure 2.4 *– Proposed synthetic strategies for the preparation of coumarins.*

Most intermolecular approaches proposed to date rely on classic organic reactions, such as Pechmann, Knoevenagel, Perkin, Reformatsky, or Wittig reactions (***Figure* 2.4**, left).[8,9] These methods often require harsh conditions, produce significant waste, and afford only moderate yields. More recently developed strategies, which exploit transition metal chemistry, have shown

promising improvements in this regards (***Figure* 2.4**, right).[9] Many of these approaches involve cyclization of aromatic precursors with unsaturated side chains (***Figure* 2.4**, upper right)[9–16] or, in general, prior installation of specific functional groups at aromatic substrates, such as 2–halosubstituted phenols, which are suitable for coupling reactions.[17–19] Simpler strategies involve the direct C–H functionalization of phenols, through oxidative Heck–type reactions[20–24] or direct alkyne hydroarylation[25–27] followed by intramolecular esterification (***Figure* 2.4**, lower right), however current protocols exhibit limited catalytic efficiencies for an application.

Taking advantage from our previous experience on gold–catalysed hydroarylation reactions,[28] we have proposed a system, based on gold(I) complexes in ionic liquids as catalysts, featuring high activity in the intermolecular hydroarylation of alkynoic acids and esters with activated arenes under mild conditions. Key to success was the use of a small molar amount (comparable to the reagents) of a suitable ionic liquid as reaction promoter, which enabled efficient reaction using one order of magnitude less gold catalyst compared to conventional organic solvents.[29,30]

2.2.2. Results and Discussion

As outlined above, gold(I)–catalyzed hydroarylation of propiolic acids/esters with *para* and/or *meta* substituted phenols allows to yield the *Z*–o–vinyl derivative with precise regio– and stereoselectivities. While the regioselectivity is governed by the substituents on the alkyne, the Z configuration of the double bond arises from anti-addition of the nucleophile to the alkyne, consistent with a Friedel–Crafts-like electrophilic substitution at the phenol by the activated, π-coordinated alkyne adduct (outer-sphere mechanism).[31,32] The resulting *Z*–*o*–coumaric acid/ester derivative has the exact stereochemistry to allow an intramolecular (trans)esterification (lactonization) to the final coumarin product. Preliminary investigations on the reaction were carried out using as model synthesis the reaction between sesamol **1** and ethyl phenylpropiolate **2** (***Figure* 2.5**).

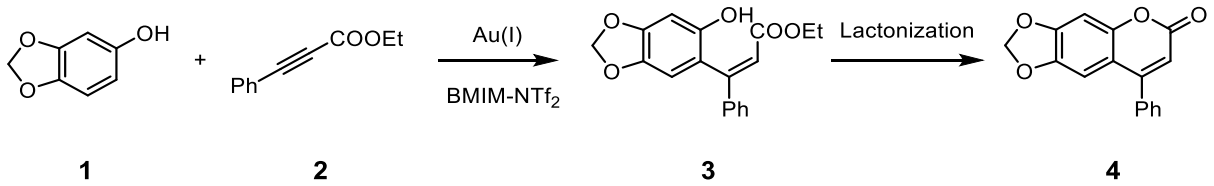

Figure 2.5 *– Coumarin synthesis used for process optimization*

The reaction was carried out at room temperature with only 0.5 mol% of the commercial gold precatalyst IPrAuCl (IPr = 1,3–bis–(2,6–diisopropylphenyl)–imidazol–2–ylidene) plus 0.5 mol% $AgSbF_6$ as an activator to remove the chlorido ligand from the gold coordination sphere and a small amount of the ionic liquid [BMIM][NTf_2], according to the synthetic protocol we previously developed.[29] Traces of coumarin **4** were recorded in the reaction mixture after one hour reaction time (***Figure* 2.6**) while the main observed product was however the corresponding coumaric ester **3**, which accumulates in solution since the cyclization (transesterification) step is slower than hydroarylation. This experimental proof underlines the intermolecular nature of the hydroarylation step. The molar fraction of **3** started to decrease only at long reaction times, whereas the molar fraction of **4** continuously increased. From the reported data, it can be also appreciated that the overall sesamol conversion almost stops at long reaction times, indicating deactivation of the catalytic system. On the other hand, conversion of **3** to **4** continues with time, suggesting that gold catalysis is not necessary for this step. Indeed, an increase in the reaction temperature to 60°C after 48 hours of reaction causes the complete conversion of **3** to **4** without increasing the sesamol conversion. This evidence supports that the lactonization process can be thermally activated rather than activated by gold(I).

Control tests confirmed that no reaction was taking place in absence of the gold catalyst, either at room temperature or at 60 °C. The ionic liquid alone or the ionic liquid with added $AgSbF_6$ was as well ineffective in promoting the reaction. To finally exclude a “silver effect” (i.e. an active role of the introducet silver(I) centers in the catalytic event, we also tested the pre–activated complex IPrAuNTf_2, which delivered results that were fully comparable to the IPrAuCl + $AgSbF_6$ system.

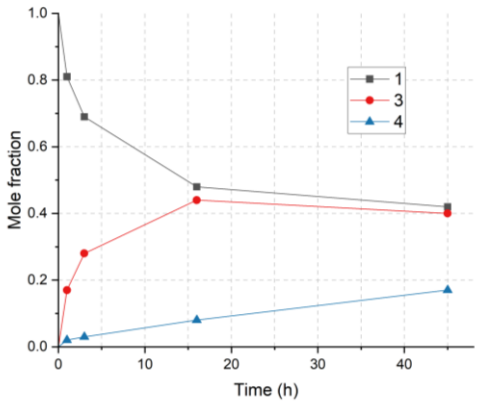

Figure 2.6 *– Composition of the reaction mixture with time for the reaction depicted in* ***Figure 2.5****. Reaction conditions: 2.5 mmol sesamol, 2.5 mmol ethyl phenylpropiolate, 0.012 mmol IPrAuCl, 0.012 mmol $AgSbF_6$, 0.75 mL BMIM–NTf_2, room temperature.*

Screening of the optimal reaction conditions gave further insight about mechanistic aspects of the reaction. The role of the ligand was first interrogated (selected results are summarized in ***Table 2.3***). The tests were performed at 40°C to better evaluate the differences in activity; quantitative conversion of **3** to **4** was accessed upon thermal treatment (60°C, ^{1}H NMR monitoring). Both pre–activated complexes bearing the anion ligand NTf_2^- or *in situ* activated chlorido complexes were employed ($AgSbF_6$ as scavenger).

In our previous contributions dealing with direct alkyne hydroarylations using simple arenes as substrates,[29] we recorded maximum activity with complexes bearing a neutral ligand L with comparatively low electron–donating properties. This is in line with a reaction mechanism in which the rate determining step is the Friedel–Crafts–like electrophilic attack on the arene by the alkyne π–coordinated to the gold(I) centre.[31,32] The best choice in that case was the one to compromise a high electrophilic character at the gold metal centre (low donating character of the ligand), and an appreciable robustness to ensure good catalytic turnovers. In the present context of sesamol **1** as nucleophilic substrate, the reaction rate was found to increase accordingly to a higher electron–donating character of the ligand at gold. Tested complexes with poorly donating ligands (e.g. triphenylphosphine and its fluorinated variant) were ineffective and this phenomenon is to attribute to the low stability of the complex in solution. It is also possible that the excess of phenol in solution may render hasher the reaction condition for the cationic complex, triggering decomposition pathways by reduction of the metal centre to form colloidal gold (rapid formation observed in solution). On the other hand, the Buchwald–type phosphine tBuXphos could successfully promote the reaction, achieving the same performance achieved with the preformed $tBu_3PAuNTf_2$ catalyst. The presence of alkyl substituents and the pendant biphenyl ring helps to stabilize the competent active species in solution. Finally, the IPr carbene ligand was found to be the best ligand both in term of catalytic activity and stability of the cationic complex. This suggests that with electron–rich, nucleophilic arenes such as sesamol, the rate determining step of the process is likely to be the protonolysis of the neutral gold–vinyl species, formed after deprotonation of the Wheland–type intermediate.[31,32] We previously recorded a similar behaviour with some electron–rich heterocycles as well.[29]

Analysis of the influence of the reaction temperature on the performance could further address the importance of the catalyst stability in solution (***Figure* 2.7**). Increasing temperature leads to increased reaction rates and yield up to 60°C. However, at temperatures above 60°C a worse performance was recorded, probably because of catalyst decomposition. Again, for higher

temperature the cyclization rate was observed to increase, favouring the formation of **4** rather than accumulation of the vinylated product **3**.

***Table 2.3**. Reactivity of different gold(I) complexes as catalysts for the reaction reported in **Figure 2.5**.*

Catalyst	Reaction time (h)	Conversion of **1** (%)	Yield of **4** (%)
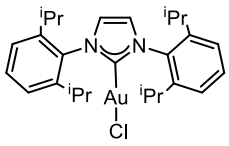	1	29	5
	3	38	15
	24	61	32
$tBu_3PAuNTf_2$	1	33	4
	3	34	13
	24	48	29
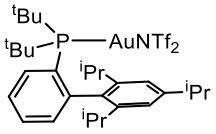	1	30	4
	3	36	11
	24	48	29
Ph_3PAuCl	24	2	1
$(m–F–Ph)_3PAuCl$	24	2	1

Reaction conditions: 2.5 mmol sesamol, 2.5 mmol ethyl phenylpropiolate, 0.012 mmol Au complex, 0.012 mmol $AgSbF_6$ (only in the case of Cl–containing Au complexes) 0.75 mL BMIM–NTf_2, 40°C.

We then started to evaluate the catalytic performance of our system with other substrates. We first targeted the reaction scope with respect to ethyl phenylpropiolate and differently substituted phenols. Tri–substituted phenols bearing electron–donating groups such as 3,4,5–trimethylphenol or 3,4,5–trimethoxyphenol showed analogous reactivity to sesamol. Substrate conversions are faster, since these phenols are more activated towards aromatic electrophilic substitutions, but the presence of two *meta* substituents results in a slower ring–closing process. Indeed, this open intermediate rapidly accumulates in solution and a simple temperature increase is in this case not sufficient to trigger its further conversion. The addition of an acid cocatalyst is needed in order to

speed up its cyclization to coumarin (***Table 2.4***). Conversely, *m*–monosubstituted phenols provided poor conversions (entries 4 and 5), and high selectivity toward the vinyl product at *ortho* positions (no traces of the 4–vinyl adduct were observed). Finally, only traces of product are obtained with a *p*–monosubstituted phenol (entry 6), since in this case, the substituent does not significantly contribute to the activation of the *o*–positions of the ring.

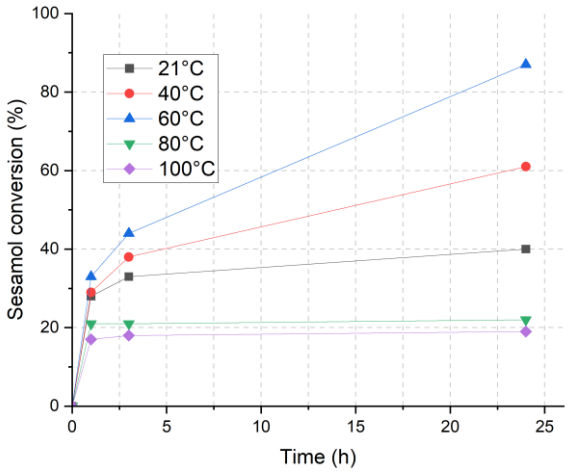

Figure 2.7 *– Effect of temperature on the conversion curve of sesamol in the reaction depicted in* ***Figure 2.5****. Reaction conditions: 2.5 mmol sesamol, 2.5 mmol ethyl phenylpropiolate, 0.012 mmol IPrAuCl, 0.012 mmol* $AgSbF_6$*, 0.75 mL BMIM–*NTf_2*, room temperature.*

Table 2.4*. Reactivity of different phenols with ethyl phenylpropiolate.*

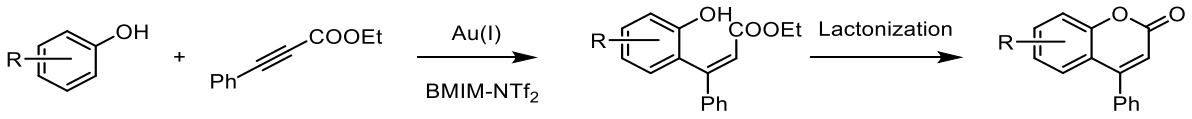

Entry	Phenol	Time (h)	Phenol conversion (%)	Coumaric ester yield (%)	Coumarin yield(%)
1	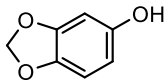	1	29	24	5
		3	48	33	15
		24	61	29	32

2	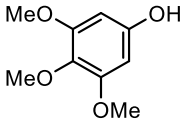	1	68	64	4
		3	72	67	5
		24	76	66	10
		24[a]	78	0	78
3	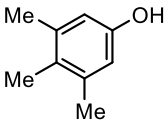	1	72	72	0
		3	77	75	2
		24	81	65	16
		24[a]	89	0	89
4	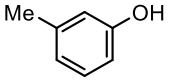	24[a]	11	0	11
5	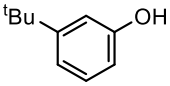	24[a]	13	0	13
6	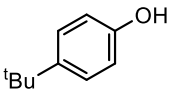	24	<5	0	traces

Reaction conditions: 2.5 mmol phenol, 2.5 mmol ethyl phenylpropiolate, 0.012 mmol IPrAuCl, 0.012 mmol $AgSbF_6$, 0.75 mL BMIM–NTf_2, 40°C. [a] 0.1 eq. HBF_4 were added to the system after 1 hour reaction time.

Different alkyne substrates also exhibited a range of reactivities (**Table 2.5**). Use of phenylpropiolic acid instead of ethyl phenylpropiolate resulted in somewhat faster reaction (entry 2) due to the fact that the acidity of the free carboxylic acid moiety may facilitate the protonolysis of the vinyl intermediate. The subsequent cyclization step (intramolecular Fischer–esterification) is also facilitated, leading to a minor accumulation of open type–**3** product. As a drawback, the use of the free carboxylic acid allows formation of decarboxylation products under reaction conditions: in particular, phenylacetylene was detected in relevant quantities (20% of by–product detected by ^{1}H NMR). This process was demonstrated to be promoted by the same gold complex, and no decarboxylation could be observed in the absence of the gold catalyst. As second issue, the use of an alkynoic acid as reagent leads to the accumulation of water as co–product from the esterification process, which is in competition with the phenol as nucleophile. We ultimately found

that adding an acid cocatalyst (10 mol%) and using 4 Å molecular sieves improved both catalytic activity and selectivity toward the alkyne (entry 3). The additional proton source facilitates the protonolysis step, which is likely the rate-determining step of our process, while also accelerating addition of water to the triple bond. Application of these reaction conditions allowed to reach comparable catalytic performance using only 0.1 mol% gold catalyst (entry 4). Furthermore, the reaction could be extended to aliphatic alkynoic acids, although in this case the activity was lower, given the lower reactivity of the triple bond (entry 5).

Table 2.5 – Reactivity of different alkynes with sesamol.

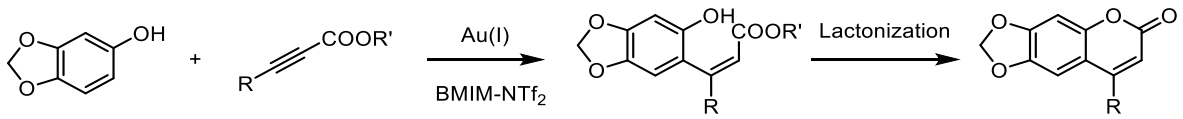

Entry	Alkyne	[Au] mol%	Time (h)	Sesamol conversion (%)	Coumarin yield (%)
1	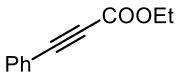	0.5	1	29	5
			3	38	15
			24	61	32
2	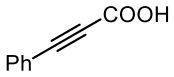	0.5	1	39	37
			3	43	40
			24	69	60
3[a]	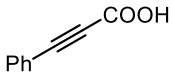	0.5	1	13	13
			3	28	28
			24	72	72
4[a]	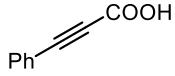	0.1	1	12	12
			3	23	23
			24	64	64

5[a]	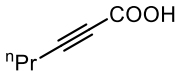	0.1	3 24	– 36	Traces 34
6	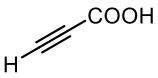	0.5	1 3	96 100	42 52
7[b]	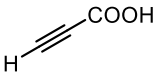	0.5	3	81	81
8[b]	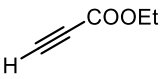	0.5	1	100	58

Reaction conditions: 2.5 mmol sesamol, 2.5 mmol alkyne, 0.012 mmol IPrAuCl, 0.012 mmol $AgSbF_6$, 0.75 mL BMIM–NTf_2, 40°C. [a] 0.1 eq. HBF_4 and 4Å molecular sieves were added to the system; [b] Reaction conditions: 2.5 mmol sesamol, 12.5 mmol alkyne, 0.1 eq. HBF_4, 0.012 mmol IPrAuCl, 0.012 mmol $AgSbF_6$, 0.75 mL BMIM–NTf_2, 25°C.

Unsubstituted propiolic acid was instead much more reactive in the process (entry 6), as it is commonly the case in transition metal catalyzed direct alkyne hydroarylations,[28] and allowed complete substrate conversion in very short reaction times. On the other hand, the higher reactivity of the unsaturated substrate resulted in some selectivity issues with formation of more complex products stemming from double hydroarylation of the alkyne (***Figure* 2.8**). Ethyl propiolate showed analogous behavior, with the only difference that the hydroarylation and especially the cyclization of the doubly hydroarylated product were much slower, so that the open intermediate accumulated as main reaction byproduct.

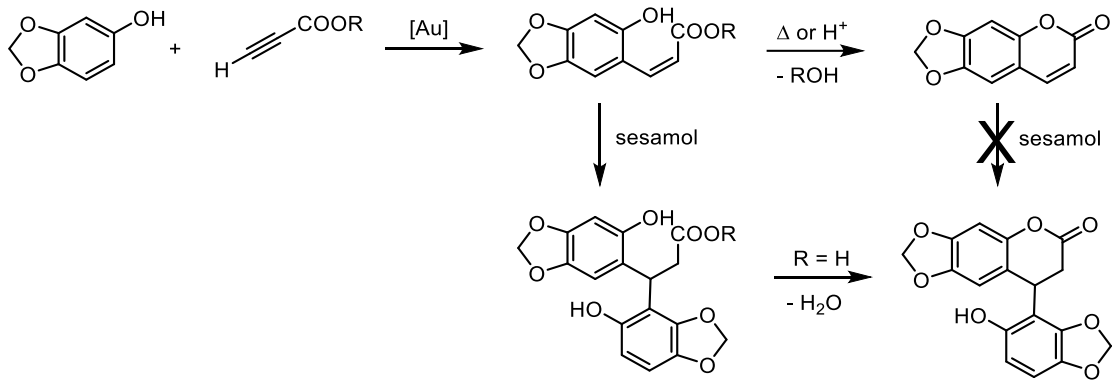

Figure 2.8 *– Sesamol hydroarylation with terminal alkynes and subsequent reactions.*

The secondary product was quickly identified as originating from a formal hydroarylation at the α,β–unsaturated bond of the coumarin. Such double–bond hydroarylation was previously reported as a side reaction with highly electron–rich heteroaromatic substrates,[29] and in our case it could occur either at the intermediate coumaric acid or at the final coumarin product. Control experiments demonstrated that the isolated coumarin cannot undergo further reaction with sesamol to give the secondary product, regardless of whether the alkyne is present, under the standard conditions (***Figure* 2.9**).

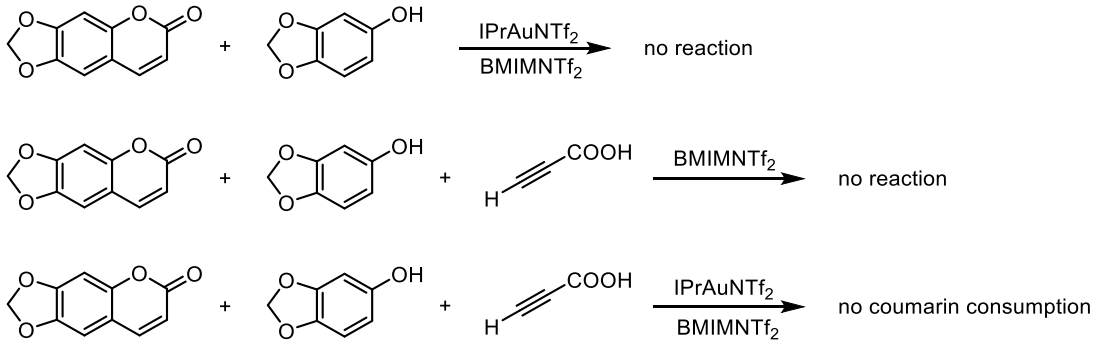

Figure 2.9. *Reactivity of coumarin towards further hydroarylation under reaction conditions.*

We established that the secondary product originates from alkene hydroarylation of the open type–**3** intermediate, by addition of a second phenol molecule, followed by lactonization. This insight enabled us to design an optimized protocol that suppresses the formation of such di–hydroarylation product. In particular, employing an excess of alkyne was found to accelerate the formation of the analogous coumarin, while increasing the competition of the open vinyl–intermediate for coordination at the metal center. In addition, lowering the reaction temperature and introducing 0.1 equiv. of HBF_4 as a cocatalyst further favors cyclization to the coumarin over

the undesired pathway. These modifications result in a marked increase in selectivity for the coumarin product (**Table 2.5**, entry 7). As a proof of concept, when ethyl propiolate was used under the same optimized conditions lower selectivity was detected, underlying that a slower lactonization rate results in a higher extent of formation for the di–hydroarylation product (entry 8).

Phenol screening with propiolic acid under the optimized conditions (***Table 2.6***) revealed that the reaction scope is broader than with substituted alkynoic acids. Besides sesamol, the system accommodates more heavily substituted phenols such as 3,4,5–trimethoxyphenol (entry 2) and 3,4,5–trimethylphenol (entry 3), as well as simpler *meta*–, *ortho*–, and *para*– monosubstituted derivatives (entries 4 to 9). Notably, with 3,4,5–trimethylphenol, the steric hindrance suppresses formation of the double–hydroarylation side product, even when only 1 equivalent of alkyne was used. On the other hand, the more electron–rich and less–hindered 3,4,5–trimethoxyphenol requires excess alkyne to achieve good selectivity. Interestingly, this substrate also gives rise to a novel secondary product: a dearomatized, bicyclic species formed via hydroarylation followed by electrophilic attack of the alkyne at the 4–position of the phenol and subsequent intramolecular Michael–type addition to the unsaturated bond (***Figure* 2.10**). While intramolecular phenol dearomatization via electrophilic or nucleophilic activation is well established,[33] intermolecular dearomatization reactions remain rare.[34,35] We are currently exploring whether this byproduct formation can be developed into a synthetically useful transformation.

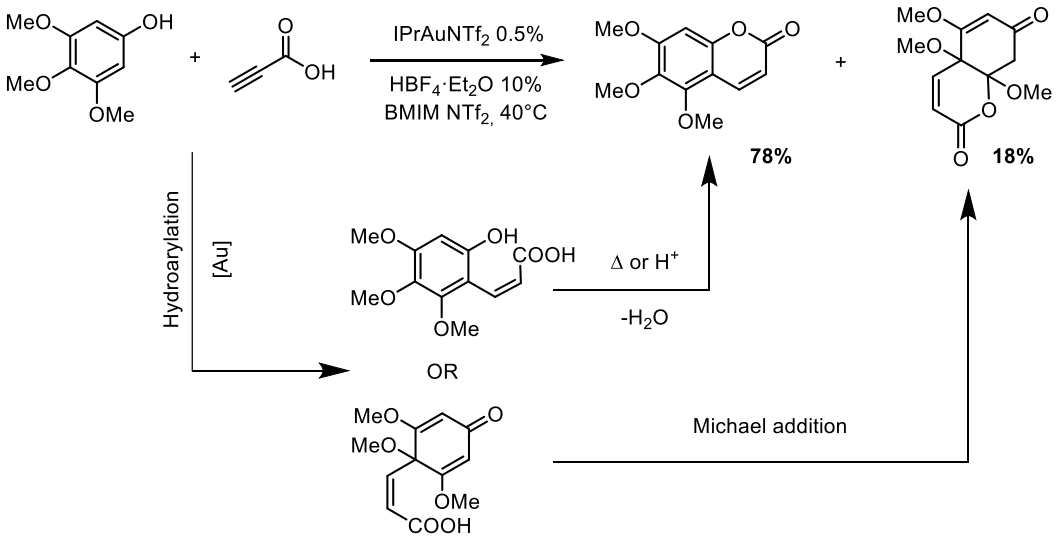

Figure 2.10 – Reactivity of 3,4,5–trimethoxyphenol with propiolic acid under reaction conditions

Simple phenol is also reactive under these conditions, but a complex mixture of products was obtained. Multiple position at the ring are available for electrophilic substitution (*ortho* and *para*) and they all may be involved under reaction conditions. The same issue has been encountered with mono–substituted phenols. In particular, in presence of a single substituent at *meta* position, two different coumarin products were obtained. This derives from the nonequivalent character of *ortho* positions to the hydroxyl group, which are both available for electrophilic attack (entries 4 and 5). However, an increase of steric hindrance nearby one of the interested positions, as in the case of *t*–butyl (entry 6) allowed for selective hydroarylation to a single coumarin product (position 6 is indeed more available to behave as nucleophile). No secondary coumarin product stemming from double hydroarylation of the alkyne was observed; however, despite quantitative phenol conversion, coumarin yields remained quite low, presumably because of the formation of side products stemming from competitive attack at the 4–position of the ring. Limitations due to the selectivity of the electrophilic attack arise also with *o*– or *p*–monosubstituted phenols. With *p*–monosubstituted phenols, coumarin yields are low to moderate and phenol conversions are not quantitative, indicating as expected a lower degree of activation of the aromatic ring towards electrophilic attack.

Table 2.6. *Reactivity of propiolic acid with different phenols under optimized reaction conditions*

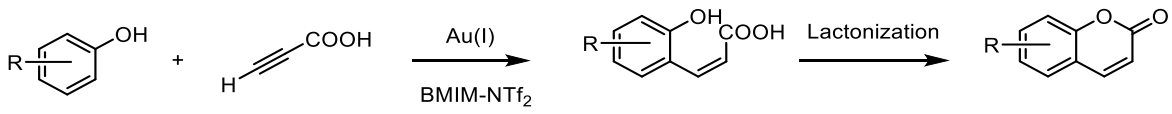

Entry	Phenol	Time (h)	Phenol conversion (%)	Coumarin yield (%)
1	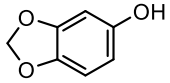	3	81	81
2	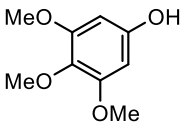	3	96	78

3[a]	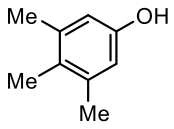	3	88	72
4	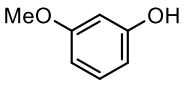	3	100	24[b] 12[c]
5	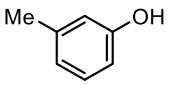	3	100	14[b] 15[c]
6	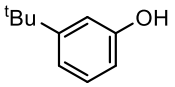	3	100	13
7	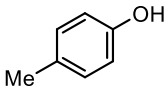	3	74	16
8	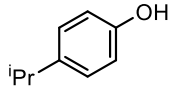	3	73	26
9	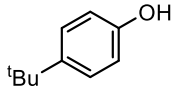	3	82	51
10	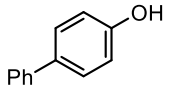	24	<5	Traces
11	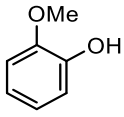	24	100	12

12	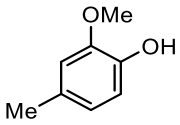	1.5	100	21

Reaction conditions: 2.5 mmol sesamol, 12.5 mmol alkyne, 0.1 eq. HBF_4, 0.012 mmol IPrAuCl, 0.012 mmol $AgSbF_6$, 0.75 mL BMIM–NTf_2, 25°C. [a] 1 eq. propiolic acid was employed. [b] Coumarin product stemming from electrophilic attack at the 6–position of the ring. [c] Coumarin product stemming from electrophilic attack at the 2–position of the ring.

Furthermore, competitive side reactions which are yet to be identified contribute to lowering the overall coumarin yield, although also in these cases no secondary coumarin product stemming from double hydroarylation of the alkyne was observed. With *o*–monosubsituted phenols, conversions are again quantitative but coumarin yields remain low (entry 11), probably because of the competitive reactivity of the 4–position of the ring. When this position is occupied, as in the case of *o,p*–disubstituted creosol, coumarin yields increase again a little (entry 12) which is interesting since creosol is a model for phenol units present in lignin,[36] hence its transformation into a coumarin could be employed for lignin derivatization. Finally, the presence of electron–withdrawing groups on the phenol generally shuts down the reaction (entry 10), in accordance with what is commonly observed in the hydroarylation of arenes with several catalytic systems.

Since the use of ionic liquids allow in principle the convenient separation and recycling of the catalytic system, we also set out to preliminarily evaluate the possibility of multiple use of the same catalyst batch. We employed sesamol and phenylpropiolic acid as substrates and $IPrAuNTf_2$ as silver–free catalyst under the reaction conditions outlined in **Table 2.5**, entry 3. After reaction and removal of a sample for the determination of the reaction yield, the reaction mixture could be conveniently extracted with diethylether, which allowed the complete removal of organic substrates and coumarin product. Residual diethylether was subsequently evaporated from the ionic liquid phase under vacuum and then a new reaction cycle was started by adding fresh substrates as well as molecular sieves and the HBF_4 cocatalyst. The results of multiple recycling according to this protocol are reported in ***Figure* 2.11**. Despite the small losses deriving from sampling of the reaction mixture, catalytic activity is substantially maintained for at least two recycles, which gives hope for the development of a more refined and efficient recycling protocol.

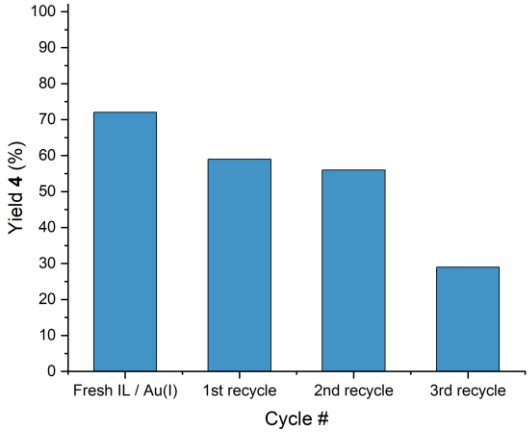

***Figure* 2.11** – Recycling tests using the reaction between sesamol and phenylpropiolic acid (**Table 2.5**, entry 3).

2.2.3. Screening and limitations of dearomatization pathways

In the previous section we showed that, under suitable conditions, the nucleophilic attack of 3,4,5–trimethoxyphenol to propiolic acid could occur not only at the unsubstituted *ortho*–position but also at the methoxy–substituted *para*–position (***Figure* 2.12**). In the latter case, the phenol undergoes electronic redistribution with consequent loss of the aromatic character by formation of a di–unsaturated carbonyl moiety (products **c** and **c'**). A Michael addition follows just for the product with the propiolic acid derivative, forming a polyunsaturated heterobicyclic structure (**c**).

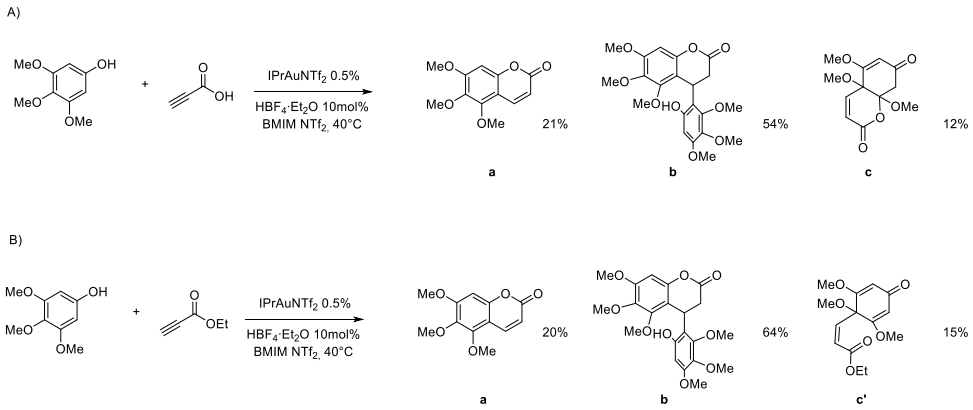

***Figure 2.12 –** Hydroarylation of propiolic acid (**A**) and ethyl propiolate (**B**) with 3,4,5–trimethoxyphenol.*

As first step, we tried to understand what conditions could favor the formation of species **c** and **c'** over the standard hydroarylation products **a** and **b**. It seems that the presence of unhindered terminal alkynes is fundamental to achieve those products. Indeed, no dearomatization process was detected using phenylpropiolic acid as substrate. We selected 2,6–di–tertbutyl–4–ethylphenol as benchmark substrate for our reaction, since it is commercially available and tert–butyl groups should provide enough steric hindrance to screen *ortho* and *meta* positions from attack by the alkyne. However, this did not work as planned, due to selectivity issues stemming from the acid–assisted cleavage of a *tert*–butyl moiety at phenol. This was further confirmed with a blank test, where the acid co–catalyst alone demonstrated to be able to cleave a tBu moiety from the phenol. Multiple conditions where attempted but no dearomatization products were formed in this reaction. On the other hand, species **D**, **E** and **F** could be synthesized in a quite selective manner by manipulating the stoichiometric ratio between the two reagents (***Table 2.7***).

Table 2.7 – *Hydroarylation of propiolic acid with 2,6–di–tertbutyl–4–ethylphenol*

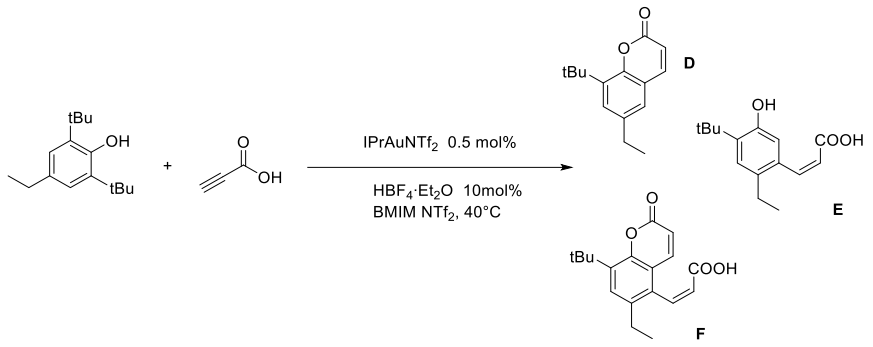

	Relative distribution		
	D	**E**	**F**
Equimolar conditions	1	2.5	1
2.5 equivs. alkyne	Traces	1.3	1
2.5 equivs. phenol	1.4	2.6	1

We are currently focusing our efforts on developing a strategy to improve the selectivity of this reaction, using 3,4,5-trimethoxyphenol as the substrate. Installing a protecting group OBoc at the –OH moiety seems to partially improve the selectivity. On the other hand, the protected phenol can be easily deprotected under reaction conditions, and even in the absence of acidic sources. Formation of a tert–butyl aryl ether may solve this issue. Moreover we experimented the effect of

dimethyl–hydrogenphosphate as templating agent for the process.[35] Again, an improvement in the reaction selectivity was detected but much lower activities are reached.

Those two strategies are the ones that gave the best results so far and will be further explored.

2.2.4. Conclusion and perspectives

In conclusion, a new Au(I)–catalyzed system has been developed to synthesize coumarin derivatives via direct hydroarylation of alkynoic acids and esters. The intermolecular nature of the hydroarylation step was confirmed by the detection of the open *Z*–vinyl product (type–3 product) via ^{1}H NMR spectroscopy. Low catalyst loadings (down to 0.1 mol%) were achieved by employing an acidic co–catalyst ($HBF_4 \cdot Et_2O$) and molecular sieves to sequester water. The process showed maximum activity when propiolic acid was used as the alkyne, and selectivity issues were addressed from a mechanistic perspective and resolved by using an excess of alkyne. Several phenols were found to be reactive under our conditions; however, major limitations in selectivity remain for mono–substituted phenols.

Preliminary attempts to selectively promote dearomatization at the phenol scaffold were also performed. Initial observations suggest that the reaction is highly substrate–specific, limiting the accessible chemical space. Different strategies to direct the electrophilic attack of the activated alkyne, such as installing a sterically hindered group or using a templating agent, are currently under investigation.

2.2.5. Experimental section

General experimental procedure for the direct synthesis of coumarins (Procedure A; *Table 2.3*, *Table 2.4* and *Table 2.5* entries 1 and 2)

The phenol (2.5 mmol) and the gold(I) catalyst (0.012 mmol, 0.5 mol%), were added in a Schlenk tube previously evacuated and filled with argon for three times. The ionic liquid (0.75 mL) was then added. In cases in which a silver salt activator was required for the gold(I) catalyst, the silver salt $AgSbF_6$ (4.3 mg, 0.013 mmol, 0.5 mol%) was pre–dissolved in the ionic liquid; stock solutions of the silver salt were prepared for this purpose and stored in refrigerator away from sources of light and heat inside vials completely covered with aluminum foil. The reaction mixture was stirred at room temperature for 2 minutes, after which the alkyne (2.5 mmol) was added. The Schlenk tube was placed in an oil bath thermostated at the desired temperature. In order to follow the catalytic system, aliquots (0.05 mL) were drawn off from the solution, solubilized in 0.5 mL deuterated solvent ($CDCl_3$ or DMSO–d_6) and analyzed by ^{1}H–NMR. Conversion of the phenol and product yields were determined by internal calibration. 1,2–Dimethoxyethane was occasionally employed as an internal standard to verify mass balance over all the phenol–derived species.

Optimized experimental procedure for the synthesis of coumarins with substituted propiolic acid (Procedure B; *Table 2.5*, entries 3–5)

The phenol (2.5 mmol, 1 eq.), molecular sieves 4Å (400 mg) and the gold(I) catalyst IPrAuCl (7.7 mg, 0.013 mmol, 0.5 mol%), were added in a Schlenk tube previously evacuated and filled with argon for three times. Then, 1.5 ml of the $AgSbF_6$ stock solution in $BMIMNTf_2$ (8.3 μM) was added and the mixture was put under stirring for two minutes. The Schlenk–flask was placed in a thermostatic oil–bath at 40°C and the acid co–catalyst $HBF_4{\cdot}Et_2O$ (0.035 ml, 0.25 mmol, 10 mol%) was added along with phenylpropiolic acid (365.4 mg, 2.5 mmol, 1 eq.). In order to follow the reaction kinetic, aliquots (0.05 mL) were drawn off from the solution, solubilized in 0.5 mL of deuterated solvent ($CDCl_3$ or DMSO–d_6) and analyzed by NMR. Conversion of the phenol and products yields were determined by internal calibration. 1,2–Dimethoxyethane was occasionally employed as an internal standard to verify mass balance over all the phenol–derived species.

Recycling procedure

In the context of the hydroarylation of phenylpropiolic acid with sesamol a recycling protocol has been established. After the reaction was finished, the crude was treated with Et_2O and the biphasic mixture was filtered through a PTFE syringe–filter into an 8 ml vial. The system was homogenized by a vortex mixer and separated after centrifugation (3000 rpm for 2 minutes). The Et_2O phase was then separated by a syringe.

The IL phase was extracted other 3 times by the same methodology and then stripped by N_2 flux to remove Et_2O residues from the solution. At this point, the catalyst–containing IL phase was transferred in a new Schlenk flask and further dried under vacuum. An ^1H NMR check was performed to ensure the complete extraction of the organic derivatives.

The catalyst–containing IL phase was then employed in another reaction cycle, adding an equivalent quantity of substrates, molecular sieves and acid co–catalyst with respect to the mass of the recovered IL phase.

Optimized experimental procedure for the synthesis of coumarins with propiolic acid (Procedure C; *Table 2.5*, entries 7–8 and *Table 2.6*)

The phenol (2.5 mmol, 1 eq.) and the gold(I) catalyst IPrAuCl (7.7 mg, 0.012 mmol, 0.5 mol%), were added in a Schlenk tube previously evacuated and filled with argon for three times. Under argon atmosphere, the silver salt $AgSbF_6$ (4.3 mg, 0.013 mmol, 0.5 mol%) dissolved in the ionic liquid $BMIMNTf_2$ (0.75 ml) was then added. The reaction mixture was stirred at room temperature for 2 minutes, after which propiolic acid (0.77 ml, 12.5 mmol, 5 eq.) was added. The Schlenk tube was placed in a thermostated oil bath at the desired temperature and the acid co–catalyst $HBF_4{\cdot}Et_2O$ (0.035 ml, 0.25 mmol) was added. In order to monitor the reaction, aliquots (0.05 ml) were drawn off from the solution, solubilized in 0.5 mL of deuterated solvent ($CDCl_3$ or DMSO–d_6) and analyzed by ^1H–NMR. Conversion of the phenol and products yields were determined by internal calibration. 1,2–Dimethoxyethane was occasionally employed as an internal standard to verify mass balance over all the phenol–derived species.

^{1}H NMR characterization of the intermediate alkene products (type 3 products, *Table 2.4*).

*Ethyl (Z)–3–(2–hydroxy–4,5–methylendioxyphenyl)–3–phenylacrylate (**Table 2.4**, entry 1)*

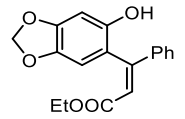

^{1}H NMR (300 MHz, $CDCl_3$): δ 6.57 (s, Ar–H, 1H), 6.48 (s, Ar–H, 1H), 6.38 (s, vinyl, 1H), 5.90 (s, OCH_2O, 2H), 5.95 (brs, O–H, s), 4.14 (q, *J* = 7.2 Hz, OCH_2CH_3, 2H), 1.24 (t, *J* = 7.2 Hz, OCH_2CH_3, 3H) ppm;

*Ethyl (Z)–3–(2–hydroxy–4,5,6–trimethoxyphenyl)–3–phenylacrylate (**Table 2.4**, entry 2)*

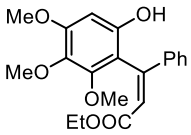

^{1}H NMR (300 MHz, DMSO–d^6): δ 6.46 (s, vinyl, 1H), 6.32 (s, Ar–H, 1H), 3.97 (q, *J* = 7.1 Hz, OCH_2CH_3, 2H), 1.08 (t, *J* = 7.1 Hz, OCH_2CH_3, 3H) ppm;

*Ethyl (Z)–3–(2–hydroxy–4,5,6–trimethylphenyl)–3–phenylacrylate (**Table 2.4**, entry 3)*

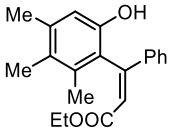

^{1}H NMR (300 MHz, DMSO–d^6): δ 6.56 (s, vinyl, 1H), 6.52 (s, Ar–H, 1H), 3.94 (q, *J* = 7.1 Hz, OCH_2CH_3, 2H), 1.04 t, *J* = 7.1 Hz, OCH_2CH_3, 3H) ppm;

All products were detected in the reaction crudes by ^{1}H NMR spectroscopy. Purification attempts by extraction and/or column chromatography led to complete lactonization of the molecules to the corresponding coumarins.

^{1}H NMR characterization of the coumarin products obtained from substituted propiolic acids or esters (*Table 2.4* and *Table 2.5*, entries 1–5)

*6,7–(methylendioxy)–4–phenylcoumarin (**Table 2.5**, entry 3)* [37]

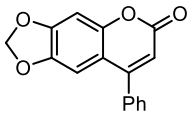

^{1}H NMR (300 MHz, $CDCl_3$): δ 7.52–7.50 (m, 3H), 7.45–7.39 (m, 2H), 6.88 (s, 1H), 6.82 (s, 1H), 6.23 (s, 1H), 6.05 (s, 2H) ppm;

*5,6,7–(trimethoxy)–4–phenyl–coumarin (**Table 2.4**, entry 2)* [38]

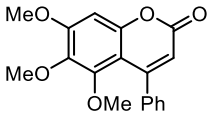

^{1}H NMR (300 MHz, $CDCl_3$): δ 7.49–7.36 (m, 3H),7.36–7.27 (m, 2H), 6.72 (s, 1H), 6.05 (s, 1H), 3.93 (s, 3H), 3.78 (s, 3H), 3.25 (s, 3H) ppm;

*5,6,7–(trimethyl)–4–phenyl–coumarin (**Table 2.4**, entry 3)* [39]

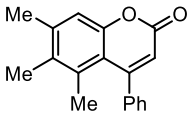

^{1}H NMR (300 MHz, $CDCl_3$): δ 7.48–7.41 (m, 3H), 7.34–7.27 (m, 2H), 7.11 (s, 1H), 6.21 (s, 1H), 2.39 (s, 3H), 2.15 (s, 3H), 1.76 (s, 3H) ppm;

*7–methyl–4–phenyl–coumarin (**Table 2.4**, entry 4)* [40]

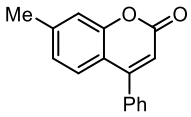

^{1}H NMR (300 MHz, $CDC1_3$): δ 7.49 (t, *J* = 3.1 Hz, 3H), 7.43–7.41 (m, 2H), 7.34 (d, *J* = 8.0 Hz, 1H), 7.19 (s, 1H), 7.01 (d, *J* = 8.0 Hz, 1H), 6.29 (s, 1H), 2.47 (s, 3H) ppm;

*7–tert–butyl–4–phenyl–coumarin (**Table 2.4**, entry 5)* [39]

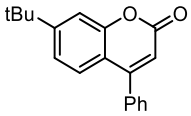

^{1}H NMR (300 MHz, $CDCl_3$): δ 7.54–7.50 (m, 3H), 7.44–7.40 (m, 4H), 7.28–7.25 (m, 1H), 6.32 (s, 1H), 1.36 (s, 9H) ppm;

*6,7–(methylendioxy)–4–n–propylcoumarin (**Table 2.5**, entry 5)* [41]

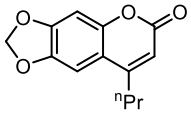

^{1}H NMR (300 MHz, $CDCl_3$): δ 6.97 (s, 1H), 6.81 (s, 1H), 6.13 (t, *J* = 0.8 Hz, 1H), 6.05 (s, 2H), 2,64 (td, *J* = 7.6, 0.8 Hz, 2H), 1.70 (ses, *J* = 7.6 Hz, 2H), 1.03 (t, *J* = 7.4 Hz, 3H) ppm;

^{1}H NMR characterization of the coumarin products obtained from propiolic acid or ethyl propiolate (*Table 2.5*, entries 6–8 and *Table 2.6*)

*6,7–(methylendioxy)–coumarin (**Table 2.6**, entry 1)* [14]

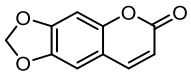

^{1}H NMR (300 MHz, $CDCl_3$): δ 7.58 (d, *J* = 9.5 Hz, 1H), 6.83 (s, 2H), 6.28 (d, *J* = 9.5 Hz, 1H), 6.07 (s, 2H) ppm;

*5,6,7–(trimethoxy)–coumarin (**Table 2.6**, entry 2)* [42]

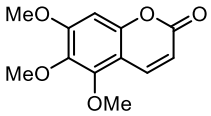

^{1}H NMR (300 MHz, $CDCl_3$): δ 7.92 (d, *J* = 9.6 Hz, 1H), 6.61 (s, 1H), 6.22 (d, *J* = 9.6 Hz, 1H), 4.02 (s, 3H), 3.92 (s, 3H), 3.85 (s, 3H) ppm;

*5,6,7–(trimethyl)–coumarin (**Table 2.6**, entry 3)* [43]

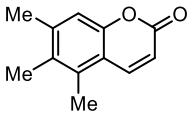

^{1}H NMR (300 MHz, $CDCl_3$): δ 7.94 (d, *J* = 9.9 Hz, 1H), 6.97 (s, 1H), 6.32 (d, *J* = 9.9 Hz, 1H), 2.40 (s, 3H), 2.34 (s, 3H), 2.21 (s, 3H) ppm;

*7–methoxy–coumarin (**Table 2.6**, entry 4)* [14]

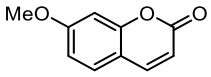

^{1}H NMR (300 MHz, $CDCl_3$): δ 7.63 (d, *J* = 9.5 Hz, 1H), 7.37 (d, *J* = 8.5 Hz, 1H), 6.84 (dd, *J* = 8.5, 2.5 Hz, 1H), 6.81 (d, *J* = 2.5 Hz, 1H), 6.24 (d, *J* = 9.5 Hz, 1H), 3.87 (s, 3H) ppm;

*5–methoxy–coumarin (**Table 2.6**, entry 4)* [14]

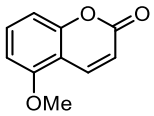

^{1}H NMR (300 MHz, $CDCl_3$): δ 8.09 (d, *J* = 9.8 Hz, 1H), 7.44 (t, *J* = 8.4 Hz, 1H), 6.93 (d, *J* = 8.4 Hz, 1H), 6.71 (d, *J* = 8.4 Hz, 1H), 6.34 (d, *J* = 9.8 Hz, 1H), 3.94 (s, 3H) ppm;

*7–methyl–coumarin (**Table 2.6**, entry 5)* [44]

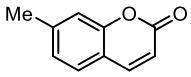

^{1}H NMR (300 MHz, $CDCl_3$): 7.67 (d, J = 9.6 Hz, 1H), 7.36 (d, J = 7.7 Hz, 1H), 7.12 (s,1H), 7.09 (d, J = 7.7 Hz, 1H), 6.35 (d, J = 9.6 Hz, 1H), 2.44 (s, 3H);

*5–methyl–coumarin (**Table 2.6**, entry 5)* [45]

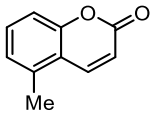

^{1}H NMR (300 MHz, $CDCl_3$): δ 7.70 (d, *J* = 9.5, 1H), 7.38 (d, *J* = 7.3, 1H), 7.32 (d, *J* = 7.5, 1H), 7.18 (t, *J* = 7.6, 1H), 6.41 (d, *J* = 9.5, 1H), 2.46 (s, 3H) ppm;

*7–tert–butyl–coumarin (**Table 2.6**, entry 6)* [46]

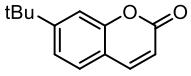

^{1}H NMR (300 MHz, $CDCl_3$): δ 7.70 (d, *J* = 9.6 Hz, 1H), 7.45–7.41 (m, 1H), 7.34–7.29 (m, 2H), 6.36 (d, *J* = 9.6 Hz, 1H), 1.35 (s, 9H) ppm;

*6–methyl–coumarin (**Table 2.6**, entry 7)* [14]

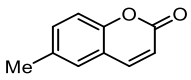

^{1}H NMR (300 MHz, $CDCl_3$): δ 7.60 (d, *J* = 9.5 Hz, 1H), 7.25 (d, *J* = 8.4 Hz, 1H), 7.20 (s, 1H), 7.14 (d, *J* = 8.4 Hz, 1H), 6.32 (d, *J* = 9.5 Hz, 1H), 2.40 (s, 3H) ppm;

*6–isopropyl–coumarin (**Table 2.6**, entry 8)* [43]

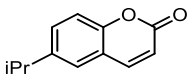

^{1}H NMR (300 MHz, $CDCl_3$): δ 7.70 (d, *J* = 9.9 Hz, 1H), 7.42–7.38 (m, 1H), 7.31–7.25 (m, 2H), 6.41 (d, *J* = 9.2 Hz, 1H), 2.99–2.96 (m, 1H), 1.28 (d, *J* = 6.8 Hz, 6H) ppm;

*6–tert–butyl–coumarin (**Table 2.6**, entry 9)* [38]

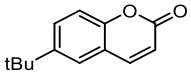

^{1}H NMR (300 MHz, $CDCl_3$): δ 7.68 (d, *J* = 9.2 Hz, 1H), 7.56–7.54 (m, 1H), 7.42 (d, *J* = 2.3 Hz, 1H), 7.24 (d, *J* = 8.4 Hz, 1H), 6.38 (d, *J* = 9.9 Hz, 1H), 1.33 (s, 9H) ppm;

*8–methoxy–coumarin (**Table 2.6**, entry 11)* [14]

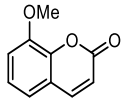

^{1}H NMR (300 MHz, $CDCl_3$): δ 7.70 (d, *J* = 9.6 Hz, 1H), 7.23 (t, *J* = 8.0 Hz, 1H), 7.10 (dd, *J* = 8.0, 1.3 Hz, 1H), 7.08 (dd, *J* = 8.0, 1.3 Hz, 1H), 6.45 (d, *J* = 9.6 Hz, 1H), 3.99 (s, 3H);

*8–methoxy–6–methyl–coumarin (**Table 2.6**, entry 12)*

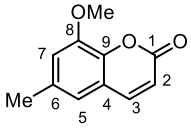

Separated after column chromatography (eluent EtOAc/Hex 1:2) of the reaction crude using creosol and propiolic acid as substrates (ratio 1:5); see the section ***"Optimized experimental procedure for the synthesis of coumarins with propiolic acid"***. The reaction was scaled down to 0.5 mmol of creosol in this case.

The product was isolated as a light–yellow powder in 21% yield (19.9 mg, 0.1 mmol).

^{1}H NMR (300 MHz, $CDCl_3$): δ 7.62 (d, *J* = 9.5 Hz, 1H, C_3–H), 6.90 (d, *J* = 1.4 Hz, 1H, C_7–H), 6.84 (d, *J* = 1.2 Hz, 1H, C_5–H), 6.41 (d, *J* = 9.5 Hz, 1H, C_2–H),

3.94 (s, 3H, –OMe), 2.40 (s, 3H, –Me); **$^{13}C\{^{1}H\}$ NMR (75.5 MHz, $CDCl_3$) :** δ 160.6 (C_1), 147.1 (C_8), 143.7 (C_3), 142.1 (C_4), 134.4 (C_6), 119.3 (C_9), 119.2 (C_5), 117.1 (C_2), 115.2 (C_7), 56.4 (–OMe), 21.4 (–Me) ppm; **HRMS (ESI+):** calcd for $[M+H]^+ = C_{11}H_{11}O_3^+$: 191.0703. Found: 191.0772;

^{1}H NMR characterization of dihydrocoumarins

4–(2'–hydroxy–4',5'–methylendioxyphenyl)–6,7–methylendioxy–3,4–dihydrocoumarin [47]

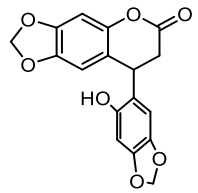

^{1}H NMR (300 MHz, DMSO–d^6): δ 6.82 (s, Ar–H, 1H), 6.60 (s, Ar–H, 1H), 6.49 (s, Ar–H, 1H), 6.21 (s, Ar–H, 1H), 6.01 (d, *J* = 4.4 Hz, OCH_2O, 2H), 5.87 (d, *J* = 4.4 Hz, OCH_2O, 2H), 4.45 (t, *J* = 5.8 Hz, 1H), 3.07–2.85 (m, 2H) ppm;

4–(2'–hydroxy–6'–methoxyphenyl)–6–methoxy–3,4–dihydrocoumarin [48]

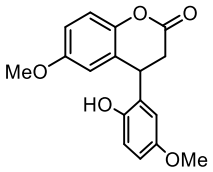

^{1}H NMR (300 MHz, $CDCl_3$): δ 7.06 (d, *J* = 8.9 Hz, 1H), 6.83 (dd, *J* = 8.9, 3.0 Hz, 1H), 6.68–6.60 (m, 3H), 6.35 (d, *J* = 2.9 Hz, 1H), 4.60 (t, *J* = 6.3 Hz, 1H), 3.73 (s, 3H), 3.65 (s, 3H), 3.18 (dd, *J* = 16.1, 6.1 Hz, 1H), 2.97 (dd, *J* = 16.1, 6.4 Hz, 1H) ppm;

4–(2'–hydroxy–5'–methylphenyl)–6–methyl–3,4–dihydrocoumarin [48]

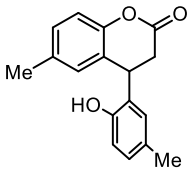

^{1}H NMR (300 MHz, $CDCl_3$): δ 7.10 (d, *J* = 8.2 Hz, 1H), 7.03 (d, *J* = 8.3 Hz, 1H), 6.90 (d, *J* = 7.9 Hz, 1H), 6.86 (s, 1H), 6.64 (d, *J* = 8.1Hz, 1H), 6.59 (s, 1H), 5.38 (brs, 1H), 4.60 (t, *J* = 6.2 Hz, 1H), 3.18 (dd, *J* = 16.0, 6.1 Hz, 1H), 2.97 (dd, *J* = 16.0, 6.5 Hz, 1H), 2.18 (s, 3H), 2.27 (s, 3H) ppm;

4–(2'–hydroxy–5'–tert–butylphenyl)–6–tertbutyl–3,4–dihydrocoumarin [48]

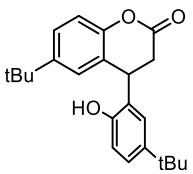

^{1}H NMR (300 MHz, $CDCl_3$): δ 7.32 (dd, *J* = 8.5, 2.2 Hz, 1H), 7.11–7.07 (m, 3H), 6.79 (d, *J* = 2.2 Hz,1H), 6.66 (d, *J* = 8.3Hz, 1H), 5.50 (brs, 1H), 4.69 (t, *J* = 6.4 Hz, 1H), 3.19 (dd, *J* =16.1, 6.4 Hz, 1H), 3.01 (dd, *J* = 16.1, 6.4 Hz, 1H), 1.25 (s, 9H), 1.17 (s, 9H) ppm;

4–(2'–hydroxy–4',5',6'–methylendioxyphenyl)–6,7–methylendioxy–3,4–dihydrocoumarin

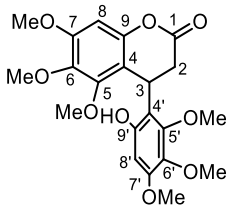

Separated after column chromatography (eluent EtOAc/Hex 1:1) of the reaction crude using 3,4,5–tri–methoxyphenol and propiolic acid as substrates in equimolar ratio; see the section ***"General experimental procedure for the direct synthesis of coumarins"***.

The product was isolated as a light–yellow powder in 54% yield (282 mg, 0.67 mmol).

^{1}H NMR (300 MHz, $CDCl_3$): δ 6.44 (s, 1H, C_8–H), 6.25 (s, 1H, $C_{6'}$–H), 6.06 (brs, 1H, –OH), 4.71 (dd, $^{2}J_{anti}$ = 9.35 Hz, $^{2}J_{sin}$ = 0.98 Hz, 1H, C_3–H), 3.83 (s, 3H, C_4–OCH_3), 3.79 (s, 6H, C_5–OCH_3), 3.74 (s, 3H, C_5–OCH_3), 3.69 (s, 3H, C_5–OCH_3), 3.67 (s, 3H, C_5–OCH_3), 2.98 (dd, $^{1}J_{gem}$ = 16.96 Hz, $^{2}J_{anti}$ = 9.35 Hz, 1H, C_2–H), 2.80 (dd, $^{1}J_{gem}$ = 16.96 Hz, $^{2}J_{sin}$ = 0.98 Hz, 1H, C_2–H) ppm; **^{13}C{^{1}H} NMR (75.5 MHz, $CDCl_3$) :** δ 167.35 (s, C_1), 153.42 (s, $C_{7'}$), 153.22 (s, C_7), 152.36 (s, $C_{5'}$), 150.82 (s, C_5), 149.15 (s, $C_{9'.}$), 147.62 (s, C_9), 138.29 (s, $C_{6'}$), 136.34 (s, C_6), 115.92 (s, $C_{4'}$), 108.93 (s, C_4), 96.96 (s, $C_{8'}$), 96.81 (s, C_8), 61.26 (s, C_5–OCH_3), 61.09 (s, C_7–OCH_3), 61.04 (s, C_6–OCH_3), 60.01 (s, $C_{5'}$–OCH_3), 56.19 (s, $C_{7'}$–OCH_3), 55.98 (s, $C_{6'}$–OCH_3), 34.37 (s, C_2), 26.72 (s, C_3) ppm; **HRMS (ESI+):** calcd for $[M+H]^+$ = $C_{21}H_{25}O_9^+$: 421.1493. Found: 421.1508;

^{1}H NMR characterization of the dearomatized product

4,5,9–tri–methoxy–7–oxo–9H–chromen–2–one

Separated after column chromatography (eluent EtOAc/Hex 2:1) of the reaction crude using 3,4,5–tri–methoxyphenol and propiolic acid as substrates (ratio 1:5); see the section ***"Optimized experimental procedure for the synthesis of coumarins with propiolic acid"***.

The product was isolated as a white powder in 18% yield (113 mg, 0.44 mmol).

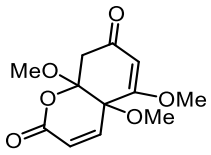

^{1}H NMR (300 MHz, $CDCl_3$): δ 6.99 (d, $^2J_{cis}$ = 10.09 Hz, 1H), 6.15 (d, $^2J_{cis}$ = 10.09 Hz, 1H), 5.56 (s, 1H), 3.74 (s, 3H, C_4–OCH_3), 3.52 (s, 3H, C_5–OCH_3), 3.46 (s, 3H, C_9–OCH_3), 3.04 (s, $^1J_{gem}$ = 16.96 Hz, 1H), 2.87 (s, $^1J_{gem}$ = 16.96 Hz, 1H) ppm; $^{13}C\{^1H\}$ NMR (75.47 MHz, $CDCl_3$) : δ 192.28 (s, C_7), 171.28 (s, C_4), 161.76 (s, C_1), 143.00 (s, C_3), 121.53 (s, C_2), 105.49 (s, $C_{9.}$), 104.17 (s, C_6), 74.95 (s, C_5), 56,82 (s, C_4–OCH_3), 54.35 (s, C_5–OCH_3), 50.56 (s, C_9–OCH_3), 40.90 (s, C_8) ppm; **HRMS (ESI+):** calcd for $[M+H]^+$ = $C_{12}H_{15}O_6^+$: 255.0863. Found: 255.0884;

2.2.6. References

[1] R. D. H. Murray, J. Méndez, S. A. Brown in *Plant, Cell & Environment*, **1982**, pp. 435–436.

[2] X. Sun, T. Liu, J. Sun, X. Wang, "Synthesis and application of coumarin fluorescence probes" *RSC Adv*. **2020**, *10*, 10826–10847.

[3] A. Pereira, S. Martins, A. Teresa Caldeira in *Phytochemicals in Human Health* (Eds.: V. Rao, D. Mans, L. Rao), IntechOpen, **2020**.

[4] T. Al–Warhi, A. Sabt, E. B. Elkaeed, W. M. Eldehna, "Recent advancements of coumarin–based anticancer agents: An up–to–date review" *Bioorganic Chemistry* **2020**, *103*, 104163.

[5] A. Stefanachi, F. Leonetti, L. Pisani, M. Catto, A. Carotti, "Coumarin: A Natural, Privileged and Versatile Scaffold for Bioactive Compounds" *Molecules* **2018**, *23*, 250.

[6] K. P. Barot, S. V. Jain, L. Kremer, S. Singh, M. D. Ghate, "Recent advances and therapeutic journey of coumarins: current status and perspectives" *Med Chem Res* **2015**, *24*, 2771–2798.

[7] F. Borges, F. Roleira, N. Milhazes, L. Santana, E. Uriarte, "Simple Coumarins and Analogues in Medicinal Chemistry: Occurrence, Synthesis and Biological Activity" *CMC* **2005**, *12*, 887–916.

[8] D. Sharma, V. Dhayalan, C. Manikandan, R. Dandela in *Strategies for the Synthesis of Heterocycles and Their Applications* (Eds.: P. Kumari, A. B. Patel), IntechOpen, **2023**.

[9] K. Szwaczko, "Coumarins Synthesis and Transformation via C–H Bond Activation—A Review" *Inorganics* **2022**, *10*, 23.

[10] J. Ferguson, F. Zeng, H. Alper, "Synthesis of Coumarins via Pd–Catalyzed Oxidative Cyclocarbonylation of 2–Vinylphenols" *Org. Lett.* **2012**, *14*, 5602–5605.

[11] A. Seoane, N. Casanova, N. Quiñones, J. L. Mascareñas, M. Gulías, "Straightforward Assembly of Benzoxepines by Means of a Rhodium(III)–Catalyzed C–H Functionalization of *o* –Vinylphenols" *J. Am. Chem. Soc.* **2014**, *136*, 834–837.

[12] X.–G. Liu, S.–S. Zhang, C.–Y. Jiang, J.–Q. Wu, Q. Li, H. Wang, "Cp*Co(III)–Catalyzed Annulations of 2–Alkenylphenols with CO: Mild Access to Coumarin Derivatives" *Org. Lett.* **2015**, *17*, 5404–5407.

[13] K. Sasano, J. Takaya, N. Iwasawa, "Palladium(II)–Catalyzed Direct Carboxylation of Alkenyl C–H Bonds with CO_2" *J. Am. Chem. Soc.* **2013**, *135*, 10954–10957.

[14] A. Cervi, Y. Vo, C. L. L. Chai, M. G. Banwell, P. Lan, A. C. Willis, "Gold(I)–Catalyzed Intramolecular Hydroarylation of Phenol–Derived Propiolates and Certain Related Ethers as a Route to Selectively Functionalized Coumarins and 2 *H* –Chromenes" *J. Org. Chem.* **2021**, *86*, 178–198.

[15] F. Ravera, M. S. Martinsen Holmsen, P. Sgarbossa, D. Bourissou, A. Biffis, "Gold(III) Catalysis in Ionic Liquids: The Case Study of Coumarin Synthesis" *Adv Synth Catal* **2025**, *367*, DOI 10.1002/adsc.202400706.

[16] F. Ravera, F. Floreani, C. Tubaro, M. Roverso, R. Pedrazzani, M. Bandini, A. Biffis, "An Improved Gold(I) Catalytic System for the Preparation of Coumarins *via* Intramolecular Cyclization" *Chemistry An Asian Journal* **2025**, *20*, DOI 10.1002/asia.202400725.

[17] G. Battistuzzi, S. Cacchi, I. De Salve, G. Fabrizi, L. M. Parisi, "Synthesis of Coumarins in a Molten *n*- Bu_4 NOAc/ *n* -Bu_4 NBr Mixture through a Domino Heck Reaction/Cyclization Process" *Adv Synth Catal* **2005**, *347*, 308–312.

[18] D. Giguère, P. Cloutier, R. Roy, "Domino Heck/Lactonization–Catalyzed Synthesis of 3– *C* –Linked Mannopyranosyl Coumarins" *J. Org. Chem.* **2009**, *74*, 8480–8483.

[19] T. D. A. Fernandes, B. Gontijo Vaz, M. N. Eberlin, A. J. M. Da Silva, P. R. R. Costa, "Palladium–Catalyzed Tandem Heck–Lactonization from *o* –Iodophenols and Enoates: Synthesis of Coumarins and the Study of the Mechanism by Electrospray Ionization Mass Spectrometry" *J. Org. Chem.* **2010**, *75*, 7085–7091.

[20] S. Aoki, J. Oyamada, T. Kitamura, "Formation of Coumarins by Palladium(II)–Catalyzed Reaction of Phenols with Ethyl Acrylates" *Bulletin of the Chemical Society of Japan* **2005**, *78*, 468–472.

[21] U. Sharma, T. Naveen, A. Maji, S. Manna, D. Maiti, "Palladium-Catalyzed Synthesis of Benzofurans and Coumarins from Phenols and Olefins" *Angew. Chem. Int. Ed.* **2013**, *52*, 12669–12673.

[22] D. Kim, M. Min, S. Hong, "One–pot catalysis of dehydrogenation of cyclohexanones to phenols and oxidative Heck coupling: expedient synthesis of coumarins" *Chem. Commun.* **2013**, *49*, 4021.

[23] C. Zhang, S. Lv, Y. Wang, J. Zhang, X.–N. Wang, J. Chang, "Metal–free intramolecular hydroarylation of alkynes" *Org. Chem. Front.* **2022**, *9*, 1300–1307.

[24] S. K. Gadakh, S. Dey, A. Sudalai, "Rh–Catalyzed Synthesis of Coumarin Derivatives from Phenolic Acetates and Acrylates *via* C–H Bond Activation" *J. Org. Chem.* **2015**, *80*, 11544–11550.

[25] V. V. Kouznetsov, C. E. Puerto–Galvis, M. C. Ortiz Villamizar, L. Y. Vargas–Mendez *Current Organic Chemistry* **2017**, *21*, 949–963.

[26] B. M. Trost, F. D. Toste, K. Greenman, "Atom Economy. Palladium–Catalyzed Formation of Coumarins by Addition of Phenols and Alkynoates via a Net C−H Insertion" *J. Am. Chem. Soc.* **2003**, *125*, 4518–4526.

[27] G. Brufani, F. Valentini, F. Sabatelli, B. Di Erasmo, A. M. Afanasenko, C.–J. Li, L. Vaccaro, "Valorisation of phenols to coumarins through one–pot palladium–catalysed double C–H functionalizations" *Green Chem.* **2022**, *24*, 9094–9100.

[28] A. Biffis, C. Tubaro, M. Baron, "Advances in Transition-Metal-Catalysed Alkyne Hydroarylations" *The Chemical Record* **2016**, *16*, 1742–1760.

[29] M. Baron, A. Biffis, "Gold(I) Complexes in Ionic Liquids: An Efficient Catalytic System for the C-H Functionalization of Arenes and Heteroarenes under Mild Conditions" *Eur. J. Org. Chem.* **2019**, *2019*, 3687–3693.

[30] S. Bonfante, P. Bax, M. Baron, A. Biffis, "Gold(I)–Catalyzed Direct Alkyne Hydroarylation in Ionic Liquids: Mechanistic Insights" *Catalysts* **2023**, *13*, 822.

[31] Z. Lu, T. Li, S. R. Mudshinge, B. Xu, G. B. Hammond, "Optimization of Catalysts and Conditions in Gold(I) Catalysis—Counterion and Additive Effects" *Chem. Rev.* **2021**, *121*, 8452–8477.

[32] C. H. Leung, M. Baron, A. Biffis, "Gold–Catalyzed Intermolecular Alkyne Hydrofunctionalizations—Mechanistic Insights" *Catalysts* **2020**, *10*, 1210.
[33] T. Nemoto, "Development of Transition–Metal–Catalyzed Dearomatization Reactions" *Chem. Pharm. Bull.* **2023**, *71*, 624–632.
[34] L. Shao, X.–P. Hu, "Copper–catalyzed intermolecular asymmetric propargylic dearomatization of phenol derivatives" *Chem. Commun.* **2017**, *53*, 8192–8195.
[35] X. Gao, T.–J. Han, B.–B. Li, X.–X. Hou, Y.–Z. Hua, S.–K. Jia, X. Xiao, M.–C. Wang, D. Wei, G.–J. Mei, "Catalytic asymmetric dearomatization of phenols via divergent intermolecular (3 + 2) and alkylation reactions" *Nat Commun* **2023**, *14*, 5189.
[36] Z. Sun, B. Fridrich, A. De Santi, S. Elangovan, K. Barta, "Bright Side of Lignin Depolymerization: Toward New Platform Chemicals" *Chem. Rev.* **2018**, *118*, 614–678.
[37] Z. Wang, X. Li, L. Wang, P. Li, "Photoinduced cyclization of alkynoates to coumarins with N–Iodosuccinimide as a free–radical initiator under ambient and metal–free conditions" *Tetrahedron* **2019**, *75*, 1044–1051.
[38] C. Jia, D. Piao, T. Kitamura, Y. Fujiwara, "New Method for Preparation of Coumarins and Quinolinones via Pd–Catalyzed Intramolecular Hydroarylation of C−C Triple Bonds" *J. Org. Chem.* **2000**, *65*, 7516–7522.
[39] F. Ravera, M. S. Martinsen Holmsen, P. Sgarbossa, D. Bourissou, A. Biffis, "Gold(III) Catalysis in Ionic Liquids: The Case Study of Coumarin Synthesis" *Adv. Synth. Catal.* **2025**, *367*, e202400706.
[40] M. L. N. Rao, V. Venkatesh, D. N. Jadhav, "Palladium-Catalyzed Synthesis of 4-Arylcoumarins Using Triarylbismuth Compounds as Atom-Efficient Multicoupling Organometallic Nucleophiles" *Eur. J. Org. Chem.* **2010**, *2010*, 3945–3955.
[41] M. D. P. Olaya, N. E. Vergel, J. L. López, D. Viña, M. F. Guerrero, "8–Propyl–6H–[1,3]dioxolo[4,5–g]chromen–6–one: A new coumarin with monoamine oxidase B inhibitory activity and possible anti–parkinsonian effects" *Braz. J. Pharm. Sci.* **2020**, *56*, e17609.
[42] C. Schultze, B. Schmidt, "Prenylcoumarins in One or Two Steps by a Microwave–Promoted Tandem Claisen Rearrangement/Wittig Olefination/Cyclization Sequence" *J. Org. Chem.* **2018**, *83*, 5210–5224.
[43] P. K. Hota, A. Jose, S. K. Mandal, "Stereo– and Regioselective Addition of Arene to Alkyne Using Abnormal NHC Based Palladium Catalysts: Elucidating the Role of Trifluoroacetic Acid in Fujiwara Process" *Organometallics* **2017**, *36*, 4422–4431.
[44] B. Zhao, B. Xu, "Visible–light promoted oxidative cyclization of cinnamic acid derivatives using xanthone as the photocatalyst" *Org. Biomol. Chem.* **2021**, *19*, 568–573.
[45] X.–G. Liu, S.–S. Zhang, C.–Y. Jiang, J.–Q. Wu, Q. Li, H. Wang, "Cp*Co(III)–Catalyzed Annulations of 2–Alkenylphenols with CO: Mild Access to Coumarin Derivatives" *Org. Lett.* **2015**, *17*, 5404–5407.
[46] B. Li, D. Guo, S. Guo, G. Pan, Y. Gao, Y. Wang, "Palladium-Catalyzed C−H Functionalization of Phenyl 2-Pyridylsulfonates" *Chem. Asian J.* **2017**, *12*, 130–144.
[47] T. Ziegler, H. Möhler, F. Effenberger, "Enolether, XVIII Eine einfache Synthese von Cumarinen" *Chem. Ber.* **1987**, *120*, 373–378.

[48] R. A. Kunkalkar, R. A. Fernandes, “Lewis acid–catalyzed annulative partial dimerization of 3–aryloxyacrylates to 4–arylchroman–2–ones: synthesis of analogues of tolterodine, RORγ inhibitors and a GPR40 agonist” *Chem*. *Commun*. **2019**, *55*, 2313–2316.

3. Gold(III)-catalysed cyclization of aryl alkynoates

3.1. Introduction

As presented in the precedent chapters, the direct addition of aromatic C–H bonds to unsaturated substrates by π-acidic catalysis (direct hydroarylation) is a fascinating and challenging chemical transformation, due to the high atom economy of the process and ready availability of substrates.[1] Scientific contributions by several groups report the use of cationic Au(I) complexes to accomplish this task, due to the enhanced carbophilicity of this metal center to promote and we contributed. However, a rather limited number of studies can be found when turning to species that are based on gold(III) metal centers. Up to now, relevant catalytic applications mainly employ simple gold(III) salts that can be activated by a silver co-catalyst,[2,3] generating complex species among which it is difficult to distinguish the catalytically competent one.[4] Moreover, N-heterocyclic carbene (NHC) complexes with a gold(I) metal center were generally found to be superior in catalytic activity with respect to analogous NHC-Au(III) species.[5,6]

Gold(III) catalysis from well-defined complexes has attracted increasing attention in recent years and significant progress has been achieved.[7] Of special note, (P,C)-cyclometalated ligands were discovered to unlock the catalytic potential of electrophilic gold(III) complexes, opening a new avenue for gold-catalyzed hydroarylation.[8] A detailed mechanistic study revealed a strict similarity between those species and the more traditional gold(I) catalysts.[9,10] An outer-sphere pathway was indeed demonstrated to be the most probable, where the coordination of the alkyne at the metal center precedes the effective C–H bond activation (***Figure 3.1***).[9,10] This mechanistic scenario was supported by kinetic isotope experiments and DFT calculations. Moreover, both the catalytically active species, as well as π-alkyne Au(III) intermediates and an off-cycle Wheland-type Au(III) σ-aryl complex were authenticated experimentally by NMR spectroscopy and/or mass spectrometry coupled to CID (collision-induced dissociation) analyses. On the other hand, the mechanistic study has not been extended beyond simple electron-rich arenes as substrates; furthermore, the potential role of the catalyst counterion on the catalytic performance has not been exhaustively explored, compared to gold(I)-catalyzed reactions.[11] For example, Zuccaccia and co-workers recently reported an in-depth study on the role of the counterion X^- (Cl^-, BF_4^- or OTf^-) in the alkyne hydration reaction catalyzed by [(2-phenylpyridine)Au(NHC)X]X complexes by a computational approach coupled to NMR studies.[12] Overall, gold(III) π-acid catalysis appears to hold much

potential in direct hydroarylation reactions, but its study and application remain preliminary at this stage.

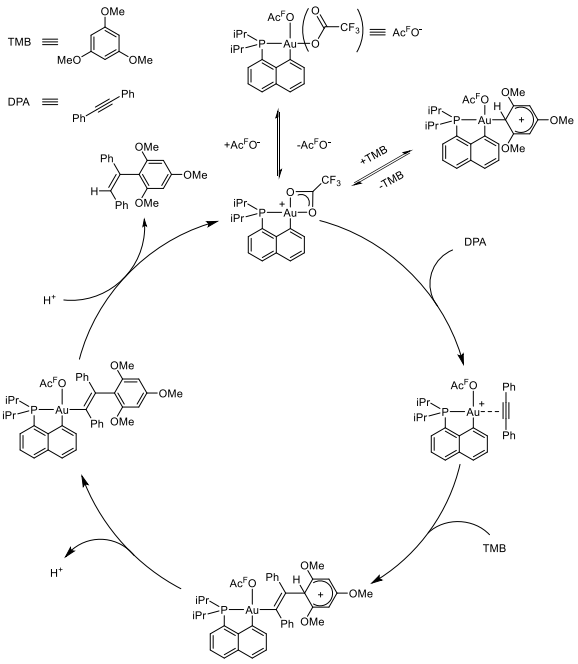

Figure 3.1. *Mechanism proposed to account for the intermolecular hydroarylation of alkynes catalyzed by (P,C)-cyclometalated gold(III) complexes.*

Being of our interest to develop new approaches for efficient and more sustainable gold-based processes, we became involved in applying the hydroarylation of alkynes to the direct synthesis of coumarins and performed a comprehensive study of this catalytic transformation with (P,C)-cyclometalated Au(III) complexes. As presented in the previous chapters, coumarins are conveniently and efficiently prepared by intra- or intermolecular metal-catalyzed hydroarylation processes, with only very few precedents involving Au(III) catalysis to date.[2,4,8] As reported hereafter, the (P,C)-cyclometalated Au(III) complexes proved very efficient catalysts for the synthesis of coumarins by intramolecular hydroarylation. Systematic screening of the reaction variables enabled us to achieve high yields (> 90%) using low amounts of gold catalyst (0.1-2 mol%) under mild and practical conditions (25-40°C, 1-24 hours). In particular, ionic liquids[13] were employed to limit the amount of Brönsted acid used to unlock the catalyst regeneration step, substantiating for the first time the interest and potential of these attractive solvents in catalysis by

well-defined Au(III) complexes.[14] The impact of the acidic additive strength and of the ionic liquid have been preliminarily assessed.

3.2. Results and discussion

Table 3.1. *Direct hydroarylation of ethyl phenylpropiolate with TMB and sesamol.*

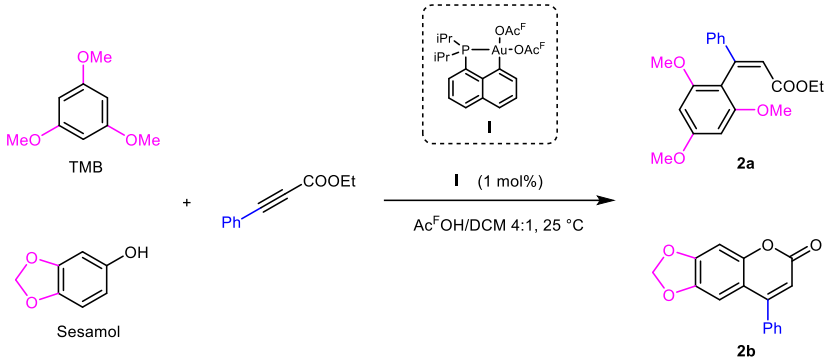

Entry	Substrate	Time [h]	Yield 2a[b] [%]	Yield 2b[b] [%]
1	TMB	0.5	> 99	**-**
2	Sesamol	2	-	Traces
3[c]	Sesamol	2	-	Traces
4[d]	Sesamol	3	-	Traces
5[e]	Sesamol + TMB	1 (24)	5 (8)	- (-)

[a] Reaction conditions: [Alkyne] = 1M, 2eq. arene; [b] yields were determined by ^{1}H NMR spectroscopy using hexamethylbenzene as internal standard; [c] 5 mol% catalyst; [d] reaction performed at 40 °C; [e] 2 eq. sesamol + 2 eq. TMB.

The direct reaction of ethyl phenylpropiolate with sesamol was selected as model reaction to access coumarins. Direct comparison with the benchmark compound 1,3,5-tri-methoxybenzene (TMB) was conducted under the standard conditions developed by Fujiwara: dichloromethane/trifluoroacetic acid 1:4 as solvent and an alkyne/arene molar ratio 1:2.[15,16]

The (iPr_2P,C)Au^{III} complex **I** (***Table 3.1***) yielded as expected 99% of product with TMB at 1 mol% loading after only 1 h at 25 °C (entry 1). However, changing the aromatic substrate to sesamol completely switched off catalysis (entry 2). Further attempts with increased loadings of gold

complex or at higher temperatures were also unsuccessful (entries 3 and 4). Direct analysis of the reaction mixture by ^{31}P NMR{^{1}H} spectroscopy (entry 3) revealed the presence of two main peaks at 90.5 and 79.5 ppm, which are both upfield compared to the signal of the isolated complex **I** (107.8 ppm in $CDCl_3$). This result suggested the presence of inactive resting states of the catalyst. To further support this view, a competitive test (entry 5) revealed that the presence of sesamol inhibits the catalytic coupling with TMB. Imputing this phenomenon to the presence of the hydroxyl moiety of the phenolic substrate and its possible interaction with the catalyst, other aimed tests were performed in order to establish a deactivation path. No evidence for such an interaction was recorded placing **I** and sesamol in ratio 1:2 under Fujiwara's conditions; however, partial conversion of the catalyst was recorded after 1 equiv. of the alkyne was added to the mixture, together with the formation of the coumarin **2b**. The reaction was protracted by further additions of the two substrates to determine almost complete consumption of the gold complex **I** after 5 turnovers. It was then clear that the deactivation mechanism involves the alkyne as well, which should initially □-coordinate to the metal center. The cleavage of a trifluoroacetate ligand by Ac^FOH is needed to start this process, since no reaction of the gold complex **I** with the substrates was observed in pure CD_2Cl_2. The addition of as little as 2% v/v of Ac^FOH (compared to 80% v/v under Fujiwara conditions) was enough to initiate the process, and enabled us to follow it by ^{1}H and ^{31}P NMR spectroscopies. Slow conversion of **I** toward a well-defined species with ^{31}P NMR signal at 90.1 ppm was detected, affording 93% conversion after 24 h. This reaction mixture was subjected to complete characterization by multinuclear NMR spectroscopy and MS spectrometry, to authenticate the newly formed species as the gold-vinyl complex **I-2b'** that is expected to form in the course of the catalytic cycle, with the vinyl group *trans* to P (***Figure 3.2***). Interestingly, when we attempted to purify complex **I-2b'** upon layering the concentrated reaction solution with *n*-hexane, we isolated a solid containing sesamol and the corresponding coumaryl complex **I-2b** (***Figure 3.2***) with ^{31}P NMR signal at 79.5 ppm. Remarkably, complex **I-2b** is much more easily protonolyzed than **I-2b'** (***Figure 3.2***; complete experimental and characterization details are given in the Experimental Section). The inertness of complex **I-2b'** toward protonolysis recalls previously reported results by Tilset and co-workers on the addition of Ac^FOH to acetylene, catalyzed by N,C-cyclometallated gold(III) complexes.[17] In that case as well, the gold-vinyl intermediate with the vinyl group *trans* to the group of the chelating ligand with lower *trans* influence was found to be inert towards protonolysis by Ac^FOH.

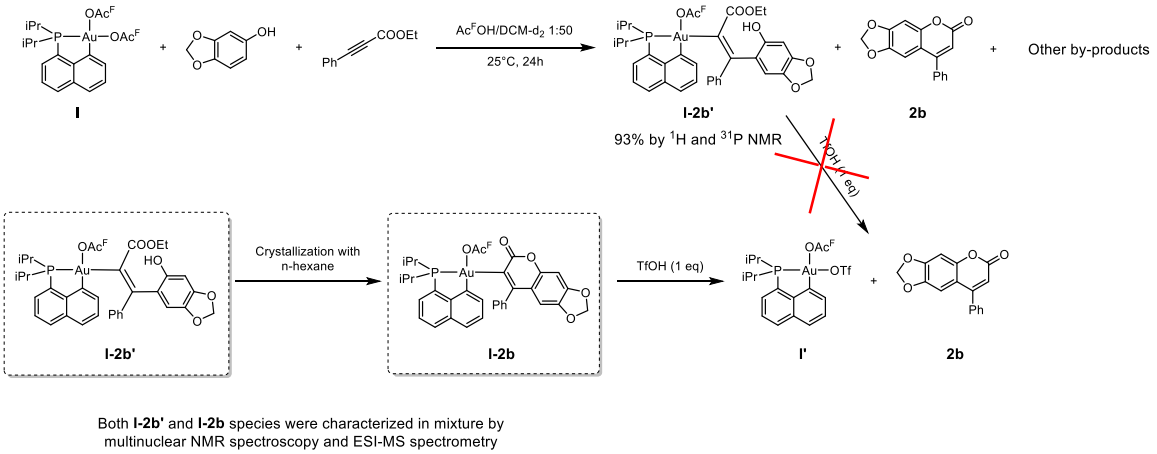

Figure 3.2. *Deactivation pathway authenticated for the intermolecular hydroarylation of alkynes with sesamol catalyzed by the (P,C)-cyclometalated gold(III) complex* ***I****.*

The results of our mechanistic investigation pointed out that the synthesis of coumarins by gold(III) catalyzed hydroarylation could be carried out much more efficiently in an intramolecular fashion, since in this case protonolysis of the resulting coumaryl intermediate should be much faster. Consequently, we started to examine the reactivity of preformed aryl propiolic esters as substrates. The model compound **1b** (***Table 3.2***) was readily synthetized and used for this purpose.

At 0.5 mol% loading, complex **I** was found to efficiently catalyze the cyclization of this substrate, affording the desired product **2b** in 98 % yield within only 1 h at 25 °C (***Table 3.2***, entries 1 and 3). No trace of the regioisomeric product **2'b** was observed. Operating at 40 °C, the catalytic loading could be lowered to 0.1 mol% without compromising the efficiency of the **1b** to **2b** cyclization (entry 3). In line with previous observations,[8] the (Ph_2P,C)-cyclometalated complex **II** demonstrated to be superior in catalytic performance, enabling complete conversion of **1b** within 30 minutes at 25°C and 0.1 mol% loading (entry 4). At this point, the (P,C)-cyclometalated complexes fulfilled our expectations in terms of activity, ease-of-process and robustness of the transformation. However, the high amount of trifluoroacetic acid cosolvent and the volatility of the organic mixture are not ideal practically. To further upgrade the catalytic system, we thus looked for conditions that would maintain similar reaction efficiencies but would at the same time improve the process sustainability and applicability.

Table 3.2. *Intramolecular hydroarylation of* ***1b*** *under Fujiwara's conditions*

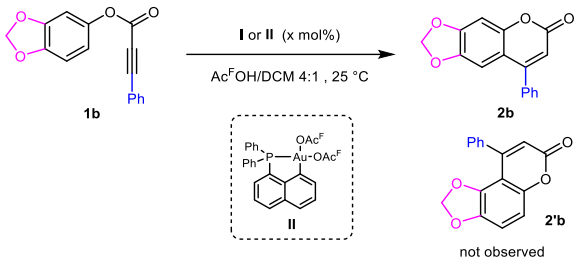

Entry	Cat. (mol%)	Time [h]	Yield 2b[b] [%]
1	**I** (0.5)	1	98
2	**I** (0.1)	3	16
3[c]	**I** (0.1)	1	99
4	**II** (0.1)	1	> 99
5	-	3	Traces

[a] *Reaction conditions: [**1b**] = 1 M;* [b] *yields were calculated by* ^{1}*H NMR spectroscopy using hexamethylbenzene as internal standard;* [c] *reaction performed at 40 °C.*

In this respect, we considered the use of Ionic Liquids (ILs) as a very interesting perspective to have a comparative analysis with the Au(I)-based catalytic system we reported previously. *In*-situ activation of the bis-iodo-(P,C)Au^{III} complexes **III** and **IV** (***Table 3.3***) was achieved by anion exchange with 2 equivalents of silver hexafluoroantimonate to ensure removal of coordinating iodide anions. Complete formation of the di-cationic species was confirmed by ESI-MS analyses (see the Experimental Section for a detailed discussion). Moreover, former kinetic studies by Blons *et al.* have excluded a possible silver effect[18] in the observed catalysis.[8]

Experimental results accounting for the effect of different acid additives (HA) on the hydroarylation of **1b** are disclosed in ***Table 3.3***. The presence of a co-catalyst is indeed mandatory to overcome the energy barrier for protonolysis of the Au–C bond and unlock catalysis (entry 1 vs 5). Three different strong acids were tested (entries 2 to 4). Very similar results were obtained (20-31 % yield after 1 h, > 99 % after 3 h using 20 mol% of HA), indicating minimal impact of the related conjugated base (A = NTf_2, BF_4, OTf). Swapping to precatalyst **IV** (entry 5) enabled to achieve quantitative yields within only 1 h with the three strong acid additives. On the other hand, employing trifluoroacetic acid (Ac^FOH), i.e. the same acid employed in Fujiwara's conditions, resulted in a significant drop in activity, which can be interpreted in terms of the lower acid strength of this additive and/or of the higher tendency of its conjugated base to coordinate to gold(III).[19]

Table 3.3. *Influence of the Brönsted acid additive on the gold(III)-catalyzed intramolecular hydroarylation of* ***1b*** *in [BMIM][NTf$_2$].*

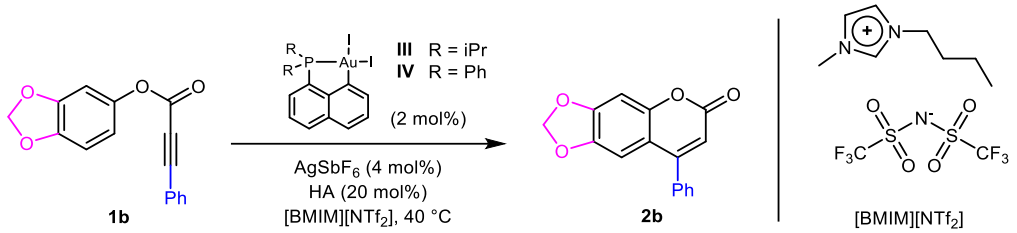

Entry	HA	Cat.	Time [h]	Yield 2b[b] [%]
1[c]	-	**IV**	24	NR[d]
2	$HNTf_2$	**III**	1 (3)	31 (> 99)
3	$HBF_4 \cdot Et_2O$	**III**	1 (3)	28 (> 99)
4	TfOH	**III**	1 (3)	20 (> 99)
5[e]	$HBF_4 \cdot Et_2O$	**IV**	1	> 99
6	Ac^FOH	**IV**	1 (24)	25 (48)
7[f]	$HBF_4 \cdot Et_2O$	**IV**	1 (3)	24 (57)
8[e]	$HBF_4 \cdot Et_2O$	-	3	Traces

[a] Reaction conditions: 0.5 mmol ***1b*** *in 0.75 ml [BMIM][NTf$_2$]; [b] yields were calculated by ^{1}H NMR spectroscopy with 1,2-dimethoxyethane as internal standard; [c] 5mol%* ***IV****, no acid co-catalyst; [d] NR: no reaction; [e] Analogous results were collected with HNTf$_2$ and TfOH; [f] CH_2Cl_2 instead of [BMIM][NTf$_2$] and 4 mol% AgNTf$_2$ as catalyst activator.*

To support our observations, we can recall that Gagné and co-workers already described the reactivity of a cationic diaurated alkenyl intermediate toward different strong acids and recorded the inability of Ac^FOH to perform demetallation of this species.[20,21] As a further example, even more similar to our case, Blum and Roth confirmed that a net positive charge at the metal complex can strongly affect its kinetic relative acidity, enabling only strong acids such as TfOH, to cleave Au–C bonds.[22] On the other hand, the basicity of the phosphine seems to have only a minor role on this step.

Furthermore, substituting [BMIM][NTf$_2$] with dichloromethane as solvent led to lower activities (entry 7), which highlights once more the positive role played by ILs over more traditional organic solvents in this reaction. It is also important to note that a control experiment performed with HBF_4 (20 mol%) but without gold complex resulted in only traces of coumarin **2b** after 3 hours (entry 8).[23]

The effect of the anion of the IL was then investigated using different ionic liquids [BMIM][X] (***Table 3.4***) with 0.5 mol% gold(III) complex **IV**. The acid co-catalyst $HBF_4{\cdot}Et_2O$ was kept as standard additive. Its pK_a is lower than that of the conjugated acids of most of the other anions X^-, with the only exception of OAc^F. In the latter case, the actual co-catalyst is Ac^FOH.[24,25]

Table 3.4. *Effect of the ionic liquid anion on the gold(III)-catalyzed intramolecular hydroarylation of* ***1b****.*

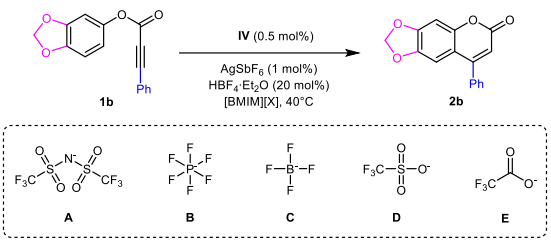

Entry	[X]	Time [h]	Yield 2b[b] [%]
1	**A**	1 (3)	34 (> 99)
2	**B**	1 (3)	90 (> 99)
3	**C**	1 (3)	90 (> 99)
4	**D**	3 (24)	28 (85)
5	**E**	24	NR[c]

[a] Reaction conditions: 0.5 mmol ***1b*** *in 0.75 ml [BMIM][X] [b] yields were calculated by ^1H NMR spectroscopy with 1,2-dimethoxyethane as internal standard; [c] NR: no reaction.*

Because of this, and because of the large excess of Ac^FO^- over gold complex, leaving no available coordination site for substrate coordination, no catalytic activity was recorded over 24 h in [BMIM][OAc^F] (entry 5).

On the other hand, anions that interact more weakly with the gold center, such as PF_6^- **B** and BF_4^- **C**, express the highest activity. The coumarin product is obtained in almost 90% yield within 1 h (entries 2 and 3). The anion NTf_2^- **A** provides somewhat lower activity, but still allows full conversion of the substrate in 3 h (entry 1). Conversely, much lower activity was observed with the anion TfO^- **D** (entry 4), 24 h being needed in this case to obtain 85 % of product. This result is likely the consequence of the higher affinity of **D** for the gold(III) metal center. Thus, the recorded differences in reactivity with different anions of the IL seem to correlate well with the coordinating ability of the anion, which in case of gold(I) catalysis has been expressed through the GAI (gold affinity index) of the anion itself.[11b] In spite of these findings, we chose to employ the ionic liquid [BMIM][NTf_2] for practical reasons, since it is easier to work with ionic liquids containing NTf_2^- compared to BF_4^- and PF_6^- due to the higher stability of the former. Aging of ILs, caused in particular by the absorption of water and consequent hydrolysis of the BF_4^- or PF_6^- anions,[26] is indeed an issue potentially causing poorly reproducible results when these solvents are employed in our reactions.

Table 3.5. *Scope of the gold(III)-catalyzed cyclization of aryl alkynoates in ionic liquids.*

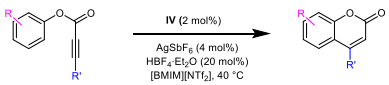

Entry	1	2	Yield [%][b]
1	1b	2b	>99 (1h) **99 (1h)**[c]
2	1c	2c	>99 (1h) **94 (1h)**[c]
3	1d	2d	>99 (0.5h) **97 (0.5h)**[c]
4	1e	2e	>99 (0.5h) **99 (0.5h)**[c]
5	1f	2f	>99 (0.5h) **98 (0.5h)**[c]
6	1g	2g	87 (24h) **80 (24h)**[c]
7	1h	2h	97 (24h)
8	1i	2i	90 (5h)
9	1j	2j	82 (5h) 94 (24h) **88 (24h)**[c]
10	1k	2k	35 (24h) 80 (3h)[d] **71 (3h)**[c,d]
11	1l	2l	>99 (24h)
12	1m	2m	16 (24h) 30 (24h)[d] **22 (24h)**[c,d]
13	1n	2n + 3n	66 (5h) 34 (5h)
14	1o	2o + 3o	87 (1h) 13 (1h)
15	1p	2p	>99 (3h)
16	1q	2q	>99 (3h) **92 (3h)**[c]

[a] *Conditions: 0.5mmol of* ***1*** *in 0.75ml [BMIM][NTf$_2$];* [b] *yields were calculated by* ^{1}*H NMR vs internal standard 1,2-dimethoxyethane (reaction time is reported in parenthesis);* [c] *isolated yield;* [d] *[BMIM][BF$_4$] instead of [BMIM][NTf$_2$], 5mol%* ***IV*** *at 60°C*

After having examined the effects of the acid additive and of the ionic liquid anion, the substrate scope of the intramolecular reaction was assessed under the above optimized conditions: complex **IV** (2 mol%), $AgSbF_6$ (4 mol%), $HBF_4.Et_2O$ (20 mol%), IL [BMIM][NTf_2] (***Table 3.5***).

In the first stage, we evaluated the substituent effect at the alkyne. Keeping constant the sesamol moiety, products were obtained in quantitative yields within 1 h for the internal alkynes (with phenyl and *n*-propyl substituents) as well as terminal alkynes (> 94 % yield in 0.5 h, entries 1 to 3). The presence of substituents at the 3-5 positions of the arene moiety showed no steric influence on the conversion to the coumarin products (entries 4 and 5). Conversely, substrates **1g** and **1h** with an unsubstituted phenyl react significantly slower, high cyclization yields requiring 24 h (entries 6 and 7). Introducing a 4-*tert*-butyl substituent is enough to restore high catalytic activity, allowing to obtain 90 % **2i** and 82 % **2j** in high yields within only 5 h (88% of **2j** was isolated after 24h reaction).

The cyclization of biphenyl-4-yl propiolate **1l** proceeded slowly but quantitatively under standard conditions (entry 11), while for the related substrate **1k**, turning to [BMIM][BF_4] as IL and heating to 60 °C proved necessary to obtain the corresponding coumarin **2k** in good yield, 71% at best (entry 10). Attempts to extend the reaction to the bromide-substituted substrate **1m** gave modest results (entry 12). For substrates with electron-depleted aryl moieties such as **1k** and **1m**, byproducts deriving from the hydrolysis of the ester moiety were consistently detected. The best obtained yields are however comparable to those reported by He and Shi with the $AuCl_3$/AgOTf system, which are the best achieved so far with these substrates upon gold catalysis.[2]

Moving to **1n** and **1o** featuring 4-methoxy substituted aryl moieties revealed an interesting selectivity issue. Indeed, with these substrates the *ipso* position is activated and may compete with the *ortho* positions for nucleophilic attack to the alkyne, giving spirocyclic lactones instead of coumarins. This side process has been already reported by Vadola *et al*., who showed that the gold(I) catalytic system (Ph_3P)AuCl + AgOTf affords the spiro lactone with high selectivity in the presence of 1 equivalent of water.[27] In our case, only traces of water are present in the [BMIM][NTf_2] ionic liquid, which probably favor the formation of the coumarin over the corresponding spirocyclic lactone. The hydroarylation proceeds faster from **1o** than **1n**, which limits the formation of spirocycle **3o** to 13% (entry 14). The competition between these two cyclization pathways prompted us to take a closer look at the effect of the reaction conditions on product selectivity, using (Ph_2P,C)-cyclometalated Au(III) complexes **II** and **IV** (***Table 3.6***).

Fujiwara's conditions were tested first. Interestingly, operating at 2 mol% catalytic loading, low activity but exclusive selectivity towards **3n** were recorded (entry 2). Increasing the catalytic loading to 5 mol% enabled to achieve complete conversion of **1n** after 24 h and to obtain the spirolactone **3n** in 89% isolated yield (entry 3). The ability of the Ac^FO^- anion to assist O-demethylation probably plays a major role in the observed chemoselectivity. The crude mixture actually displays a ^{1}H NMR signal at δ 3.99 ppm accounting for the concomitant formation of the trifluoroacetate methyl ester. As for the IL conditions, it was also possible to obtain **3n** in high yield (97 %) using [BMIM][OTf] and 5 mol% of complex **IV** (entry 5). The TfO^- anion is more nucleophilic than the NTf_2^- anion in the commonly employed IL [BMIM][NTf_2] and may better assist the O-demethylation; it also makes the IL more hygroscopic, which may explain the complete selectivity for the dearomative spirocyclization.

Table 3.6. *Impact of the reaction conditions on the coumarin vs spirolactone formation from* ***1n****.*

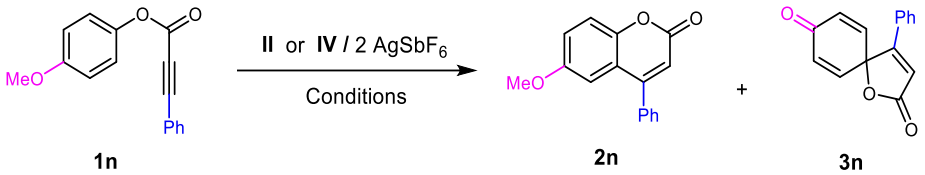

1n **2n** **3n**

Entry	Conditions[a,b]	Cat. (mol%)	Time [h]	Conv. 1n[c] [%]	Yield 2n[c] [%]	Yield 3n[c] [%]
1	IL, [X]=[NTf_2]	**IV** (2)	5	>99	66	34
2	Fujiwara's	**II** (2)	24	37	-	37
3	Fujiwara's	**II** (5)	24	98	Traces	92 (89)[d]
4	IL, [X]=[OTf]	**IV** (2)	24	30	-	29
5	IL, [X]=[OTf]	**IV** (5)	24	>99	-	97

[a] IL conditions: 0.5 mmol ***1n*** *in 0.75 ml [BMIM][X], 20 mol% $HBF_4{\cdot}Et_2O$, 40°C; [b] Fujiwara's conditions: DCM/Ac^FOH 1:4 v/v, [**1n**]=1M at 25°C; [c] yields and conversions were calculated by ^1H NMR spectroscopy using hexamethylbenzene (Fujiwara's conditions) or 1,2-dimethoxyethane (IL conditions) as internal standards; [d] isolated yield.*

Finally, to probe the impact of the aryl group (phenyl *vs* naphthyl) on the hydroarylation/spirocyclization competition, we prepared and tested substrates **1p** and **1q**. Here, the corresponding coumarins were quantitatively obtained within 3 h whatever the position of the methoxy group (entries 15 and 16, ***Table 3.5***). Moreover 92% of **2q** could be isolated after complete conversion of the alkynoate (entry 16).

The last part of the work was focused on the activation of more electron-rich alkynes. Aryl propargyl ethers were selected to explore a further application of our system to the synthesis of chromenes (***Table 3.7***).

Remarkably rapid conversion of substrates **4h** and **4o** was observed under the same conditions developed for coumarin synthesis (entries 1 and 2). However, complex mixtures were obtained due to the fast degradation of the obtained chromenes under reaction conditions. Chromene **5o** accumulated in the reaction mixture and its consumption was monitored over-time (entries 4 and 5). Fujiwara's conditions allowed to reach 67% of **5o**, stopping the reaction after 30 minutes (entry 4). On the other hand, any attempt to expand the scope to substrates **4h** (entry 3) and **4c** (entries 6

to 8) produced much poorer results, due to the fast degradation of the chromenes with respect to cyclization rates.

Table 3.7. *Synthesis of chromenes*

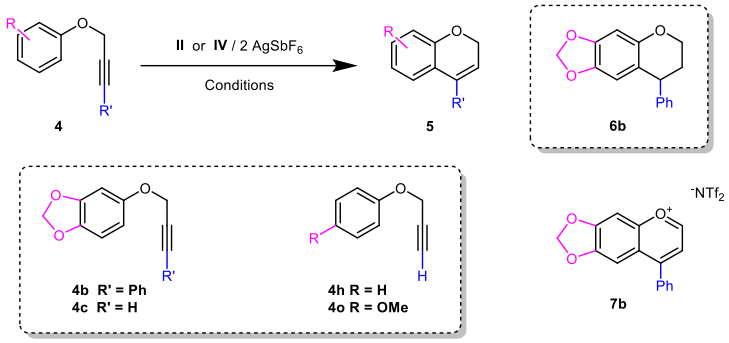

Entry	Conditions [a,b]	Substrate	Cat. (mol%)	Time [h]	Conv. 4[c] [%]	Yield 5[c] [%]
1	IL	**4h**	**IV** (2)	1	94%	n.d.[d]
2	IL	**4o**	**IV** (2)	1	>99	n.d.[d]
3	Fujiwara's	**4h**	**II** (0.5)	3 (24)	15 (47)	n.d.[d]
4	Fujiwara's	**4o**	**II** (0.5)	0.5 (6)	>99	67 (< 5)
5[e]	IL	**4o**	**IV** (2)	0.5 (1)	>99	30 (12)
6[e]	IL	**4c**	**IV** (2)	0.5	>99	n.d.[d]
7	Fujiwara's	**4c**	**II** (0.5)	0.5	>99	n.d.[d]
8[f]	IL	**4c**	**IV** (2)	1 (4)	75 (>99)	21 (Traces)
9	IL	**4b**	**IV** (2)	5	95	n.d.[d,g]
10[f]	IL	**4b**	**IV** (2)	1 (24)	40 (84)	30 (13)[h]

*[a] IL conditions: 0.5mmol **1n** in 0.75 ml [BMIM][NTf_2], 20 mol% HBF_4·Et_2O or $HNTf_2$ at 40°C; [b] Fujiwara's conditions: DCM/Ac^FOH 1:4 v/v, [**4**]=1M at 25°C; [c] yields and conversions were calculated by ^1H NMR using hexamethylbenzene (Fujiwara's conditions) or 1,2-dimethoxyethane (IL conditions) as internal standards; [d] n.d.: not detected; [e] reaction performed at 25°C; [f] No acid co-catalyst was employed; [g] **6b** was detected with 72% yield; [h] **6b** was detected in traces and then with 20% yield respectively at 1 h and 24 h reaction time;*

No improvements were recorded operating under IL conditions rather than Fujiwara's ones. However, an interesting result was obtained from **4b**, leading to the formation of the chromane **6b** as major product (72% yield, entry 9). Overreduction of chromenes was already reported by Sames

et al. as a side-process in the intramolecular hydroarylation of aryl propargyl ethers using $Pd(OAc)_2$ under Fujiwara's conditions.[28] Assuming that the acid conditions play a role in the reduction of the initially formed chromene, we performed some blank tests reacting **5b** along with HBF_4 and [BMIM][NTf_2] as reaction medium (see the Experimental Section for details). Formation of chromane **6b** was observed, along with the corresponding benzopyrilium salt **7b**, which was unambiguously authenticated by ^1H NMR spectroscopy. To our knowledge, this disproportionation process has never been reported before in the case of chromenes, while a similar acid-initiated process is known for 1,2-dihydronaphtalene and quinoline derivatives.[23,29,30] This new reactivity could be usefully applied for synthetic purposes. Benzopyrilium salts are indeed valuable intermediates for the synthesis of 4H-chromenes or 2-subtituted chromenes, upon nucleophilic attack at 4 or 2 position, respectively.[31,32] Moreover, taking as an example the work conducted by Chang and co-workers[23] we successfully synthesized **7b** directly from **4b** by addition of 1 equivalent of $HNTf_2$ in dichloromethane (details are reported in the Experimental Section).

Whereas formation of **7b** seems to require acid conditions, formation of the chromane **6b** was recorded also under neutral conditions in the presence of gold complex **IV** after 1 day of reaction (entry 10). It is clear that the gold catalyst also contributes to consume the chromene product over time (entries 8 and 10). More studies are needed to clarify what is the nature of those secondary processes.

3.3. Conclusions and perspectives

In this chapter, we presented a practical methodology to access coumarins employing (P,C)-cyclometalated Au(III) complexes as hydroarylation catalysts in ILs. Direct cyclization of aryl alkynoates was demonstratedly operated at low loading of gold (0.1-2 mol%) employing sub-stoichiometric quantities of Brønsted acid additive (20 mol%).

The reaction scope showed good compatibility toward different propiolate fragments. The transformation works best when the aromatic ring bears electron donating groups, with the exception of *para*-methoxy substituents due to competitive dearomative spirocyclization. Conversely, we found that it is possible to obtain the spirolactone with complete selectivity under both Fujiwara's and IL conditions. In general, the gold(III)-based catalytic system proved to be competitive with other gold(I)-based systems previously described in the literature.

Attempts to further extend the application of the gold(III) catalyst system to the cyclization of aryl propargyl ethers were difficult due to the instability of the ensuing chromenes under the employed reaction conditions. However, an acid-mediated disproportionation process leading to chromanes and benzopyrilium salts was disclosed.

Future work will aim at exploring and developing gold(III) catalysis in ILs. In particular, ligand design will be optimized in order to overcome catalyst deactivation currently hampering efficient coumarin synthesis by intermolecular direct alkyne hydroarylation with phenols.

3.4. References

[1] a) C. Nevado, A. M. Echavarren, *Chem. Eur. J.* **2005**, *11*, 3155–3164; b) H. C. Shen, *Tetrahedron* **2008**, *64*, 3885–3903; c) T. Ghosh, J. Chatterjee, S. Bhakta, *Org. Biomol. Chem.* **2022**, *20*, 7151–7187.

[2] Z. Shi, C. He, *J. Org. Chem.* **2004**, *69*, 3669–3671.

[3] Z. Li, Z. Shi, C. He, *J. Organomet. Chem.* **2005**, *690*, 5049–5054.

[4] M. T. Reetz, S. Sommer, *Eur. J. Org. Chem.* **2003**, 3485–3496.

[5] P. De Frémont, R. Singh, E. D. Stevens, J. L. Petersen, S. P. Nolan, *Organometallics* **2007**, *26*, 1376–1385.

[6] C. Tubaro, M. Baron, A. Biffis, M. Basato, *Beilstein J. Org. Chem.* **2013**, *9*, 246–253.

[7] a) W. Henderson, *Adv. Organomet. Chem.* **2006**, *54*, 207-265; b) R. Kumar, C. Nevado, *Angew. Chem. Int. Ed.* **2017**, *56*, 1994–2015; c) L. Rocchigiani, M. Bochmann, *Chem. Rev.* **2021**, *121*, 8364-8451.

[8] C. Blons, S. Mallet-Ladeira, A. Amgoune, D. Bourissou, *Angew. Chem. Int. Ed.* **2018**, *57*, 11732–11736.

[9] M. S. M. Holmsen, C. Blons, A. Amgoune, M. Regnacq, D. Lesage, E. D. Sosa Carrizo, P. Lavedan, Y. Gimbert, K. Miqueu, D. Bourissou, *J. Am. Chem. Soc.* **2022**, *144*, 22722–22733.

[10] M. Regnacq, D. Lesage, M. S. M. Holmsen, K. Miqueu, D. Bourissou, Y. Gimbert, *Dalton Trans.* **2023**, *52*, 13528–13536.

[11] a) M. Jia, M. Bandini, *ACS Catal.* **2015**, *5*, 1638–1652; b) Z. Lu, J. Han, O. E. Okoromoba, N. Shimizu, H. Amii, C. F. Tormena, G. B. Hammond, B. Xu, *Org. Lett.* **2017**, *19*, 5848–5851; c) J. Schießl, J. Schulmeister, A. Doppiu, E. Wörner, M. Rudolph, R. Karch, A. S. K. Hashmi, *Adv. Synth. Catal.* **2018**, *360*, 2493–2502; d) L. Biasiolo, A. Del Zotto, D. Zuccaccia, *Organometallics* **2015**, *34*, 1759–1765; e) M. Trinchillo, P. Belanzoni, L. Belpassi, L. Biasiolo, V. Busico, A. D'Amora, L. D'Amore, A. Del Zotto, F. Tarantelli, A. Tuzi, D. Zuccaccia, *Organometallics* **2016**, *35*, 641–654.

[12] J. Segato, E. Aneggi, W. Baratta, F. Campagnolo, L. Belpassi, P. Belanzoni, D. Zuccaccia, *Organometallics* **2023**, *42*, 2973−2982.

[13] For previous reports on the advantageous use of ionic liquids in metal-catalyzed, direct alkyne hydroarylation processes, see a) C. E. Song, D.-U. Jung, S. Y. Choung, E. J. Roh, S.-G. Lee, *Angew. Chem. Int. Ed.* **2004**, *43*, 6183 –6185; b) D. S. Choi, J. H. Kim, U. S. Shin, R. R. Deshmukh, C. E. Song, *Chem. Commun.* **2007**, 3482– 3484; c) M. Y. Yoon, J. H. Kim, D. S. Choi, U. S. Shin, J. Y. Lee, C. E. Song, *Adv. Synth. Catal.* **2007**, 349, 1725– 1737; d) A. Biffis, L. Gazzola, C. Tubaro, M. Basato, *ChemSusChem* **2010**, *3*, 834–839; e) M. Baron, A. Biffis, *Eur. J. Org. Chem.* **2019**, 3687–3693; f) S. Bonfante, P. Bax, M. Baron, A. Biffis, *Catalysts* **2023**, *13*, 822.

[14] Simple gold(III) salts in ionic liquids have been occasionally employed in catalysis, without identifying the actual catalytically competent species: a) I. Ambrogio, A. Arcadi, S. Cacchi, G. Fabrizi, F. Marinelli, *Synlett* **2007**, *2007*, 1775–1779; b) A. Corma, I. Dominguez, T. Rodenas, M. Sabater, *J. Catal.* **2008**, *259*, 26–35; c) F. Neaţu, V. I. Pârvulescu, V. Michelet, J.-P. Gênet, A. Goguet, C. Hardacre, *New J. Chem.* **2009**, *33*, 102–106; d) L. F. Bobadilla, T. Blasco, J. A.

Odriozola, *Phys. Chem. Chem. Phys.* **2013**, *15*, 16927-16934; e) N. Morita, K. Ikeda, H. Chiaki, R. Araki, K. Tanaka III, Y. Hashimoto, O. Tamura, *HETEROCYCLES* **2021**, *103*, 714-722.

[15] C. Jia, W. Lu, J. Oyamada, T. Kitamura, K. Matsuda, M. Irie, Y. Fujiwara, *J. Am. Chem. Soc.* **2000**, *122*, 7252–7263.

[16] C. Jia, D. Piao, T. Kitamura, Y. Fujiwara, *J. Org. Chem.* **2000**, *65*, 7516–7522.

[17] M. S. M. Holmsen, A. Nova, D. Balcells, E. Langseth, S. Øien-Ødegaard, R. H. Heyn, M. Tilset, G. Laurenczy, *ACS Catal.* **2017**, *7*, 5023–5034.

[18] For previous reports on "silver effect", see a) D. Wang, R. Cai, S. Sharma, J. Jirak, S. K. Thummanapelli, N. G. Akhmedov, H. Zhang, X. Liu, J. L. Petersen, X. Shi, *J. Am. Chem. Soc.* **2012**, *134*, 9012–9019; b) A. Homs, I. Escofet, A. M. Echavarren, *Org. Lett.* **2013**, *15*, 5782–5785; c) Z. Lu, J. Han, G. B. Hammond, B. Xu, *Org. Lett.* **2015**, *17*, 4534–4537; d) A. Zhdanko, M. E. Maier, *ACS Catal.* **2015**, *5*, 5994–6004.

[19] S. Komiya, J. K. Kochi, *J. Am. Chem. Soc.* **1976**, *98*, 7599–7607.

[20] D. Weber, M. A. Tarselli, M. R. Gagné, *Angew. Chem. Int. Ed.* **2009**, *48*, 5733–5736.

[21] D. Weber, M. R. Gagné, *Chem. Sci.* **2013**, *4*, 335–338.

[22] K. E. Roth, S. A. Blum, *Organometallics* **2010**, *29*, 1712–1716.

[23] a) C. Zhang, S. Lv, Y. Wang, J. Zhang, X.-N. Wang, J. Chang, *Org. Chem. Front.* **2022**, *9*, 1300–1307; b) H. Choi, J. Kim, K. Lee, *Tetrahedron Lett.* **2016**, *57*, 3600–3603; c) O. Zaitceva, V. Bénéteau, D. S. Ryabukhin, B. Louis, A. V. Vasilyev, P. Pale, *ChemCatChem* **2020**, *12*, 326–333; d) D. S. Ryabukhin, A. V. Vasilyev, S. Yu. Vyazmin, *Russ. Chem. Bull.* **2012**, *61*, 843–846.

[24] A. Kütt, T. Rodima, J. Saame, E. Raamat, V. Mäemets, I. Kaljurand, I. A. Koppel, R. Yu. Garlyauskayte, Y. L. Yagupolskii, L. M. Yagupolskii, E. Bernhardt, H. Willner, I. Leito, *J. Org. Chem.* **2011**, *76*, 391–395.

[25] E. Paenurk, K. Kaupmees, D. Himmel, A. Kütt, I. Kaljurand, I. A. Koppel, I. Krossing, I. Leito, *Chem. Sci.* **2017**, *8*, 6964–6973.

[26] M. G. Freire, C. M. S. S. Neves, I. M. Marrucho, J. A. P. Coutinho, A. M. Fernandes, *J. Phys. Chem. A* **2010**, *114*, 3744–3749.

[27] M. D. Aparece, P. A. Vadola, *Org. Lett.* **2014**, *16*, 6008–6011.

[28] S. J. Pastine, S. W. Youn, D. Sames, *Org. Lett.* **2003**, *5*, 1055–1058.

[29] K. Sisido, H. Nozaki, *J. Am. Chem. Soc.* **1948**, *70*, 1609–1612.

[30] T. P. Forrest, G. A. Dauphinee, S. A. Deraniyagala, *Can. J. Chem.* **1985**, *63*, 412–417.

[31] R. Doodeman, F. P. J. T. Rutjes, H. Hiemstra, *Tetrahedron Lett.* **2000**, *41*, 5979–5983.

[32] Z. Wen, K. Yang, J. Deng, L. Chen, *Adv. Synth. Catal.* **2023**, *365*, 1290–1331.

3.5. Experimental section

Synthesis of (P,C) pro-ligands [4,5]

1,8-Diiodonaphtalene (304.0 mg, 0.80 mmol, 1.0 eq.) was dissolved in THF (15 ml) and a solution of ^{n}BuLi (1.6 M or 2.5 M in hexanes, 0.84 mmol, 1.05 eq.) was added dropwise at -78 °C. The reaction mixture was stirred at -78 °C for 1 h. Then iPr_2PCl or Ph_2PCl (0.80 mmol, 1.0 eq.) was added dropwise and the reaction mixture was allowed to warm to room temperature and stirred over-night. All volatiles were removed under reduced pressure and the residue subjected to column chromatography over silica gel (gradient from pure hexane to Tol/Hex 1:1 v/v). The desired products were obtained upon evaporation of the relevant fractions as yellowish solids. Yields and spectroscopic data are in line with the ones previously reported.

1-iodo-8-di-isopropylphosphino-naphtalene [4]

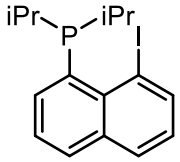

^{1}H NMR (300 MHz, C_6D_6): δ 8.25 (dd, *J* = 7.4, 1.3 Hz, 1H), 7.63 (d, *J* = 6.7 Hz, 1H), 7.42 (d, *J* = 7.5 Hz, 2H), 6.59 (t, *J* = 7.5 Hz, 2H), 2.09 (heptd, *J* = 7.0 Hz, $^{2}J_{H\text{-}P}$ = 2.2 Hz, 2H), 1.15 (dd, $J_{P\text{-}H}$ = 13.7 Hz, *J* = 7.0 Hz, 6H), 0.95 (dd, $^{3}J_{H\text{-}P}$ = 12.7 Hz, *J* = 7.0 Hz, 6H) ppm; **^{31}P{^{1}H} (121 MHz, C_6D_6):** δ = -7.8 (s) ppm;

1-iodo-8-di-phenylphosphino-naphtalene [5]

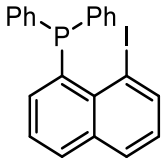

^{1}H NMR (300 MHz, $CDCl_3$): δ 8.30 (dd, *J* = 7.4, 1.1 Hz, 1H), 7.86 (dtd, *J* = 8.1, 1.4, 0.3 Hz, 1H), 7.80 (dd, *J* = 7.6, 1.9 Hz, 1H), 7.24 – 7.36 (m, 12H), 7.09 (dd, *J* = 8.0, 7.4 Hz, 1H) ppm ; **^{31}P{^{1}H} NMR (121 MHz, $CDCl_3$):** δ -12.6 (s) ppm;

Synthesis of the bis-iodo-gold(III) complexes III and IV [5,6]

Gold iodide (130 mg, 0.4 mmol) was suspended in toluene (5 ml) and a solution of the selected ligand (0.4 mmol) in toluene (10 ml) was added dropwise at room temperature. The reaction mixture was stirred at 60°C for 5h. Complete conversion of the ligand was confirmed by ^{31}P NMR (no-lock experiment). All volatiles were removed *in vacuo* to yield the desired complex, which was successfully crystallized by layering a saturated DCM solution with n-hexane.* Yields and analytic data are in line to the ones previously reported.

* if needed, the final product can be further purified by column chromatography (eluent DCM/Hex 1:1).

Bis-iodo-(8-di-isopropyl-1-naphthyl)-cyclometalated gold (III) – Complex III *

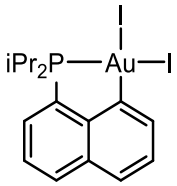

^{1}H NMR (300 MHz, $CDCl_3$): δ 9.38 (d, *J* = 7.6 Hz, 1H), 8.06 (dd, *J* = 7.9, 3.2 Hz, 1H), 7.84 (dd, *J* = 8.0, 2.4 Hz, 1H), 7.80-7.72 (m, 1H), 7.60 (td, *J* = 7.5, 3.2 Hz, 1H), 7.08 (t, *J* = 7.9 Hz, 1H), 3.42 (heptd, *J* = 6.9, 3.5 Hz, 2H), 1.43 (dd, *J* = 19.6, 7.0 Hz, 6H), 1.37 (dd, *J* = 17.8, 7.0 Hz, 6H) ppm; **^{31}P{^{1}H} NMR (121 MHz, $CDCl_3$):** δ 88.8 (s) ppm;

* spectra are in agreement with the ones previously reported in C_6D_6.

Bis-iodo-(8-di-phenyl-1--naphthyl)-cyclometalated gold (III) – Complex IV

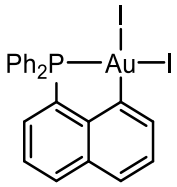

^{1}H NMR (300 MHz, $CDCl_3$): δ 9.37 (ddd, *J* = 7.5, 1.3, 1.0 Hz, 1H), 8.00 – 8.06 (m, 1H), 7.78–7.91 (m, 5H), 7.45–7.66 (m, 9H) ppm; **^{31}P{^{1}H} NMR (121 MHz, $CDCl_3$):** δ 51.8 (s) ppm;

Synthesis of the bis-(trifluoroacetate)-gold(III) complexes I and II [7]

Complex **III** or **IV** (0.05 mmol, 1eq.) was dissolved in 1 mL of DCM and added to a suspension of silver trifluoroacetate (22.1 mg, 0.1 mmol, 2 eq.) in 1 mL of DCM. The mixture was stirred for 30 min during which AgI precipitated as the solution color varied from reddish/orangish to colorless. The suspension was filtered over a Celite® pad, and the solvent removed under reduced pressure to afford the desired product. Yields and spectroscopic data are in accordance with the ones previously reported.

Bis-(trifluoroacetate)-(8-di-isopropyl-1-naphthyl)-cyclometalated gold (III) – Complex I *

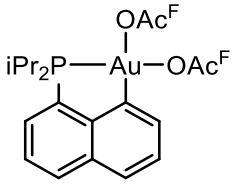

^{1}H NMR (300 MHz, $CDCl_3$): δ 8.10 (ddd, *J* = 7.8, 3.4, 1.3 Hz, 1H), 7.87 (dd, *J* = 7.9, 3.0 Hz, 1H), 7.78 (ddd, *J* = 7.6, 3.1, 0.6 Hz, 1H), 7.72 (ddd, *J* = 8.7, 3.0, 1.1 Hz, 1H), 7.67 (ddd, *J* = 7.6, 7.2, 4.3 Hz, 1H), 7.51 (t, *J* = 7.9, 1H), 3.12 (heptd, *J* = 7.1, 2.1 Hz, 2H), 1.40 (dd, , *J* = 19.2, 7.1 Hz, 6H), 1.39 (dd, *J* = 20.2, 7.1 Hz 6H) ppm ; **^{31}P{^{1}H} NMR (121 MHz, $CDCl_3$):** δ 107.8 (s) ppm ; **^{19}F{^{1}H} NMR (282 MHz, $CDCl_3$):** δ -74.1 (s, OAc^F trans to C) ppm;**

Bis-(trifluoroacetate)-(8-di-phenyl-1--naphthyl)-cyclometalated gold (III) – Complex II *

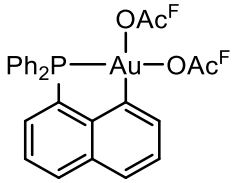

^{1}H NMR (300 MHz, $CDCl_3$): δ 8.12 (ddd, *J* = 7.9, 3.6, 0.8 Hz, 1H), 7.90 (dd, *J* = 8.1, 3.6 Hz, 1H), 7.88–7.78 (m, 5H), 7.76–7.68 (m, 3H), 7.67 (ddd, *J* = 8.0, 7.3, 4,3 Hz, 1H), 7.64–7.56 (m, 4H), 7.55 (t, *J* = 7.9 Hz, 1H) ppm ; **^{31}P{^{1}H} NMR (121 MHz, $CDCl_3$):** δ 64.4 (s) ppm ; **^{19}F NMR (282 MHz, $CDCl_3$):** δ -73.9 (brs, OAc^F trans to P), -74.1 (brs, OAc^F trans to C) ppm;

* the spectra are in agreement with the ones previously reported in CD_2Cl_2. [7]

** -OAc^F *trans* to P was not detected using $CDCl_3$ as deuterated solvent, while it was observed in

CD_2Cl_2 as a broad singlet located at -73.3 ppm.

Synthesis of aryl-alkynoates

• Aryl-alkynoates **1b**, **1d**, **1e**, **1f**, **1g**, **1h**, **1i**, **1j**, **1k**, **1l**, **1m** and **1n** were synthetized according to the following literature procedure.[8]

In a round-bottom flask, a stirred solution of the phenol (3.0 mmol, 1.0 eq.) in DCM (12 ml) was cooled to 0°C and the propiolic acid derivative (3.3 mmol, 1.1 eq.) was added. Subsequently, a mixture of DCC (873.0 mg, 4.4 mmol, 1.5 eq.) and DMAP (36.0 mg, 0.3 mmol, 0.1 eq.) in DCM (6 mL) was added dropwise to the round-bottom flask. The resulting mixture was allowed to warm up and stirred at room temperature for 12 hours. Then the mixture was filtered and the solid residue on the filter was washed with DCM (15 mL). The combined organic phases were concentrated under reduced pressure and the obtained residue purified by flash chromatography over silica gel. The desired product was isolated upon evaporation of the relevant fractions.

• Aryl-propiolates **1c**, **1o**, **1p** and **1q** were obtained by the following synthetic route.[9]

A stirred solution of the phenol (1.0 mmol, 1.0 eq.) in THF (10 ml) at 0°C was pretreated with sodium hydride (60% suspension in mineral oil, 1.1 mmol, 1.1 eq.). In a second flask, a solution of propiolic acid (3.3 mmol, 3.3 eq.) in THF (10 ml) was cooled to 0 °C and then treated with DCC (3.3 mmol, 3.3 eq.) followed by the phenolate solution that was previously prepared. The resulting mixture was allowed to warm up to room temperature and stirred for 16 h. The mixture was then concentrated under reduced pressure and taken up in acetonitrile (10 ml) before filtration. The filtrate was again concentrated under reduced pressure, and the residue subjected to flash chromatography over silica gel. The desired product was isolated upon evaporation of the relevant fractions.

Spectroscopic data of all known compounds were consistent with the ones reported in the literature. The molecular connectivity of **1b**, **1d**, **1f**, **1j** and **1q** was univocally determined by correlation NMR experiments and their chemical identity was further confirmed after cyclization tests.

3',4'-Methylendioxy-phenyl 3-phenyl-propiolate – 1b [10]

Isolated as a white solid (eluent EtOAc/Hex 1:10 v/v) with 74% yield (593 mg, 2.22 mmol).

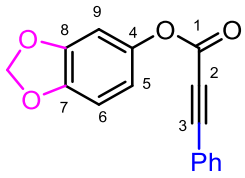

^{1}H NMR (300 MHz, $CDCl_3$): δ 7.66–7.60 (m, 2H, -Ph, C_{ortho}-H), 7.53–7.36 (m, 3H, -Ph, C_{meta}-H and C_{para}-H), 6.80 (d, 1H, $^{3}J_{ortho}$= 8.4Hz, C_6-H), 6.71 (d, 1H, $^{4}J_{meta}$= 2.4Hz, C_9-H), 6.64 (dd, 1H, $^{3}J_{ortho}$= 8.4Hz, $^{4}J_{meta}$= 2.4Hz, C_5-H), 5.99(s, 2H) ppm; **^{13}C{^{1}H} NMR (75.5 MHz, $CDCl_3$):** δ 152.76 (s, C_1), 148.20 (s, C_7), 145.90 (s, C_8), 144.43 (s, C_4), 133.28 (s, -Ph, C_{ortho}), 131.16 (s, -Ph, C_{para}), 128.78 (s, -Ph, C_{meta}), 119.31 (s, -Ph, C_{ipso}), 114.05 (s, C_5), 108.15 (s, C_6), 103.68 (s, C_9), 101.95 (s, O-CH_2-O), 88.88 (s, C_3), 80.26 (s, C_2) ppm;

3',4'-Methylendioxy-phenyl propiolate – 1c [9]

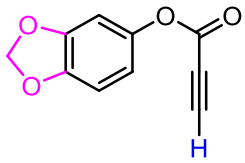

Isolated as a white solid (eluent Et_2O/Hex 1:4 v/v) with 72% yield (206 mg, 1.08 mmol).

^{1}H NMR (300 MHz, $CDCl_3$): δ 6.79 (d, J = 8.4 Hz, 1H), 6.66 (d, J = 2.4 Hz, 1H), 6.59 (dd, J = 8.4, 2.4 Hz, 1H), 6.00 (s, 2H), 3.06 (s, 1H) ppm;

3',4'-Methylendioxy-phenyl 2-hexynoate – 1d

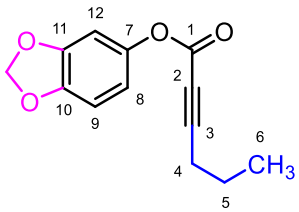

Isolated as a white solid (eluent EtOAc/Hex 1:10 v/v) with 57% yield (395 mg, 1.70 mmol).

^{1}H NMR (300 MHz, $CDCl_3$): δ 6.77 (d, 1H, $^{3}J_{ortho}$= 8.4Hz, C_9-H), 6.64 (d, 1H, $^{4}J_{meta}$= 2.4Hz, C_{12}-H), 6.57 (dd, 1H, $^{3}J_{ortho}$= 8.4Hz, $^{4}J_{meta}$= 2.4Hz, C_8-H), 5.98 (s, 2H, O-CH_2-O), 2.37 (t, 2H, ^{3}J= 7.1Hz, C_3-CH_2-C_5), 1.65 (ses, 2H, ^{3}J= 7.2Hz, C_4-CH_2-C_6), 1.04 (t, 3H, ^{3}J= 7.4Hz, -CH_3) ppm; **^{13}C{^{1}H} NMR (75.5 MHz, $CDCl_3$):** δ 152.50 (s, C1), 148.17 (s, C_{10}), 145.83 (s, C_{11}), 144.49 (s,

C_7), 114.05 (s, C_8), 108.13 (s, C_9), 103.72 (s, C_{12}), 101.93 (s, O-CH_2-O), 92.39 (s, C_3), 72.90 (s, C_2), 21.14 (s, C_5), 20.88 (s, C_4), 13.61 (s, C_6) ppm; **HRMS (ESI+):** calcd for $[M+H]^+ = C_{13}H_{13}O_4^+$: 233.0808. Found: 233.0844;

3',4',5'-Tri-methoxy-phenyl 3-phenyl-propiolate – 1e [11]

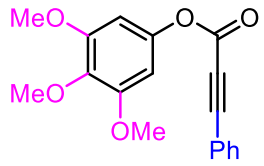

Isolated as a yellow solid (eluent EtOAc/Hex 1:5 v/v) with 60% yield (561 mg, 1.80 mmol).

^{1}H NMR (300 MHz, $CDCl_3$): δ 7.67–7.58 (m, 2H), 7.54–7.35 (m, 3H), 6.44 (s, 2H), 3.85 (s, 6H), 3.84 (s, 3H) ppm;

3',4',5'-Tri-metyl-phenyl 3-phenyl-propiolate – 1f

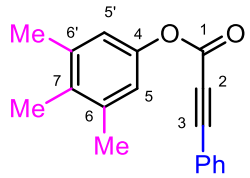

Isolated as a white solid (eluent EtOAc/Hex 1:10 v/v) with 48% yield (384 mg, 1.45 mmol).

^{1}H NMR (300 MHz, $CDCl_3$): δ 7.69–7.61 (m, J = 7.8 Hz, 2H, -Ph, C_{ortho}-H), 7.55–7.36 (m, 3H, -Ph, C_{meta}-H and C_{para}-H), 6.85 (s, 2H, $C_{5/5''}$-H), 2.31 (s, 6H, $C_{6/6'}$-Me), 2.16 (s, 3H, C_7-Me) ppm; **^{13}C{^{1}H} NMR (75.5 MHz, $CDCl_3$):** δ 152.96 (s, C_1), 147.26 (s, C_4), 138.00 (s, $C_{6/6'}$), 133.50 (s, C_7), 133.23 (s, -Ph, C_{ortho}), 131.03 (s, -Ph, C_{para}), 128.73 (s, -Ph, C_{meta}), 120.16 (s, $C_{5/5'}$), 119.40 (s, -Ph, C_{ipso}), 88.30 (s, C_3), 80.49 (s, C_2), 20.82 (s, $C_{6/6'}$-Me), 15.13 (s, C_7-Me) ppm; **HRMS (ESI+):** calcd for $[M+H]^+ = C_{18}H_{17}O_2^+$: 265.1223. Found: 265.1256;

Phenyl 3-phenyl-propiolate – 1g [10]

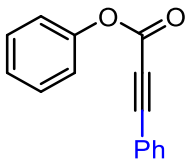

Isolated as a white solid (eluent EtOAc/Hex 1:20 v/v) with 62% yield (415 mg, 1.87 mmol).

^{1}H NMR (300 MHz, $CDCl_3$): δ 7.66–7.61 (m, 2H), 7.53–7.37 (m, 5H), 7.32–7.27 (m, 1H), 7.23–7.17 (m, 2H) ppm;

Phenyl propiolate – 1h [9]

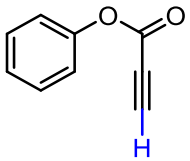

Isolated as a colorless oil (eluent EtOAc/Hex 1:20 v/v) with 55% yield (241 mg, 1.65 mmol).

^{1}H NMR (300 MHz, $CDCl_3$): δ 7.32 (t, J = 7.7 Hz, 2H), 7.19 (t, J = 7.7 Hz, 1H), 7.07 (d, J = 7.7 Hz, 2H), 2.99 (s, 1H) ppm;

4'-Tert-butyl-phenyl 3-phenyl-propiolate – 1i [11]

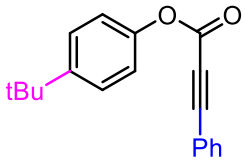

Isolated as a white solid (eluent EtOAc/Hex 1:20 v/v) with 67% yield (559 mg, 2.01 mmol).

^{1}H NMR (300 MHz, $CDCl_3$): δ 7.67–7.60 (m, 2H), 7.54–7.36 (m, 5H), 7.15–7.08 (m, *J* = 8.8 Hz, 2H), 1.33 (s, 9H) ppm;

3'-Tert-butyl-phenyl 3-phenyl-propiolate – 1j

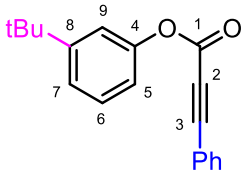

Isolated as a greenish oil (eluent EtOAc/Hex 1:20 v/v) with 44% yield (366 mg, 1.31 mmol).

^{1}H NMR (300 MHz, $CDCl_3$): δ 7.66–7.60 (m, 2H, -Ph, C_{ortho}-H), 7.53–7.45 (m, 1H, -Ph, C_{para}-H), 7.44–7.37 (m, 2H, -Ph, C_{meta}-H), 7.34 (d, $^3J_{ortho}$ = 7.6

Hz, 1H, C_6-H), 7.31 (dt, $^3J_{ortho}$ = 7.8 Hz, $^4J_{meta}$ = 1.6 Hz, 1H, C_7-H), 7.19 (t, $^3J_{meta}$ = 1.9 Hz, 1H, C_9-H), 7.03 (dt, $^3J_{ortho}$ = 7.5 Hz, $^4J_{meta}$ = 1.9 Hz, 1H, C_5-H), 1.34 (s, 9H, -tBu) ppm; **$^{13}C\{^1H\}$ NMR (75.5 MHz, $CDCl_3$):** δ 153.48 (s, C_8), 152.64 (s, C_1), 150.22 (s, C_4), 133.31 (s, -Ph, C_{ortho}), 131.11 (s, -Ph, C_{para}), 129.18 (s, C_6), 128.80 (s, -Ph, C_{meta}), 123.55 (s, C_7), 119.49 (s, -Ph, C_{ipso}), 118.60 (s, C_5 and C_9), 88.67 (s, C_3), 80.51 (s, C_2), 34.98 (s, tBu, C_{quat}), 31.37 (s, tBu, -Me) ppm; **HRMS (ESI+):** calcd for $[M+H]^+$ = $C_{19}H_{19}O_2^+$: 279.1380. Found: 279.1408;

Biphenyl-4'-yl 3-phenyl-propiolate – 1k [12]

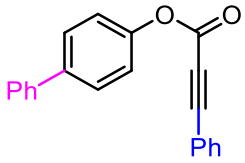

Isolated as a white solid (eluent Tol/Hex 1:1 v/v) with 68% yield (608 mg, 2.04 mmol).

^1H NMR (300 MHz, $CDCl_3$): δ 7.68–7.60 (m, 5H), 7.60–7.55 (m, 2H), 7.55–7.33 (m, 6H), 7.31–7.24 (m, 2H) ppm;

Biphenyl-4'-yl propiolate – 1l [13]

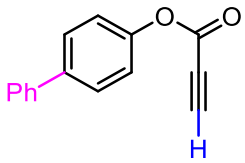

Isolated as a white solid (eluent Tol/Hex 1:1 v/v) with 65% yield (433 mg, 1.95 mmol).

^1H NMR (300 MHz, $CDCl_3$): δ 7.64–7.59 (m, 2H), 7.59–7.54 (m, 2H), 7.48–7.41 (m, 2H), 7.39–7.32 (m, 1H), 7.26–7.20 (m, 2H), 3.09 (s, 1H) ppm;

4'-bromo-phenyl 3-phenyl-propiolate – 1m [12]

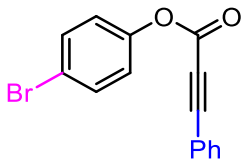

Isolated as a white solid (eluent EtOAc/Hex 1:10 v/v) with 82% yield (738 mg, 2.45 mmol).

^1H NMR (300 MHz, $CDCl_3$): δ 7.67–7.60 (m, 2H), 7.57–7.51 (m, *J* = 8.8 Hz, 2H), 7.51–7.46 (m, 1H), 7.46–7.37 (m, 2H), 7.14–7.06 (m, *J* = 8.8 Hz, 2H)

ppm;

4'-Methoxy-phenyl 3-phenyl-propiolate – 1n [14]

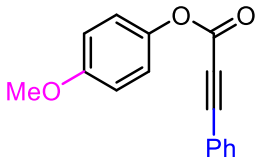

Isolated as a white solid (eluent EtOAc/Hex 1:10 v/v) with 79% yield (596 mg, 2.36 mmol).

^{1}H NMR (300 MHz, $CDCl_3$): δ 7.66–7.59 (m, 2H), 7.52–7.45 (m, 1H), 7.45–7.36 (m, 2H), 7.15–7.08 (m, *J* = 9.1 Hz, 2H), 6.96–6.88 (d, *J* = 9.1 Hz, 2H), 3.81 (s, 3H) ppm;

4-Methoxyphenyl propiolate – 1o [14]

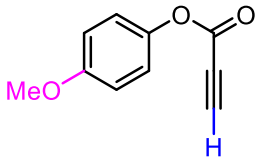

Isolated as a white solid (eluent Et_2O/Hex 1:4 v/v) with 99% yield (263 mg, 1.49 mmol).

^{1}H NMR (300 MHz, $CDCl_3$): δ 7.10–7.03 (m, *J* = 9,1 Hz, 2H), 6.93–6.87 (m, *J* = 9.1 Hz, 2H), 3.80 (s, 3H), 3.06 (s, 1H) ppm;

7-Methoxynaphtalen-2-yl propiolate – 1p [9]

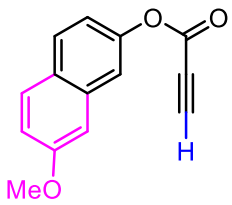

Isolated as a crystalline, colorless solid (eluent Et_2O/Hex 1:4 v/v) with 53% yield (359.3 mg, 1.59 mmol).

^{1}H NMR (300 MHz, $CDCl_3$): δ 7.79 (d, J = 8.8 Hz, 1H), 7.74 (d, *J* = 8.8 Hz, 1H), 7.52 (d, *J* = 2.2 Hz, 1H), 7.18–7.08 (m, 3H), 3.92 (s, 3H), 3.09 (s, 1H) ppm;

6-Methoxynaphtalen-2-yl propiolate – 1q

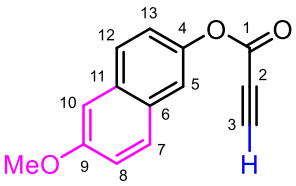

Isolated as a crystalline, colorless solid (eluent EtOAc/Hex 1:20 v/v) with 28% yield (191 mg, 0.85 mmol).

^{1}H NMR (300 MHz, $CDCl_3$): δ 7.76 (d, *J* = 7.9 Hz, 1H, C_{12}-H), 7.71 (d, *J* = 7.9 Hz, 1H, C_7-H), 7.56 (d, *J* = 2.4 Hz, 1H, C_5-H), 7.24 (dd, *J* = 8.8, 2.4 Hz, 1H, C_{13}-H), 7.19 (dd, *J* = 8.8, 2.6 Hz, 1H, C_8-H), 7.16–7.13 (m, 1H, C_{10}-H), 3.92 (s, 3H, -OMe), 3.09 (s, 1H, C_3-H) ppm; **^{13}C{^{1}H} NMR (75.5 MHz, $CDCl_3$):** δ 158.03 (s, C_9), 151.42 (s, C_1), 145.94 (s, C_4), 133.08 (s, C_6), 129.32 (s, C_{11}), 129.01 (s, C_7), 128.42 (s, C_{12}), 120.88 (s, C_{13}), 119.92 (s, C_8), 118.53 (s, C_5), 105.93 (s, C_{10}), 76.92 (s, C_3), 74.50 (s, C_2), 55.49 (s, -OMe) ppm; **HRMS (ESI+):** calcd for $[M+H]^+ = C_{14}H_{11}O_3^+$: 227.0703. Found: 227.0690;

Synthesis of 3-phenyl-2-propyn-1-ol

The synthesis has been accomplished according to procedures from the literature.[15,16]

In a 100 ml round-bottom flask, phenylacetylene (1.1 ml, 10 mmol, 1.0 eq) in THF (20 mL) at -78 °C was treated with n-BuLi 2.5 M in hexanes (4.8 mL, 12 mmol, 1.2 eq). After stirring at -78 °C for 1 h, paraformaldehyde (360.4 mg, 12 mmol, 1.2 eq) was added to the mixture. Then the flask was allowed to warm up to room temperature, and stirred over-night. The mixture was then quenched with a saturated NH_4Cl solution (40 mL) and extracted with EtOAc (3x30 mL). The collected organic phases were washed a further time with brine (30 mL) and dried over Na_2SO_4. Volatiles were removed under reduced pressure to give the desired product as a yellow oil with a yield of 92% (1.22 g, 9.23 mmol). No further purification was needed for our synthetic purposes. Spectroscopic data were in agreement with the ones previously reported in the literature.

3-Phenyl-2-propyn-1-ol [15]

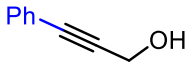

^{1}H NMR (300 MHz, $CDCl_3$): δ 7.48–7.39 (m, 2H), 7.35–7.27 (m, 3H), 4.5 (s, 2H) ppm;

Synthesis of aryl-propargyl ether derivatives

• Aryl-propargyl ethers **4c**, **4h** and **4o** were prepared according to a modified literature procedure.[17,18]

A solution of the phenol (3.0 mmol, 1eq.) in anhydrous DMF (10 ml) was treated with propargyl bromide (80% solution in toluene, 4.5 mmol, 1.5 eq.) in the presence of potassium carbonate (1.2 eq.). The crude was taken up in DCM (30 ml) and washed with H_2O (3x20 ml). Only for compound **4c**, traces of unreacted sesamol were removed by additional extractions with a sodium hydroxide aqueous solution at 1M concentration (3x20 ml). After a further washing with brine (1x20 ml), the organic phase was then dried over Na_2SO_4, and evaporated under reduced pressure to obtain the desired product. Spectroscopic data were in agreement with the ones previously reported in the literature.

3',4'-Methylendioxy-phenyl-propargyl-ether – 4c [18]

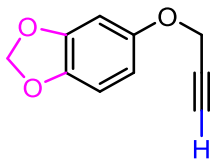

The compound was isolated as a brown oil with 92% yield (486 mg, 2.76 mmol).

^{1}H NMR (300 MHz, $CDCl_3$): δ 6.72 (d, *J* = 8.4 Hz, 1H), 6.57 (d, *J* = 2.5 Hz, 1H), 6.41 (dd, *J* = 8.4, 2.5 Hz, 1H), 5.93 (s, 2H), 4.62 (d, *J* = 2.4 Hz, 2H), 2.52 (t, *J* = 2.4 Hz, 1H) ppm;

Phenyl-propargyl-ether – 4h [17]

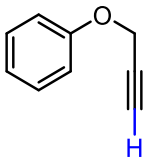

The compound was isolated as a brown oil with quantitative yield (396 mg, 3.00 mmol).

^{1}H NMR (300 MHz, $CDCl_3$): δ 7.36–7.27 (m, 2H), 7.05–6.95 (m, 3H), 4.70 (d, *J* = 2.4, 2H), 2.52 (t, *J* = 2.4, 1H) ppm;

4'-Methoxy-phenyl-propargyl-ether – 4o [18]

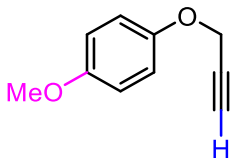

The compound was isolated as a brown oil with 98% yield (475 mg, 2.93 mmol)

^{1}H NMR (300 MHz, $CDCl_3$): δ 6.97–6.90 (m, *J* = 9.2 Hz, 2H), 6.88–6.82 (m, *J* = 9.2 Hz, 2H), 4.64 (d, *J* = 2.4, 2H), 3.78 (s, 3H), 2.51 (t, *J* = 2.4, 1H) ppm;

• Compound **4b** was prepared by Mitsunobu reaction of sesamol with 3-phenyl-2-propyn-1-ol by the following procedure.[17,19]

Sesamol (414.4 mg, 3.0 mmol, 1 eq.), 3-phenyl-2-propyn-1-ol (0.38ml, 3. mmol, 1eq.) and triphenylphosphine (2.21 g, 8.4 mmol, 1.4 eq.) were added to a round bottom flask and dissolved in THF (15 ml). The solution was cooled to 0°C and diisopropyl azodicarboxylate (0.83 ml, 4.2 mmol, 1.4eq.) was added dropwise. The reaction mixture was then allowed to warm up to room temperature and stirred for 24 hours. The solvent was then evaporated under reduced pressure and the residue purified by flash chromatography on silica gel (gradient from pure hexane to EtOAc/Hex 1:20 v/v). The desired product **4b** was obtained as a white solid with a yield of 26% (194.4mg, 0.77mmol) upon collecting and evaporating the relevant fractions. Spectroscopic data were in agreement with the ones previously reported in the literature.

3',4'-Methylendioxy-phenyl-3-phenyl-2-propyn-1-yl-ether – 4b [20]

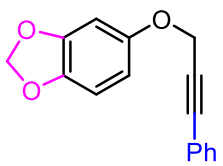

^{1}H NMR (300 MHz, $CDCl_3$): δ 7.50–7.38 (m, 2H), 7.37–7.26 (m, 3H), 6.74 (d, *J* = 8.4 Hz, 1H), 6.63 (d, *J* = 2.5 Hz, 1H), 6.48 (dd, *J* = 8.4, 2.5 Hz, 1H), 5.93 (s, 2H), 4.84 (s, 2H) ppm;

General procedures for catalytic tests:

Fujiwara's conditions (intermolecular hydroarylation) [7]

The arene (2.0 mmol) was placed in a flame-dried Schlenk tube under argon atmosphere along with 0.8 ml of Ac^FOH. Gold complex **I** (6.7 mg, 0.01 mmol)* and hexamethylbenzene (25.0 mg, 0.15 mmol) were dissolved in 0.2 ml of DCM and added to the flask. A t_0 NMR check was performed after taking an aliquot of the reaction mixture in 0.5 ml $CDCl_3$. The flask was then cooled down to 0°C and ethyl phenyl-propiolate (0.17 ml, 1.0 mmol) was added. After 5 min stirring at 0°C, the mixture was placed in a 25°C thermostatic bath and the reaction monitored by ^1H NMR using hexamethylbenzene as internal standard, as for the t_0 NMR check.

*The procedure remained the same when different catalyst loadings were employed.

Fujiwara's conditions (intramolecular hydroarylation)

The substrate (1 mmol) and hexamethylbenzene (25.0 mg, 0.15 mmol) were placed in a flame-dried Schlenk tube under argon atmosphere along with 0.9 ml of a solution 1:4 v/v DCM/Ac^FOH. A t_0 NMR check was performed after taking an aliquot of the reaction mixture in 0.5 ml $CDCl_3$. Then the gold complex **I** or **II** (0.001 mmol or 0.005 mmol) in 0.1 ml of the DCM/Ac^FOH mixture was added to the mixture. The flask was then placed in a thermostatic bath at 25 or 40°C, and the reaction monitored by ^1H NMR using hexamethylbenzene as internal standard, as for the t_0 NMR check.

Only for product **3n**: upon completion of the reaction, the crude was diluted in DCM (20 ml) and quenched with a saturated solution of $NaHCO_3$. The aqueous phase was then counter-extracted with DCM (3x10 ml) and the whole combined organic phases were dried over Na_2SO_4 before removing all volatiles under reduced pressure. The obtained residue was subjected to flash chromatography over silica gel (eluent EtOAc/Hex 2:5 v/v) to obtain the pure product as a white solid with a yield of 89% (105.6 mg, 0.44 mmol).

IL conditions

The substrate (0.5 mmol) and the gold complex **III** or **IV** (0.01 mmol)* were placed in a flame-dried Schlenk tube under argon atmosphere. A freshly prepared solution of the silver salt $AgSbF_6$ (6.9 mg, 0.02 mmol) in [BMIM][X] (0.75 ml) and 1,2-dimethoxyethane (0.05 ml, 0.48 mmol) were added to the flask and the mixture was stirred for 5 min at room temperature. A t_0 NMR check was performed after taking an aliquot of the reaction mixture in 0.5 ml $CDCl_3$. The acid co-catalyst HA (0.1 mmol) was then added to the mixture and the flask was placed in a thermostatic bath at 40°C. The reaction was monitored by ^1H NMR using 1,2-dimethoxyethane as internal standard, as for the t_0 NMR check.

* When 5 mol% gold complex (19.1 mg, 0.025 mmol) were employed, it was preferred to load $AgSbF_6$ (17.2 mg, 0.05 mmol) in the flask directly as a solid rather than in solution. For catalyst loadings lower than 2 mol%. the procedure remained unvaried.

Compounds **2b-g**, **2j**, **2k**, **2m**, and **2q** were synthesized by the same procedure and isolated as follows:

The reaction crude was taken-up in DCM (15 ml) and the resulting organic phase was quenched with a saturated $NaHCO_3$ aqueous solution. The aqueous phase was then counter-extracted with DCM (3x10 ml) and the whole combined organic phases were dried over Na_2SO_4 before removing all volatiles under reduced pressure. The obtained residue was subjected to flash chromatography over silica gel to obtain the pure products upon collecting and evaporating the relevant fractions.

Compounds **5b** and **6b** were respectively isolated from the reaction mixtures of the entries 10 and 9 of ***Table 3.7***:
After extraction of the crude with n-hexane (3x5 ml), the collected organic phases were evaporated to remove volatiles. The obtained residue was purified by flash column chromatography over silica gel (gradient EtOAc/Hex 1:10 to 1:5) to isolate the desired product **5b** or **6b** as a white solid.

Spectroscopic data of all known compounds were consistent with the ones reported in the literature. The molecular connectivity of **2d**, **2f**, **5b** and **6b** was univocally determined by correlation NMR experiments. The chemical identity of **2f** and **5b** was further confirmed by HRMS-ESI analyses.

Ethyl (Z)-3-phenyl-3-(2,4,6-trimethoxyphenyl)prop-2-enoate – 2a [7]

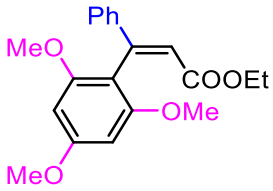

^{1}H NMR (300 MHz, $CDCl_3$): 7.37–7.31 (m, 5H), 6.89 (s, 2H), 6.66 (s, 1H), 4.04 (q, *J* = 7.1 Hz, 2H), 2.31 (s, 3H), 2.01 (s, 6H), 1.06 (t, *J* = 7.1 Hz, 3H) ppm;

4-Phenyl-6,7-methylendioxy-2H-chromen-2-one – 2b [21]

Isolated as a white solid (eluent EtOAc/Hex 1:4 v/v) with 99% yield (52.5 mg, 0.197 mmol).

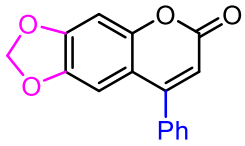

^{1}H NMR (300 MHz, $CDCl_3$): δ 7.52–7.50 (m, 3H), 7.45–7.39 (m, 2H), 6.89 (s, 1H), 6.82 (s, 1H), 6.23 (s, 1H), 6.04 (s, 2H) ppm; **^{13}C{^{1}H} NMR (75.5 MHz, $CDCl_3$):** δ 161.30, 156.02, 151.50, 151.29, 144.97, 135.83, 129.73, 129.03, 128.38, 113.01, 112.37, 104.51, 102.49, 98.71 ppm; **ESI-MS (m/z):** 289 (**2b** + Na^+);

6,7-Methylendioxy-2H-chromen-2-one – 2c [9]

Isolated as a white solid (eluent DCM) with 94% yield (35.9 mg, 0.189 mmol).

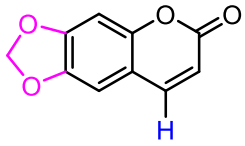

^{1}H NMR (300 MHz, $CDCl_3$): δ 7.57 (d, J = 9.5 Hz, 1H), 6.82 (s, 1H), 6.82 (s, 1H), 6.27 (d, J = 9.5 Hz, 1H), 6.06 (s, 2H) ppm; **^{13}C{^{1}H} NMR (75.5 MHz, $CDCl_3$):** δ 161.34, 151.42, 151.41, 145.05, 143.60, 113.54, 112.83, 105.16, 102.48, 98.54 ppm; **ESI-MS (m/z):** 213 (**2c** + Na^+);

4-n-propyl-6,7-methylendioxy-2H-chromen-2-one – 2d [22]

Isolated as a brownish solid (eluent EtOAc/Hex 1:4 v/v) with 97% yield (45.2 mg, 0.195 mmol).

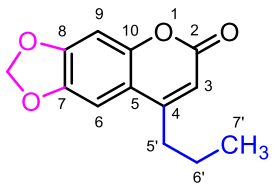

^{1}H NMR (300 MHz, $CDCl_3$): δ 6.98 (s, 1H, C_9-H), 6.82 (s, 1H, C_6-H), 6.15 (t, ^{4}J= 0.8 Hz, 1H, C_3-H), 6.06 (s, 1H, O-CH_2-O), 2,65 (td, ^{3}J= 7.6 Hz, ^{4}J= 0.8 Hz, 2H, C_4-CH_2-$C_{6'}$), 1.71 (ses, 2H, ^{3}J= 7.6 Hz, $C_{5'}$-CH_2-$C_{7'}$), 1.04 (t, 3H, ^{3}J= 7.4 Hz, $C_{6'}$-CH_3) ppm; **^{13}C{^{1}H} NMR (75.5 MHz, $CDCl_3$):** δ 161.69 (s, C_2), 156.35 (s, C_5), 150.99 (s, C_7), 150.98 (s, C_{10}), 145.09 (s, C_8), 113.34 (s, C_4), 111.28 (s, C_3), 102.44 (s, O-CH_2-O), 102.05 (s, C_9), 98.70 (s, C_6), 34.38 (s, $C_{5'}$), 21.52 (s, $C_{6'}$), 14.04 (s, $C_{7'}$) ppm; **ESI-MS (m/z):** 255 (**2d** + Na^+);

4-Phenyl-5,6,7-trimetoxy-2H-chromen-2-one – 2e [11]

Isolated as a yellowish solid (eluent EtOAc/Hex 1:4 v/v) with 99% yield (61.9 mg, 0.198 mmol).

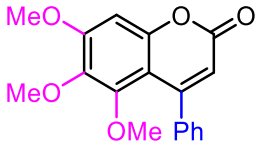

^{1}H NMR (300 MHz, $CDCl_3$) δ 7.49–7.36 (m, 3H, aryl), 7.36–7.27 (m, 2H, aryl), 6.72 (s, 1H, aryl), 6.05 (s, 1H, vinyl), 3.93 (s, 3H, OCH_3), 3.78 (s, 3H, OCH_3), 3.25 (s, 3H, OCH_3) ppm; **^{13}C{^{1}H} NMR (75.5 MHz, $CDCl_3$):** δ 160.73, 157.03, 155.50, 151.82, 151.20, 139.58, 139.16, 128.14, 127.63, 127.33, 114.19, 107.40, 96.40, 61.16, 61.03, 56.38 ppm; **ESI-MS (m/z):** 335 (**2e** + Na^+);

4-Phenyl-5,6,7-trimethyl-2H-chromen-2-one – 2f

Isolated as a dark yellow (eluent EtOAc/Hex 1:4 v/v) with 98% yield (51.6 mg, 0.195 mmol).

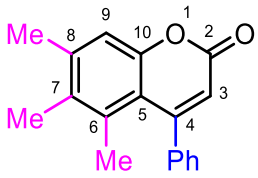

^{1}H NMR (300 MHz, $CDCl_3$): δ 7.48–7.40 (m, 3H, -Ph, C_{ortho}-H and C_{para}-H), 7.32–7.24 (m, 3H, -Ph, C_{meta}-H), 7.11 (s, 1H, C_9-H), 6.19 (s, 1H, C_3-H), 2.37 (s, 3H, C_8-Me), 2.13 (s 3H, C_7-Me), 1.75 (s, 3H, C_6-Me) ppm; **^{13}C{^{1}H} NMR (75.5 MHz, $CDCl_3$):** δ 160.84 (s, C_2), 156.83 (s, C_4), 153.05 (s, C_{10}), 141.47 (s, C_8), 140.44 (s, -Ph, C_{ipso}), 135.21 (s, C_6), 133.24 (s, C_7), 128.85 (s, -Ph, C_{ortho}), 128.82 (s, -Ph, C_{para}), 127.25 (s, -Ph, C_{meta}), 116.66 (s, C_3), 116.49 (s, C_5), 116.10 (s, C_9), 21.50 (s, C_8-Me), 20.64 (s, C_6-Me), 15.87 (s, C_7-Me) ppm; **HRMS (ESI+):** calcd for $[M+H]^+$ = $C_{18}H_{17}O_2^+$: 265.1223. Found: 265.1243;

4-Phenyl-2H-chromen-2-one – 2g [23]

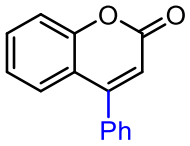

Isolated as a white solid (eluent EtOAc/Hex 1:8 v/v) with 80% yield (35.7 mg, 0.161 mmol).

^{1}H NMR (300 MHz, $CDCl_3$): δ 7.58–7.40 (m, 8H), 7.26–7.21 (m, 1H), 6.37 (s, 1H) ppm; **$^{13}C\{^{1}H\}$ NMR (75.5 MHz, $CDCl_3$):** δ 160.84, 155.78, 154.32, 135.33, 132.04, 129.89, 128.99, 128.55, 127.13, 124.28, 119.11, 117.43, 115.31 ppm; **ESI-MS (m/z):** 245 (**2g** + Na^+);

2H-chromen-2-one- 2h [9]

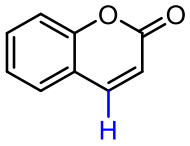

^{1}H NMR (300 MHz, $CDCl_3$): δ 7.64 (d, J = 9.6 Hz, 1H), 7.45 (t, J = 7.9 Hz, 1H), 7.42 (d, J = 7.9 Hz, 1H), 7.25 (d, J = 7.9 Hz, 1H), 7.21 (t, J = 7.9 Hz, 1H), 6.39 (d, J = 9.6 Hz, 1H);

4-Phenyl-6-tert-butyl-2H-chromen-2-one – 2i [11]

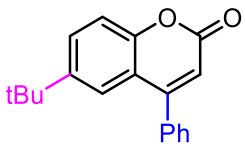

^{1}H NMR (300 MHz, $CDCl_3$): δ 7.60 (dd, 1H, aryl), 7.54 (m, 6H, aryl), 7.35 (d, 1H, aryl), 6.36 (s, 1H, vinyl), 1.27 (s, 9H, tert-butyl) ppm;

4-Phenyl-7-tert-butyl-2H-chromen-2-one – 2j [21]

Isolated as a viscous pale whitish oil (eluent EtOAc/Hex 1:8 v/v) with 88% yield (48.9 mg, 0.176 mmol).

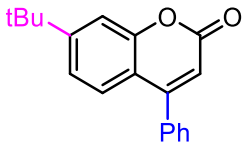

^{1}H NMR (300 MHz, $CDCl_3$): δ 7.54–7.50 (m, 3H), 7.44–7.40 (m, 4H), 7.28–7.25 (m, 1H), 6.32 (s, 1H), 1.36 (s, 9H); **^{13}C{^{1}H} NMR (75.5 MHz, $CDCl_3$):** δ 161.28, 156.58, 155.67, 154.39, 135.56, 129.73, 128.95, 128.54, 126.66, 121.82, 116.62, 114.36, 114.25, 35.32, 31.16 ppm; **ESI-MS (m/z):** 301 (**2j** + Na^+);

4,6-Di-phenyl-2H-chromen-2-one – 2k [24]

Isolated as a white solid (eluent EtOAc/Hex 1:5 v/v) with 71% yield (42.4 mg, 0.142 mmol).

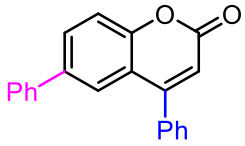

^{1}H NMR (300 MHz, $CDCl_3$): δ 7.75 (dd, J = 8.6, 2.2 Hz, 1H), 7.66 (d, J = 2.2 Hz, 1H), 7.55–7.51 (m, 3H), 7.51–7.43 (m, 5H), 7.43–7.37 (m, 2H), 7.36–7.30 (m, 1H), 6.42 (s, 1H) ppm; **^{13}C{^{1}H} NMR (75.5 MHz, $CDCl_3$):** δ 160.79, 155.83, 153.76, 139.80, 137.73, 135.31, 131.02, 129.92, 129.12, 129.09, 128.57, 127.83, 127.22, 125.37, 119.33, 117.86, 115.70 ppm; **ESI-MS (m/z):** 321 (**2k** + Na^+);

6-Phenyl-2H-chromen-2-one – 2l [24]

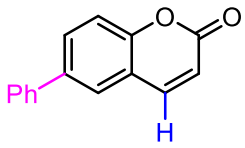

^{1}H NMR (300 MHz, $CDCl_3$): δ 7.77–7.72 (m, 2H), 7.66 (d, 1H), 7.58–7.56 (m, 2H), 7.49–7.45 (m, 2H), 7.40–7.37 (m, 2H), 6.46 (d, 1H) ppm;

4-Phenyl-6-bromo-2H-chromen-2-one – 2m [23]

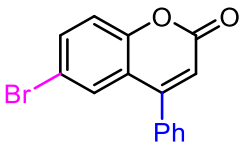

Isolated as a white solid (eluent EtOAc/Hex 1:10 v/v) with 22% yield (33.7 mg, 0.112 mmol).

^{1}H NMR (300 MHz, $CDCl_3$): δ 7.59–7.66 (m, 2H), 7.55–7.57 (m, 3H), 7.43–7.45 (m, 2H), 7.30 (d, *J* = 8.8 Hz, 1H), 6.40 (s, 1H) ppm; **^{13}C{^{1}H} NMR (75.5 MHz, $CDCl_3$):** δ 160.07, 154.67, 153.21, 134.87, 134.64, 130.14, 129.48, 129.25, 128.44, 120.79, 119.20, 117.14, 116.26 ppm; **ESI-MS (m/z):** 323 (**2m** + Na^+);

4-Phenyl-6-methoxy-2H-chromen-2-one – 2n [9]

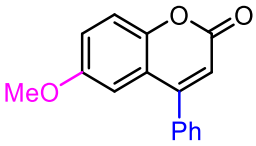

^{1}H NMR (300 MHz, $CDCl_3$): δ 7.53 (m, 3H), 7.46 (m, 2H), 7.34 (d, J = 9.0 Hz, 1H), 7.13 (dd, J = 9.0 and 3.0 Hz, 1H), 6.93 (d, J = 3.0 Hz, 1H), 6.38 (s, 1H), 3.74 (s, 3H) ppm;

4-Phenyl-1-oxaspiro[4,5]deca-3.5,8-trien-2,7-dione – 3n [14]

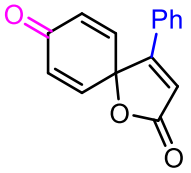

Isolated as a white solid (eluent EtOAc/Hex 1:20 v/v) with 89% yield (105.6 mg, 0.44 mmol).

^{1}H NMR (300 MHz, $CDCl_3$): δ 7.52–7.46 (m, 3H), 7.42–7.37 (m, 2H), 6.72 (d, *J* = 10.2 Hz, 2H), 6.57 (s, 1H), 6.51 (d, *J* = 9.9 Hz, 2H) ppm; **^{13}C{^{1}H} NMR (75.5 MHz, $CDCl_3$):** δ 184.14, 170.58, 165.40, 143.48, 132.15, 131.93, 129.45, 129.00, 127.28, 116.96, 81.46 ppm; **ESI-MS (m/z):** 261 (**3n** + Na^+);

6-Methoxy-2H-chromen-2-one – 2o [9]

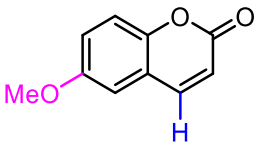

^{1}H NMR (300 MHz, $CDCl_3$): δ 7.65 (d, J = 9.6 Hz, 1H), 7.26 (d, J = 9.0 Hz, 1H), 7.11 (dd, J = 9.0, 2.9 Hz, 1H), 6.91 (d, J = 2.9 Hz, 1H), 6.42 (d, J = 9.6 Hz, 1H), 3.85 (s, 3H) ppm;

1-Oxaspiro[4,5]deca-3.5,8-trien-2,7-dione – 3o [14]

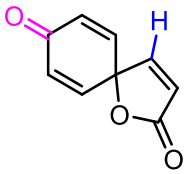

^{1}H NMR (300 MHz, $CDCl_3$): δ 7.17 (d, J = 5.7 Hz, 1H), 6.55 (d, J = 10.2 Hz, 2H), 6.41 (d, J = 10.2 Hz, 2H), 6.36 (d, J = 5.7 Hz, 1H);

9-Methoxy-3H-benzo[f]chromen-3-one – 2p [9]

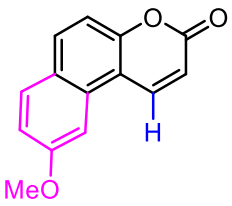

^{1}H NMR (300 MHz, $CDCl_3$): δ 8.44 (d, J = 9.8 Hz, 1H), 7.91 (d, J = 8.9 Hz, 1H), 7.81 (d, J = 8.9 Hz, 1H), 7.51 (d, J = 2.4 Hz, 1H), 7.32 (d, J = 8.9 Hz, 1H), 7.22 (dd, J = 8.9, 2.4 Hz, 1H), 6.55 (d, J = 9.8 Hz, 1H), 4.00 (s, 3H) ppm;

8-Methoxy-3H-benzo[f]chromen-3-one – 2q [25]

Isolated as a white solid (eluent EtOAc/Hex 1:10 v/v) with 92% yield (41.8 mg, 0.185 mmol).

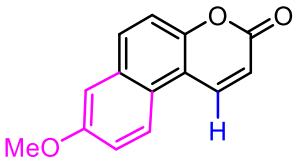

^{1}H NMR ($CDCl_3$, 300 MHz): δ 8.43 (d, *J* = 9.8 Hz, 1H), 8.12 (d, *J* = 9.2 Hz, 1H), 7.88 (d, *J* = 9.0 Hz, 1H), 7.44 (d, *J* = 9.0 Hz, 1H), 7.34 (dd, *J* = 9.2 and 2.6 Hz, 1H), 7.22 (d, *J* = 2.6 Hz, 1H), 6.56 (d, *J* = 9.8 Hz, 1H), 3.95 (s, 3H); **^{13}C{^{1}H} NMR (75.5 MHz, $CDCl_3$):** δ 161.17, 157.89, 152.61, 139.26, 132.04, 131.80, 124.02, 123.00, 120.59, 117.62, 115.98, 113.35, 107.66,

55.62 ; **ESI-MS (m/z):** 249 (**2k** + Na^+);

6,7-Methylendioxy-2H-chromene – 5c [26]

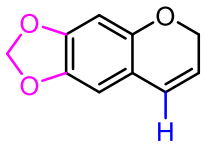

^{1}H NMR (300 MHz, $CDCl_3$): δ 6.47 (s, 1H), 6.38 (s, 1H), 6.31 (dt, J = 9.7, 2.0 Hz, 1H), 5.89 (s, 2H), 5.66 (dt, J = 9.7, 3.6 Hz, 1H), 4.70 (dd, J = 3.6, 2.0 Hz, 2H) ppm;

2H-chromene – 5h [27]

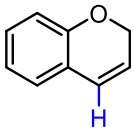

^{1}H NMR (300 MHz, $CDCl_3$): δ 4.82 (dd, *J* = 1.8 Hz, *J* = 1.4 Hz, 2 H,), 5.78–5.74 (m, 1 H), 6.42 (d, *J* = 8.1 Hz, 1 H), 6.77 (d, *J* = 8.1 Hz, 1 H), 6.86 (t, *J* = 7.4, 7.3 Hz, 1 H), 6.94 (d, *J* = 7.3 Hz, 1 H), 7.08 (t, *J* = 8.1, 7.3 Hz, 1 H) ppm;

6-Methoxy-2H-chromene – 5o [27]

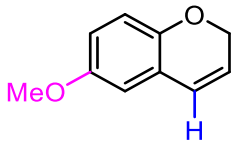

^{1}H NMR (300 MHz, $CDCl_3$): δ 6.65 (d, 1H), 6.59 (s, 1H), 6.47 (d, 1H), 6.31 (s, 1H), 5.73 (dt, 1H), 4.67 (dd, 2H), 3.67 (s, 3H) ppm;

4-Phenyl-6,7-methylendioxy-2H-chromene – 5b

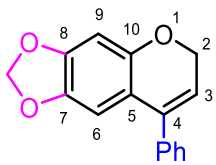

^{1}H NMR (300 MHz, $CDCl_3$): δ 7.43–7.28 (m, 5H, -Ph), 6.51 (s, 1H, C_9-H), 6.50 (s, 1H, C_6-H), 5.89 (s, 2H, -O-CH_2-O-), 5.69 (t, ^3J = 4.1 Hz, 1H, C_3-H), 4.75 (d, ^3J = 4.1 Hz, 2H, C_3-CH_2) ppm; **^{13}C{^{1}H} NMR (75.5 MHz, $CDCl_3$):** δ 150.51 (s, C_{10}), 147.72 (s, C_7), 141.92 (s, C_8), 138.62 (s, -Ph, C_{ipso}), 137.66 (s, C_4), 128.72 (s, -Ph, C_{ortho}), 128.55 (s, -Ph, C_{meta}), 127.95 (s, -Ph, C_{para}), 117.21 (s, C_3), 117.11 (s, C_5), 105.71 (s, C_6), 101.25 (s, O-CH_2-O), 98.89 (s, C_9), 65.44 (s, C_2) ppm; **HRMS (ESI+):** calcd for $[M–H]^+$ = $C_{16}H_{11}O_3^+$: 251.0703. Found: 251.0716;

4-Phenyl-6,7-methylendioxy-chromane – 6b [28]

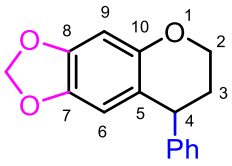

^{1}H NMR (300 MHz, $CDCl_3$): δ 7.35–7.18 (m, 3H, -Ph, C_{ortho}-H and C_{para}-H), 7.18–7.10 (m, 2H, -Ph, C_{meta}-H), 6.41 (s, 1H, C_6-H), 6.26 (s, 1H, C_9-H), 5.87–5.82 (m, 2H, O-CH_2-O), 4.11 (t, *J* = 5.1 Hz, 2H, C_3-CH_2), 4.07 (t, *J* = 6.5 Hz, 1H, C_4-H), 2.35–2.20 (m, 1H, C_3-H), 2.11–1.95 (m, 1H, C_3-H) ppm; **^{13}C{^{1}H} NMR (75.5 MHz, $CDCl_3$):** δ 150.07 (s, C_{10}), 146.98 (s, C_8), 145.94 (s, -Ph, C_{ipso}), 141.57 (s, C_7), 128.69 (s, -Ph, C_{ortho}), 128.60 (s, -Ph, C_{meta}), 126.63 (s, -Ph, C_{para}), 116.07 (s, C_5), 109.17 (s, C_9), 100.96 (s, O-CH_2-O), 98.45 (s, C_6), 63.98 (s, C_2), 41.19 (s, C_4), 31.93 (s, C_3) ppm;

Acid-mediated disproportionation of 5b

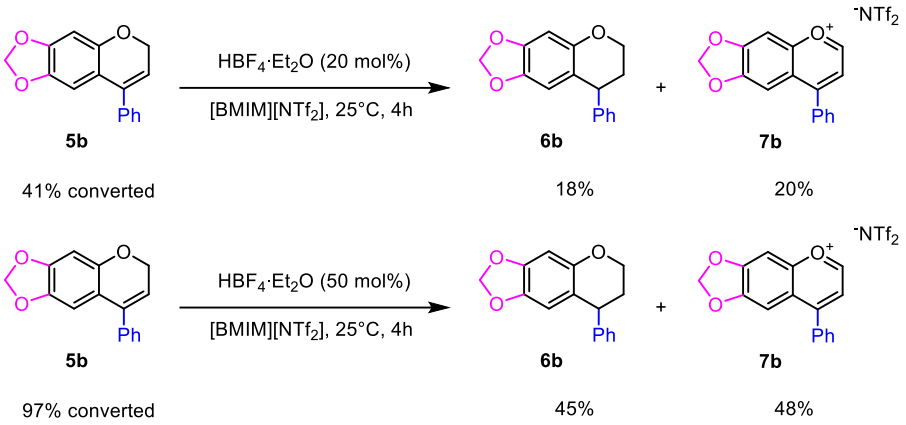

Two blank tests were performed adding 0.2 or 0.5 equivs. of $HBF_4 \cdot Et_2O$ (3 or 7 µl that corresponds to 0.02 or 0.05 mmol, respectively) to a mixture of **5b** (25.2 mg, 0.1 mmol, 1 eq.) in 0.15ml [BMIM][NTf_2] under argon atmosphere at 25°C. The stoichiometric formation of **6b** and of the analogous benzopyrylium ion **7b** was observed under the reported reaction conditions. ^{1}H NMR analysis using 1,2-dimethoxyethane as internal standard confirmed the mass conservation over these two products and the unreacted **5b**. To further confirm our hypothesis, HMRS-ESI analysis of the precursor **5b** allowed to assess the formation of the main fragmentation peak at 251.0716 m/z ,

by loss of a formal hydride moiety from the chromene scaffold. Unfortunately, purification of the crude by column chromatography was unsuccessfully attempted due to the fast oxidation of **7b** over silica-gel: **1b** was surprisingly isolated instead. However, **7b** could be separately synthesized by the following methodology.

Synthesis of the benzopyrylium bistriflimide 7b

The ether **4b** (25.2 mg, 0.1 mmol, 1eq.) was charged in a 5ml round-bottom flask and dissolved in 0.5 ml of DCM. The acid $HNTf_2$ (28.1 mg, 0.1 mmol, 1eq.) was dissolved in 0.5ml of DCM and slowly added to the other flask. Immediately after the addition, the mixture turned dark and opaque. After stirring over-night, volatiles were removed under reduced pressure and the mixture was redissolved in a minimum quantity of DCM. The solution was then treated with hexane at 0°C, decantated, and the solid residue washed with cold Et_2O (2x3ml) to afford **7b** as a greenish solid in 43% yield (22.8 mg, 0.043 mmol).

4-Phenyl-6,7-methylendioxy-chromane – 7b

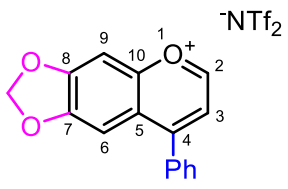

^{1}H NMR (300 MHz, $CDCl_3$): δ 9.15 (d, *J* = 4.6 Hz, 1H, C_2-H), 7.84 (d, *J* = 4.6 Hz, 1H, C_3-H), 7.75–7.62 (m, 5H, -Ph), 7.54 (s, 1H, C_9-H), 7.45 (s, 1H, , C_6-H), 6.42 (s, 2H, O-CH_2-O) ppm; **^{13}C{^{1}H} NMR (75.5 MHz, $CDCl_3$):** δ 166.47 (s, C_5), 160.93 (s, C_2), 160.86 (s, C_8), 159.94 (s, C_{10}), 152.16 (s, C_7), 133.66 (s, C_4), 133.29 (s, -Ph, C_{para}), 130.11 (s, -Ph, C_{ortho}), 130.05 (s, -Ph, C_{meta}), 123.26 (s, -Ph, C_{ipso}), 119.83 (q, $J_{C\text{-}F}$ = 321 Hz, -CF_3), 119.14 (s, -Ph, C_3), 105.82 (s, -Ph, O-CH_2-O), 103.40 (s, C_9), 99.22 (s, C_6) ppm; **^{19}F{^{1}H} NMR (188.3 MHz, $CDCl_3$):** δ -78.8 (s, -CF_3) ppm; **HRMS (ESI+):** calcd for $[M]^+$ = $C_{16}H_{11}O_3^+$: 251.0703. Found: 251.0714; **HRMS (ESI-):** calcd for $[M]^-$ = $C_2F_6NO_4S_2^-$: 279.9173. Found: 279.9189;

Spectroscopic $^{13}C\{^1H\}$ and $^{19}F\{^1H\}$ data for bistriflimide anion were in agreement with the ones previously reported.[29]

Hydroarylation tests with a stoichiometric amount of complex I

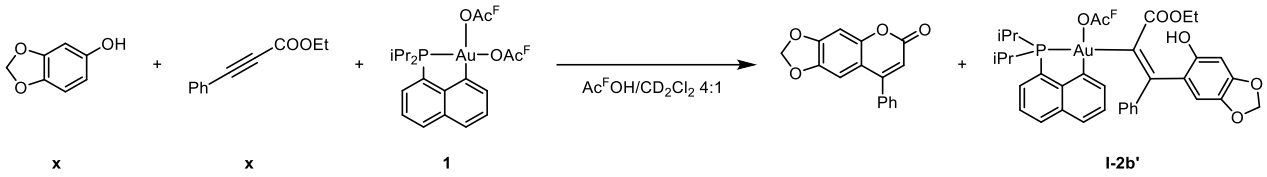

x x 1 I-2b'

Complex **I** (16.8 mg, 0.025 mmol) was placed in a Schlenk tube under argon atmosphere together with sesamol (3.5 mg, 0.025 mmol) and 0.75 ml of Ac^FOH/ DCM-d^2 4:$1_{v/v}$. The obtained greenish mixture was transferred to an NMR tube that was previously flushed with argon and a first ^1H and $^{31}P\{^1H\}$ NMR spectrum was collected. Ethyl phenylpropiolate (4.2 µl, 0.025 mmol) was then added to the tube, which made the solution turn color to reddish: consumption of the alkyne occurred within few minutes, with the solution turning back to the previously observed greenish color. The sample was subjected to the same analytic routine to determine both the formation of the coumarin **2b** and a not negligible conversion of complex **I** to a new species. Further additions of sesamol and the alkyne were performed, to detect the almost complete consumption of **I** after addition of 10 eq, of the two substrates.

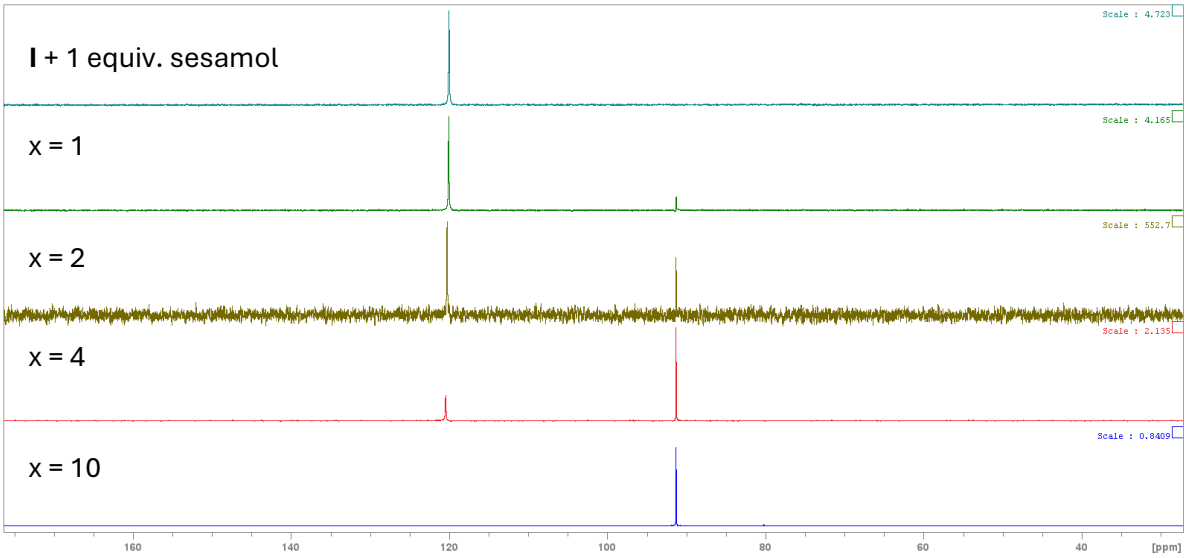

***Figure* 3.3** – $^{31}P\{^1H\}$ NMR spectra of the reaction mixture at different loads of the substrates (x = number of eq. of substrates added).

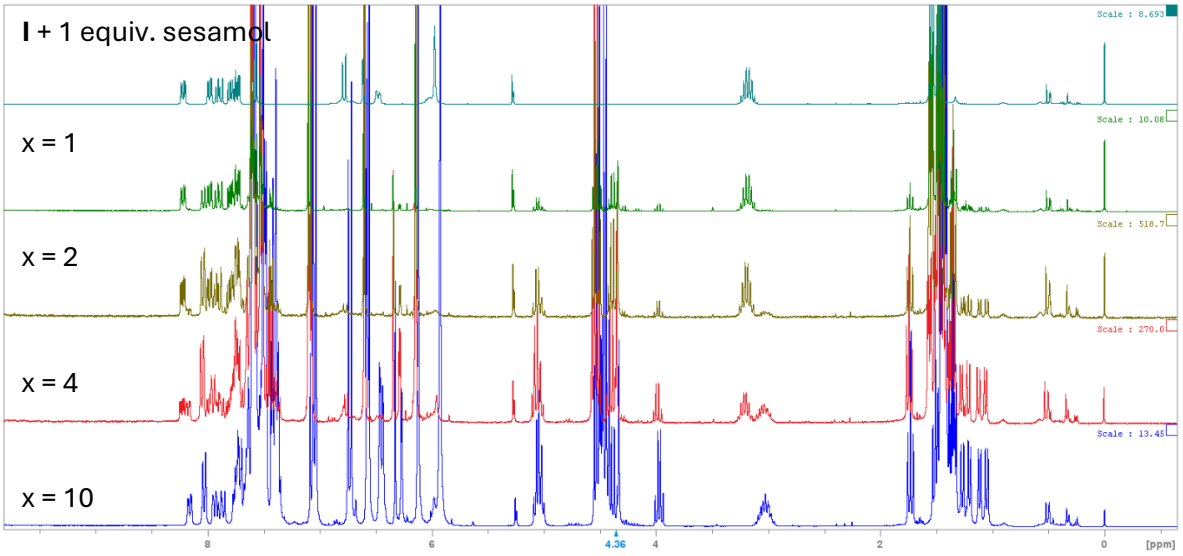

***Figure* 3.4** – ^{1}H NMR spectra of the reaction mixture at different loads of the substrates (x = number of eq. of substrates added).

The same experiment was performed by maintaining the original 1:2 alkyne/phenol ratio, obtaining analogous results and almost complete conversion of **I** after addition of 5 eq, of the alkyne and 10 eq. of sesamol, respectively.

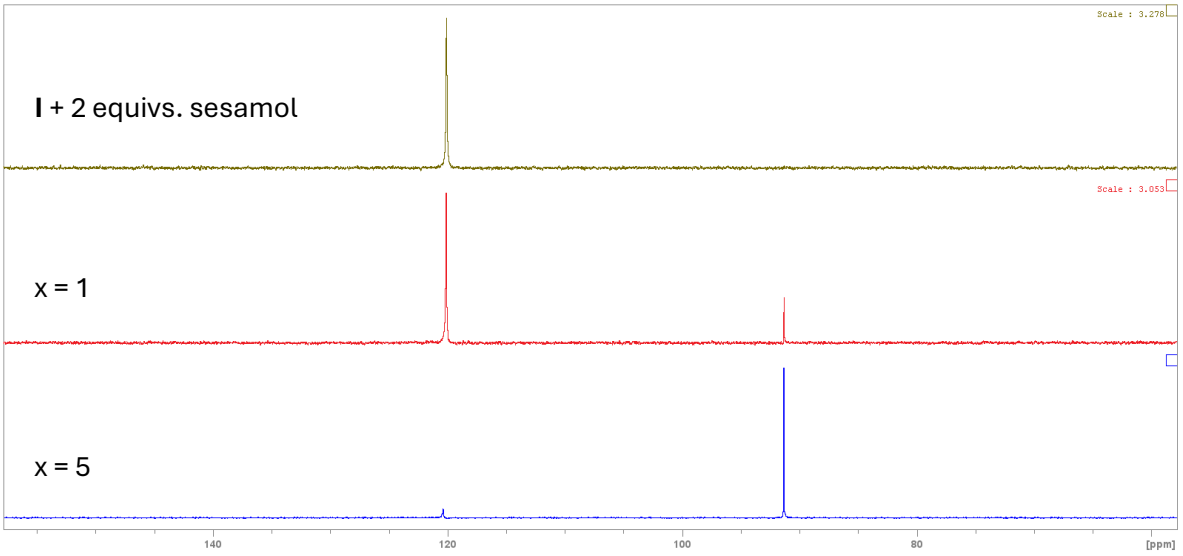

***Figure* 3.5** – ^{31}P NMR spectra of the reaction mixture after successive additions of the substrates (x = eq. alkyne; 2x = eq. sesamol).

The experiment was repeated using as solvent 0.74 ml Ac^FOH/DCM-d^2 1:20 ([Ac^FOH]/[Au] = 17.2). Complete conversion of the complex is detected after 30 minutes and only traces of the hydroarylation product are detected.

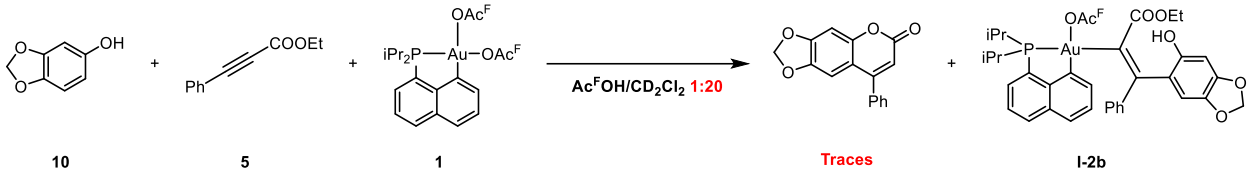

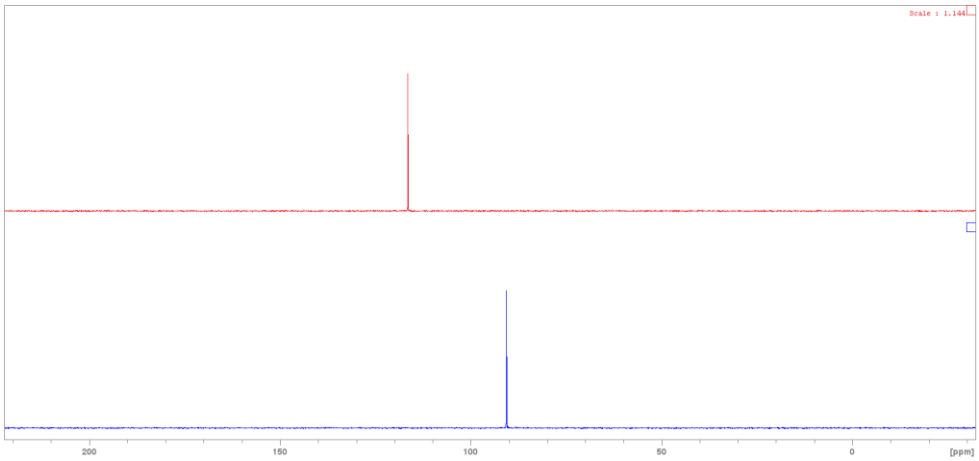

***Figure* 3.6** – $^{31}P\{^1H\}$ NMR spectra of the reaction mixture before (red line) and after (blue line) addition of ethyl phenylpropiolate.

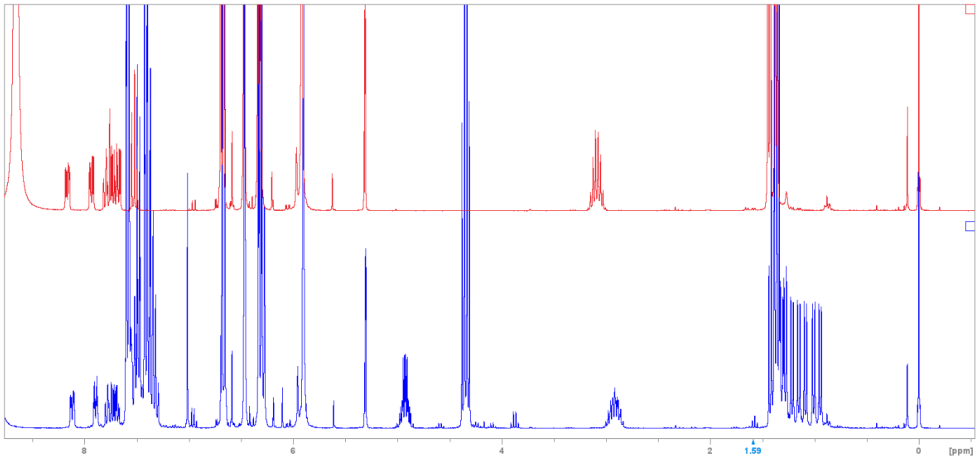

***Figure* 3.7** – ^1H NMR spectra of the reaction mixture before (red line) and after (blue line) addition of ethyl phenylpropiolate.

The reaction crude was then concentrated under vacuum and subjected to ESI-MS analyses (HPLC-acetonitrile as solvent).

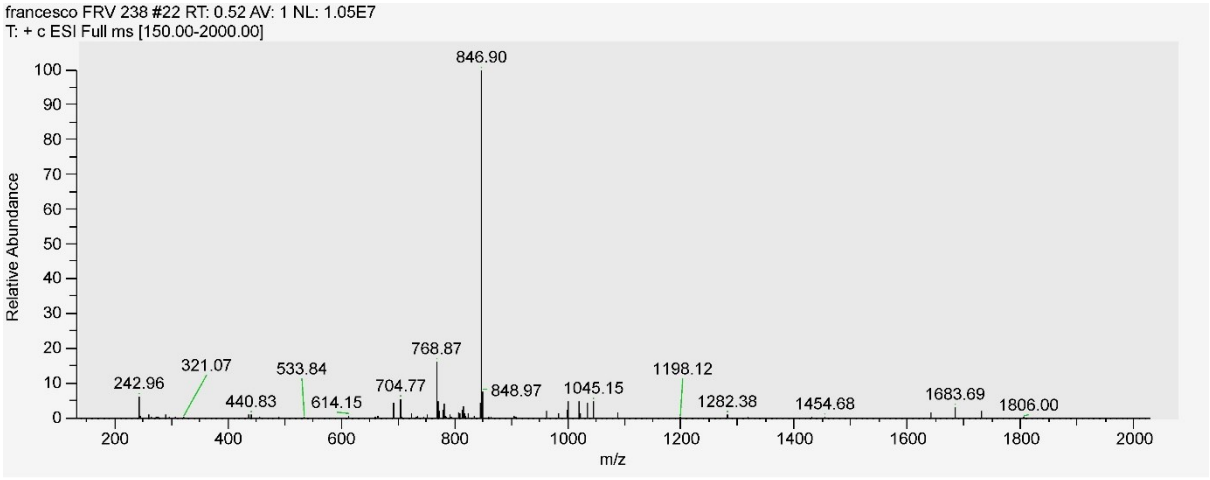

***Figure* 3.8** – ESI-MS analysis of the reaction mixture.

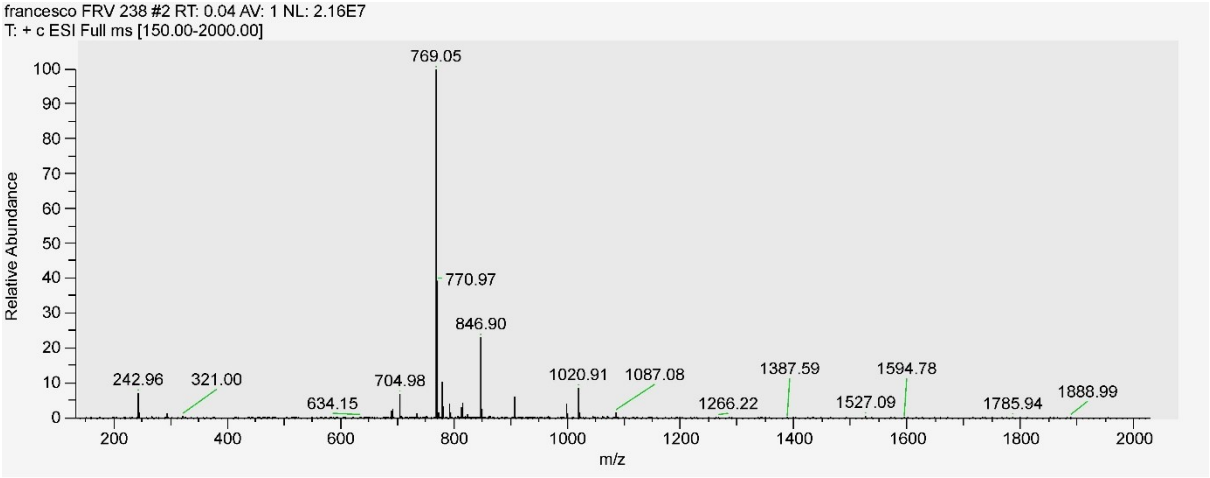

***Figure* 3.9** – ESI-MS analysis, chloride exchange at the charged species under diluted conditions.

The two reported mass spectra refer to the same solution under different dilution conditions. The signal at 769 m/z is indeed a secondary signal due to the exchange of a trifluoroacetate anion with a chloride. Analysis of the spectra allowed to assign to the two peaks the chemical formula $[C_{36}H_{34}AuF_3O_6P]^+$ and $[C_{34}H_{34}AuClO_4P]^+$. The isotopic distribution of both the fragments are in line

with the simulated ones. MS/MS experiments allowed to identify the following fragmentations peaks:

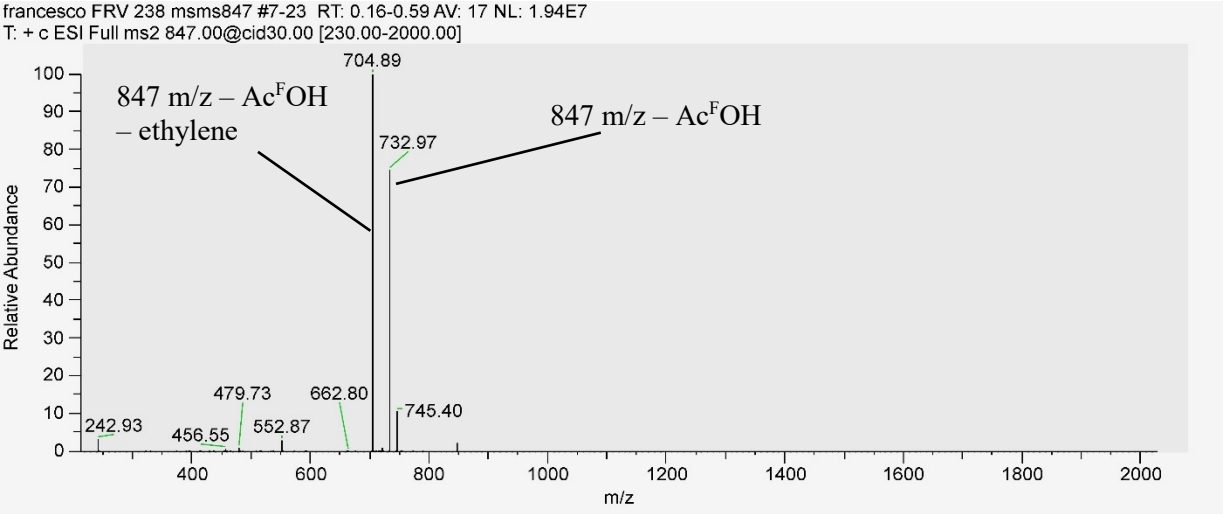

***Figure* 3.10** – MS/MS fragmentation spectrum of 847 m/z

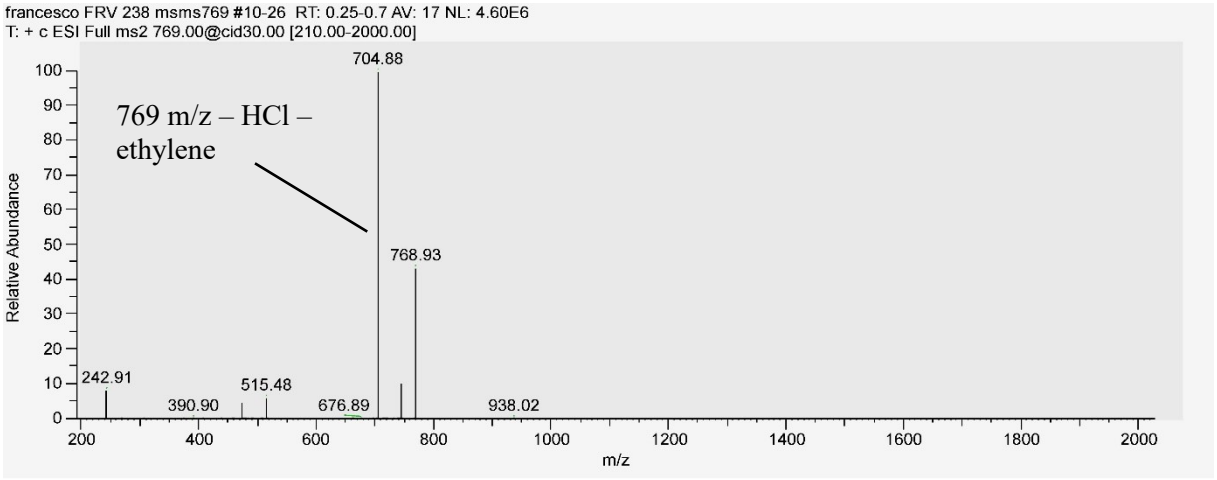

***Figure* 3.11** – MS/MS fragmentation spectrum of 769 m/z

Synthesis and characterization of I-2b'

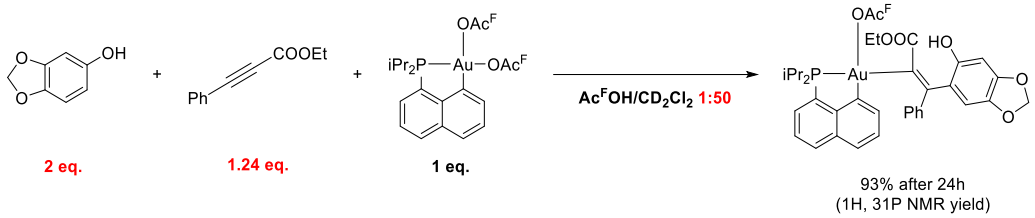

Complex **I** (16.8 mg, 0.025 mmol, 1 eq.) and sesamol (7.0 mg, 0.05 mmol) were placed in a flame-dried Schlenk flask under argon. The two solids were solubilized in 0.7 ml of DCM-d^2 and transferred into an NMR tube that was previously purged with argon. At this point, the alkyne (5.1 µl, 0.03 mmol) was added and ^{1}H and $^{31}P\{^{1}H\}$ spectra were collected as reference. The reaction started upon addition of 14 µl Ac^FOH to convert 93% of **I** to **I-2b'** after 24 hours.

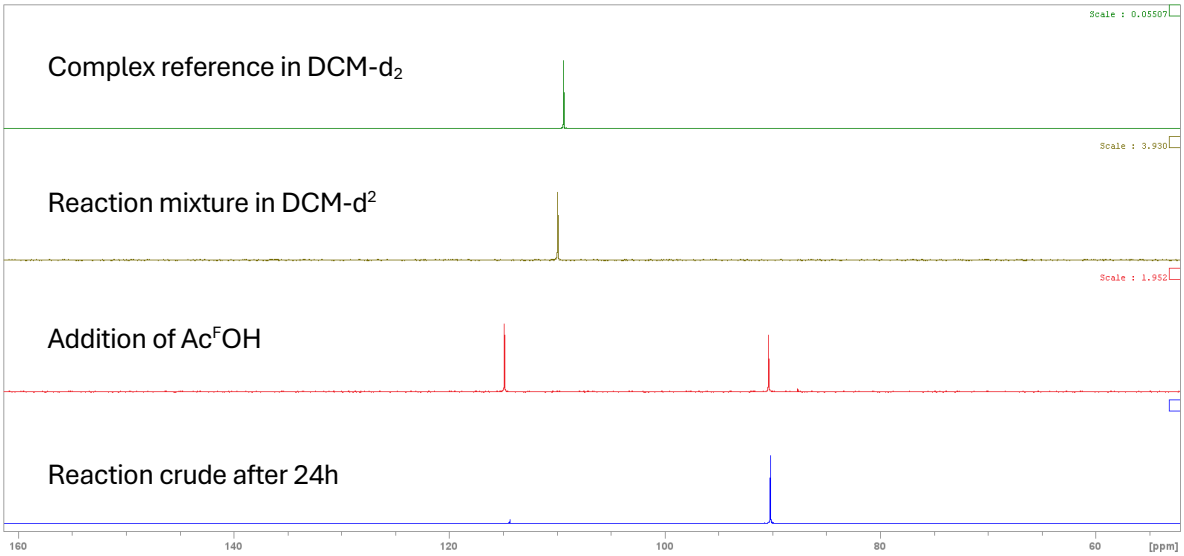

***Figure* 3.12** – $^{31}P\{^{1}H\}$ NMR monitoring of the reaction

Complete characterization of the reaction mixture by NMR spectroscopy (^{1}H, $^{13}C\{^{1}H\}$, DEPT-135, $^{31}P\{^{1}H\}$ and 2D correlation experiments).

(IPr$_2$P,C)Au(III)-vinyl complex – I-2b'

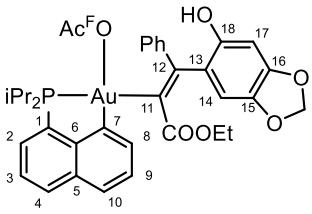

^{1}H NMR (300 MHz, CD_2Cl_2/Ac^{F}OH 50:1): δ 8.12 (ddd, *J* = 7.9, 3.0, 1.3 Hz, 1H, H_4), 7.89 (dt, *J* = 7.3, 2.0 Hz, 1H, H_{10}), 7,77 (ddd, *J* = 9.8, 7.1, 1.2, 1H, H_2), 7.70 (dd, *J* = 7.8, 3.1, 1H, H_3), 7.58-7.53 (m, 2H, H_{ortho} and H_{meta}), 7.51-7.45 (m, 1H, H_{para}), 7.45-7.41 (m, 1H, H_{ortho}), 7.40 (s, 1H, H_{17}), 7.37-7.28 (m, 3H, H_8, H_9 and H_{meta}), 7.02 (s, 1H, H_{14}), 6.29 (d, *J* = 0.7Hz, -O-CH_2-O-), 5.05-4.85 (m, 2H, -Et, -CH_2-), 3.02-2.83 (heptd, *J* = 9.7, 7.1 Hz, 2H, -iPr, CH), 1.43 (t, *J* = 7.1 Hz, 3H, -Et, -CH_3), 1.34 (dd, *J* = 16.7, 7.1 Hz, 3H, -iPr, -CH_3), 1.25 (dd, *J* = 19.5, 7.1 Hz, 3H, -iPr, -CH_3), 1.12 (dd, *J* = 19.0, 7.1 Hz, 3H, -iPr, -CH_3), 0.97 (dd, *J* = 18.6, 6.9 Hz, 3H, -iPr, -CH_3) ppm; **^{13}C{^{1}H} NMR (75.5 MHz, CD_2Cl_2/Ac^{F}OH 50:1): δ** 170.26 (d, *J* = 1.1 Hz, C_{12}), 169.86 (d, *J* = 4.4 Hz, C=O), 159.40 (q, *J* = 41.5 Hz, OAc^F and HOAc^F, C=O), 155.58 (s, C_{16}), 151.29 (s, C_{18}), 149.74 (d, *J* = 0.8 Hz, C_{15}), 148.46 (d, *J* = 27.3 Hz, C_6), 144.80 (d, *J* = 125.8 Hz, C_{11}), 137.70 (d, *J* = 3.0 Hz, $C_{Ph,\ ipso}$), 135.39 (d, *J* = 14.8 Hz, C_5), 135.13 (d, *J* = 0.5 Hz C_8), 134.29 (d, *J* = 2.6 Hz, C_4), 132.96 (d, *J* = 1.6 Hz, C_7), 132.37 (d, J = 1.6 Hz, C_2), 130.94 (s, $C_{Ph,\ para}$), 129.71 (s, $C_{Ph,\ meta}$), 129.55 (s, $C_{Ph,\ ortho}$), 129.35 (s, $C_{Ph,\ meta}$), 129.42 (s, C_{10}), 128.39 (s, C_9), 128.37 (s, $C_{Ph,\ ortho}$), 127.41 (d, *J* = 9.3 Hz, C_3), 123.44 (d, *J* = 55.0 Hz, C_1), 119.59 (d, *J* = 6.4 Hz, C_{13}), 115.34 (q, *J* = 286.0 Hz, OAc^F and HOAc^F, -CF_3), 105.00 (s, -O-CH_2-O-), 104.77 (d, *J* = 0.5 Hz, C_{14}), 98.59 (s, C_{17}), 71.45 (s, -OEt, -CH_2-), 26.52 (d, *J* = 27.3 Hz, iPr, CH), 26.31 (d, *J* = 27.4 Hz, iPr, CH), 18.07 (s, iPr, -CH_3), 17.99 (d, *J* = 1.9 Hz, iPr, -CH_3), 17.79 (d, *J* = 3.3 Hz, iPr, -CH_3), 17.03 (d, *J* = 1.5 Hz, iPr, -CH_3), 14.17 (s, -OEt, -CH_3) ppm; **^{31}P{^{1}H} NMR (121.5 MHz, CD_2Cl_2/Ac^{F}OH 50:1): δ** 90.1 (s) ppm;

Synthesis and characterization of I-2b

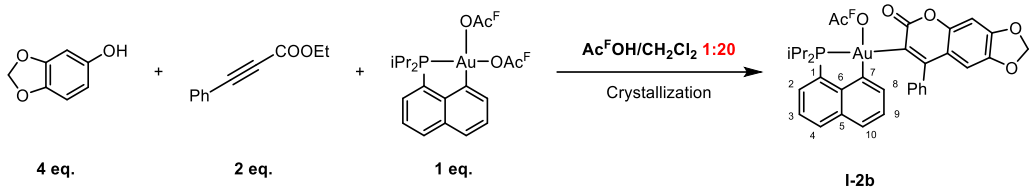

Gold complex **I** (30.0 mg, 0.045 mmol, 1 eq.) and sesamol (24.9 mg, 0.18 mmol, 4 eq.) were placed in a flame-dried round-bottom flask under argon. The two solids were solubilized in 2 ml of Ac^{F}OH/DCM 1:20; ethyl phenylpropiolate (15 µl, 0.09 mmol, 2 eq.) was then added and the reaction was stirred for 2 hours. A first attempt of isolating **I-2b'** by column chromatography was ineffective. On the other hand, the direct crystallization by layering *n*-hexane on a concentrated DCM solution gave better results, allowing to isolate a mixture of sesamol and **I-2b** which could be analyzed by the same characterization routine as above.

(IPr$_2$P,C)Au(III)-coumarinyl complex – I-2b

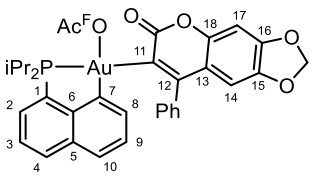

^{1}H NMR (300 MHz, CD$_2$Cl$_2$): δ 8.01 (ddd, *J* = 7.9, 2.5, 1.0 Hz, 1H, H$_4$), 7.78 (dd, *J* = 8.1, 1.2 Hz, 1H, H$_{10}$), 7.71 (d, *J* = 7.4 Hz, 1H, H$_8$), 7.66 (ddd, *J* = 9.0, 7.1, 1.2 Hz, 1H, H$_2$), 7.59 (dd, *J* = 7.9, 2.6 Hz, 1H, H$_3$), 7.58-7.52 (m, 1H, H$_{Ph,\ ortho}$), 7.46-7.38 (m, 1H, H$_{Ph,\ meta}$), 7.31 (t, *J* = 7.8 Hz, 1H, H$_9$), 7.30-7.23 (m, 2H, H$_{Ph,\ para}$ and H$_{Ph,\ ortho}$), 7.18-7.10 (m, 1H, H$_{Ph,\ meta}$), 6.90 (s ,1H, H$_{17}$), 6.58 (s ,1H, H$_{14}$), 6.01 (s, -O-CH$_2$-O-), 2.92 (heptd, 9.5, 7.1 Hz, 2H, -iPr, CH), 1.26 (dd, J = 16.6, 7.0 Hz, 3H, -iPr, -CH$_3$), 1.21 (dd, J = 19.3, 7.1 Hz, 3H, -iPr, -CH$_3$), 0.99 (dd, J = 18.8, 7.1 Hz, 3H, -iPr, -CH$_3$), 0.93 (dd, J = 17.3, 7.0 Hz, 3H, -iPr, -CH$_3$) ppm; **^{13}C{^{1}H} NMR (75.5 MHz, CD$_2$Cl$_2$): δ** 163.97 (d, *J* = 6.9 Hz, C=O), 160.60 (q, *J* = 36.6 Hz, OAc^F, C=O), 154.69 (d, *J* = 1.5 Hz, C$_{12}$), 153.81 (d, *J* = 129.3 Hz, C$_{11}$), 150.99 (s, C$_{18}$), 150.27 (s, C$_{16}$), 148.56 (d, *J* = 32.1 Hz, C$_6$), 144.81 (brs, C$_{15}$), 138.98 (d, *J* = 4.3 Hz, C$_{Ph,\ ipso}$), 135.63 (s, C$_8$), 134.86 (d, *J* = 14.4 MHz, C$_5$), 133.48 (s, C$_7$), 133.42 (d, *J* = 2.4 Hz, C$_4$), 131.32 (s, C$_2$), 130.05 (s, C$_{Ph,\ ortho}$), 128.84 (s,

$C_{Ph,\ meta}$), 128.68 (s, 2C, $C_{Ph,\ ortho}$ and $C_{Ph,\ meta}$), 128.46 (s, $C_{Ph,\ para}$), 128.15 (s, C_{10}), 128.10 (s, C_9), 126.31 (d, *J* = 8.4 Hz, C_3), 125.06 (d, *J* = 51.6 Hz, C_1), 117.40 (q, *J* = 290.4 Hz, OAc^F, $-CF_3$), 116.57 (d, *J* = 0.9 Hz, C_{13}), 104.67 (s, C_{14}), 102.69 (s, -O-CH_2-O-), 98.50 (s, C_{17}), 26.16 (d, *J* = 25.7 Hz, iPr, CH), 26.06 (d, *J* = 25.7 Hz, iPr, CH), 17.83 (d, *J* = 2.3 Hz, iPr, -CH_3), 17.78 (s, iPr, -CH_3), 17.76 (d, *J* = 1.5 Hz, iPr, -CH_3), 17.23 (d, *J* = 2.4 Hz, iPr, -CH_3) ppm; **$^{31}P\{^1H\}$ NMR (121.5 MHz, CD_2Cl_2): δ** 80.8 (s) ppm; **^{19}F NMR (188.3 MHz, CD_2Cl_2): δ** -74.3 (s) ppm; **ESI-MS (m/z):** 705 (**I-2b** – Ac^FO^-);

Direct protonolysis of the Au-C bond was carried out by addition of TfOH (4.0 µl, 0.045 mmol, 1 eq.). Formation of the coumarin **2b** was detected, along with a consistent shift of the ^{31}P signal at lower field, due to the labile character of the triflate anion tethered to gold.

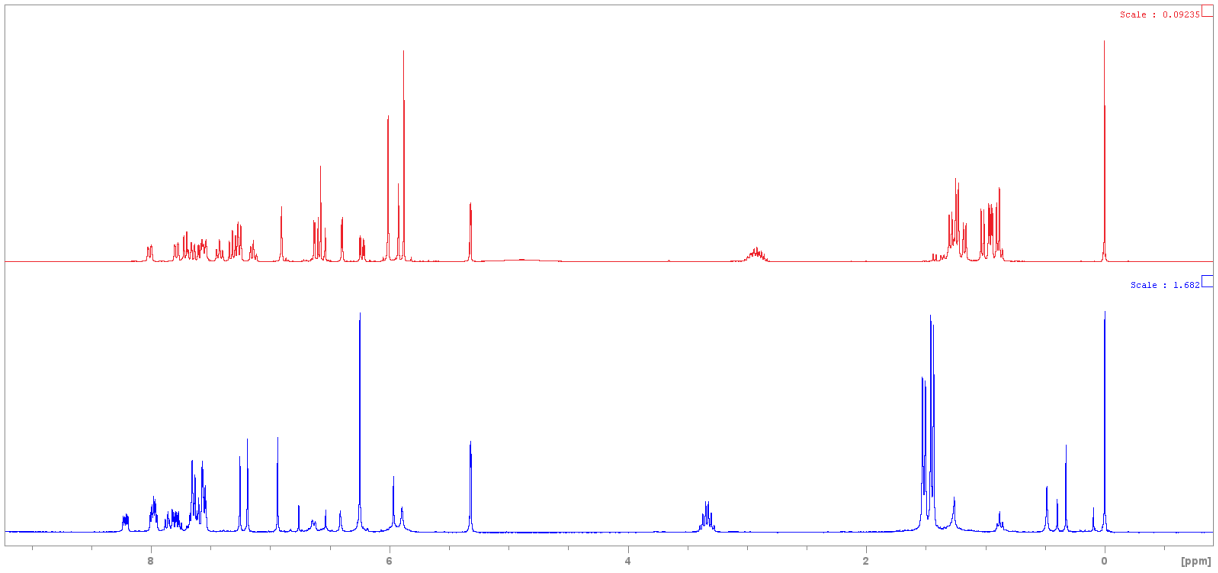

***Figure* 3.13** – ^1H NMR before (red line) and after (blue line) addition of 1 equiv. TfOH.

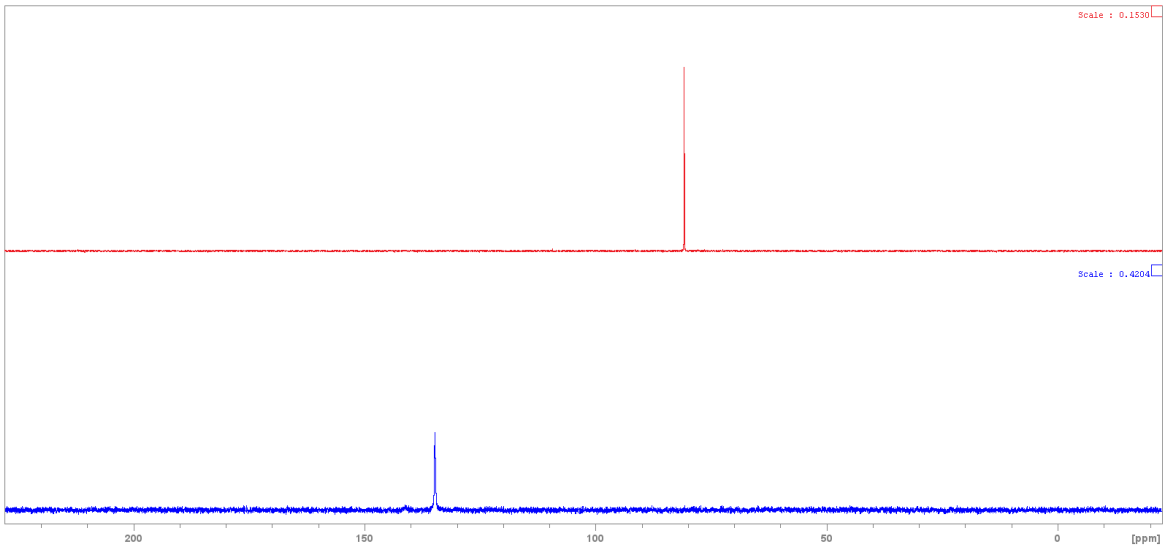

***Figure* 3.14** – $^{31}P\{^{1}H\}$ NMR before (red line) and after (blue line) addition of 1 equiv. TfOH.

Attempts to achieve Au-C bond cleavage in **I-2b'** by addition of 1 eq. of TfOH were ineffective; partial degradation of the gold complex was detected instead.

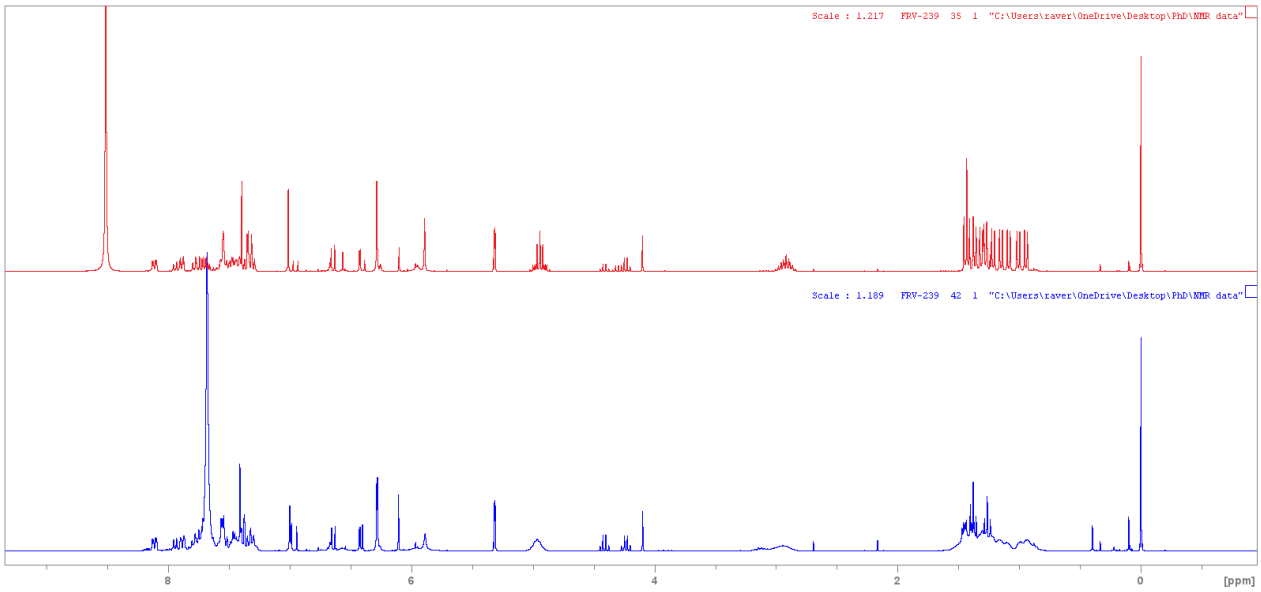

***Figure* 3.15** – ^{1}H NMR before (red line) and after (blue line) addition of 1 equiv. TfOH.

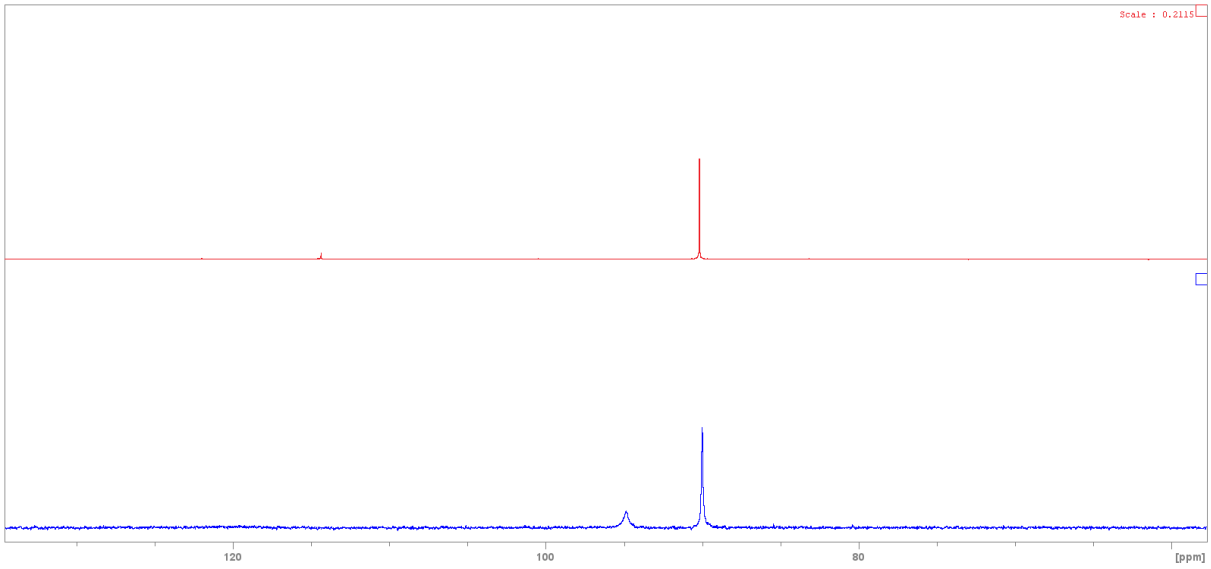

***Figure* 3.16** – $^{31}P\{^{1}H\}$ NMR before (red line) and after (blue line) addition of 1 equiv. TfOH.

ESI-MS analyses of catalyst activation

The complete extrusion of the iodide moieties at the gold(III) pre-catalysts **III** and **IV** upon catalyst activation was confirmed by ESI-MS analyses. In a 1 ml round-bottom flask, direct activation of the complex **III** (2.8 mg, 4.0 μmol) was performed by adding 0.3 ml of a freshly prepared solution of $AgSbF_6$ (2.8 mg, 8.1 μmol, 2.0 eq.) in [BMIM][NTf_2] (0.3 ml) under argon atmosphere. The mixture was stirred for one hour and the crude was then passed through a PTFE syringe-filter to remove the precipitated silver iodide. An aliquot of the filtered mixture was dissolved in HPLC-grade ACN and analyzed by ESI-MS (***Figure 3.17***). Separately, analytical data of the employed silver salt solution and the pure [BMIM][NTf_2] were also collected (***Figure*s 3.18** and **3.19** respectively).

The recorded data of the medium were in agreement with the fragmentation pattern previously reported in the literature. A minor impurity peak was also visible, due to traces of silver coming from former analyses we performed. Interestingly, this signal was located at 383 m/z (Ag^+ + 276 m/z) and it could be undoubtedly assigned to Ag^+ ions in the ionic liquid medium by means of the unique isotopic distribution of this metal ion (^{107}Ag : ^{109}Ag = 51.8 : 48.2). The shift of the observed m/z value was imputed to the formation of adducts with neutral decomposition fragments of the imidazolium cation. Several reports in the literature already described the formation of free N-heterocyclic carbenes (NHCs) by abstraction of the relatively acidic proton at the pro-carbene carbon atom.[30–34] Detection of free carbenes is possible only upon installation of a charge-tag at the organic precursor,[35–38] since imidazole-2-ylidenes and, in general, most NHCs are formally neutral. Despite the absence of a strong H-bond donor in the ionic couple, the high vacuum conditions ensured by the mass spectrometer apparatus may allow the formation of these species. Hence, we have reason to believe that the presence of soft metal ions, such as Ag or Au, may result in an easier stabilization and detection of newly formed NHC ligands under ESI conditions.

From this analysis we could assign the peak at 996 m/z as the cationic gold(III) complex with the loss of a bistriflimide moiety: m/z = [(iPr_2P,C)Au(NTf_2)]$^+$ + 276. The additional mass of 276 Da fits well with two NHCs moieties which originated from the [BMIM]$^+$ precursor. As well, the isotopic distributions of both fragments [Ag$(NHC)_2$]$^+$ and [(iPr_2P,C)Au$(NHC)_2$]NTf_2^+ are in agreement with the calculated ones while no traces of iodides at the gold complex could be observed.

To confirm this result, control tests were conducted upon treating **III** (15 mg) with $AgNTf_2 \cdot ACN$ (2 eq.) in DCM (1 ml) under argon atmosphere. After 1 hour stirring, the suspension was filtered through a PTFE syringe filter and the volatiles removed under reduced pressure. ESI-MS analyses of the obtained yellow solid allowed to observe an intense signal at 720 m/z (***Figure 3.20*** and **3.21**). This peak corresponds to the mono-cationic fragment $[(iPr_2P,C)Au(NTf_2)]^+$, generated by loss of a bistriflimide moiety from the neutral $[(iPr_2P,C)Au(NTf_2)_2]$ complex. This fragmentation pattern was already reported for the analogous bis-trifluoroacetate (iPr_2P,C)-catalyst **I**. However, dissolving the solid in $[BMIM][NTf_2]$ determined an analogous result as activating **III** directly in the IL medium: the peak corresponding to the metal complex was indeed found shifted at 996 m/z (***Figure 3.22***). This result further confirms the complete cleavage of the iodide moieties at the gold metal center after treatment with 2 eq. $AgSbF_6$.

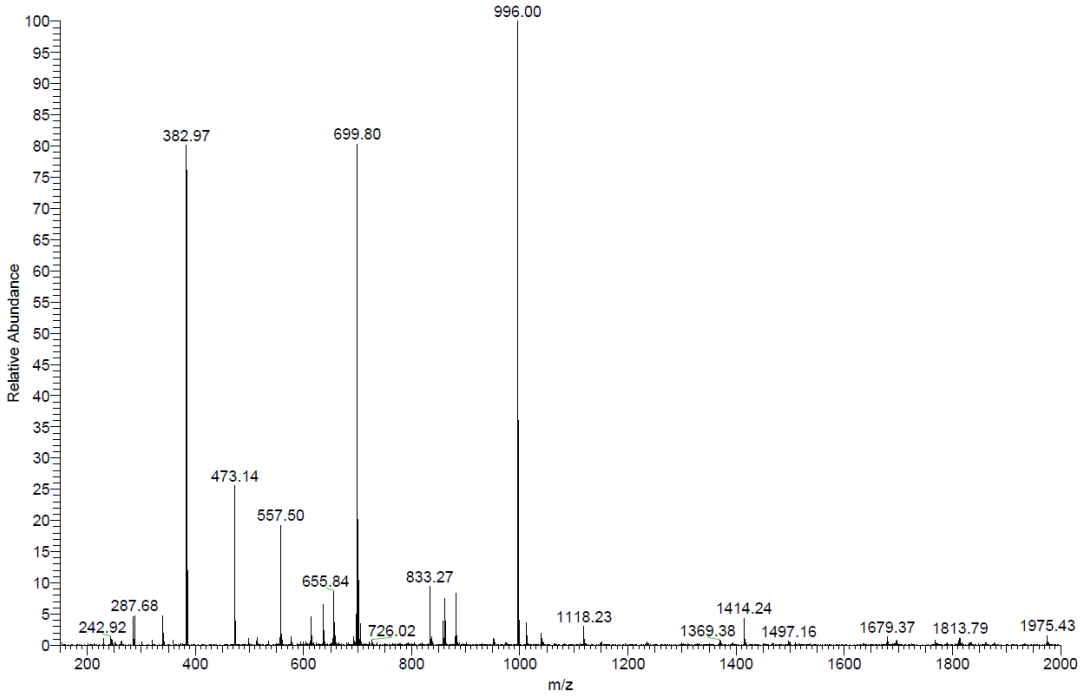

Figure 3.17 – ESI-MS spectrum of complex **III** activated in BMIM NTf_2

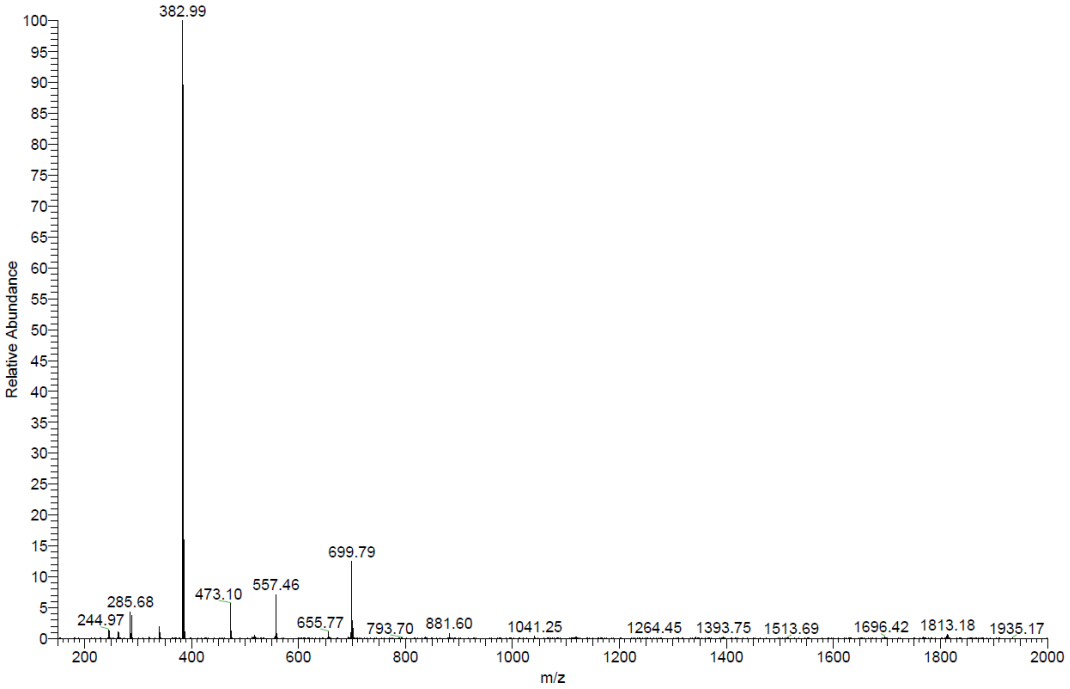

Figure 3.18 – ESI-MS spectrum of the silver salt $AgSbF_6$ in BMIM NTf_2

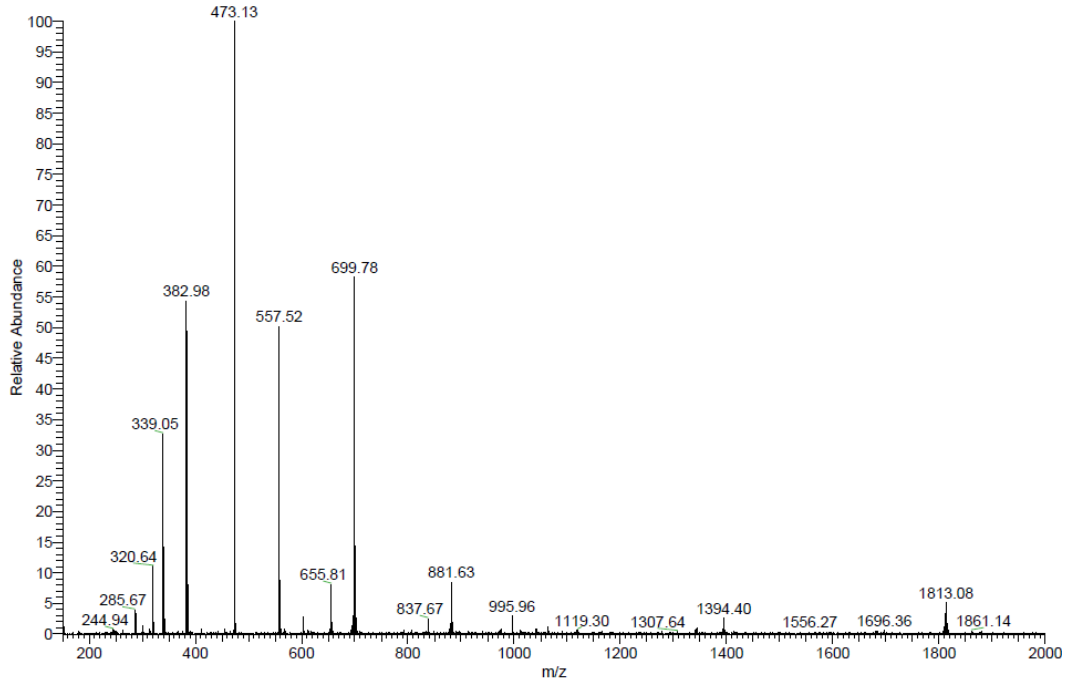

Figure 3.19 – ESI-MS spectrum of BMIM NTf_2

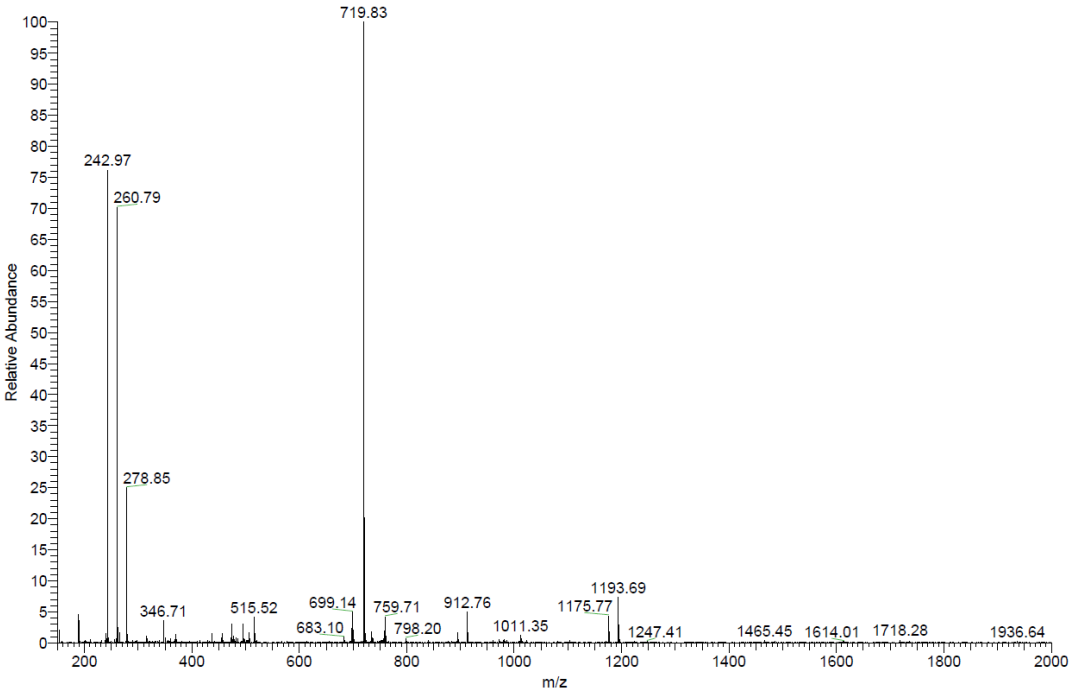

Figure 3.20 – ESI-MS spectrum of complex **III** activated in DCM

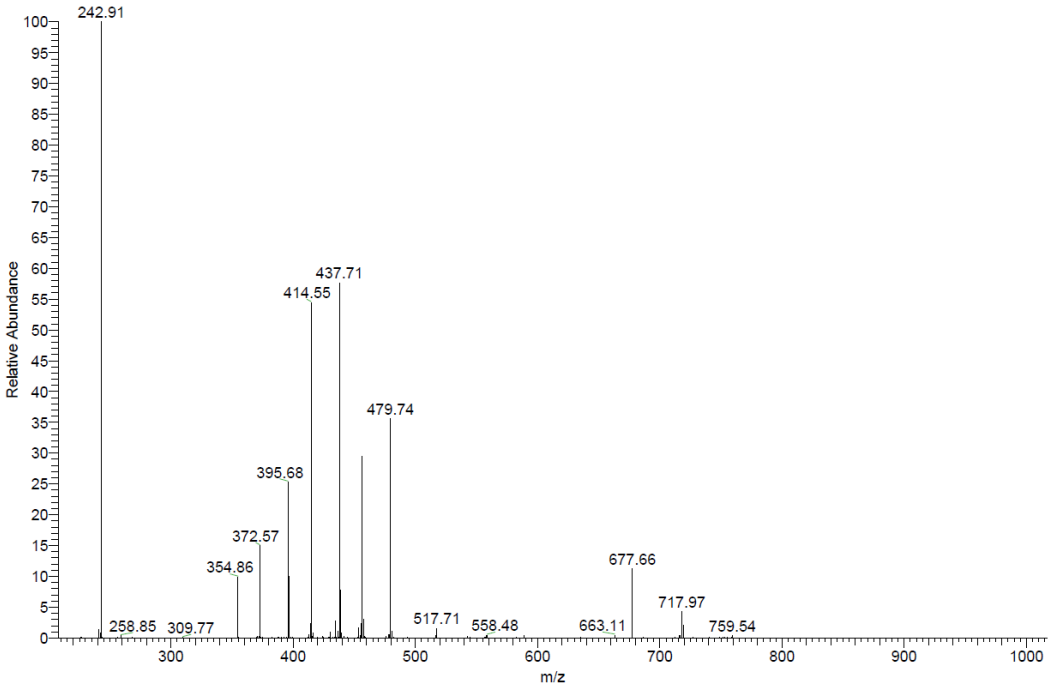

Figure 3.21 – MS/MS experiment of the peak at 720 m/z

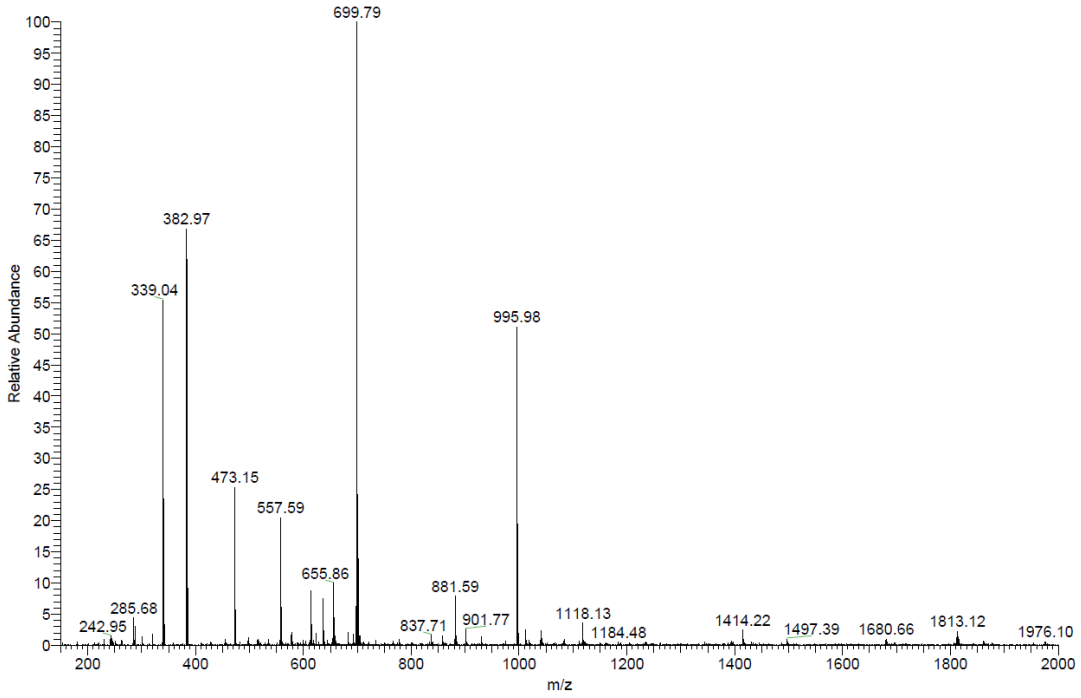

Figure 3.22 – Catalyst activated in DCM and dissolved in BMIM NTf_2

3.6. References

[1] G. R. Fulmer, A. J. M. Miller, N. H. Sherden, H. E. Gottlieb, A. Nudelman, B. M. Stoltz, J. E. Bercaw, K. I. Goldberg, *Organometallics* **2010**, *29*, 2176–2179.

[2] N. R. Babij, E. O. McCusker, G. T. Whiteker, B. Canturk, N. Choy, L. C. Creemer, C. V. D. Amicis, N. M. Hewlett, P. L. Johnson, J. A. Knobelsdorf, F. Li, B. A. Lorsbach, B. M. Nugent, S. J. Ryan, M. R. Smith, Q. Yang, *Org. Process Res. Dev.* **2016**, *20*, 661–667.

[3] R. K. Harris, E. D. Becker, R. Goodfellow, P. Granger, *Pure Appl. Chem.* **2001**, *73*, 1795–1818.

[4] S. Bontemps, M. Devillard, S. Mallet-Ladeira, G. Bouhadir, K. Miqueu, D. Bourissou, *Inorg. Chem.* **2013**, *52*, 4714–4720.

[5] J. Guenther, S. Mallet-Ladeira, L. Estevez, K. Miqueu, A. Amgoune, D. Bourissou, *J. Am. Chem. Soc.* **2014**, *136*, 1778–1781.

[6] F. Rekhroukh, R. Brousses, A. Amgoune, D. Bourissou, *Angew Chem Int Ed* **2015**, *54*, 1266–1269.

[7] C. Blons, S. Mallet-Ladeira, A. Amgoune, D. Bourissou, *Angew. Chem. Int. Ed.* **2018**, *57*, 11732–11736.

[8] H. Li, S. Liu, Y. Huang, X.-H. Xu, F.-L. Qing, *Chem. Commun.* **2017**, *53*, 10136–10139.

[9] A. Cervi, Y. Vo, C. L. L. Chai, M. G. Banwell, P. Lan, A. C. Willis, *J. Org. Chem.* **2021**, *86*, 178–198.

[10] A. Mathuri, B. Pal, M. Pramanik, P. Mal, *J. Org. Chem.* **2023**, *88*, 10096–10110.

[11] C. Jia, D. Piao, T. Kitamura, Y. Fujiwara, *J. Org. Chem.* **2000**, *65*, 7516–7522.

[12] S. Sau, P. Mal, *Chem. Commun.* **2021**, *57*, 9228–9231.

[13] M. Bio, G. Nkepang, Y. You, *Chem. Commun.* **2012**, *48*, 6517–6519.

[14] M. D. Aparece, P. A. Vadola, *Org. Lett.* **2014**, *16*, 6008–6011.

[15] A. D. Worthy, C. L. Joe, T. E. Lightburn, K. L. Tan, *J. Am. Chem. Soc.* **2010**, *132*, 14757–14759.

[16] J. Li, H.-W. Xing, F. Yang, Z.-S. Chen, K. Ji, *Org. Lett.* **2018**, *20*, 4622–4626.

[17] S. J. Pastine, S. W. Youn, D. Sames, *Org. Lett.* **2003**, *5*, 1055–1058.

[18] Y.-Y. Chen, K.-L. Chen, Y.-C. Tyan, C.-F. Liang, P.-C. Lin, *Tetrahedron* **2015**, *71*, 6210–6218.

[19] O. Renaudet, J.-L. Reymond, *Org. Lett.* **2004**, *6*, 397–400.

[20] J.-S. Tian, Y. He, Z.-Y. Gao, X. Liu, S.-F. Dong, P. Wu, T.-P. Loh, *Org. Lett.* **2021**, *23*, 6594–6598.

[21] Z. Wang, X. Li, L. Wang, P. Li, *Tetrahedron* **2019**, *75*, 1044–1051.

[22] M. D. P. Olaya, N. E. Vergel, J. L. López, D. Viña, M. F. Guerrero, *Braz. J. Pharm. Sci.* **2020**, *56*, e17609.

[23] Z. Shi, C. He, *J. Org. Chem.* **2004**, *69*, 3669–3671.

[24] D. Kim, M. Min, S. Hong, *Chem. Commun.* **2013**, *49*, 4021–4023.

[25] Y.-S. Hon, T.-W. Tseng, C.-Y. Cheng, *Chem. Commun.* **2009**, 5618–5620.

[26] B. Martín-Matute, C. Nevado, D. J. Cárdenas, A. M. Echavarren, *J. Am. Chem. Soc.* **2003**, *125*, 5757–5766.

[27] T. Danelzik, S. Joseph, C. Mück-Lichtenfeld, C. G. Daniliuc, O. García Mancheño, *Org. Lett.* **2022**, *24*, 6105–6110.

[28] V. C. Pandurang, A. D. Dattatray, A. Sudalai, *PROCESS FOR THE PRODUCTION OF 4-SUBSTITUTED CHROMANES VIA GOLD CATALYSIS*, **2013**, WO 2013/088455 Al.
[29] A. J. Ward, A. F. Masters, T. Maschmeyer, *RSC Adv.* **2014**, *4*, 23327–23337.
[30] O. Hollóczki, D. Gerhard, K. Massone, L. Szarvas, B. Németh, T. Veszprémi, L. Nyulászi, *New J. Chem.* **2010**, *34*, 3004–3009.
[31] R. Lambert, P. Coupillaud, A. Wirotius, J. Vignolle, D. Taton, *Macromol. Rapid Commun.* **2016**, *37*, 1143–1149.
[32] A. C. Baumruck, D. Tietze, A. Stark, A. A. Tietze, *J. Org. Chem.* **2017**, *82*, 7538–7545.
[33] J. R. Diniz, T. B. De Lima, R. Galaverna, A. L. De Oliveira, D. A. C. Ferreira, F. C. Gozzo, M. N. Eberlin, J. Dupont, B. A. D. Neto, *Phys. Chem. Chem. Phys.* **2018**, *20*, 24716–24725.
[34] I. Chiarotto, L. Mattiello, F. Pandolfi, D. Rocco, M. Feroci, *Front. Chem.* **2018**, *6*, 355.
[35] E. Alcalde, N. Mesquida, M. Vilaseca, *Rapid Commun. Mass Spectrom.* **2000**, *14*, 1443–1447.
[36] J. W. Remsburg, R. J. Soukup-Hein, J. A. Crank, Z. S. Breitbach, T. Payagala, D. W. Armstrong, *J. Am. Soc. Mass Spectrom.* **2008**, *19*, 261–269.
[37] C. Salvitti, I. Chiarotto, F. Pepi, A. Troiani, *ChemPlusChem* **2021**, *86*, 209–223.
[38] C. Salvitti, F. Pepi, M. Managò, M. Bortolami, C. Michenzi, I. Chiarotto, A. Troiani, G. De Petris, *Rapid Comm Mass Spectrometry* **2022**, *36*, e9338.

4. Direct hydroarylations of organic isocyanates with heteroarenes

4.1. Introduction

Organic isocyanates are a class of molecules characterized by the heterocumulene –N=C=O functional group.[1,2] They can be conveniently synthesized either by direct phosgenation of a primary amine or by a Curtius rearrangement of acyl azides under thermal conditions;[2–4] the latter method is particularly suited for laboratory–scale syntheses. From an industrial point of view, catalytic decomposition of carbamates is as well a valuable strategy, avoiding the use of dangerous reagents, such as phosgene or analogous species (**Figure 4.1**).[2,5,6]

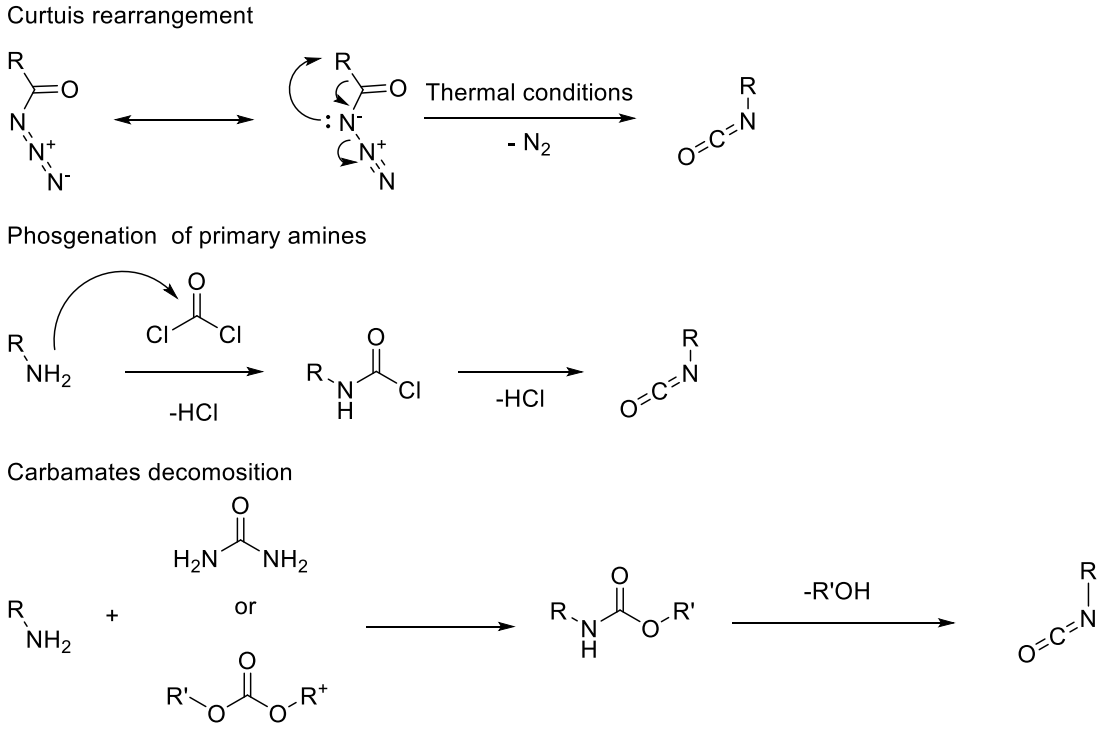

Figure 4.1 – Common methods for the synthesis of organic isocyanates;

The enhanced electrophilic character of the heteroallene carbon makes these molecules prone to nucleophilic attack by a wide range of Lewis bases, affording diverse carboxamide derivatives (*e.g.* urethanes, ureas, amides). Moreover, organic diisocyanates are widely employed in the industrial manufacture of polyurethane materials.[5]

Turning to organometallic chemistry, isocyanate coordination to transition metal centers (*e.g.* Ni, Fe, Ti) has been comprehensively reviewed by Pierre Braunstein and Dominique Nobel.[7] Such coordination can trigger migratory insertion reactions of the –N=C=O group into various M–X bonds (with X= H, O, N or C), thereby expanding the synthetic utility of this functional group. More complex pathways involving unsaturated or polyunsaturated substrates may lead to cycloisomers through multiple insertions driven by the metal center. Additionally, isocyanates can serve as precursors to carbodiimides and participate in diverse cycloaddition pathways.

Over the past two decades, particular attention has been directed toward the synthesis of amides via insertion of the –N=C=O fragment into M–C bonds. Traditionally, the synthesis of amides from carboxylic acids and amines is quite straightforward, but it often require the use of coupling reagents (di-substituted carbodiimides or azodicarboxylates) to promote the condensation of the two reacting moieties, with the inevitable formation of stoichiometric quantities of by-products. This new approach has proven applicable across a wide range of metal centers, enabling interception of various organometallic intermediates to afford the desired amides with an improved atom-economy and without waste production (**Figure 4.2**).[8–15]

More recently, independent works by Hashmi[16] and Melen[17] introduced a novel activation mode based on direct Lewis–acid–mediated activation of this heterocumulene fragment (**Figure 4.3**). Withdrawal of electron density from the –N=C=O group increases the electrophilicity of the carbon atom, thereby facilitating attack by nucleophiles. Specifically, Melen and co–workers reported that N–substituted indoles undergo conversion to 3–aminocarboxy derivatives using 0.3 equivalents of $B(C_6F_5)_3$ as a catalyst,[17] while Hashmi reported that the salt $AuBr_3$ can similarly activate isocyanates to promote addition and ring–opening reactions of azirines.[16]

In the final part of this thesis, we describe the direct activation of organic isocyanates using a well–defined Au(I) complex to enable hydroarylation across the N=C fragment. Optimization of reaction conditions revealed a narrow window of choice concerning the ligand tethered to gold. In particular, only the NHC-carbene complex $IPrAu^+$ and the cyclometalated $(iPr_2P,C)Au^{2+}$ complex showed appreciable activity at 0.5 mol% loading, utilizing either $[BMIM][NTf_2]$ or dichloromethane. Under neat conditions, the process could be further optimized and the substrate scope examined. Both aryl– and alkyl–isocyanates were successfully employed, affording modest to good yields. Additionally, a variety of nucleophiles, including substituted pyrroles and indoles, were found to participate with comparable results.

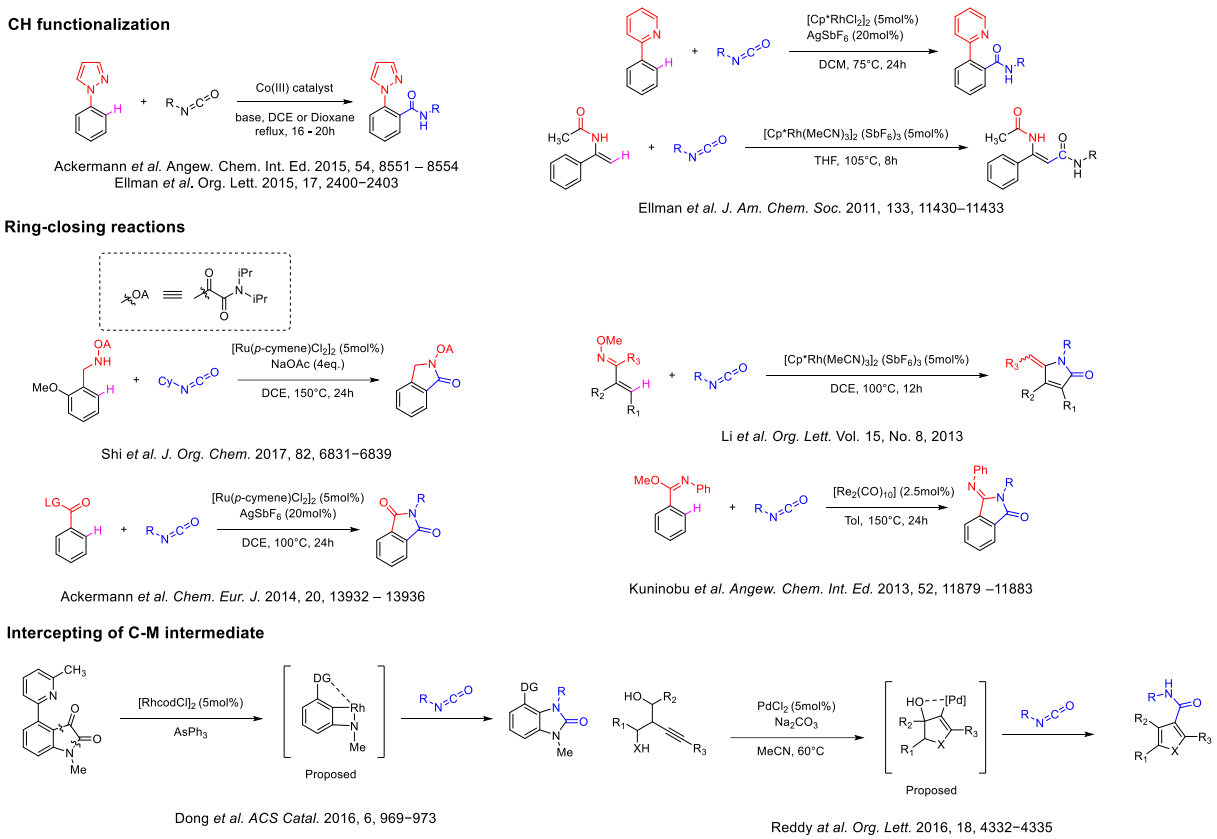

Figure 4.2 *– Selected examples from the literature of transformation with isocyanates in organic synthesis.*

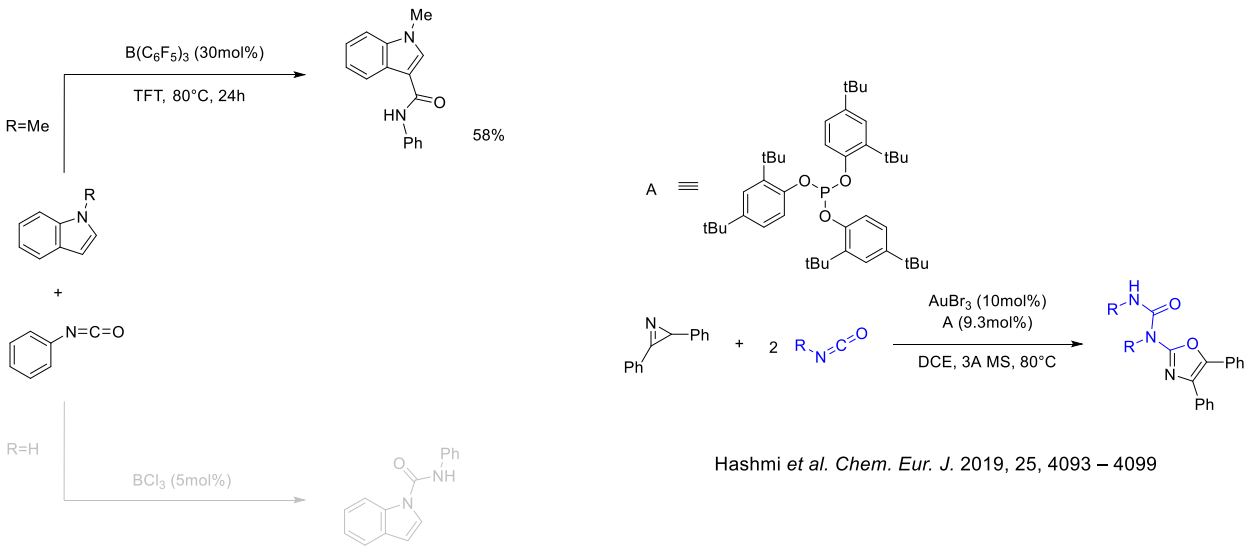

Figure 4.3 *– Previously reported examples of direct activation of organic isocyanates by Melen and Hashmi.*

Mechanistic studies suggest that the process operates via an outer–sphere pathway. Both Hammett analysis and kinetic isotope effect (KIE) experiments indicate that direct auration of N–methylpyrrole contributes only minimally to the reaction kinetic. This aspect is important since there is no evidence in the literature for a TM-catalyzed hydroarylation at isocyanates residues by an outer-sphere mechanism. To value our hypothesis we obtained evidence for the formation of a family of well–defined IPrAu–(isocyanate) adducts. These adducts were characterized by multinuclear NMR spectroscopy (^{1}H, ^{13}C, ^{15}N, and 2D experiments) at variable temperatures and shown to generate the corresponding products in the presence of N–methylpyrrole.

4.2. Process Optimization and Reaction Scope

The direct amidation of N–methylpyrrole with phenylisocyanate was selected as benchmark reaction for optimization. The results of this screening are summarized below (***Figure 4.4***).

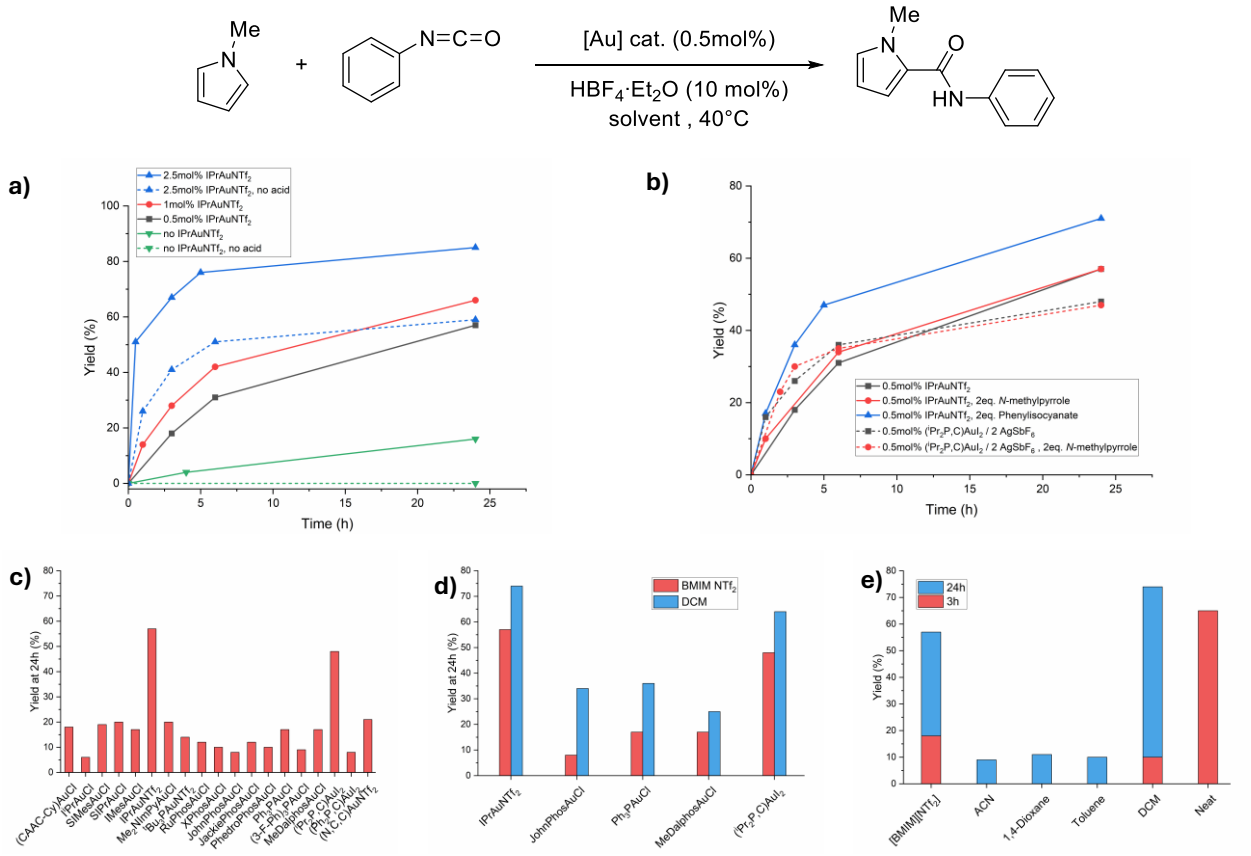

Figure 4.4 *– a) Effect of the IPrAuNTf$_2$ loading on the reaction kinetic; b) effect of different reagents stoichiometries on the reaction kinetic; c) screening of the catalyst (solvent [BMIM][NTf$_2$], chlorido complexes are activated in–situ with AgSbF$_6$); d) subgroup of the catalyst scope tested in DCM (activation performed in–situ with AgNTf$_2$); e) effect of the solvent.*

The reaction proceeded under mild conditions (T = 40 °C) with moderate catalyst loadings (down to 0.5 mol% $IPrAuNTf_2$). A blank test underscored the essential role of the gold complex in promoting reactivity (***Figure 4.4a***, green lines). The presence of an acidic additive significantly increased the reaction rate, enabling a reduction in the required catalyst quantity (***Figure 4.4a***). An increased reaction rate was also observed with an excess of phenylisocyanate (2 equivalents), while no change was detected using 2 equivalents of N–methylpyrrole; this observation was consistent when employing $(iPr_2P,C)AuI_2$ as the catalyst (***Figure 4.4b***). Notably, only the aforementioned complexes exhibited appreciable catalytic activity among those tested (***Figure 4.4c***, $[BMIM][NTf_2]$ as the solvent). The structures of the employed ligands are shown in **Figure 4.30** of the "***Experimental section***". The result is confirmed by testing a subset of these complexes in DCM (***Figure 4.4d***): $IPrAuNTf_2$ and the (P,C)–gold(III) complex remained the most active catalysts, while other complexes mediated the process with lower yields (<40%). More in specific about the choice of the medium, DCM as a solvent afforded higher yields, whereas $[BMIM][NTf_2]$ provided faster initial kinetics followed by attenuation of the reaction rate(***Figure 4.4f***), likely due to competing processes such as oligomerization of N-methylpyrrole mediate by acid or formation of aniline from phenyl isocyanate via hydration/decarboxylation of the allene. Interestingly, changing the complex anion to hexafluoroantimonate did not improve the catalytic performance, which is an unusual behavior if compared to most of gold(I)-catalyzed processes where the anion choice cover an important role for optimization (***Figure 4.5***). [18,19]

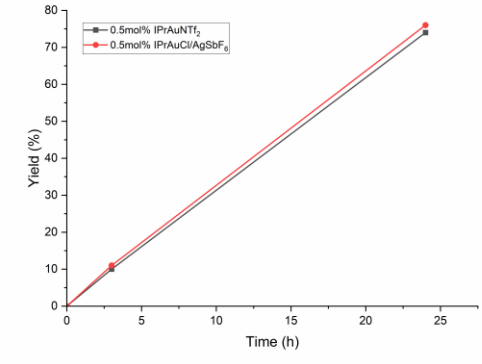

Figure 4.5 *– Anion effect on the reaction kinetic.*

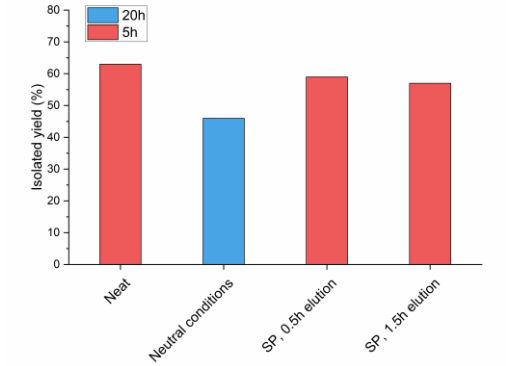

Figure 4.6 *– Attempts to improve the yield.*

Ultimately, employing neat conditions proved most effective for increasing the reaction rate, achieving full conversion of N–methylpyrrole within 3 hours. Attempts to further increase the yield

were unsuccessful: neutral conditions led to lower yields and longer reaction times (46% in 24 h), while syringe–pump methods provided similar results to bulk conditions (***Figure 4.6***).

The reaction scope was investigated on a 0.5–1 mmol scale (***Figure 4.7***). Aryl isocyanates with both electron–withdrawing (EW) and electron–donating (ED) substituents were successfully utilized showcasing a low influence of the electronic effects on the final yield. On the other hand, in the presence of hindered groups near the nitrogen atom affected negatively the performance (e.g., substrate **3ai** vs. **3ab** and **3af**). Specifically, mesityl and 2,6–dimethylphenyl derivatives afforded modest yields only after 20 h, whereas the Dipp–substituted isocyanate remained unreactive, likely due to higher energy barriers for nucleophilic attack. This behavior contrasts with methodologies that rely on H-bond-directed catalysis, which are less affected by ortho-substituents on aryl isocyanates, as independently reported by Neri and Song.[20][21] This suggests that the active adduct is probably different from the H-bonded aggregates formed in protic environments such as resorcinarene capsules or HFIP (hexafluoroisopropanol). Other isocyanates bearing unsaturated residues such as naphthyl, benzyl, and allyl groups were successfully employed (**3ao**, **3aq** and **3ar**), though reporting a modest yield for the latter. Finally, alkyl isocyanates could be included as well to the scope (**3as** and **3at**). In contrast, ethyl isocyanate and phenyl isothiocyanate failed under the same conditions over 24h reaction time (**3au** and **3ap**). While the thio-derivative was expected to have a more inert character toward nucleophilic attacks, the reason why ethylisocyanate was found unreactive stays controversial. In this case, the low steric hindrance may result detrimental for the formation of the active adduct.

The methodology demonstrated of good generality with respect to the nucleophile scope. Both unsubstituted and N–phenyl pyrroles showed appreciable reactivity, with a higher yield obtained for the less hindered nucleophile (67% of **3ba** vs 44% of **3ca**). Expectedly, increasing the number of EDGs at the heterocycle enhanced the yield (**3da**, 74% yied), according to a higher nucleophilic character at the carbon atom at position 2. Selective amidation at position 3 was achieved when positions 2 and 5 were blocked by methyl groups (**3ea**, 45% yield) and the introduction of a carboxylate function as EWG was also possible, albeit increasing the reaction time due to lack in activity (**3fa**, 32% yield). Indoles were tested and displayed moderate reactivity. Protection at the N–position was essential to maintain good selectivity, due to potential hydroamination side reactions. This was evident when comparing 1–, 2–, and 4–methyl indoles: 1–methyl or 1,2–dimethyl indoles did not form hydroamination products, although lower yields were determined, which correlates

with a higher steric hindrance near the nucleophilic carbon (**3ga** vs. **3ha** vs. **3ia**). Conversely, 2–methylindole yielded both the hydroarylation and hydroamination products, although proceeding with comparable yields regarding the amide **3ja** (38% vs. 43% for **3ha**). In 4–methylindole, steric hindrance slowed the hydroarylation rate, concurrently to a decrease in selectivity toward **3ka**, that could be isolated in 21% yield.

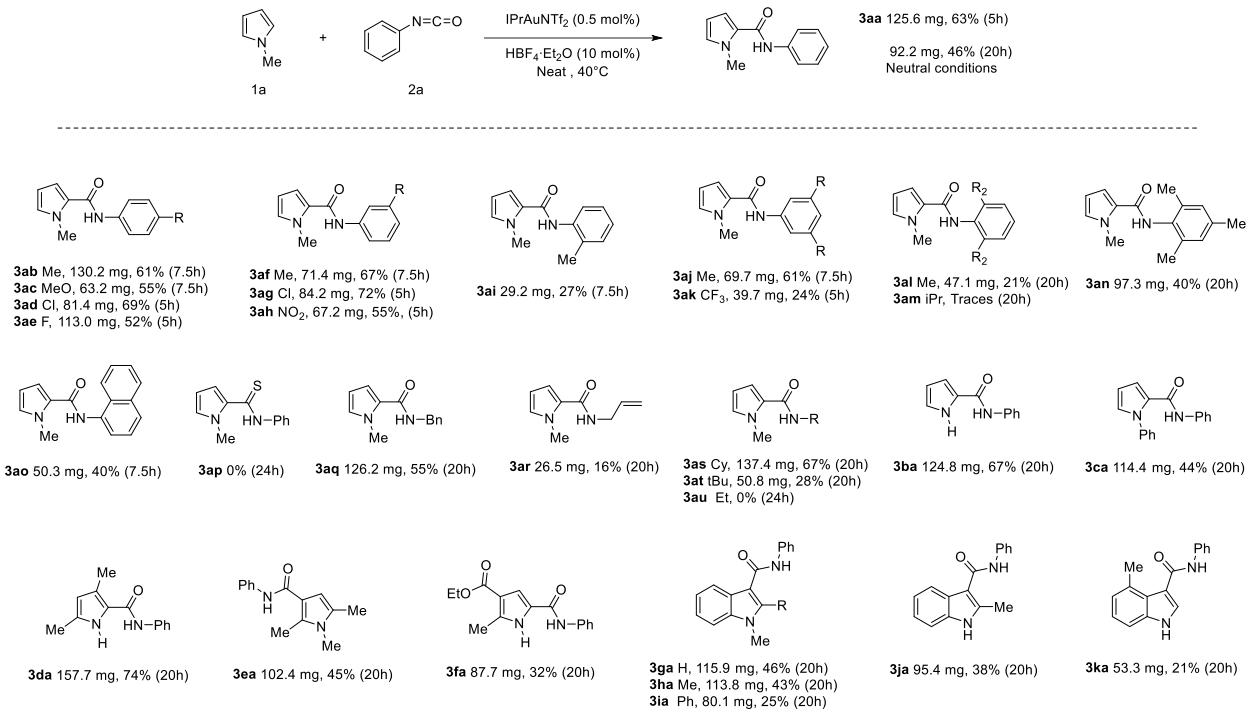

***Figure 4.7** – Reaction scope*

4.3. Mechanistic Studies

To elucidate the reaction mechanism, a Hammett analysis was performed using selected aryl isocyanates in DCM–d_2 at 25 °C (***Figure 4.8***). The kinetic constants were determined via linear fitting of pseudo zero–order kinetics. Substrates with ED-substituents (*p*–methoxy, *p*–chloro, *p*–methyl) exhibited increased kinetic constants, while a modest decrement in the k values was recorded for *p*-acetyl and *m*-nitro derivatives. A slightly negative slope indicated that electron–donating groups stabilize the transition state without generating explicit positive charges, suggesting that the *rate–determining step* may either involve nucleophilic attack at the activated Au–isocyanate adduct or protodeauration of the Au–amido intermediate.[10,22]

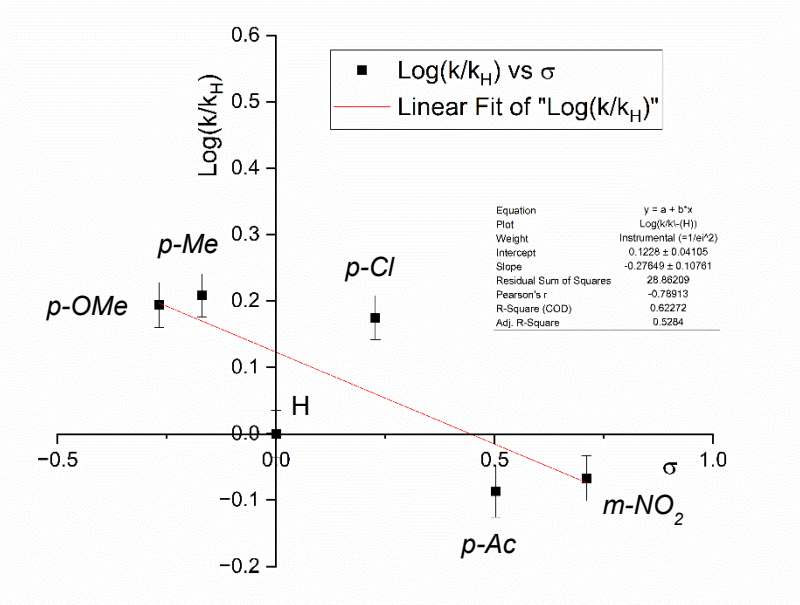

Figure 4.8 *– Hammett plot*

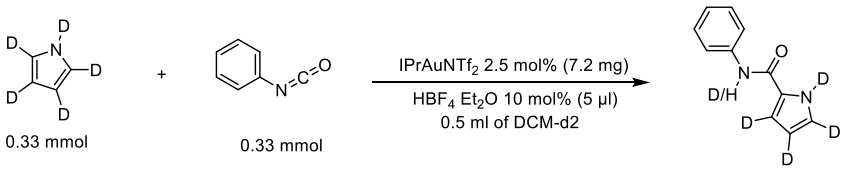

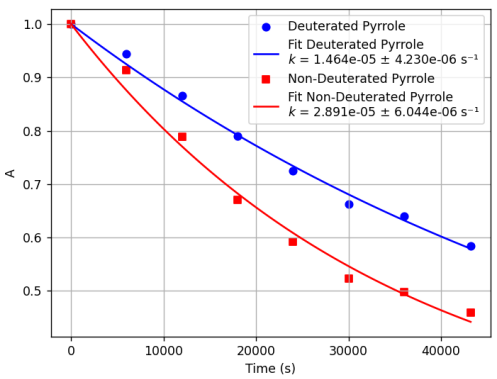

KIE (A vs t) = 2.0

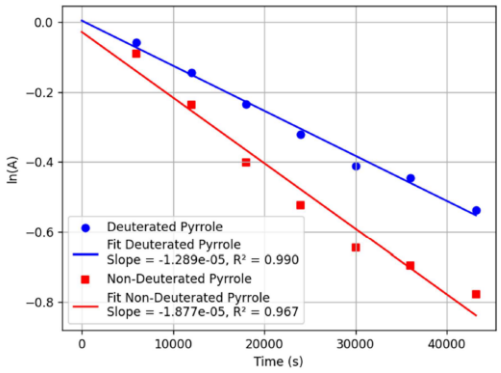

KIE (lnA vs t) = 1.5

Figure 4.9 *– KIE determination*

Complementary KIE studies (kinetic isotopic effect, ***Figure 4.9***) comparing pyrrole and pyrrole–d_5 revealed a discrepancy of the obtained kinetic constants by a factor 2.0 (1.5 in the linear plot). This implies that the direct metalation of pyrrole plays a minor role in influencing the reaction kinetics and that the C–H bond cleavage at the pyrrole moiety is unlikely to be rate–determining.[23]

4.4. Au(I)–Isocyanate Adduct Characterization

Further studies focused on generating and characterizing Au(I)–isocyanate adducts were performed. $IPrAuSbF_6$ was identified as the most suitable scaffold to model the adduct formation. The choice was made due to the instability of other phosphine ligands and higher degree of complexity introduced by the (P,C)–cyclometalated Au(III) structure. In this last case, the presence of two coordination sites may result in different coordination isomers and other undesired decomposition pathways.

- **[IPrAu(mesitylisocyanate)][SbF_6]**

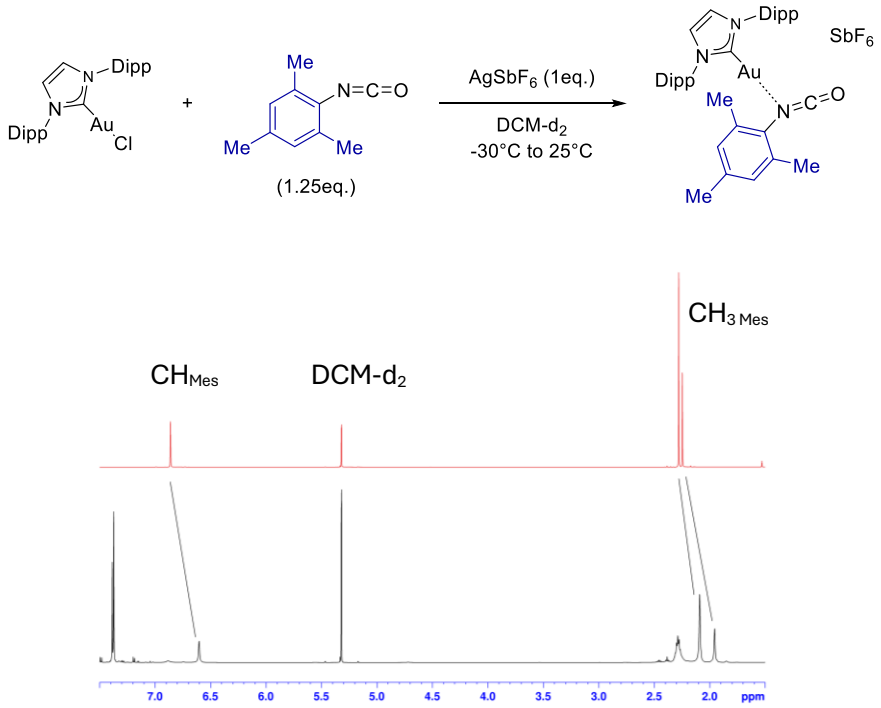

Figure 4.10 – Reaction mixture at rt (blue line) vs isolated Mes–NCO (red line)

Mesityl isocyanate (Mes–NCO) was used to sterically stabilize the allene carbon. The coordination was confirmed by NOESY NMR (***Figure 4.11***), showing cross–peaks between the mesityl ring and IPr ligand (**a**), and exchange between free and coordinated Mes–NCO (**b**).

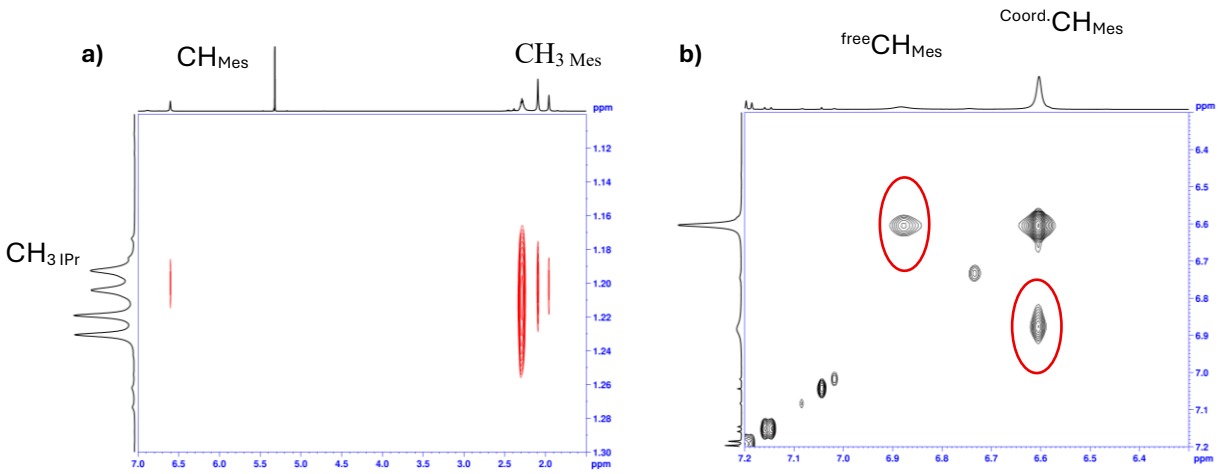

Figure 4.11 – NOESY spectrum **a)** zoom on the NOE cross–peaks **b)** zoom on the exchange cross–peaks

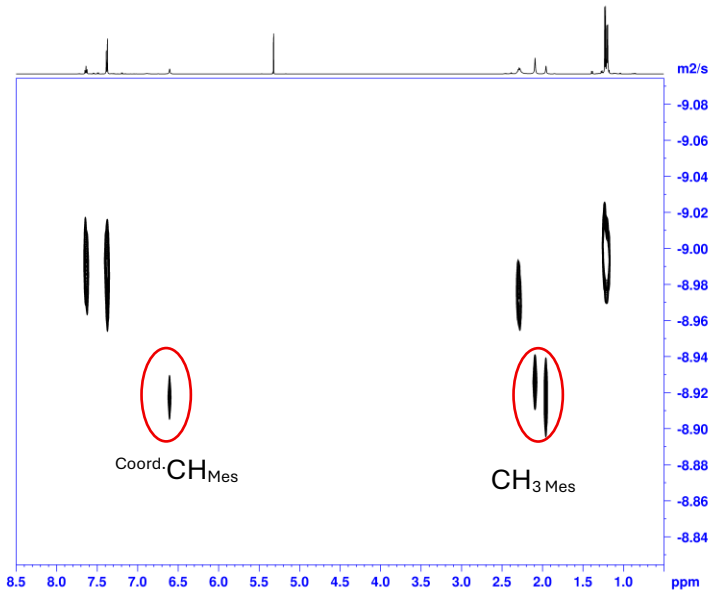

Figure 4.12 *– DOSY spectrum*

DOSY analysis supported coordination (***Figure 4.12***), allowing us to observed a D value of $(1.17\pm0.02)\cdot10^{-9}$ m^2/s for the coordinated species vs. the $(2.20\pm0.11)\cdot10^{-9}$ m^2/s of Mes–NCO in absence of gold. That value is also similar to the D value determined for the $IPrAu^+$ fragment $D_{Au\text{-}complex} = (9.8\pm0.3)\cdot10^{-10}\,m^2/s$.

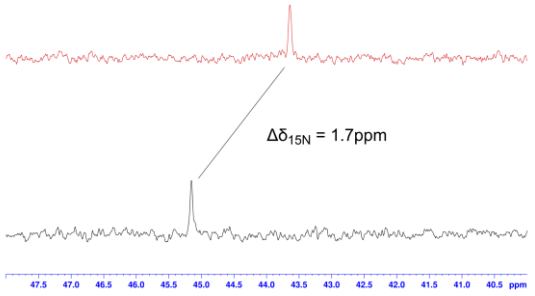

Figure 4.13 *– ^{15}N NMR spectra of free (red line) vs coordinated (black line) Mes–NCO (T = –20 °C)*

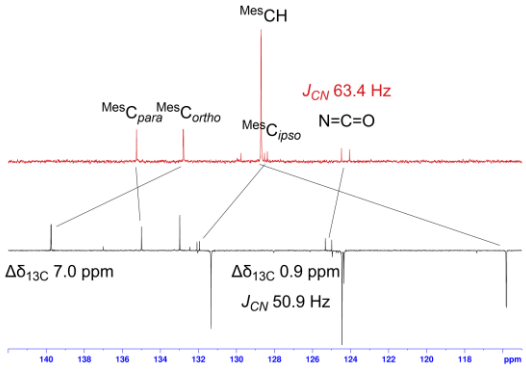

Figure 4.14 *– ^{13}C NMR spectra of free (red line) vs coordinated (black line) Mes–NCO (T = –20 °C)*

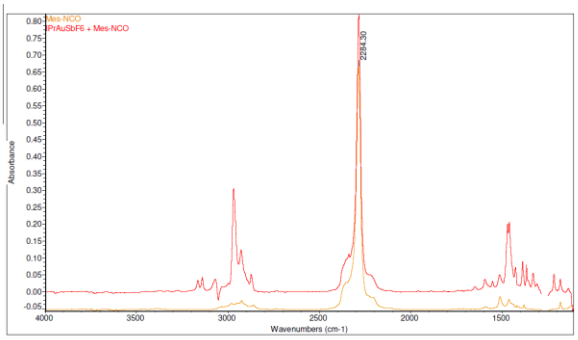

Figure 4.15 *– IR spectra in DCM of Mes–NCO in presence (red line) or absence (yellow line) of $IPrAuSbF_6$*

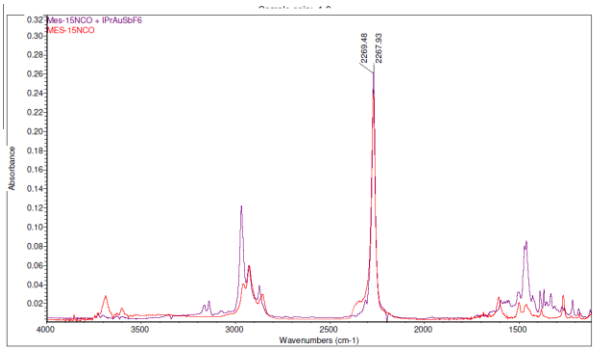

Figure 4.16 *– IR spectra in DCM–d_2 of Mes–^{15}NCO in presence (purple line) or absence (red line) of $IPrAuSbF_6$*

Moreover, ^{15}N-labeling enabled detection of minor variations in the nitrogen atom chemical shift upon coordination at -20°C ($\Delta\delta_{15N}$ = 1.7ppm, **Figure 4.13**). Monitoring of the heteroallene carbon showed an analogous result, recording a minor deshielding ($\Delta\delta_{13C}$ = 0.9ppm, **Figure 4.14**). More diagnostic was a variation in the J_{CN} coupling constant value that decreases from 63.4Hz (free Mes–^{15}NCO) to 50.9Hz (adduct), suggesting a weaker character of the N=C double bond upon coordination to the metal center. A much stronger deshielding affects the caron atoms at the mesityl ring, especially the ones at *ortho* positions for which the relative signal is found dowfield by 7.0ppm (**Figure 5b**). Conversely, no important changes in the measured J_{NC} values are detected. IR spectra of the obtained species were inconclusive, showing only negligible shifts in the

antisymmetric –N=C=O stretch prior and after coordination to gold for both Mes–NCO the ^{15}N-labeled reagent (**Figures 4.15** and **4.16**).

- **[IPrAu(phenylisocyanate)][SbF$_6$]**

Phenylisocyanate (Ph–NCO) coordinates with the gold complex in the presence of $AgSbF_6$. Partial formation of the adduct is observed, while uncoordinated $IPrAuSbF_6$ decomposes to form $[(IPr)_2Au][SbF_6]$ (***Figure 4.17***). This last species was separately synthesized from a control test and characterized by ^{1}H and ^{13}C NMR spectroscopies.

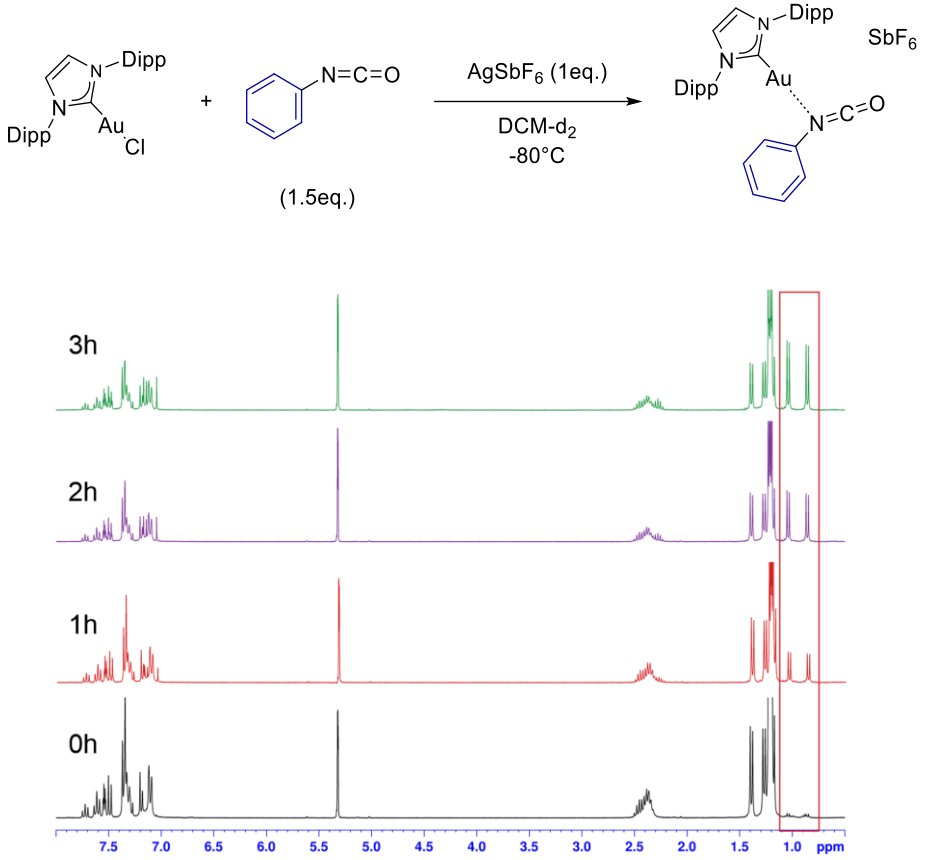

Figure 4.17 *– Evolution of the reaction mixture over–time; the decomposition product $[(IPr)_2Au][SbF_6]$ is highlighted in the red rectangle*

Addition of N–methylpyrrole (1 eq.) led at first to isocyanate displacement and formation of a new species that we had identified as a π–complex of N-methylpyrrole. After 24h at 25°C, product **3aa** was identified in solution, as a new π–coordinated ligand at gold (***Figures 4.18, 4.19*** and ***4.20***). The

HRMS data further corroborate this results; **HRMS (ESI+):** calcd for $[M]^+ = C_{39}H_{48}AuN_4O^+$: 785.3494 m/z. Found: 785.3502 m/z.

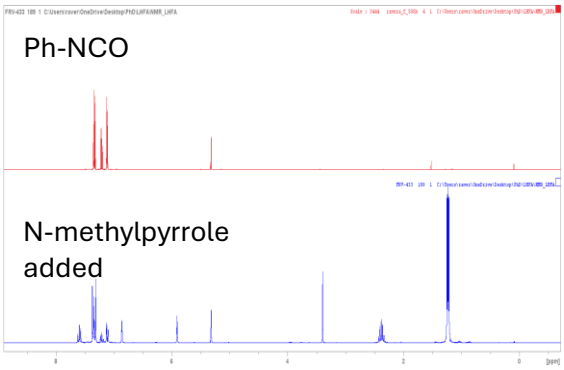

Figure 4.18 *– Reaction mixture after adding 1 eq. N–methylpyrrole (blue line) vs. pure phenylisocyanate in DCM–d_2 (red line).*

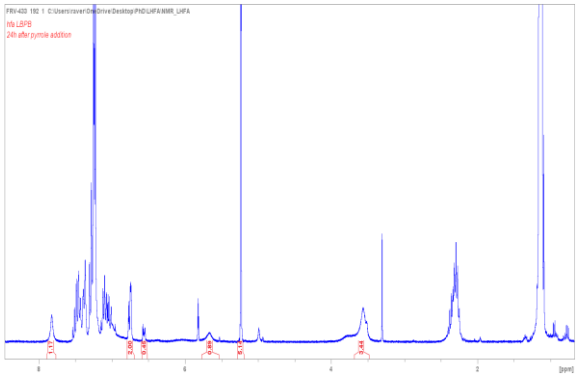

Figure 4.19 *– Reaction mixture after 24h from the addition of N–methylpyrrole (T = 25 °C).*

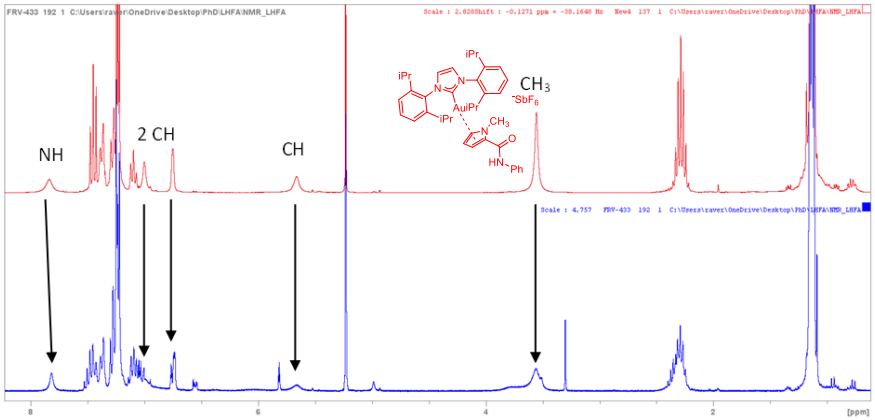

Figure 4.20 *– Reaction mixture after 24h from the addition of N–methylpyrrole (blue line) vs IPrAuSbF$_6$ +* ***3aa*** *in DCM–d_2 (red line).*

- **[IPrAu(benzylisocyanate)][SbF$_6$]**

Similar reactivity was observed with benzylisocyanate (Bn–NCO), but the differences between coordinated and uncoordinated species were evident only at low temperatures, with coalescence of the ^{1}H NMR signals at –20 °C (***Figure 4.21***). NOESY NMR was inconclusive due to low sensitivity, but exchange between the coordinated and non-coordinated Bn-NCO was evident. DOSY (**Figure 4.22**) suggests coordination of Bn–NCO to the cationic complex. Direct comparison of the D values corresponding to the CH_2 at benzyl position outlines a significative difference $D_{free}/D_{coord.} \approx 3$.

Moreover, D value calculated for the coordinated isocyanate is similar to the one determined at the IPr signals $D_{Au\text{-}complex} = (7.8\pm0.8)\cdot10^{-11}\,m^2/s$.

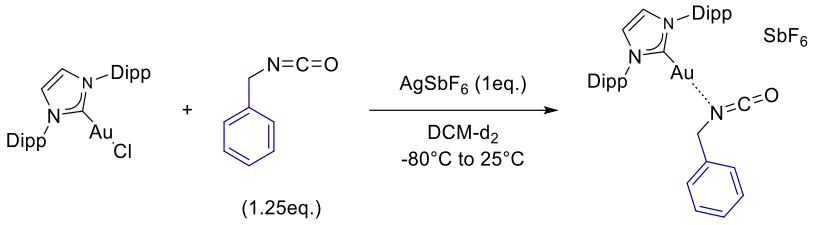

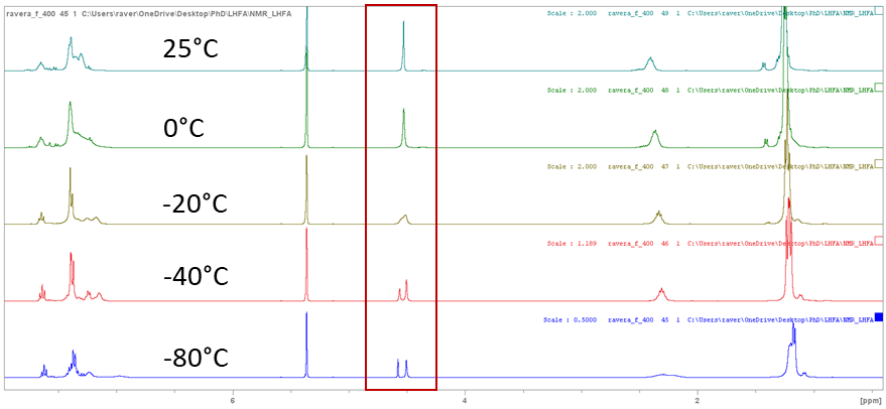

Figure 4.21 *– VT–^{1}H NMR.*

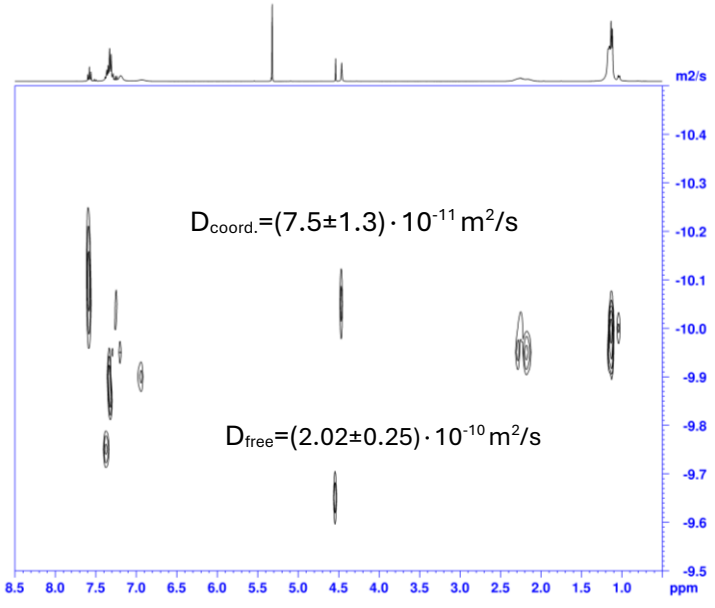

Figure 4.22 *– DOSY NMR spectrum (T = –80°C).*

- **[IPrAu(cyclohexylisocyanate)][SbF_6]**

Coordination attempts with cyclohexylisocyanate (Cy–NCO) yielded as previously observed two species in solution: likely coordinated and uncoordinated forms. The most relevant signals in ***Figures 4.23*** and ***4.24*** were attributed by ^{1}H-^{13}C HSQC and HMBC analyses. HMBC indicated a 17 ppm shift in the allene carbon of one species (***Figure 4.25***). This results is interesting and would be in line with the increased electrophilicity experimented by Cy-NCO in presence of the gold complex.

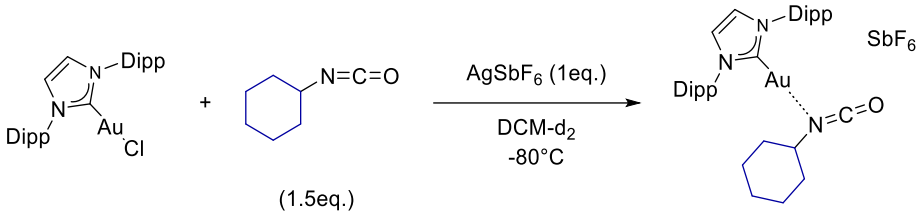

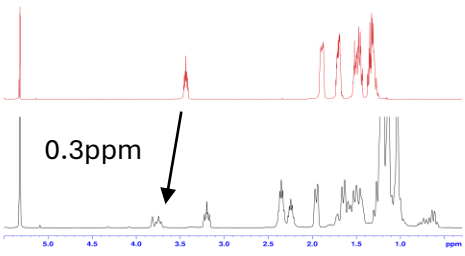

Figure 4.23 – ^{1}H NMR spectra of the reaction mixture (blue line, –80°C) vs pure Cy–NCO in DCM–d_2 (red line, RT spectrum).

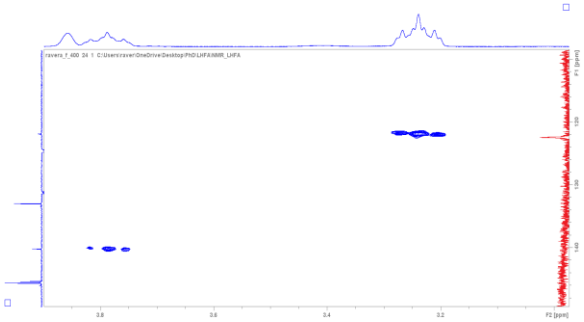

Figure 4.24 – ^{1}H–^{13}C HMBC spectrum of the reaction mixture, zoom on the allene carbon; the red line is Cy–NCO in DCM–d_2.

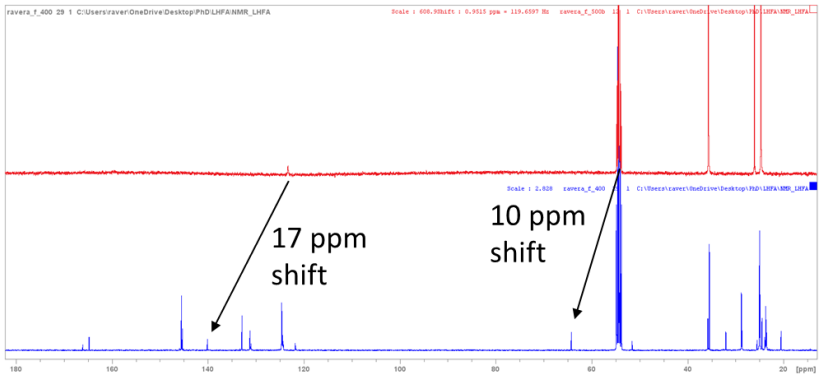

Figure 4.25 – $^{13}C\{^{1}H\}$ NMR spectra of the pure Cy–NCO in DCM–d2 (red line, RT spectrum) and the reaction mixture (blue line, –80°C).

4.5. Gold–N-methylpyrrole Complex

A new π–complex formed upon addition of N–methylpyrrole to Au(I)–isocyanate adducts, characterized by ^{1}H, ^{13}C, and 2D NMR. The signals of the N-methylpyrrole are indeed retained in solution but found at different ppm values than the pure species in DCM-d_2. The signals of the N-methylpyrrole are indeed retained in solution but found at different ppm values than the pure species in solution. Signals of residual N-methyl pyrrole are also found, but they are shifted at higher ppm values than expected: probably due to other interaction in solution. NOESY analysis confirmed the coordination at gold (**Figure 4.26**). This can be stated observing the cross-peaks between the heteroaromatic ring and the CH_3 groups of the IPr ligand.

The complex was isolated *via* precipitation n–pentane on a 0.1 mmol scale (81.6 mg, 90% yield). Crystals suitable for XRD were obtained by layering n–pentane over a saturated DCM solution at 25–30 °C. The observed coordination lengths were consistent with previously reported π–complexes of phosphine/NHCs–supported Au(I) metal centers with arenes and styrene–derivatives.[24]

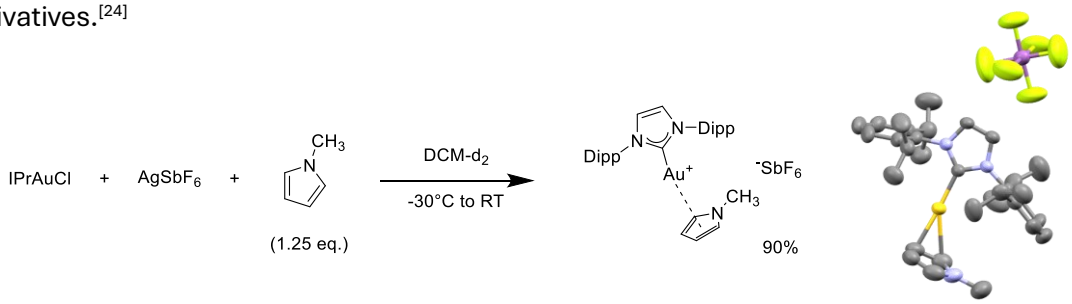

XRD-structure

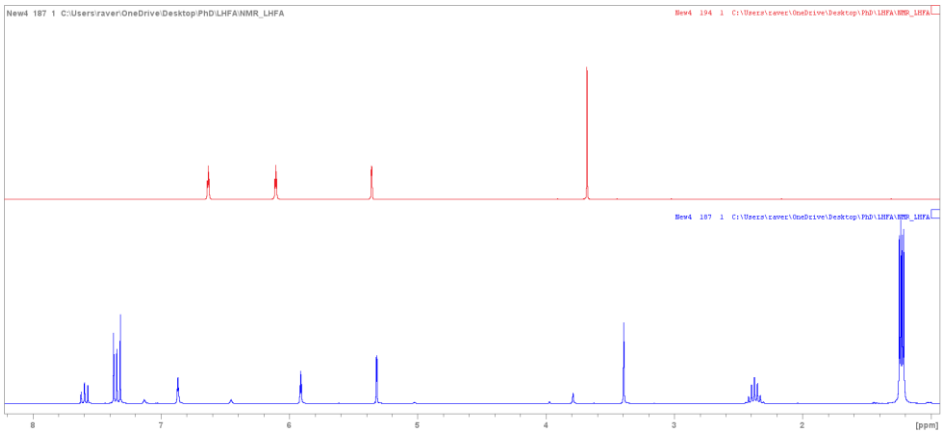

Figure 4.26 *– ^{1}H NMR spectrum after generating the adduct (upper spectrum) and comparison with the pure N-methylpyrrole in DCM-d_2 (bottom spectrum).*

Guinchard and co-workers have recently presented a new class of cationic Au(I) complexes bearing Buchwald-type phosphines as ancillary ligands and indole derivatives as π-donor moiety.[25] In analogy, the complex **II-a** exhibits unequal distances between gold and the C3 and C2 carbon atoms of 2.21 and 2.53 Å, respectively. This result is in line to the higher electron density localized at the C3 position of *N*-methylpyrrole. These structural features hinder for the direct metalation of *N*-methylpyrrole by the gold catalyst, making unlikely the operation of an inner-sphere mechanism under our reaction conditions.

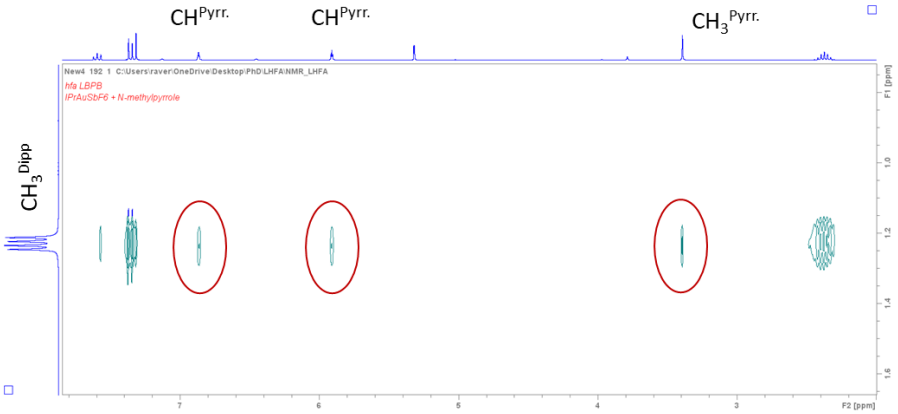

Figure 4.27 *– Synthesis of [IPrAu–(N–methylpyrrole)][SbF_6] with XRD and NOESY analysis.*

A direct comparison with the ^{13}C NMR spectrum of N-methylpyrrole shows that the aromatic carbon of the molecule are the ones that are more affected after coordination to gold. On the other hand, the signal corresponding to the methyl group stays at similar ppm values (37.1ppm vs 36.3ppm for the π-complex and the free substrate, respectively).

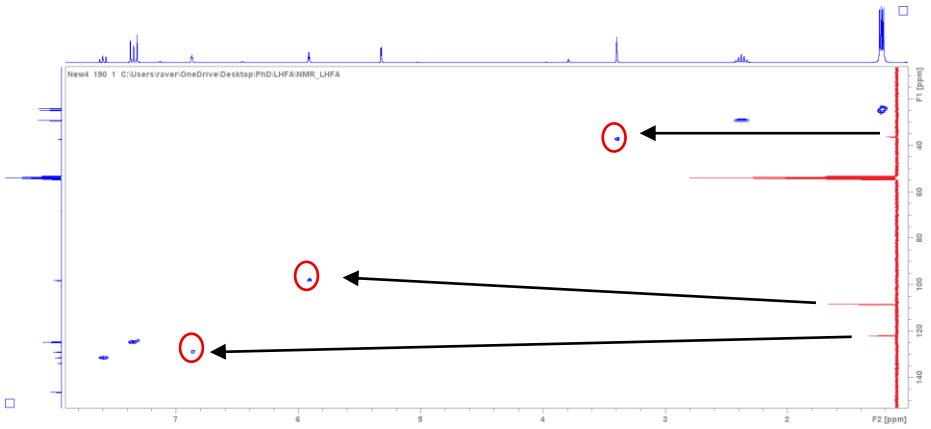

Figure 4.28 *– ^{1}H-^{13}C HMBC spectra and comparison with the pure N-methylpyrrole $^{13}C\{^{1}H\}$ spectrum (red line).*

This species is stable in solution (marginal decomposition observed within 1 day) and it is stable in presence of air and/or water. The formation of this complex may indeed stabilize IPrAu^{+} under catalytic conditions, however, the N-methylpyrrole is also a strong competitor for coordination at the metal center. This π–complex represents a clear example of resting state for our catalytic cycle, which can be drawn as follows.

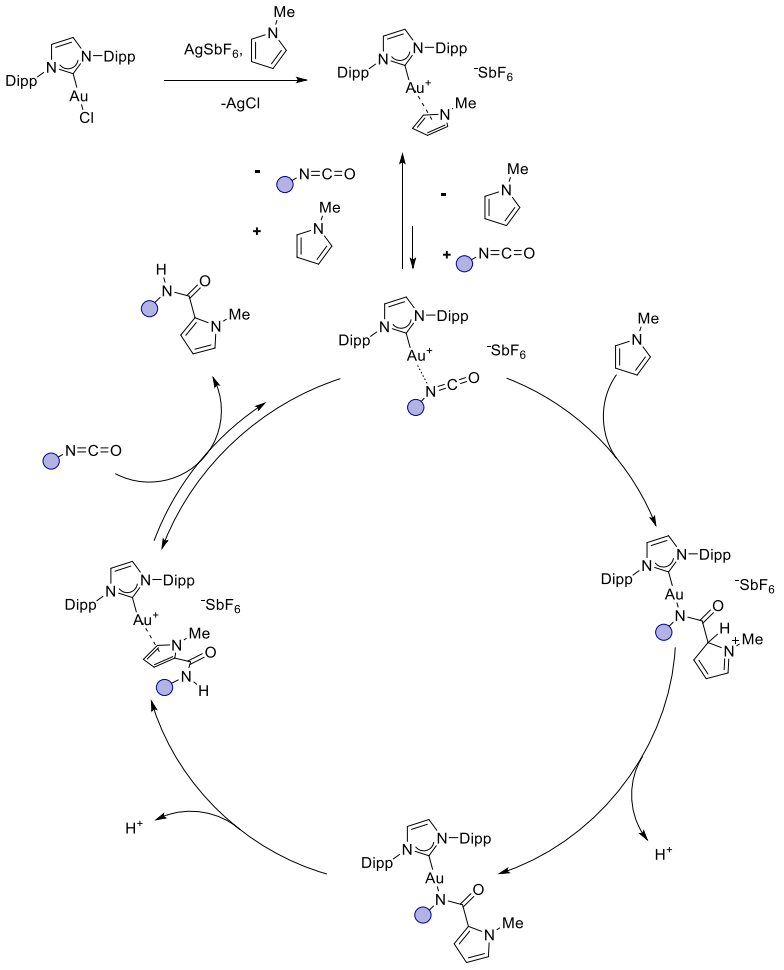

Figure 4.29 *– Revised mechanism for the direct hydroarylation of organic isocyanates by IPrAuNTf$_2$.*

4.6. Conclusions

The direct activation of organic isocyanates using a well–defined Au(I) complex has been disclosed and it represents the first case of TM–catalyzed hydroarylation of isocyanate by an outer sphere mechanism. An initial optimization of the reaction conditions revealed a strict dependence on the catalyst employed: only $IPrAu^{+}$ and $(iPr_2P,C)Au^{2+}$ exhibited appreciable activity at 0.5 mol% loading and 40 °C (solvents [BMIM][NTf_2] or DCM). Under neat conditions, the process activity was maximized, enabling the analysis of the substrate scope. Various aryl and alkyl isocyanates were employed, achieving modest to good yields. Additionally, different nucleophiles, including substituted pyrroles and indoles, were incorporated with comparable results.

Mechanistic studies suggest that the process operates via an outer–sphere mechanism. Both the Hammett analysis and KIE determination experiments indicate a limited contribution of direct auration of N–methylpyrrole to the reaction kinetics. Evidences for the formation of genuine IPrAu–isocyanate complexes were obtained by NMR spectroscopy (^{1}H, ^{13}C, ^{15}N, and 2D experiments). The adduct with phenylisocyanate was shown to lead to product formation in the presence of N–methylpyrrole. Under this framework, an unprecedent IPrAu–N–methylpyrrole π–complex was also found as a potential resting state of the catalytic cycle.

4.7. Experimental section

General remarks

Unless differently stated, all manipulations and reactions were carried out under an argon atmosphere, using standard Schlenk techniques and flame–dried glassware. Dry, oxygen–free solvents were employed: tetrahydrofuran (THF), dichloromethane (DCM), toluene (Tol) and acetonitrile (ACN) were dried on a MBraun SPS–800 solvent purification system, and degassed by two freeze–pump–thaw cycles. Deuterated solvents, DCM–d_2 and THF–d_8 were dried over CaH_2 and stored in presence of freshly activated 3Å molecular sieves. Phenyl–, cyclohexyl– and benzyl–isocyanates used for coordination tests were distilled over P_2O_5, degassed and stored in a glovebox at –20°C. Unless otherwise noted, all starting materials used for synthesis and catalytic tests were purchased and used directly as received. The complexes IPrAuNTf$_2$,[26] SIPrAuCl,[27] IMesAuCl,[27] SIMesAuCl,[27] IiPrAuCl,[28] Me$_2$NImPyAuCl,[29] PedroPhosAuCl,[30] (iPr$_2$P,C)AuI$_2$,[31] (Ph$_2$P,C)AuI$_2$[31] and (N,C,C)AuCl[32] were synthesized by previously reported procedures (see **Scheme S1**). Purifications were performed by flash–column chromatography on silica gel, using mixtures of ethyl acetate (EtOAc) with petroleum ether (PE) or n–hexane (Hex) at different compositions. Analytical thin layer chromatography (TLC) was performed to optimize the eluent and monitor the isolated fractions; the TLC plates were visualized under UV–light or by staining with potassium permanganate or iodine/silica indicators. Multinuclear NMR spectra (^{1}H, ^{13}C, ^{31}P, ^{19}F and ^{15}N nuclei) were recorded on Bruker Avance 300, 400, 500 or 600 at 298K, unless otherwise stated. The ^{1}H and ^{13}C chemical shifts (δ) were calibrated with respect to signals of the deuterated solvent (^{13}C) and its protonated residue (^{1}H).[33,34] Chemical shifts of ^{31}P, ^{19}F and ^{15}N heteronuclei were calibrated indirectly[35] and referenced to 85% H_3PO_4, $CFCl_3$ and liquid NH_3, respectively. The following abbreviations and their combinations are used for the compressed notation of the characterization data: br, broad; p, pseudo; s, singlet; d, doublet; t, triplet; q, quartet; quint, quintet; m, multiplet; hept, heptet. Data elaboration was performed with the software TopSpin 4.4.1. DOSY experiments were analyzed with the software Dynamics Center 2.8.5. HRMS data were recorded in positive (or negative) mode on a Waters UPLC Xevo G2 Q TOF apparatus for ESI. GC–MS analyses were performed on a MS Perkin Elmer Clarus MS560, GC PerkinElmer Clarus 500 and Agilent HP6890. IR spectra were collected in DCM or DCM–d_2 using a Thermo Scientific™ Spectrometer or a ReactIR™ 15 apparatus for reaction monitoring.

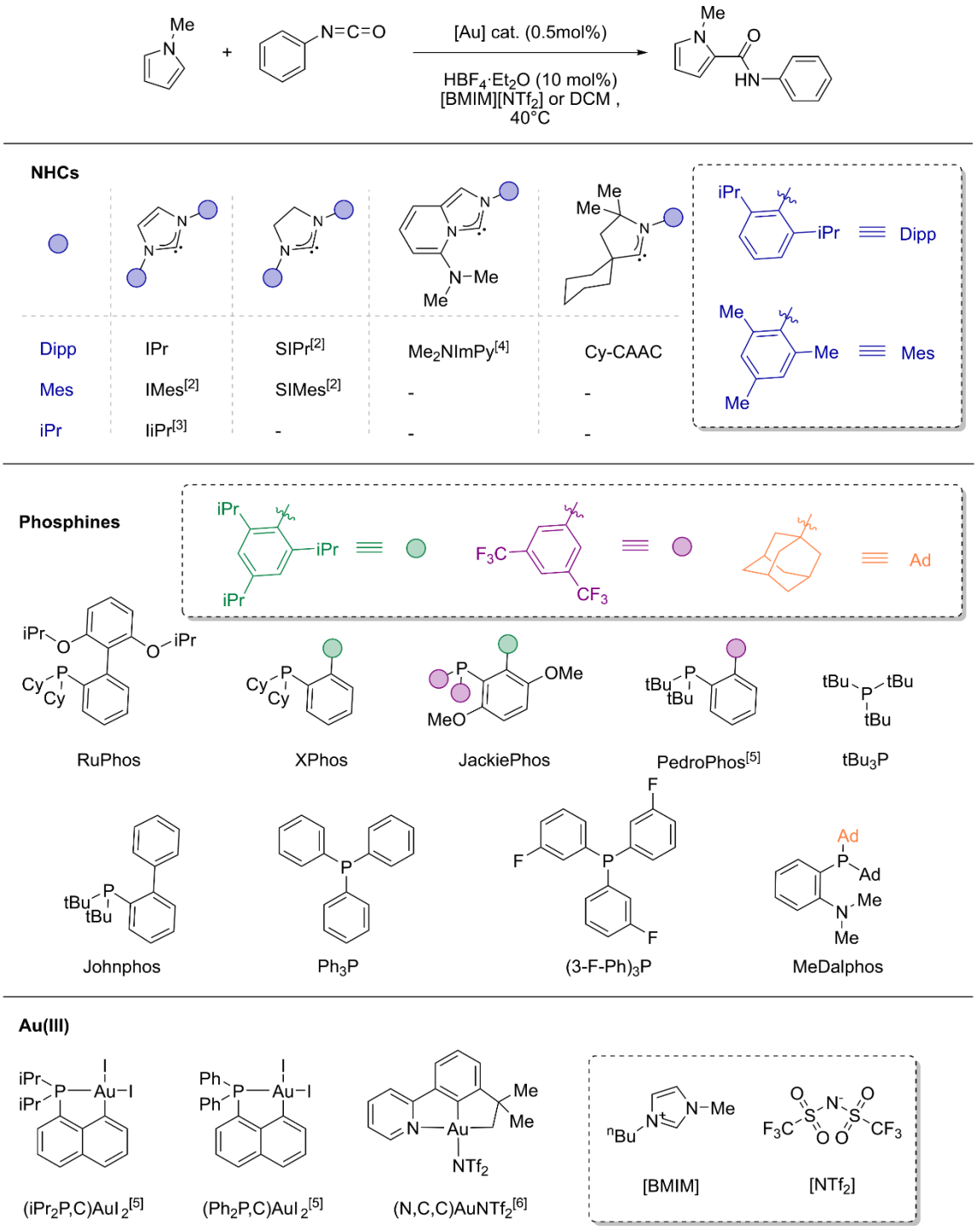

Figure 4.30 *– Summary of the ligands at Au(I) and Au(III) complexes employed for the catalyst scope.*

Synthesis of IPrAuCl

IPrAuCl was synthesized by a modified procedure in the literature (weak–base route):[27]

In a Schlenk flask with IPr·HCl (400mg, 0.94mmol, 1.0eq.), [Au(DMS)Cl] (278.1mg, 0.94mmol, 1.0eq.) and K_2CO_3 (200mg, 1.45mmol, 1.5eq.). The flask was capped with a rubber septum and purged by three vacuum/argon cycles and acetone (5.0ml) was added. The resulting white suspension was slowly taken to reflux while stirring. Progressive darkening of the mixture was observed overtime. The mixture was monitored by ^{1}H NMR (acetone presaturation), after sampling an aliquot of the crude and diluting it in $CDCl_3$. Once IPr·HCl was completely consumed (1.5–3h), volatiles were evaporated in *vacuo*. The resulting residue was taken up in DCM (5ml), filtered through silica and the filtering pad was further washed with DCM (3x5ml). The collected solution was concentrated (ca. 3ml) and cold pentane (20ml) was added to it, resulting in a fine white suspension of the desired complex. The solid was left to sediment at –20°C for 4h and then it was filtered off, washed with pentane (2x5ml) and dried under vacuum. IPrAuCl was isolated as a white powder in 92% yield (537.9mg, 0.87mmol). Spectroscopic data are in agreement with the ones previously reported.[36]

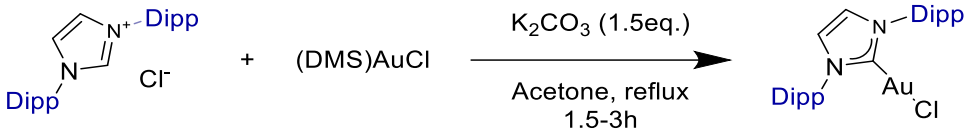

^{1}H NMR (300MHz, $CDCl_3$): δ 7.50 (t, ^{3}J = 7.8 Hz, 2H, Dipp, CH_{para}), 7.29 (d, ^{3}J = 7.8 Hz, 2H, Dipp, CH_{meta}), 7.17 (s, 2H, vinyl, CH), 2.55 (hept, ^{3}J = 6.9Hz, 4H, iPr, CH), 1.34 (d, ^{3}J = 6.9Hz, 6H, iPr, CH_3), 1.22 (d, ^{3}J = 6.9Hz, 6H, iPr, CH_3) ppm.

Synthesis of (CAAC–Cy)AuCl

The complex (CAAC–Cy)AuCl was synthesized by a modified procedure reported for the synthesis of the complex (CAAC–Cy)Rh(COD)Cl[37] (strong–base route):

Inside a glovebox, (DMS)AuCl (44.2mg, 0.15mmol. 1.0eq.) and CAAC–Cy·2HCl (59.6mg, 0.15mmol, 1eq.) were added to a 10ml Schlenk flask and suspended in 3ml of THF. In a separate vessel, KHMDS (60.2mg, 0.30mmol, 2.0eq.) was solubilized in THF (5ml). The resulting solution was charged in a syringe and the needle capped with a rubber septum. Out of the glovebox, the

(DMS)AuCl suspension was cooled to –80°C and the KHMDS solution was added dropwise. The mixture was kept under stirring for 15min at low temperature before it was allowed to slowly warm–up to RT and further stirred for 16h. The resulting crude was then evaporated in *vacuo*, allowing to remove all volatiles. The resulting residue was taken up in DCM (5ml), filtered through silica and the filtering pad was further washed with DCM (2x3ml). The obtained solution was concentrated (ca. 1ml) and layered with pentane (4ml) to yield the desired complex as an off–white solid in 69% yield (57.5 mg, 0.10mmol). Spectroscopic data are in agreement with the ones previously reported.[38] Complete assignments were made based on COSY, HSQC and HMBC analyses.

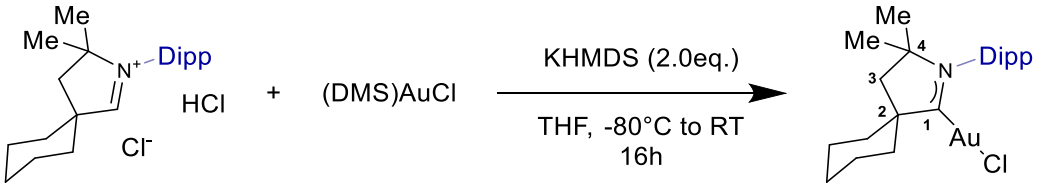

^{1}H NMR (300MHz, DCM–d_2): δ 7.48 (t, 1H, ^{3}J = 7.7Hz, Dipp, CH_{para}), 7.30 (d, 2H, ^{3}J = 7.7Hz, Dipp, CH_{meta}), 2.77 (hept, 2H, ^{3}J = 6.7Hz, iPr, CH), 2.36–2.22 (m, 2H, Cy), 2.17 (s, 2H, C_3, CH_2), 1.89–1.77 (m, 2H, Cy), 1.77–1.68 (m, 1H, Cy), 1.61–1.50 (m, 1H, Cy), 1.48–1.34 (m, 15H, Cy, $^{iPr}CH_3$ and $^{CAAC}CH_3$), 1.31 (d, ^{3}J = 6.7Hz, iPr, CH_3) ppm; **^{13}C{^{1}H} (75.48MHz, DCM–d_2): δ** 236.0 (s, 1C, C_1), 145.5 (s, 2C, Dipp, C_{ortho}), 134.4 (s, 1C, Dipp, C_{ipso}), 130.3 (s, 1C, Dipp, C_{para}), 125.5 (s, 2C, Dipp, C_{meta}), 80.7 (s, 1C, C_4), 59.3 (s, 1C, C_2), 45.6 (s, 1C, C_3), 36.7 (s, 2C, Cy), 29.8 (s, 2C, CAAC, CH_3), 29.4 (s, 2C, iPr, CH), 27.1 (s, 2C, iPr, CH_3), 25.5 (s, 1C, Cy), 22.9 (s, 2C, iPr, CH_3), 22.1 (s, 2C, Cy) ppm; **HRMS (ESI+):** calcd for $[M+ACN]^+ = C_{25}H_{38}AuN_2^+$: 563.2701m/z. Found: 563.2700 m/z.

General procedure for catalytic tests

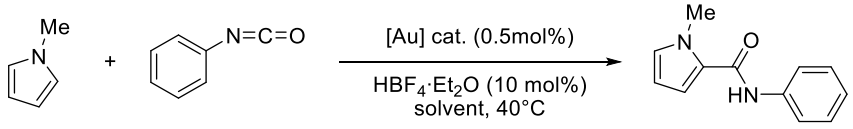

Inside a glovebox, the gold catalyst (2.5μmol, 0.5mol%) and a stoichiometric amount of $AgSbF_6$ or $AgNTf_2$ (2.5μmol, 0.5mol%) were placed in a 10ml Schlenk flask. The flask was then moved under a fume–hood, where dimethylsulfone (internal standard, 10mg, 0.1mmol), the solvent (0.75ml) and N–methylpyrrole (44μl, 0.5mmol, 1.0eq.) were sequentially added under a positive back–flow of argon. The solution was stirred for two minutes, after which a t_0 NMR check was taken. Phenylisocyanate (54μl, 0.5mmol, 1.0eq.) and $HBF_4 \cdot Et_2O$ (7.0μl, 0.05mmol, 0.1eq.) were added to

the solution, and the reaction was placed in a thermostatic bath at 40°C. The reaction was monitored over–time by ^{1}H NMR spectroscopy of sampled aliquots of the reaction crude.

Addenda to the procedure:

- For the sampling, an aliquot of 0.05ml was taken and diluted in 0.5ml of $CDCl_3$; presaturation of the solvent signal was used to better visualize the signal of interest;
- No solvent was added when neat conditions were employed;
- No acid was added when neutral conditions were employed;
- Blank tests were performed in absence of the gold catalyst;
- Any changes in the reagents stoichiometry, loading of catalyst and/or temperature of the reaction were applied without further modifications of the described procedure;
- The ionic liquid [BMIM][NTf_2] allows to form stable solutions of the salt $AgSbF_6$, which are easier to manipulate than the solid;
- The silver salt was omitted when pre–activated complexes were employed, such as IPrAuNTf_2, tBu_3PNTf_2 and (N,C,C)AuNTf_2;
- Complete cationization of bis–iodo (P,C)–cyclometalated Au(III) complexes was achieved employing 2 equivalents of $AgSbF_6$ or $AgNTf_2$;

General procedure for catalytic tests with syringe–pump setup

IPrAuNTf_2 (4.3mg, 5.0μmol, 0.5mol%) was placed in a 10ml Schlenk flask and the vessel purged with inert gas by three vacuum/argon cycles. N–methylpyrrole (ca. 120μl) was then charged in a 250μl Hamilton™ syringe coupled with a PTFE cannula (the junction was manually sealed with PTFE tape and parafilm). Phenylisocyanate (108μl, 1.0mmol, 1.0eq.) and $HBF_4 \cdot Et_2O$ (14.0μl, 0.1mmol, 0.1eq.) were added to the flask, and the reaction was placed in a thermostatic bath at 40°C. N–methylpyrrole (88μl, 1.0mmol, 1.0eq.) was slowly added to the mixture by aid of a syringe–pump setup.* In particular, the elution rate was decided to complete the addition within 0.5h and 1.5h in two different tests and the cannula removed immediately after the injection of N–methylpyrrole was completed. The reaction was kept stirring at 40°C for 5h since the syringe pump system was started. The obtained residue was taken up in DCM (40ml, dissolution was helped by sonication) and quenched with a saturated solution of $NaHCO_3$. The aqueous solution was counter–extracted

with DCM (2x20ml) and the combined organic phase dried over Na_2SO_4. The solution was filtered, evaporated to obtain a residue that was purified by column chromatography (EtOAc/PE 1:5). Evaporation of the relevant fractions allowed to obtain the desired product **3aa** as a white solid. Spectroscopic data were in agreement with the ones previously reported.

* The free–end of the cannula was constantly kept submerged in the reaction mixture along the entire injection process. This ensured a uniform addition of N–methylpyrrole, rather than a slow dropwise addition;

General procedure for the synthesis and isolation of products 3aa–3ax and 3ba–3

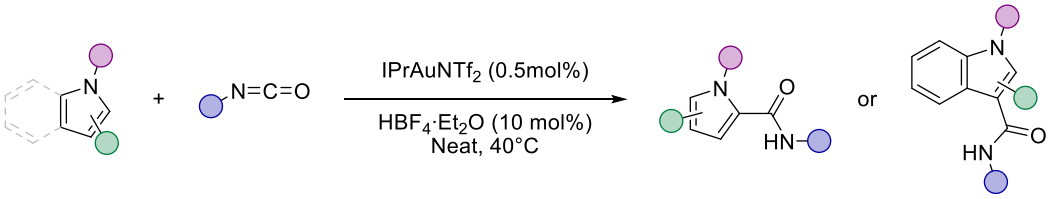

To a 10ml Schlenk flask, $IPrAuNTf_2$ (2.2mg, 2.5µmol, 0.5mol%) was added, and the vessel was purged with inert gas by three vacuum/argon cycles. The aromatic nucleophile (0.5mmol, 1eq.) and the isocyanate (0.5mmol, 1eq.) were then added under a positive argon backflow, and the mixture was stirred for two minutes. Subsequently, $HBF_4 \cdot Et_2O$ (7.0µl, 0.05mmol, 0.1eq.) was added, and the vessel was immediately transferred to a thermostatic bath at 40 °C. The reaction was stirred at this temperature for the time indicated in the table. The obtained residue was taken up in DCM (40ml, dissolution was helped by sonication) and quenched with a saturated solution of $NaHCO_3$. The aqueous solution was counter–extracted with DCM (2x20ml) and the combined organic phase dried over Na_2SO_4. The solution was filtered, evaporated and the resulting residue was purified by column chromatography. Evaporation of the relevant fractions allowed to obtain the corresponding secondary amide.

* The same protocol was adapted to 1mmol scale syntheses without modifications of the procedure.

P.1 – 1–Methyl–N–phenylpyrrole–2–carboxamide (**3aa**)

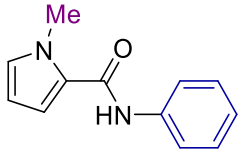

Synthesized at 1mmol scale using N–methylpyrrole and phenyl–isocyanate as starting materials. The reaction was quenched after 5h and purified by column chromatography on silica gel (eluent EtOAc/Hex 1:5). Isolated as a white solid in 63% yield (125.6mg,

0.63mmol). **Rf(EtOAc/Hex 1:5)** = 0.31; **m.p.** 104.0–104.8°C; **^{1}H NMR (400MHz, $CDCl_3$): δ** 7.64 (brs, 1H, NH), 7.58–7.53 (m, 2H, Ph, CH), 7.37–7.31 (m, 2H, Ph, CH), 7.14–7.08 (m, 1H, Ph, CH), 6.78 (pt, J = 2.1Hz, 1H, $CH_{pyrrole}$), 6.70 (dd, J = 4.0, 1.6Hz, $CH_{pyrrole}$), 6.14 (dd, J = 4.0, 2.6Hz, $CH_{pyrrole}$), 3.98 (s, 3H, CH_3) ppm; **^{13}C{^{1}H} NMR (100.6MHz, $CDCl_3$): δ** 160.1 (s, 1C), 138.1 (s,1C), 129.0 (s, 2C), 128.8 (s, 1C), 125.8 (s, 1C), 124.0 (s, 1C), 120.2 (s, 2C), 112.4 (s, 1C), 107.5 (s, 1C), 36.8 (s, 1C) ppm.

Spectroscopic data were consistent with the ones previously reported. [20]

P.2 – 1–Methyl–N–(4–methylphenyl)pyrrole–2–carboxamide (**3ab**)

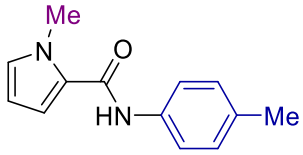

Synthesized at 1mmol scale using N–methylpyrrole and p–tolyl–isocyanate as starting materials. The reaction was quenched after 7.5h and purified by column chromatography on silica gel (eluent EtOAc/Hex 1:5). Isolated as an off–white solid in 61% yield (130.2mg, 0.61mmol). **Rf(EtOAc/Hex 1:5)** = 0.31; **m.p.** 78.8–79.5°C; **^{1}H NMR (400MHz, $CDCl_3$): δ** 7.78 (brs, 1H, NH), 7.48–7.43 (m, J = 8.4Hz, 2H, p–Tol, CH), 7.16–7.10 (m, J = 8.3Hz, 2H, p–Tol, CH), 6.76 (pt, J = 2.1Hz, 1H, $CH_{pyrrole}$), 6.71 (dd, J = 4.0, 1.6Hz, $CH_{pyrrole}$), 6.12 (dd, J = 4.0, 2.6Hz, $CH_{pyrrole}$), 3.95 (s, 3H, $CH_{3pyrrole}$), 2.33 (s, 3H, p–Tol, CH_3) ppm; **^{13}C{^{1}H} NMR (100.6MHz, $CDCl_3$): δ** 160.0 (s, 1C), 135.5 (s, 1C), 133.5 (s, 1C), 129.4 (s, 2C), 128.6 (s, 1C), 125.9 (s, 1C), 120.3 (s, 2C), 112.2 (s, 1C), 107.4 (s, 1C), 36.7 (s, 1C), 20.8 (s, 1C) ppm.

Spectroscopic data were consistent with the ones previously reported. [20]

P.3 – N–(4–methoxyphenyl)–1–methylpyrrole–2–carboxamide (**3ac**)

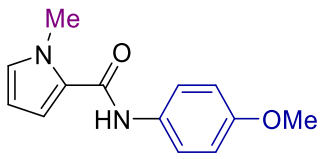

Synthesized at 0.5mmol scale using N–methylpyrrole and 4–methoxyphenyl–isocyanate as starting materials. The reaction was quenched after 7.5h and purified by column chromatography on silica gel (eluent EtOAc/Hex 1:5). Isolated as a white solid in 55% yield (63.2mg, 0.27mmol). **Rf(EtOAc/Hex 1:5)** = 0.21; **m.p.** 114.0–

114.5°C; **^{1}H NMR (400MHz, $CDCl_3$): δ** 7.52 (brs, 1H, NH), 7.47–7.42 (m, J = 9.0Hz, 2H, 4–MeO–Ph, CH), 6.91–6.86 (m, J = 9.0Hz, 2H, 4–MeO–Ph, CH), 6.77 (pt, J = 2.1Hz, 1H, $CH_{pyrrole}$), 6.67 (dd, J = 4.0, 1.6Hz, $CH_{pyrrole}$), 6.13 (dd, J = 4.0, 2.6Hz, $CH_{pyrrole}$), 3.97 (s, 3H, CH_3), 3.80 (s, 3H, OCH_3) ppm; **^{13}C{^{1}H} NMR (100.6MHz, $CDCl_3$): δ** 160.1 (s, 1C), 156.4 (s, 1C), 131.1 (s, 1C), 128.6 (s, 1C), 125.9 (s, 1C), 122.2 (s, 2C), 114.3 (s, 2C), 112.1 (s, 1C), 107.5 (s, 1C), 55.6 (s, 1C), 36.9 (s, 1C) ppm.

Spectroscopic data are consistent with the ones previously reported. [20]

P.4 – N–(4–chlorophenyl)–1–methylpyrrole–2–carboxamide (**3ad**)

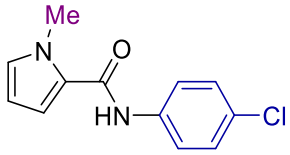

Synthesized at 0.5mmol scale using N–methylpyrrole and 4–chlorophenyl–isocyanate as starting materials. The reaction was quenched after 5h and purified by column chromatography on silica gel (eluent EtOAc/Hex 1:5). Isolated as a white solid in 69% yield (81.4mg, 0.35mmol). **Rf(EtOAc/Hex 1:5)** = 0.34; **m.p.** 141.8–142.6°C; **^{1}H NMR (400MHz, $CDCl_3$): δ** 7.74 (brs, 1H, NH), 7.53–7.46 (m, J = 8.9Hz, 2H, 4–Cl–Ph, CH), 7.30–7.23 (m, J = 8.9Hz, 2H, 4–Cl–Ph, CH), 6.78 (pt, J = 2.1Hz, 1H, $CH_{pyrrole}$), 6.71 (dd, J = 4.0, 1.7Hz, $CH_{pyrrole}$), 6.12 (dd, J = 4.0, 2.5Hz, $CH_{pyrrole}$), 3.94 (s, 3H, CH_3) ppm; **^{13}C{^{1}H} NMR (100.6MHz, $CDCl_3$): δ** 160.0 (s, 1C), 136.7 (s, 1C), 129.2 (s, 1C), 129.0 (s, 2C), 128.9 (s, 1C), 125.4 (s, 1C), 121.4 (s, 2C), 112.6 (s, 1C), 107.7 (s, 1C), 36.9 (s, 1C) ppm.

Spectroscopic data are consistent with the ones previously reported. [20]

P.5 – N–(4–fluorophenyl)–1–methylpyrrole–2–carboxamide (**3ae**)

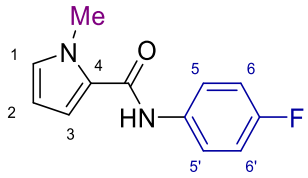

Synthesized at 1mmol scale using N–methylpyrrole and 4–fluorophenyl–isocyanate as starting materials. The reaction was quenched after 5h and purified by column chromatography on silica gel (eluent EtOAc/PE 1:5). Isolated as a white solid in 52% yield (113.0mg, 0.52mmol). **Rf(EtOAc/PE 1:5)** = 0.49; **m.p.** 131.4–132.2°C; **^{1}H NMR (300MHz, $CDCl_3$): δ** 7.59 (brs, 1H, NH), 7.54–7.46

(m, $^{3}J_{HH}$ = 9.1Hz, $^{4}J_{HF}$ = 4.8Hz, 2H, 4–F–Ph, $C_{5/5'}$–H), 7.08–6.97 (m, $^{3}J_{HH}$ = $^{3}J_{HF}$ = 9.0Hz, 2H, 4–F–Ph, $C_{6/6'}$–H), 6.79 (pt, ^{3}J = 2.1Hz, 1H, C_1–H), 6.69 (dd, ^{3}J = 4.0Hz, ^{4}J = 1.7Hz, C_2–H), 6.14 (ddd, ^{3}J = 4.0Hz, ^{4}J = 2.6Hz, ^{5}J = 0.6Hz, C_3–H), 3.97 (s, 3H, CH_3) ppm; **$^{13}C\{^{1}H\}$ NMR (75.5MHz, $CDCl_3$): δ** 160.0 (s, 1C, C=O), 159.4 (d, $^{1}J_{CF}$ = 242.9Hz, 1C, C–F), 134.1 (d, $^{4}J_{CF}$ = 2.8Hz, 1C, C_{ipso}–NH), 129.0 (s, 1C, C_1), 125.6 (s, 1C, C_4), 122.0 (d, $^{3}J_{CF}$ = 8.0Hz, 2C, $C_{5/5'}$), 115.8 (d, $^{2}J_{CF}$ = 22.5Hz, 2C, $C_{6/6'}$), 112.4 (s, 1C, C_2), 107.7 (s, 1C, C_3), 37.0 (s, 1C, CH_3) ppm; **$^{19}F\{^{1}H\}$ NMR (282.4MHz, $CDCl_3$): δ** –118.4 (s, 1F) ppm; **HRMS (ESI+):** calcd for $[M+H]^+$ = $C_{12}H_{12}FN_2O^+$: 219.0928 m/z. Found: 219.0937 m/z.

Complete assignments were made based on COSY, HSQC and HMBC analyses. The J_{HF} coupling constants were assessed by a comparative $^{1}H\{^{19}F\}$experiment.

P.6 – 1–Methyl–N–(3–methylphenyl)pyrrole–2–carboxamide (**3af**)

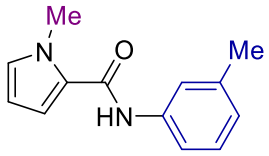

Synthesized at 0.5mmol scale using N–methylpyrrole and m–tolyl–isocyanate as starting materials. The reaction was quenched after 7.5h and purified by column chromatography on silica gel (eluent EtOAc/Hex 1:5). Isolated as a white solid in 67% yield (71.4mg, 0.33mmol). **Rf(EtOAc/Hex 1:5)** = 0.35; **m.p.** 99.9–100.7°C; **^{1}H NMR (400MHz, $CDCl_3$): δ** 7.70 (brs, 1H, NH), 7.46 (pt, J = 1.8Hz, 1H, m–Tol, CH), 7.32 (dd, J = 8.0, 1.8Hz, 1H, m–Tol, CH), 7.22 (pt, J = 7.8Hz, 1H, m–Tol, CH), 6.95–6.91 (m, J = 7.6Hz, 1H, m–Tol, CH), 6.77 (pt, J = 2.1Hz, 1H, $CH_{pyrrole}$), 6.71 (dd, J = 4.0, 1.7Hz, 1H, $CH_{pyrrole}$), 6.13 (dd, J = 4.0, 2.6Hz, 1H, $CH_{pyrrole}$), 3.97 (s, 3H, $CH_{3pyrrole}$), 2.35 (s, 3H, m–Tol, CH_3) ppm; **$^{13}C\{^{1}H\}$ NMR (100.6MHz, $CDCl_3$): δ** 160.0 (s, 1C), 138.9 (s, 1C), 138.0 (s, 1C), 128.84 (s, 1C), 128.79 (s, 1C), 125.9 (s, 1C), 124.8 (s, 1C), 120.7 (s, 1C), 117.1 (s, 1C), 112.3 (s, 1C), 107.5 (s, 1C), 36.9 (s, 1C), 21.5 (s, 1C) ppm; **HRMS (ESI+):** calcd for $[M+H]^+$ = $C_{13}H_{15}N_2O^+$: 215.1179 m/z. Found: 215.1185 m/z.

P.7 – N–(3–chlorophenyl)–1–methylpyrrole–2–carboxamide (**3ag**)

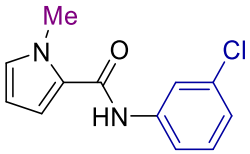

Synthesized at 0.5mmol scale using N–methylpyrrole and 3–chlorophenyl–isocyanate as starting materials. The reaction was quenched after 5h and purified by column chromatography on silica gel (eluent EtOAc/Hex 1:5). Isolated as a white solid in 72% yield (84.2mg, 0.36mmol). **Rf(EtOAc/Hex 1:5)** = 0.38; **m.p.** 93.6–94.2°C; **^{1}H NMR (400MHz, $CDCl_3$): δ** 7.75 (brs, 1H, NH), 7.69 (pt, J = 2.1Hz, 1H, 3–Cl–Ph, CH), 7.37 (ddd, J = 8.0, 2.0, 0.8 Hz, 1H, 3–Cl–Ph, CH), 7.22 (pt, J = 8.0Hz, 1H, 3–Cl–Ph, CH), 7.06 (ddd, J = 8.0, 2.0, 1.0Hz, 1H, m–Tol, CH), 6.78 (pt, J = 2.1Hz, 1H, $CH_{pyrrole}$), 6.71 (dd, J = 4.0Hz, 1.7Hz, $CH_{pyrrole}$), 6.13 (dd, J = 4.0, 2.6Hz, 1H, $CH_{pyrrole}$), 3.95 (s, 3H, $CH_{3pyrrole}$) ppm; **^{13}C{^{1}H} NMR (100.6MHz, $CDCl_3$): δ** 159.9 (s, 1C), 139.3 (s, 1C), 134.7 (s, 1C), 130.0 (s, 1C), 129.3 (s, 1C), 125.3 (s, 1C), 124.0 (s, 1C), 120.1 (s, 1C), 118.0 (s, 1C), 112.7 (s, 1C), 107.7 (s, 1C), 37.0 (s, 1C) ppm; **HRMS (ESI+):** calcd for $[M+H]^+$ = $C_{12}H_{12}{}^{35}ClN_2O^+$: 235.0633 m/z. Found: 235.0690 m/z. $[M+H]^+$ = $C_{12}H_{12}{}^{37}ClN_2O^+$: 237.0606 m/z. Found: 237.0662 m/z.

P.8 – 1–Methyl–N–(4–nitrophenyl)pyrrole–2–carboxamide (**3ah**)

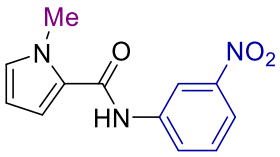

Synthesized at 0.5mmol scale using N–methylpyrrole and 3–nitrophenyl–isocyanate as starting materials. The reaction was quenched after 5h and purified by column chromatography on silica gel (eluent EtOAc/Hex 1:5). Isolated as a yellow solid in 55% yield (67.2mg, 0.27mmol). **Rf(EtOAc/Hex 1:5)** = 0.25; **m.p.** 153.9–154.7°C; **^{1}H NMR (400MHz, $CDCl_3$): δ** 8.46 (pt, J = 2.2Hz, 1H, 3–NO_2–Ph, CH), 7.97–7.92 (m, 2H, 3–NO_2–Ph, CH), 7.82 (brs, 1H, NH), 7.49 (pt, J = 8.2Hz, 1H, 3–NO_2–Ph, CH), 6.83 (pt, J = 2.1Hz, 1H, $CH_{pyrrole}$), 6.77 (dd, J = 4.1Hz, 1.7Hz, $CH_{pyrrole}$), 6.17 (dd, J = 4.1, 2.6Hz, 1H, $CH_{pyrrole}$), 3.99 (s, 3H, $CH_{3pyrrole}$) ppm; **^{13}C{^{1}H} NMR (100.6MHz, $CDCl_3$): δ** 159.9 (s, 1C), 148.8 (s, 1C), 139.4 (s, 1C), 129.9 (s, 1C), 129.8 (s, 1C), 125.6 (s, 1C), 124.9 (s, 1C), 118.6 (s, 1C), 114.6 (s, 1C), 113.1 (s, 1C), 108.0 (s, 1C), 37.1 (s, 1C) ppm; **HRMS (ESI+):** calcd for $[M+H]^+$ = $C_{12}H_{12}N_3O_3^+$: 246.0873 m/z.

Found: 246.0872 m/z.

P.9 – 1–Methyl–N–(2–methylphenyl)pyrrole–2–carboxamide (**3ai**)

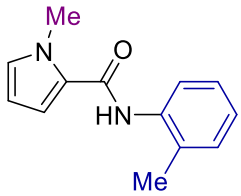

Synthesized at 0.5mmol scale using N–methylpyrrole and o–tolyl–isocyanate as starting materials. The reaction was quenched after 7.5h and purified by column chromatography on silica gel (eluent EtOAc/Hex 1:5). Isolated as a white solid in 27% yield (29.2mg, 0.27mmol). **Rf(EtOAc/Hex 1:5)** = 0.34; **m.p.** 114.7–115.2°C; **^{1}H NMR (400MHz, $CDCl_3$): δ** 7.89 (ds, J = 8.0, 0.6Hz, 1H, o–Tol, CH), 7.49 (brs, 1H, NH), 7.28–7.19 (m, 2H, o–Tol, CH), 7.09 (td, J = 7.4, 1.2Hz, 1H, o–Tol, CH), 6.80 (pt, J = 2.1Hz, 1H, $CH_{pyrrole}$), 6.71 (dd, J = 4.1Hz, 1.7Hz, $CH_{pyrrole}$), 6.16 (dd, J = 4.1, 2.6Hz, 1H, $CH_{pyrrole}$), 3.98 (s, 3H, $CH_{3pyrrole}$), 2.32 (s, 3H, o–Tol, CH_3) ppm; **^{13}C{^{1}H} NMR (100.6MHz, $CDCl_3$): δ** 160.0 (s, 1C), 135.9 (s, 1C), 130.6 (s, 1C), 129.0 (s, 1C), 128.8 (s, 1C), 126.9 (s, 1C), 126.0 (s, 1C), 124.9 (s, 1C), 122.9 (s, 1C), 112.1 (s, 1C), 107.6 (s, 1C), 36.9 (s, 1C), 17.9 (s, 1C) ppm.

Spectroscopic data are consistent with the ones previously reported. [20]

P.10 – N–(3,5–dimethylphenyl)–1–methylpyrrole–2–carboxamide (**3aj**)

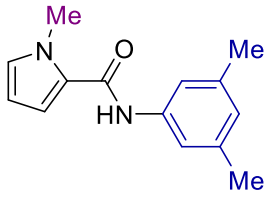

Synthesized at 0.5mmol scale using N–methylpyrrole and 3,5–dimethylphenyl–isocyanate as starting materials. The reaction was quenched after 7.5h and purified by column chromatography on silica gel (eluent EtOAc/Hex 1:5). Isolated as a crystalline white solid in 61% yield (69.7mg, 0.31mmol). **Rf(EtOAc/Hex 1:5)** = 0.41; **m.p.** 151.3–152.0°C; **^{1}H NMR (400MHz, $CDCl_3$): δ** 7.53 (brs, 1H, NH), 7.20 (s, 2H, 3,5–Me–Ph, CH), 6.78 (pt, J = 2.1Hz, 1H, $CH_{pyrrole}$), 6.77–6.75 (m, 1H, 3,5–Me–Ph, CH) 6.67 (dd, J = 4.0Hz, 1.7Hz, $CH_{pyrrole}$), 6.14 (dd, J = 4.0, 2.6Hz, 1H, $CH_{pyrrole}$), 3.98 (s, 3H, $CH_{3pyrrole}$), 2.31 (s, 6H, 3,5–Me–Ph, CH_3) ppm; **^{13}C{^{1}H} NMR (100.6MHz, $CDCl_3$): δ** 160.0 (s, 1C), 138.9 (s, 2C), 138.0 (s, 1C), 128.8 (s, 1C), 126.0 (s, 1C), 125.9 (s, 1C), 117.7 (s, 2C), 112.1 (s, 1C), 107.5 (s, 1C), 37.0 (s, 1C), 21.5 (s, 2C) ppm; **HRMS (ESI+):**

calcd for $[M+H]^+ = C_{14}H_{17}N_2O^+$: 229.1335 m/z. Found: 229.1345 m/z.

P.11 – N–[3,5–bis(trifluoromethyl)phenyl]–1–methylpyrrole–2–carboxamide (**3ak**)

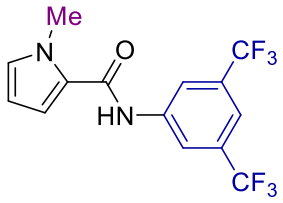

Synthesized at 0.5mmol scale using N–methylpyrrole and 3,5–bis–trifluoromethylphenyl–isocyanate as starting materials. The reaction was quenched after 5h and purified by column chromatography on silica gel (gradient from pure Hex to EtOAc/Hex 1:10). Isolated as a crystalline white solid in 24% yield (39.7mg, 0.12mmol). **Rf(EtOAc/Hex 1:10)** = 0.32; **m.p.** 121.5–122.3°C; **^{1}H NMR (400MHz, $CDCl_3$): δ** 8.08 (s, 2H, 3,5–CF_3–Ph, CH), 7.90 (brs, 1H, NH), 7.58 (brs, 1H, 3,5–CF_3–Ph, CH), 6.83 (pt, J = 2.1Hz, 1H, $CH_{pyrrole}$), 6.77 (dd, J = 4.0Hz, 1.7Hz, $CH_{pyrrole}$), 6.17 (dd, J = 4.0, 2.6Hz, 1H, $CH_{pyrrole}$), 3.98 (s, 3H, $CH_{3pyrrole}$) ppm; **^{13}C{^{1}H} NMR (100.6MHz, $CDCl_3$): δ** 159.9 (s, 1C), 139.8 (s, 1C), 132.5 (q, $^2J_{CF}$ = 33.4Hz, 2C), 130.1 (s, 1C), 124.7 (s, 1C), 123.3 (q, $^1J_{CF}$ = 273.0Hz, 2C), 119.6 (q, $^3J_{CF}$ = 3.3Hz, 2C), 119.2 (s, 1C), 117.2 (hept, $^3J_{CF}$ = 3.8Hz, 1C), 113.4 (s, 1C), 37.1 (s, 1C); **^{19}F NMR (376.5MHz, $CDCl_3$): δ** –63.0 (s, 6F) ppm.

Spectroscopic data are consistent with the ones previously reported. [39]

P.12 – N–(2,6–dimethylphenyl)–1–methylpyrrole–2–carboxamide (**3al**)

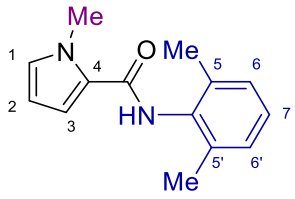

Synthesized at 1mmol scale using N–methylpyrrole and 2,6–dimethylphenyl–isocyanate as starting materials. The reaction was quenched after 20h and purified by column chromatography on silica gel (eluent EtOAc/PE 1:10). Isolated as a light–brown solid in 21% yield (47.1mg, 0.21mmol). **Rf(EtOAc/PE 1:10)** = 0.13; **m.p.** 121.9–123.0°C; **^{1}H NMR (300MHz, $CDCl_3$): δ** 7.18 (brs, 1H, NH), 7.14–7.07 (m, 3H, 2,6–Me–Ph, CH_{meta} and CH_{para}), 6.79 (pt, J = 2.1Hz, 1H, C_1–H), 6.76 (brs, 1H, 3,5–Me–Ph, C_2–H) 6.16 (pt, J = 3.0Hz, C_3–H), 3.96 (s, 3H, N–CH_3), 2.28 (s, 6H, 2,6–Me–Ph, $C_{5/5'}$–CH_3) ppm; **^{13}C{^{1}H} NMR (75.5MHz, $CDCl_3$): δ** 160.3 (s, 1C, C=O), 135.8 (s, 1C, $C_{5/5'}$), 133.9 (s, 1C, NH–C_{ipso}), 128.5 (s, 1C, C_1), 128.3 (s, 2C, $C_{6/6'}$), 127.3 (s, 1C, C_7), 125.7 (s, 1C, C_4), 112.1 (s, 1C, C_2),

107.5 (s, 1C, C_3), 36.8 (s, 1C, N–CH_3), 18.6 (s, 2C, $C_{5/5'}$–CH_3) ppm; **HRMS (ESI+):** calcd for $[M+H]^+ = C_{14}H_{17}N_2O^+$: 229.1335 m/z. Found: 229.1342 m/z.

Complete assignments were made based on COSY, HSQC and HMBC analyses.

P.13 – 1–Methyl–N–(2,4,6–trimethylphenyl)pyrrole–2–carboxamide (**3an**)

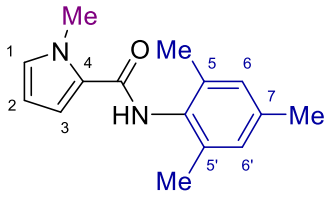

Synthesized at 1mmol scale using N–methylpyrrole and 2,4,6–dimethylphenyl–isocyanate as starting materials. The reaction was quenched after 20h and purified by column chromatography on silica gel (gradient EtOAc/PE 1:20 to 1:6). Isolated as a pale yellow solid in 40% yield (97.3mg, 0.40mmol). **Rf(EtOAc/PE 1:6)** = 0.29; **m.p.** 133.9–125.1°C; **^{1}H NMR (300MHz, $CDCl_3$): δ** 7.09 (brs, 1H, NH), 6.92 (s, 2H, Mes, CH_{meta}), 6.78 (pt, J = 2.1Hz, 1H, C_1–H), 6.76 (d, 1H, Mes, J = 2.8Hz C_2–H) 6.16 (pt, J = 2.8Hz, C_3–H), 3.96 (s, 3H, N–CH_3), 2.29 (s, 3H, Mes, C_7–CH_3), 2.23 (s, 6H, Mes, $C_{5/5'}$–CH_3) ppm; **^{13}C{^{1}H} NMR (75.5MHz, $CDCl_3$): δ** 160.4 (s, 1C, C=O), 136.9 (s, 1C, C_7), 135.6 (s, 2C, $C_{5/5'}$), 131.2 (s, 1C, NH–C_{ipso}), 129.0 (s, 2C, $C_{6/6'}$), 128.4 (s, 1C, C_1), 125.8 (s, 1C, C_4), 112.0 (s, 1C, C_2), 107.4 (s, 1C, C_3), 36.8 (s, 1C, N–CH_3), 21.1 (s, 1C, Mes, C_7–CH_3), 18.6 (s, 2C, Mes, $C_{5/5'}$–CH_3) ppm; **HRMS (ESI+):** calcd for $[M+H]^+ = C_{15}H_{19}N_2O^+$: 243.1492 m/z. Found: 243.1497 m/z.

Complete assignments were made based on COSY, HSQC and HMBC analyses.

P.14 – 1–Methyl–N–naphthalen–1–ylpyrrole–2–carboxamide (**3ao**)

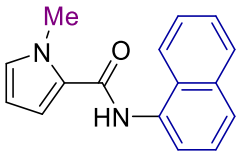

Synthesized at 0.5mmol scale using N–methylpyrrole and 1–naphthyl–isocyanate as starting materials. The reaction was quenched after 7.5h and purified by column chromatography on silica gel (eluent EtOAc/Hex 1:5). Isolated as a crystalline white solid in 40% yield (50.3mg, 0.20mmol). **Rf(EtOAc/Hex 1:5)** = 0.29; **m.p.** 115.8–116.1°C; **^{1}H NMR (400MHz, $CDCl_3$): δ** 8.01 (brs, 1H, NH), 7.95 (d, J = 7.6Hz, 1H, Nap, CH), 7.93–7.86 (m, 2H, Nap, CH), 7.72 (d, J = 8.3Hz, Nap, CH), 7.56–7.47 (m, 3H, Nap, CH), 6.86 (dd, J

= 4.0, 1.6Hz, 1H, $CH_{pyrrole}$), 6.83 (pt, J = 2.1Hz, $CH_{pyrrole}$), 6.20 (dd, J = 4.0, 2.6Hz, 1H, $CH_{pyrrole}$), 4.00 (s, 3H, CH_3) ppm; **$^{13}C\{^1H\}$ NMR (100.6MHz, $CDCl_3$): δ** 160.5 (s, 1C), 134.3 (s, 1C), 132.5 (s, 1C), 129.0 (s, 1C), 128.9 (s, 1C), 127.6 (s, 1C), 126.4 (s, 1C), 126.1 (s, 1C), 125.9 (s, 1C), 125.81 (s, 1C), 125.76 (s, 1C), 121.1 (s, 1C), 120.9 (s, 1C), 112.4 (s, 1C), 107.7 (s, 1C), 37.0 (s, 1C) ppm;

Spectroscopic data are consistent with the ones previously reported. [20]

P.15 – N–benzyl–1–methylpyrrole–2–carboxamide (**3aq**)

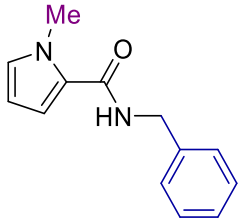

Synthesized at 1mmol scale using N–methylpyrrole and benzyl–isocyanate as starting materials. The reaction was quenched after 20h and purified by column chromatography on silica gel (gradient EtOAc/Hex 1:20 to 1:5). Isolated as a white solid in 55% yield (126.2mg, 0.55mmol). **Rf(EtOAc/Hex 1:5)** = 0.16; **m.p.** 72.4–73.6°C; **^1H NMR (400MHz, $CDCl_3$): δ** 7.38–7.31 (m, 4H, benz, CH), 7.31–7.26 (m, 1H, benz, CH), 6.73 (pt, J = 2.1Hz, 1H, $CH_{pyrrole}$), 6.53 (dd, J = 4.0Hz, 1.6Hz, $CH_{pyrrole}$), 6.15 (brs, 1H, NH), 6.07 (dd, J = 4.0, 2.6Hz, 1H, $CH_{pyrrole}$), 4.57 (d, J = 5.6Hz, benz, CH_2), 3.97 (s, 3H, CH_3) ppm; **$^{13}C\{^1H\}$ NMR (100.6MHz, $CDCl_3$): δ** 161.9 (s, 1C), 138.8 (s, 1C), 128.8 (s, 2C), 128.1 (s, 1C), 127.8 (s, 2C), 127.6 (s, 1C), 125.8 (s, 1C), 111.6 (s, 1C), 107.3 (s, 1C), 43.4 (s, 1C), 36.9 (s, 1C) ppm;

Spectroscopic data are consistent with the ones previously reported. [20]

P.16 – N–allyl–1–methyl–pyrrole–2–carboxamide (**3ar**)

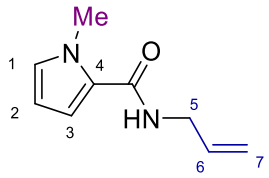

Synthesized at 1mmol scale using N–methylpyrrole and allyl–isocyanate as starting materials. The reaction was quenched after 20h and purified by column chromatography on silica gel (gradient EtOAc/Hex 1:20 to 1:5). Isolated as a clear viscous oil in 16% yield (26.5mg, 0.55mmol). **Rf(EtOAc/Hex 1:5)** = 0.15; **^1H NMR (400MHz, $CDCl_3$): δ** 6.71 (pt, J = 2.1Hz, 1H, $CH_{pyrrole}$), 6.54 (dd, J = 4.0Hz, 1.7Hz, $CH_{pyrrole}$), 6.08 (dd, J = 4.0, 2.6Hz, 1H, $CH_{pyrrole}$), 5.98–5.85 (m, 2H, NH and C_6–H), 5.24 (dq, $^3J_{trans}$ = 17.1Hz, $^2J_{gem}$ = ^4J = 1.5Hz, 1H,

C_7–H_{trans}), 5.16 (dq, $^3J_{trans}$ = 10.2Hz, $^2J_{gem}$ = ^4J = 1.5Hz, 1H, C_7–H_{cis}), 4.00 (tt, ^3J = 5.8Hz, ^4J = 1.6Hz, 2H, allyl, N–CH_2), 3.94 (s, 3H, CH_3) ppm; **$^{13}C\{^1H\}$ NMR (100.6MHz, $CDCl_3$): δ** 161.9 (s, 1C, C=O), 134.8 (s, 1C, C_6), 128.1 (s, 1C, C_1), 125.8(s, 1C, C_4), 116.4 (s, 1C, C_7), 111.5 (s, 1C, C_2), 107.3 (s, 1C, C_3), 41.7(s, 1C, C_5), 36.8 (s, 1C, CH_3) ppm;

Complete assignments were made based on COSY, HSQC and HMBC analyses. Spectroscopic data are consistent with the ones previously reported. [10]

P.17 – N–cyclohexyl–1–methylpyrrole–2–carboxamide (**3as**)

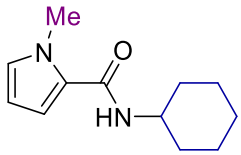

Synthesized at 1mmol scale using N–methylpyrrole and cyclohexyl–isocyanate as starting materials. The reaction was quenched after 20h and purified by column chromatography on silica gel (gradient EtOAc/PE 1:20 to 1:5). Isolated as a white solid in 67% yield (137.4mg, 0.67mmol). **Rf(EtOAc/PE 1:5)** = 0.28; **m.p.** 100.7–101.6°C; **^1H NMR (300MHz, $CDCl_3$): δ** 6.69 (pt, J = 2.1Hz, 1H, $CH_{pyrrole}$), 6.49 (dd, J = 4.0Hz, 1.7Hz, $CH_{pyrrole}$), 6.06 (dd, J = 4.0, 2.6Hz, 1H, $CH_{pyrrole}$), 5.76 (brd, J = 6.0Hz, 1H, NH), 3.92 (s, 3H, CH_3), 3.91–3.80 (m, 1H, Cy, N–CH), 2.03–1.91 (m, 2H, Cy, CH_2), 1.73 (dquint, J = 13.3, 3.9Hz, 2H, Cy, CH_2), 1.63 (dquint, J = 12.6, 3.9Hz 1H, Cy, CH_2), 1.39 (qt, J = 12.6, 3.4Hz, 2H, Cy, CH_2), 1.27–1.13 (m, 3H, CH_2) ppm; **$^{13}C\{^1H\}$ NMR (75.5MHz, $CDCl_3$): δ** 161.2 (s, 1C), 127.7 (s, 1C), 126.2 (s, 1C), 111.0 (s, 1C), 107.1 (s, 1C), 48.1 (s, 1C), 36.8 (s, 1C), 33.5 (s, 2C), 25.7 (s, 1C), 25.1 (s, 2C) ppm;

Spectroscopic data are consistent with the ones previously reported. [40]

P.18 – N–tert–butyl–1–methylpyrrole–2–carboxamide (**3at**)

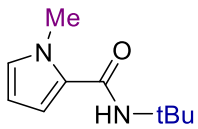

Synthesized at 1mmol scale using N–methylpyrrole and tertbutyl–isocyanate as starting materials. The reaction was quenched after 20h and purified by column chromatography on silica gel (gradient EtOAc/PE 1:20 to 1:5). Isolated as a white solid in 28% yield (50.8mg, 0.28mmol). **Rf(EtOAc/PE 1:5)** = 0.25; **m.p.** 84.5–85.6°C;

^{1}H NMR (300MHz, $CDCl_3$): δ 6.66 (pt, J = 2.1Hz, 1H, $CH_{pyrrole}$), 6.43 (dd, J = 4.0Hz, 1.7Hz, $CH_{pyrrole}$), 6.04 (dd, J = 3.8, 2.6Hz, 1H, $CH_{pyrrole}$), 5.71 (brs, 1H, NH), 3.91 (s, 3H, CH_3), 1.42 (s, 9H, tBu, CH_3) ppm; **^{13}C{^{1}H} NMR (75.5MHz, $CDCl_3$): δ** 161.8 (s, 1C), 127.6 (s, 1C), 127.0 (s, 1C), 110.9 (s, 1C), 106.9 (s, 1C), 51.3 (s, 1C), 36.8 (s, 1C), 29.2 (s, 3C) ppm;

Spectroscopic data are consistent with the ones previously reported. [41]

P.19 – N–phenyl–1H–pyrrole–2–carboxamide (**3ba**)

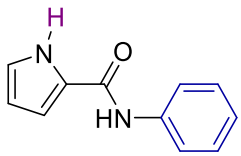

Synthesized at 1mmol scale using pyrrole and phenyl–isocyanate as starting materials. The reaction was quenched after 20h and purified by column chromatography on silica gel (eluent EtOAc/Hex 1:5). Isolated as a white solid in 67% yield (124.8mg, 0.67mmol). **Rf(EtOAc/Hex 1:5)** = 0.20; **m.p.** 152.9–153.7°C; **^{1}H NMR (400MHz, $CDCl_3$): δ** 10.03 (brs, 1H, $NH_{pyrrole}$), 7.71 (brs, 1H, NH), 7.64–7.59 (m, 2H, Ph, CH), 7.39–7.32 (m, 2H, Ph, CH), 7.17–7.10 (m, 1H, Ph, CH), 6.97 (dt, J = 2.6, 1.3Hz, 1H, $CH_{pyrrole}$), 6.74(ddd, J = 3.8, 2.6, 1.3 Hz, $CH_{pyrrole}$), 6.28 (dt, J = 3.8, 2.6Hz, $CH_{pyrrole}$) ppm; **^{13}C{^{1}H} NMR (100.6MHz, $CDCl_3$): δ** 159.4 (s, 1C), 137.9 (s, 1C), 129.2 (s, 2C), 126.1 (s, 1C), 124.4 (s, 1C), 122.7 (s, 1C), 120.3 (s, 2C), 110.2 (s, 1C), 109.8 (s, 1C) ppm.

Spectroscopic data were consistent with the ones previously reported. [20]

P.20 – N,1–diphenylpyrrole–2–carboxamide (**3ca**)

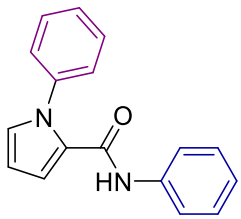

Synthesized at 1mmol scale using 1–phenyl–pyrrole and phenyl–isocyanate as starting materials. The reaction was quenched after 20h and purified by column chromatography on silica gel (eluent EtOAc/Hex 1:10). Isolated as a crystalline white solid in 44% yield (114.4mg, 0.44mmol). **Rf(EtOAc/Hex 1:10)** = 0.19; **m.p.** 152.9–153.7°C; **^{1}H NMR (400MHz, $CDCl_3$): δ** 7.50–7.35 (m, 8H, NH and CH_{Ph}), 7.30–7.24 (m, 2H, Ph, CH), 7.09–7.03 (m, 1H, Ph, CH), 7.06 (dt, J = 7.4, 1.1Hz, 1H, $CH_{pyrrole}$), 6.95 (ddd, J = 13.8, 2.7, 1.7 Hz,

$CH_{pyrrole}$), 6.32 (dd, J = 3.9, 2.7Hz, $CH_{pyrrole}$) ppm; **$^{13}C\{^1H\}$ NMR (100.6MHz, $CDCl_3$): δ** 159.0 (s, 1C), 140.3 (s, 1C), 138.1 (s, 1C), 129.2 (s, 2C), 129.1 (s, 2C), 128.7 (s, 1C), 128.0 (s, 1C), 127.5 (s, 1C), 126.0 (s, 2C), 124.1 (s, 1C), 119.9 (s, 2C), 115.0 (s, 1C), 109.2 (s, 1C) ppm.

Spectroscopic data were consistent with the ones previously reported. [20]

P.21 – 3,5–Dimethyl–N–phenyl–1H–pyrrole–2–carboxamide (**3da**)[42]

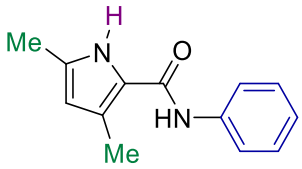

Synthesized at 1mmol scale using 2,4–dimethyl–pyrrole and phenyl–isocyanate as starting materials. The reaction was quenched after 20h and purified by column chromatography on silica gel (eluent EtOAc/Hex 1:5). Isolated as an off–white solid in 74% yield (157.7mg, 0.74mmol). **Rf(EtOAc/Hex 1:5)** = 0.25; **m.p.** 155.7–156.5°C; **^1H NMR (400MHz, $CDCl_3$): δ** 9.92 (brs, 1H, $NH_{pyrrole}$), 7.63–7.58 (m, 2H, Ph, CH), 7.48 (brs, 1H, NH), 7.37–7.31 (m, 2H, Ph, CH), 7.14–7.08 (m, 1H, Ph, CH), 5.82–5.81 (d, J = 2.8Hz, $CH_{pyrrole}$), 2.45 (s, 3H, CH_3), 2.23 (s, 3H, CH_3) ppm; **$^{13}C\{^1H\}$ NMR (100.6MHz, $CDCl_3$): δ** 160.2 (s, 1C), 138.2 (s, 1C), 132.3 (s, 1C), 129.1 (s, 2C), 124.0 (s, 1C), 121.7 (s, 1C), 121.3 (s, 1C), 120.2 (s, 2C), 111.6 (s, 1C), 13.7 (s, 1C), 12.9 (s, 1C) ppm.

Spectroscopic data were consistent with the ones previously reported.

P.22 – 1,2,5–Trimethyl–N–phenylpyrrole–3–carboxamide (**3ea**)[17]

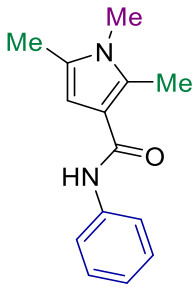

Synthesized at 1mmol scale using 2,4–dimethyl–pyrrole and phenyl–isocyanate as starting materials. The reaction was quenched after 20h and purified by column chromatography on silica gel (gradient EtOAc/PE 1:5 to 1:1). The remaining impurities were removed by precipitation with PE from a saturated EtOAc solution at –20°C. Isolated as an off–white solid in 45% yield (102.4mg, 0.45mmol). **Rf(EtOAc/PE 1:1)** = 0.38; **m.p.** 197.9–199.1°C; **^1H NMR (300MHz, $CDCl_3$): δ** 7.62–7.54 (m, 2H, Ph, CH), 7.44 (brs, 1H, NH), 7.36–7.27 (m, 2H, Ph, CH), 7.11–7.02 (m, 1H,

Ph, CH), 6.07 (s, 1H, $CH_{pyrrole}$), 3.40 (s, 3H, CH_3), 2.56 (s, 3H, CH_3), 2.21 (s, 3H, CH_3) ppm; **$^{13}C\{^1H\}$ NMR (75.5MHz, $CDCl_3$): δ** 164.3 (s, 1C), 138.8 (s, 1C), 134.6 (s, 1C), 129.0 (s, 2C), 128.2 (s, 1C), 123.5 (s, 1C), 119.9 (s, 2C), 113.5 (s, 1C), 103.7 (s, 1C), 30.3 (s, 1C), 12.5 (s, 1C), 11.4 (s, 1C) ppm.

Spectroscopic data were consistent with the ones previously reported.

P.23 – Ethyl 2–methyl–5–(phenylcarbamoyl)–1H–pyrrole–3–carboxylate (**3fa**)

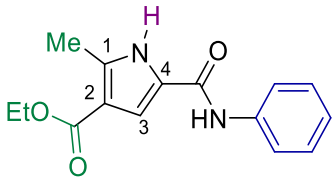

Synthesized at 1mmol scale using ethyl 2–methylpyrrole–3–carboxylate and phenyl–isocyanate as starting materials. The reaction was quenched after 20h and purified by column chromatography on silica gel (gradient EtOAc/PE 1:20 to 1:5). Isolated as a white solid in 32% yield (87.7mg, 0.32mmol). **Rf(EtOAc/PE 1:5)** = 0.16; **m.p.** 208.7–210.0°C; **^1H NMR (300MHz, $CDCl_3$): δ** 9.98 (brs, 1H, $NH_{pyrrole}$), 7.62–7.55 (m, 3H, CH_{ortho} and NH), 7.40–7.32 (m, 2H, CH_{meta}), 7.18–7.09 (m, 2H, CH_{para} and $CH_{pyrrole}$), 4.30 (q, ^3J = 7.1Hz, 2H, Et, CH_2), 2.57 (s, 3H, C_1–CH_3), 1.37 (t, ^3J = 7.1Hz, 3H, Et, CH_3) ppm; **$^{13}C\{^1H\}$ NMR (75.5MHz, $CDCl_3$): δ** 164.9 (s, 1C, COOEt, C=O), 158.8 (s, 1C, CONH, C=O), 139.4 (s, 1C, C_2), 137.6 (s, 1C, C_{ipso}), 129.3 (s, 2C, C_{meta}), 124.6 (s, 1C, C_{para}), 123.8 (s, 1C, C_4), 120.2 (s, 2C, C_{ortho}), 114.0 (s, 1C, C_1), 111.7 (s, 1C, C_3), 60.0 (s, 1C, Et, CH_2), 14.6 (s, 1C, Et, CH_3), 13.5 (s, 1C, C_1–CH_3) ppm; **HRMS (ESI+):** calcd for $[M+H]^+$ = $C_{15}H_{17}N_2O_3^+$: 273.1234 m/z. Found: 273.1245 m/z.

Complete assignments were made based on COSY, HSQC and HMBC analyses.

P.24 – 1–Methyl–N–phenylindole–3–carboxamide (**3ga**)

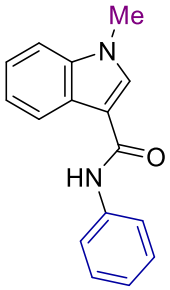

Synthesized at 1mmol scale using N–methylindole and phenyl–isocyanate as starting materials. The reaction was quenched after 20h and purified by column chromatography on silica gel (gradient EtOAc/Hex 1:10 to 1:2). Isolated as a white solid in 46% yield (115.9mg, 0.46mmol). **Rf(EtOAc/Hex 1:2)** = 0.24; **m.p.** 165.1–165.9°C; **^{1}H NMR (400MHz, $CDCl_3$): δ** 8.08–8.02 (m, 1H, CH_{ind}), 7.75 (s, 1H, CH_{ind}) 7.70–7.63 (m, 3H, NH and CH_{Ph}), 7.43–7.29 (m, 5H, CH_{ind} and CH_{Ph}), 7.16–7.10 (m, 1H, CH_{Ph}), 3.86 (s, 3H, CH_3) ppm; **^{13}C{^{1}H} NMR (100.6MHz, $CDCl_3$): δ** 163.4 (s, 1C), 138.7 (s, 1C), 137.5 (s, 1C), 132.7 (s, 1C), 129.2 (s, 2C), 125.6 (s, 1C), 124.0 (s, 1C), 122.9 (s, 1C), 121.9 (s, 1C), 120.3 (s, 1C), 120.2 (s, 2C), 111.2 (s, 1C), 110.3 (s, 1C), 33.4 (s, 1C) ppm.

Overlap of the NH signal with others makes it difficult to identify. Changing solvent from $CDCl_3$ to DMSO–d_6 allows to identify this signal. Moreover, the spin system of the indole moiety can be resolved.

^{1}H NMR (400MHz, DMSO–d_6): δ 9.71 (brs, 1H, NH), 8.26 (s, 1H, CH_{ind}), 8.21 (dt, J = 7.8, 1.0Hz, 1H, CH_{ind}), 7.80–7.74 (m, 2H, CH_{Ph}), 7.53 (dt, J = 8.2, 0.8Hz, 1H, CH_{ind}), 7.36–7.30 (m, 2H, CH_{Ph}), 7.26 (ddd, J = 8.2, 7.1, 1.2Hz, 1H, CH_{ind}), 7.19 (ddd, J = 7.8, 7.0, 1.1Hz, 1H, CH_{ind}), 7.04 (tt, J = 7.4, 1.0Hz, 1H, CH_{ind}), 3.88 (s, 3H, CH_3) ppm; Spectroscopic data were consistent with the ones previously reported.[43,44]

P.25 – 1,2–Dimethyl–N–phenylindole–3–carboxamide (**3ha**)

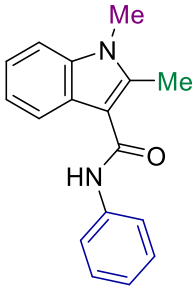

Synthesized at 1mmol scale using 1,2–dimethylindole and phenyl–isocyanate as starting materials. The reaction was quenched after 20h and purified by column chromatography on silica gel (gradient EtOAc/PE 1:20 to 1:5). Isolated as a white solid in 43% yield (113.8mg, 0.43mmol). **Rf(EtOAc/PE 1:5)** = 0.18; **m.p.** 189.1–190.0°C; **^{1}H NMR (300MHz, $CDCl_3$): δ** 7.83–7.76 (m, 1H, CH_{ind}), 7.74 (brs, 1H, NH), 7.69–7.62 (m, 2H, CH_{Ph}), 7.42–7.33 (m, 3H, CH_{Ph}

and CH_{ind}), 7.31–7.22 (m, 2H, CH_{ind}), 7.13 (m, 1H, CH_{Ph}), 3.70 (s, 3H, N–CH_3), 2.76 (s, 3H, CH_3) ppm; **$^{13}C\{^1H\}$ NMR (75.5MHz, $CDCl_3$): δ** 164.5 (s, 1C), 143.2 (s, 1C), 138.8 (s, 1C), 136.6 (s, 1C), 129.2 (s, 2C), 125.0 (s, 1C), 123.9 (s, 1C), 122.0 (s, 1C), 121.6 (s, 1C), 120.0 (s, 2C), 118.4 (s, 1C), 109.9 (s, 1C), 107.9 (s, 1C), 29.7 (s, 1C), 11.**7** (s, 1C) ppm.

Spectroscopic data were consistent with the ones previously reported.[17]

P.26 – 1–Methyl–N,2–diphenylindole–3–carboxamide (**3ia**)

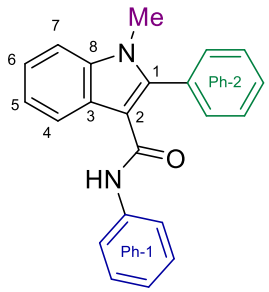

Synthesized at 1mmol scale using 1–methyl–2–phenylindole and phenyl–isocyanate as starting materials. The reaction was quenched after 20h and purified by column chromatography on silica gel (gradient EtOAc/PE 1:20 to 1:5). Isolated as a white solid in 25% yield (80.1mg, 0.25mmol). **Rf(EtOAc/PE 1:5)** = 0.44; **m.p.** 118.4–119.2°C; **^1H NMR (300MHz, $CDCl_3$): δ** 8.56–8.48 (m, 1H, C_6–H), 7.69–7.60 (m, 3H, Ph–2, CH_{meta} and CH_{para}), 7.60–7.53 (m, 3H, CH), 7.42–7.30 (m, 3H, CH), 7.25–7.13 (m, 4H, CH), 7.06–6.95 (m, 2H, NH and CH_{para}) ppm; **$^{13}C\{^1H\}$ NMR (75.5MHz, $CDCl_3$): δ** 163.2 (s, 1C, C=O), 141.3 (s, 1C, C_1), 138.6 (s, 1C, Ph–1, C_{ipso}), 136.9 (s, 1C, C_8), 130.98 (s, 2C, Ph–2. CH_{ortho}), 130.97 (s, 1C, Ph–2, C_{ipso}), 130.4 (s, 1C, Ph–2. C_{para}), 129.7 (s, 2C, Ph–2. C_{meta}), 128.9 (s, 2C, Ph–1. C_{meta}), 127.3 (s, 1C, C_3), 123.4 (s, 1C, C_4), 123.3 (s, 1C, Ph–1. C_{para}), 122.4 (s, 1C, C_6), 122.2 (s, 1C, C_5), 119.1 (s, 2C, Ph–1. CH_{ortho}), 109.7 (s, 1H, C_7), 109.3 (s, 1C, C_2), 30.9 ppm; **HRMS (ESI+):** calcd for $[M+H]^+ = C_{22}H_{19}N_2O^+$: 327.1492 m/z. Found: 327.1500 m/z.

Complete assignments were made based on COSY, HSQC and HMBC analyses.

P.27 – 2–Methyl–N–phenyl–1H–indole–3–carboxamide (**3ja**)

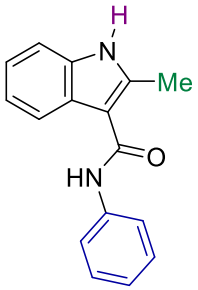

Synthesized at 1mmol scale using 2–methylindole and phenyl–isocyanate as starting materials. The reaction was quenched after 20h and purified by column chromatography on silica gel (gradient EtOAc/Hex 1:10 to 1:2). Isolated as a white solid in 38% yield (95.4mg, 0.38mmol). **Rf(EtOAc/Hex 1:2)** = 0.24; **m.p.** 166.9–167.8°C; **^{1}H NMR (400MHz, $CDCl_3$): δ** 8.62 (brs, 1H, NH_{ind}), 7.82–7.77 (m, 1H, CH_{ind}), 7.72 (brs, 1H, NH), 7.68–7.62 (m, 2H, CH_{Ph}), 7.41–7.34 (m, 3H, CH_{ind} and CH_{Ph}), 7.24 (quintd, J = 7.4, 1.8Hz, 2H, CH_{ind}) 7.16–7.10 (m, 1H, CH_{Ph}), 2.74 (s, 3H, CH_3) ppm; **^{13}C{^{1}H} NMR (100.6MHz, $CDCl_3$): δ** 164.5 (s, 1C), 141.9 (s, 1C), 138.6 (s, 1C), 134.9 (s, 1C), 129.2 (s, 2C), 125.6 (s, 1C), 124.1 (s, 1C), 122.4 (s, 1C), 121.8 (s, 1C), 120.1 (s, 2C), 118.4 (s, 1C), 111.5 (s, 1C), 108.4 (s, 1C), 13.8 (s, 1C) ppm.

Spectroscopic data were consistent with the ones previously reported.[45]

P.28 – 4–Methyl–N–phenyl–1H–indole–3–carboxamide (**3ka**)

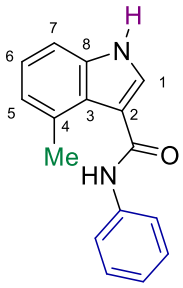

Synthesized at 1mmol scale using 4–methylindole and phenyl–isocyanate as starting materials. The reaction was quenched after 20h and purified by column chromatography on silica gel (gradient EtOAc/Hex 1:10 to 1:2). Isolated as a white solid in 21% yield (53.3mg, 0.21mmol). **Rf(EtOAc/Hex 1:2)** = 0.20; **m.p.** 210.8–211.3°C; **^{1}H NMR (400MHz, $CDCl_3$): δ** 10.68 (brs, 1H, NH_{ind}), 9.27 (brs, 1H, NH_{ind}), 7.89–7.83 (m, 3H, C_1–H and CH_{ortho}), 7.36–7.28 (m, $^{3}J_{ind}$ = 7.6Hz, 3H, CH_{meta} and C_7–H), 7.09 (t, ^{3}J = 7.4, 1H, C_6–H), 7.08–7.03 (m, 1H, Ph, CH_{para}), 6.92 (d, ^{3}J = 7.2Hz, 1H, C_5–H), 2.70 (s, 3H, CH_3) ppm; **^{13}C{^{1}H} NMR (100.6MHz, $CDCl_3$): δ** 165.1 (s, 1C, C=O), 141.2 (s, 1C, Ph, C_{ipso}), 137.8 (s, 1C, C_8), 132.1 (s, 1C, C_4), 129.4 (s, 2C, Ph, C_{meta}), 128.3 (s, 1C, C_1), 125.6 (s, 1C, C_3), 123.7 (s, 1C, Ph, C_{para}), 123.4 (s, 1C, C_6), 123.1 (s, 1C, C_5), 120.3 (s, 2C, Ph, C_{ortho}), 115.3 (s, 1C, C_2), 110.3 (s, 1C, C_7), 21.6 (s, 1C, CH_3) ppm; **HRMS (ESI+):** calcd for $[M+H]^+$ = $C_{16}H_{15}N_2O^+$: 251.1179 m/z. Found:

251.1207m/z.

Complete assignments were made based on COSY, HSQC and HMBC analyses.

General procedure for the synthesis of isocyanates

Isocyanates were synthesized from the corresponding aryl–amine by a modified literature procedure:

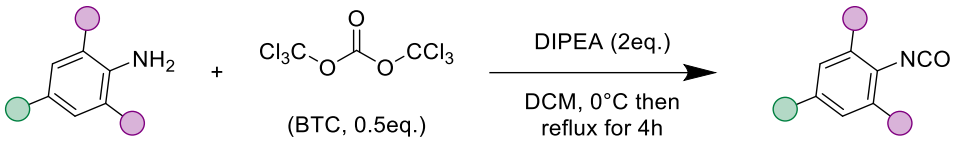

The aromatic amine (4.0mmol, 1.0eq.) and DIPEA (1.4ml, 8.0mmol, 2.0eq.) where added to a Schlenk flask and dissolved in DCM (10ml). In a separate vessel, BTC (600mg, 2.0mmol, 0.5eq.) was dissolved in DCM (10ml) under an atmosphere of argon. The flask was cooled with an ice–bath and the amine/DIPEA solution was slowly added at that temperature. The resulting mixture was stirred for 10 minutes, before the ice–bath was removed. The reaction was gently taken to reflux and stirred for 4h (reaction monitoring by TLC). After this time, the crude was allowed to cool to RT and directly filtered through silica. The filtering pad was rinsed with DCM (ca. 30ml) until no more compound could be extracted The desired compound was isolated after evaporation of the solvent and stored in a glovebox at low temperature.

ISO.1 – Mesityl–isocyanate (Mes–NCO)

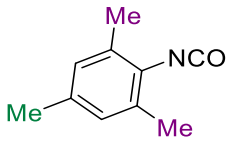

Synthesized using mesityl–amine as starting material. The corresponding isocyanate was isolated as a colorless, crystalline solid in 97% yield (622.7mg, 3.86mmol). The ^{1}H NMR characterization is in agreement with previously reported data.[46]

^{1}H NMR (600MHz, DCM–d_2): δ 6.86 (s, 2H, C_{Ar}–H), 2.28 (s, 6H, $^{meta}CH_3$), 2.25 (s, 3H, $^{para}CH_3$) ppm; **^{13}C{^{1}H} NMR (150.9MHz, DCM–d_2): δ** 135.6 (s, 1C, C_{para}), 133.1 (s, 2C, C_{ortho}), 129.1 (s, 2C, C_{meta}), 128.9 (s, 1C, C_{ipso}), 124.7 (s, 1C, N=C=O), 20.9 (s, 1C, $^{para}CH_3$), 18.8 (s, 2C, $^{ortho}CH_3$) ppm.

Complete assignments were made based on COSY, HSQC and HMBC

analyses.

ISO.2 – 2,6–Di–methyl–phenyl–isocyanate (Dmep–NCO)

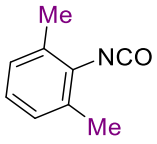

Synthesized using 2,6–di–methyl–phenyl–amine as starting material. The corresponding isocyanate was isolated as a clear, colorless oil in 94% yield (553.8mg, 3.76mmol). The ^{1}H NMR characterization is in agreement with previously reported data.[46]

^{1}H NMR (300MHz, $CDCl_3$): δ 7.07–6.97 (m, 3H, C_{Ar}–H), 2.33 (s, 6H, CH_3) ppm.

ISO.3 – 2,6–Di–isopropyl–phenyl–isocyanate (Dipp–NCO)

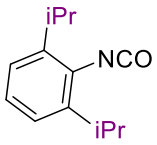

Synthesized using 2,6–di–isopropyl–phenyl–amine as starting material. The corresponding isocyanate was isolated as a pale yellow oil in 95% yield (774.7mg, 3.81mmol). The ^{1}H NMR characterization is in agreement with previously reported data.[46]

^{1}H NMR (300MHz, $CDCl_3$): δ 7.21–7.09 (m, 3H, C_{Ar}–H), 3.22 (hept, J = 6.8Hz, 2H, iPr, CH), 1.26 (d, 12H, J = 6.8Hz, iPr, CH_3) ppm.

ISO.4 – 2,6–Di–mesityl–phenyl–isocyanate (Dmp–NCO)

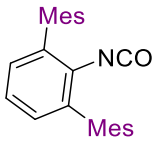

Synthesized at 1mmol scale, using 2,6–di–mesityl–phenyl–amine as starting material (the employed volume of DCM stays unchanged). The corresponding isocyanate was isolated as a white solid in 99% yield (352.2mg, 0.99mmol). The ^{1}H and ^{13}C NMR characterizations are consistent with previously reported data in C_6D_6.[47]

^{1}H NMR (600MHz, DCM–d_2): δ 7.36–7.33 (m, $^{3}J_{ortho}$ = 7.6Hz, 1H, CH_{para}), 7.13 (d, $^{3}J_{ortho}$ = 7.6Hz, 2H, CH_{meta}), 7.00–6.97 (m, 4H, Mes, CH_{meta}), 2.33 (s, 6H, Mes, $^{para}CH_3$), 2.02 (s, 12H, Mes, $^{ortho}CH_3$) ppm; **^{13}C{^{1}H} NMR (150.9MHz, DCM–d_2): δ** 138.1 (2C, Mes, C_{para}), 137.3 (2C, C_{ortho}), 136.7 (4C, Mes, C_{ortho}), 135.6 (2C, Mes, C_{ipso}), 131.9 (1C, C–N), 129.7 (2C, C_{meta}), 128.6 (4C, Mes, C_{meta}), 126.5 (1C, C_{para}), 126.1 (1C, N=C=O), 21.2 (2C, Mes, $^{para}CH_3$), 20.3 (4C, Mes, $^{ortho}CH_3$) ppm.

Complete assignments were made based on COSY, HSQC and HMBC analyses.

The 2,6–di–mesityl–phenyl–azide (Dmp–N_3) was synthesized according to a reported literature procedure, starting from 1,3–di–chloro benzene.[48,49] Tosyl–azide (TsN_3) synthesis was as well previously described,[50] whereas the Grignard reagent MesMgBr was prepared by a modified procedure.[51]

Preparation of Dmp–NH_2

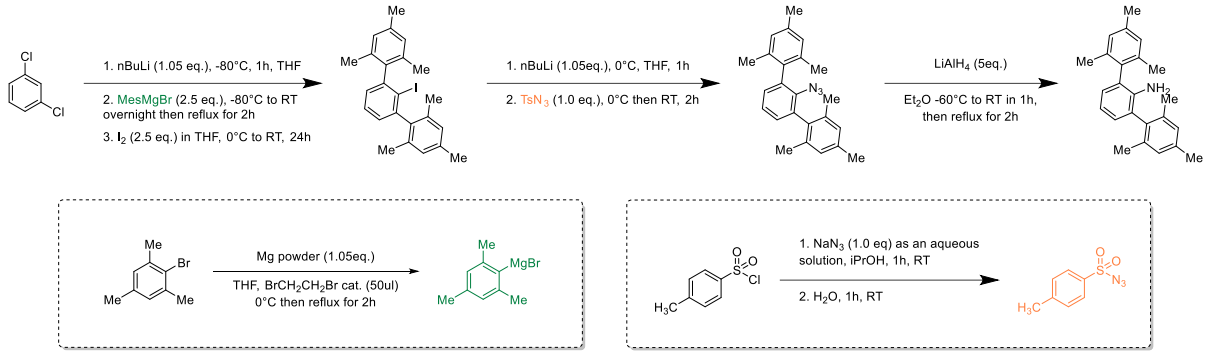

Preparation of MesMgBr

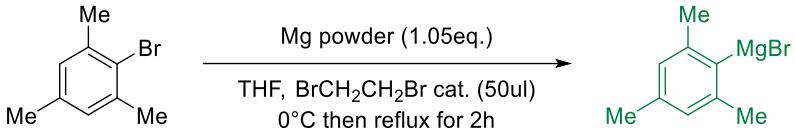

Magnesium powder (2.55g, 105mmol, 1.05eq.) was added to a 100ml Schlenk–flask inside a glovebox. The flask was then taken under a fume–hood, where THF (50ml), mesityl bromide (15.3ml, 100mmol, 1.0eq.) and 1,2–di–bromo–ethane (50µl, 0.55mmol, 0.006eq.) were sequentially added under a back–flow of argon. As soon as the reaction started (exothermic reaction) the flask was cooled down to 0°C and stirred for 30 minutes. The ice bath was then removed and the mixture was refluxed for 2h. The resulting dark–green solution was cooled to room temperature and directly used for the preparation of Dmp–I.

Preparation of Dmp–I

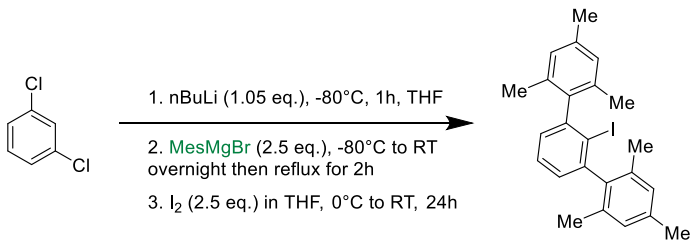

To a solution of 1,3–dichlorobenzene (4.6ml, 40mmol, 1.0eq.) in THF (125ml), nBuLi (1.6M, 26.3ml, 42mmol, 1.05eq.) was added dropwise at –80°C over a period of 30 minutes. After stirring for 1.5h at this temperature, a freshly prepared solution of MesMgBr (100mmol, 2.5eq.) in THF (50ml) was added via filter cannula at –80 °C over a period of 1h. The resulting mixture was allowed to slowly warm up to RT, stirred overnight at that temperature and then refluxed for further 2h. The flask was then cooled with an ice–bath and a solution of I_2 (25.4g, 100mmol, 2.5eq.) in THF (100ml) is added dropwise over a period of 1h. The resulting brownish solution is allowed to warm up to RT and stirred overnight. The mixture was finally quenched with a saturated $NaSO_3$ solution (300ml) and separated by aid of a separation funnel. The aqueous layer was back–extracted with Et_2O (3x300ml), and the combined organic concentrated and dried over Na_2SO_4. The solution was filtrated and the volatiles removed under vacuum. The resulting yellowish crystalline residue is dissolved in hot ethanol and crystallize overnight at –20°C. The supernatant is removed by decantation and the crystalline residue is washed with cold ethanol (2x100ml) and dried in vacuo. The desired product was isolated as a white crystalline solid in 58% yield (10.23g, 23.2mmol). Spectroscopic data are consistent with the one previously reported.[49]

^{1}H NMR (300MHz, $CDCl_3$): δ 7.43 (t, $^3J_{ortho}$ = 7.5Hz, 1H, CH_{para}), 7.15 (d, $^3J_{ortho}$ = 7.5Hz, 2H, CH_{meta}), 6.94 (s, 4H, Mes, CH_{meta}), 2.37 (s, 6H, Mes, $^{para}CH_3$), 2.09 (s, 12H, Mes, $^{ortho}CH_3$) ppm;

Preparation of TsN_3

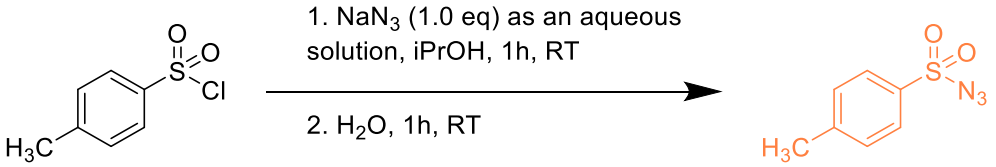

To a 500ml round bottom flask, *p*–toluenesulfonyl chloride (15.25g, 80mmol, 1.0eq.) was added along with isopropanol (45ml) in an air atmosphere. Separately, a solution of NaN_3 (6.24g, 96mmol, 1.2eq.) in H_2O (25ml) was prepared and immediately added to the TsCl suspension. The reaction mixture was stirred for 1h at RT. After that, H_2O (250ml) was added and the mixture stirred for another 1 h. The crude was transferred to a separation–funnel and extracted with DCM (4x200ml). The combined organic phase was finally washed with brine and dried over Na_2SO_4. The solution was filtered and the solvent removed by aid of a rotary evaporator to obtain a colorless oil. Eventual traces of DCM were removed by stripping with argon flow. Tosyl–azide was obtained in 94% yield

(14.85g, 75.3mmol). Spectroscopic data are consistent with previously characterized products in the literature.[50]

^{1}H NMR (300MHz, $CDCl_3$): δ 7.84 (pd, J = 8.5Hz, 2H, CH), 7.41 (pd, J = 8.5Hz, 2H, CH), 2.48 (s, 3H, CH_3) ppm.

Preparation of Dmp–N_3

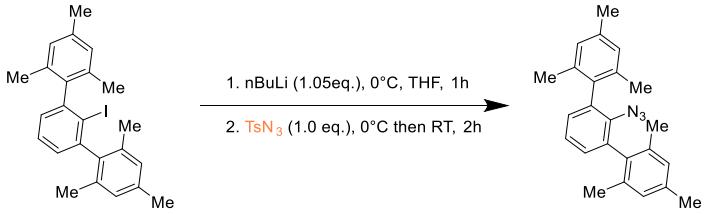

In an inert atmosphere of argon, Dmp–I (2.22g, 5.0mmol, 1.0eq.) was suspended in Et_2O (100ml). The flask was cooled in an ice–bath and ^{n}BuLi (1.6M, 3.3ml, 5.28mmol, 1.05eq.) was added dropwise at 0 °C over a period of 30 minutes with stirring which results in a golden solution. After stirring for one hour at this temperature, p–toluenesulfonylazide (0.77ml, 5.0mmol, 1.0eq.) was added dropwise at 0 °C. The bath was removed, and the resulting yellowish solution was stirred at RT for 2h. An aqueous solution of sodium hydroxide NaOH (0.05M, 50mL) was then added, and the yellowish organic layer was separated and washed again with $NaOH_{(aq)}$ (0.05M, 50mL). The combined aqueous phase was counter–extracted with diethylether (3x100ml). The obtained Et_2O solution was then dried over Na_2SO_4, filtered, and volatiles were removed in vacuo to yield a yellowish crystalline solid. Recrystallization in a minimum quantity of Et2O provided the desired compound as a colorless, crystalline solid in 90% yield (1.61g, 4.5mmol). Spectroscopic data are consistent with the one previously reported.[48]

^{1}H NMR (300MHz, DCM–d_2): δ 7.35–7.28 (m, $^3J_{ortho}$ = 7.6Hz, 1H, CH_{para}), 7.09 (d, $^3J_{ortho}$ = 7.6Hz, 2H, CH_{meta}), 7.02–6.96 (m, 4H, Mes, CH_{meta}), 2.33 (s, 6H, Mes, $^{para}CH_3$), 1.98 (s, 12H, Mes, $^{ortho}CH_3$) ppm;

Preparation of Dmp–NH_2

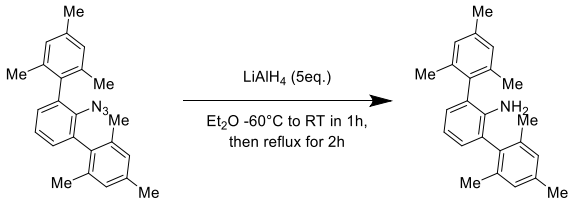

Inside a glovebox, $LiAlH_4$ (380mg, 10mmol) was loaded in a 100ml Schlenk–flask and suspended in Et_2O (40ml). Out of the glovebox, a solution of Dmp–N_3 (718mg, 2.0mmol) in Et_2O (20ml) was

separately prepared, loaded in a syringe and added dropwise to the $LiAlH_4$ suspension the at –60 °C. The resulting yellowish mixture was allowed to slowly warm–up to ambient temperature and heated to reflux for further 2h. The mixture was quenched with $NaOH_{(aq)}$ (0.01 M, 20mL) at 0°C. The organic layer was separated and again extracted with an aqueous solution of sodium hydroxide NaOH (0.01 M, 50mL). The two aqueous layer were collected and back–extracted with Et_2O (3x100ml). The combined organic fractions were dried over Na2SO4, filtrated and the solvent removed in vacuo to yield a yellowish solid. Recrystallisation from n–pentane allowed to obtain the desired product as a white crystalline solid in 84% yield (562mg, 1.7mmol). Spectroscopic data are consistent with the one previously reported.[48]

^{1}H NMR (300MHz, $CDCl_3$): δ 7.00 (s, 4H, Mes, CH_{meta}), 6.97–6.85 (m, 1H, CH_{meta} and CH_{para}), 3.17 (brs, 2H, NH_2), 2.36 (s, 6H, Mes, $^{para}CH_3$), 2.09 (s, 12H, Mes, $^{ortho}CH_3$) ppm;

Synthesis of ^{15}N–labeled mesityl isocyanate (Mes–^{15}NCO)

^{15}N–labeled mesityl–amine was synthesized according to a modified literature procedure:[52]

Mesityl–boronic acid (164.5mg, 1.0mmol, 1.0eq.) and methanol (2ml), $^{15}NH_{3(aq)}$ (6M, 0.42ml, 2.52mmol, 2.5eq.) and Cu_2O (0.1mmol, 14.7mg, 0.1eq.) were sequentially added to a round–bottom flask. The flask was not sealed, and the mixture was allowed to stir at 25°C for 24h. The mixture was then filtered and volatiles were removed in vacuo. The obtained residue was purified by column chromatography on silica gel (EtOAc/PE 1:20) to provide the desired product as a dark–brown oil in 57% yield (78.0mg, 0.57mmol).

The synthesis of the labeled Mes–^{15}NCO was performed following the ***general procedure for the synthesis of isocyanates*** previously described:

The ^{15}N–labeled mesityl–amine (0.2mmol, 1.0eq.) and DIPEA (1.4ml, 0.4mmol, 2.0eq.) where added to a Schlenk flask and dissolved in DCM (5ml). In a separate vessel, BTC (600mg, 0.1mmol, 0.5eq.) was dissolved in DCM (5ml) under an atmosphere of argon. The flask was cooled with an ice–bath and the amine/DIPEA solution was slowly added at that temperature. The resulting mixture was stirred for 10 minutes, before the ice–bath was removed. The reaction was gently taken to reflux and stirred for 4h (reaction monitoring by TLC). After this time, the crude was allowed to cool to RT and directly filtered through silica. The filtering pad was rinsed with DCM (ca. 10ml) until no more compound could be extracted. The obtained solution was evaporated until all volatiles were removed, taken up in PE (5ml) and filtered again through silica. The pad was then rinsed with PE (ca.

15ml). The desired compound was isolated as a colorless crystalline solid in 82% yield (27.5mg, 0.17mmol). Mes–^{15}NCO was immediately transferred in a glovebox and stored at low temperatures (–20°C).

N.1 – 2,4,6–trimethylphenyl–amine (^{15}N–labeled)

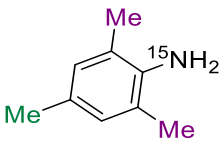

^{1}H NMR (600MHz, $CDCl_3$): δ 6.80–6.78 (m, CH_{meta}), 3.52 (brs, 2H, NH_2), 2.23 (s, 3H, $^{para}CH_3$), 2.18 (s, 6H, $^{ortho}CH_3$) ppm; **^{13}C{^{1}H} NMR (150.9MHz, $CDCl_3$): δ** 140.1 (d, $^{1}J_{CN}$ = 10.3Hz, 1C, C–NH_2), 129.0 (s, 2C, C_{meta}), 127.3 (s, 1C, C_{para}), 122.0 (d, $^{2}J_{CN}$ = 2.1Hz, 2C, C_{ortho}), 20.5 (s, 1C, $^{para}CH_3$), 17.7 (d, $^{3}J_{CN}$ = 1.1Hz, 2C, $^{ortho}CH_3$) ppm; **^{15}N NMR (60.8MHz, $CDCl_3$): δ** 48.5 ppm.

Complete assignments were made based on COSY, HSQC and HMBC analyses. The ^{13}C{^{1}H, ^{15}N} NMR spectrum is in line with previously reported data for the non–labeled 2,4,6–trimethylphenyl–amine.[52]

^{13}C{^{1}H, ^{15}N} NMR (150.9MHz, DCM–d_2): δ 140.1 (s, 1C, C–NH_2), 129.0 (s, 2C, C_{meta}), 127.3 (s, 1C, C_{para}), 122.0 (s, 2C, C_{ortho}), 20.5 (s, 1C, $^{para}CH_3$), 17.7 (s, 2C, $^{ortho}CH_3$) ppm.

N.2 – 2,4,6–trimethylphenyl–isocyanate (^{15}N–labeled)

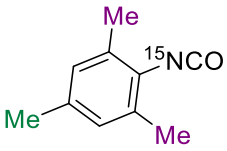

^{1}H NMR (600MHz, DCM–d_2): δ 6.86 (s, CH_{meta}), 2.28 (s, 6H, $^{ortho}CH_3$), 2.24 (s, 3H, $^{para}CH_3$) ppm; **^{13}C{^{1}H} NMR (150.9MHz, DCM–d_2): δ** 135.6 (s, 1C, C_{para}), 133.1 (d, $^{2}J_{CN}$ = 2.5Hz, 2C, C_{ortho}), 129.1 (d, $^{3}J_{CN}$ = 2.1Hz, 2C, C_{meta}), 128.9 (d, $^{1}J_{CN}$ = 18.9Hz, 1C, C–N), 124.7 (d, $^{1}J_{CN}$ = 52.5Hz, 1C, N=C=O), 20.9 (s, 1C, $^{para}CH_3$), 18.8 (d, $^{3}J_{CN}$ = 1.4Hz, 2C, $^{ortho}CH_3$) ppm; **^{15}N NMR (60.8MHz, DCM–d_2): δ** 43.1 ppm.

Complete assignments were made based on COSY, HSQC and HMBC analyses. The ^{13}C{^{1}H, ^{15}N} NMR spectrum agrees with the one obtained from the non–labeled Mes–NCO.[46]

^{13}C{^{1}H, ^{15}N} NMR (150.9MHz, DCM–d_2): δ 135.6 (s, 1C, C_{para}), 133.1 (s, 2C, C_{ortho}), 129.1 (s, 2C, C_{meta}), 128.9 (s, 1C, C_{ipso}), 124.7 (s, 1C, N=C=O), 20.9 (s, 1C, $^{para}CH_3$), 18.8 (s, 2C, $^{ortho}CH_3$) ppm.

General procedure for the preparation of [IPrAu(isocyanate)]SbF_6 adducts

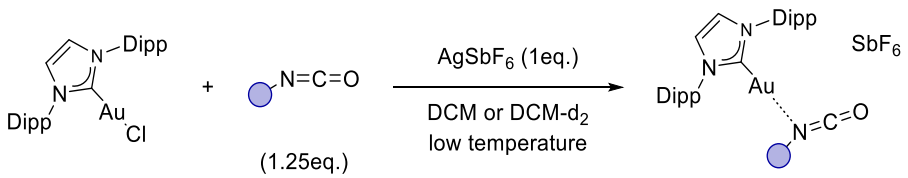

Inside a glovebox, a screw–cap NMR tube was loaded with $AgSbF_6$ (10.3mg, 0.03mmol, 1eq.) and 0.2ml of DCM–d_2. In separate vial, a solution of IPrAuCl (18.6mg, 0.03mmol, 1eq.) and the isocyanate (0.038mmol, 1.25eq.) in DCM–d_2 (0.5ml) was prepared, loaded in a syringe and the needle capped with a septum. Out of the glovebox, the NMR tube was cooled at low temperatures (–80°C to –30°C) and the solution was slowly added along the walls to ensure the liquid could properly cool down before reaching the second reagent. After 2 minutes from the addition, the tube was taken and gently shaken while keeping the low temperature. Immediate formation of AgCl was observed, while the solution remained colorless. The tube was directly inserted inside a NMR machine at variable temperature.

Comments to the procedure:

- Decomposition with formation of colloidal gold is recorded overtime at different extents depending on the relative stability of the adduct and the temperature;
- Exposure of the adduct to moisture or using regular solvents leads to the formation of the corresponding [IPrAu–aniline]SbF_6 complex, via hydration and decarboxylation of the isocyanate moiety;
- In some cases (Mes–NCO, Bn–NCO) the mixture can be moved inside a glovebox and manipulated at RT for short periods of time;
- The IPrAu(Mes–NCO) adduct can be prepared directly in the glovebox at RT using DCM or DCM–d_2 as solvent and filtered through a PTFE syringe–filter to remove AgCl. Nevertheless, the mixture must be stored at low temperature (–20°C) to avoid decomposition;

C.1 – [IPrAu(Mes–NCO)]SbF_6

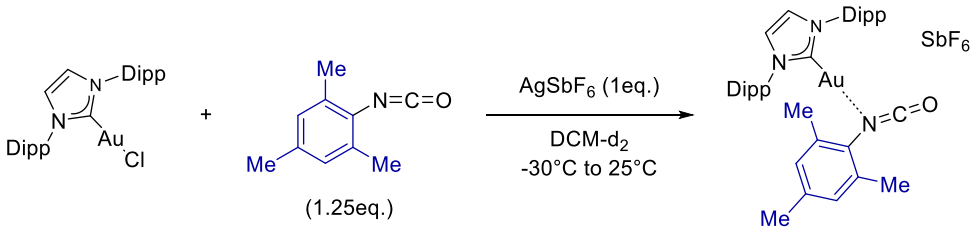

^{1}H NMR (600MHz, DCM–d_2): δ 7.64 (t, $^{3}J_{ortho}$ = 7.8Hz, 2H, Dipp, CH_{para}), 7.38 (d, $^{3}J_{ortho}$ = 7.8Hz, 4H, Dipp, CH_{meta}), 7.37 (s, 2H, CH_{indole}), 6.60 (brs, 2H, Mes, CH_{meta}), 2.29 (hept, ^{3}J = 6.8Hz, 4H, iPr, CH), 2.09 (brs, 6H, Mes, $^{ortho}CH_3$), 1.96 (brs, 3H, Mes, $^{para}CH_3$), 1.23 (d, ^{3}J = 6.8Hz, 12H, iPr, CH_3), 1.20 (d, ^{3}J = 6.8Hz, 12H, iPr, CH_3) ppm; **^{13}C{^{1}H} NMR (150.9MHz, DCM–d_2): δ** 169.4 (s, 1C, C–Au), 146.1 (s, 4C, Dipp, C_{ortho}–iPr), 140.0 (s, 2C, Mes, C_{ortho}), 135.4 (s, 1C, Mes, C_{para}), 133.5 (s, 2C, Dipp, C_{ipso}–N), 132.6 (brs, 1C, Mes, C_{ipso}–N), 131.8 (s, 2C, Dipp, C_{para}), 125.6 (brs, 1C, N=C=O), 124.8 (s, 6C, $^{Dipp}C_{meta}$ and $CH_{imidazol}$), 116.4 (s, 2C, Mes, C_{meta}), 29.1 (s, 4C, iPr, CH), 24.7 (s, 4C, iPr, CH_3), 24.1 (s, 4C, iPr, CH_3), 21.7 (brs, 1C, Mes, $^{para}CH_3$), 19.5 (brs, 2C, Mes, $^{ortho}CH_3$) ppm.

Complete assignments were made based on COSY, HSQC and HMBC analyses. The ^{13}C signal of the N=C=O carbon atom was identified by comparison with J–mod and DEPT–135 experiments. No information regarding the nitrogen atom could be collected by 2D ^{1}H–^{15}N experiments. NOESY and DOSY analyses are consistent with coordination of mesityl–isocyanate to the $IPrAu^{+}$ fragment.

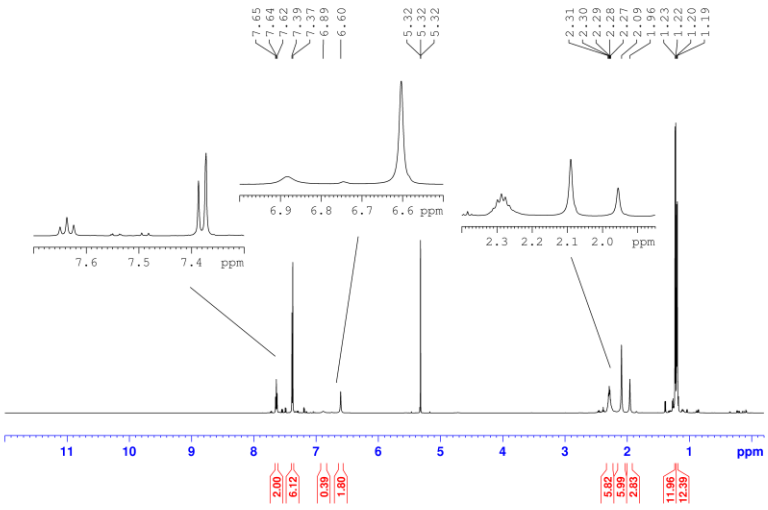

Figure 4.31– *^{1}H NMR (600MHz, DCM–d_2) spectrum of [IPrAu(Mes–NCO)]SbF_6.*

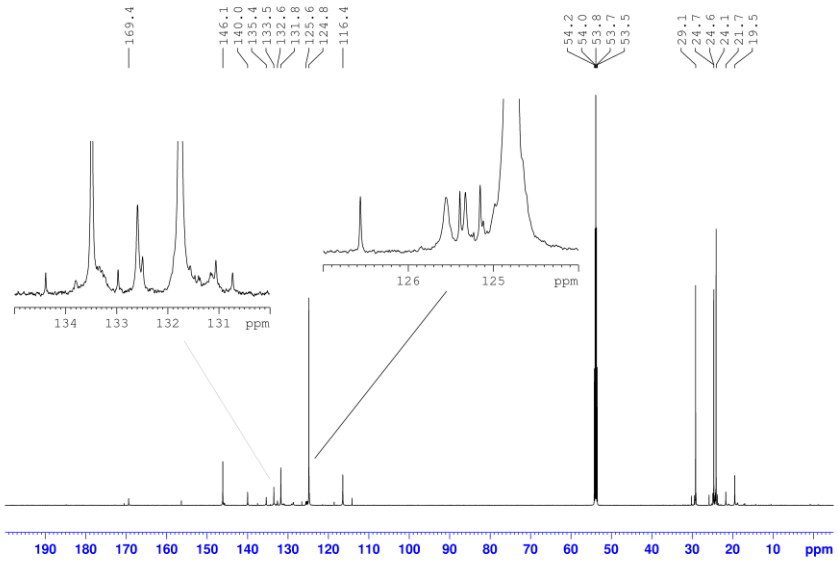

Figure 4.32 *– $^{13}C\{^{1}H\}$ NMR (600MHz, DCM–d_2) spectrum of [IPrAu(Mes–NCO)]SbF_6.*

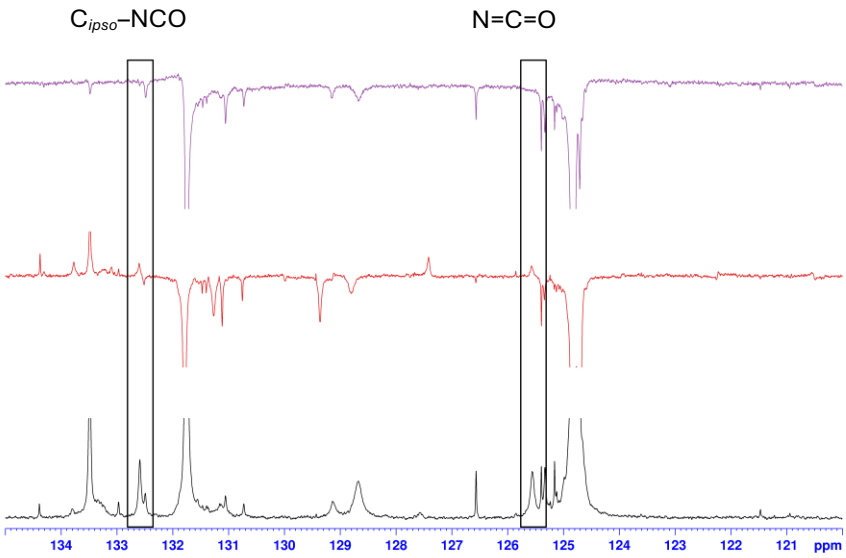

Figure 4.33 *– Stacked $^{13}C\{^{1}H\}$, J–mod and DEPT–135 spectra (600MHz, DCM–d_2), zoom on the heteoallene carbon region.*

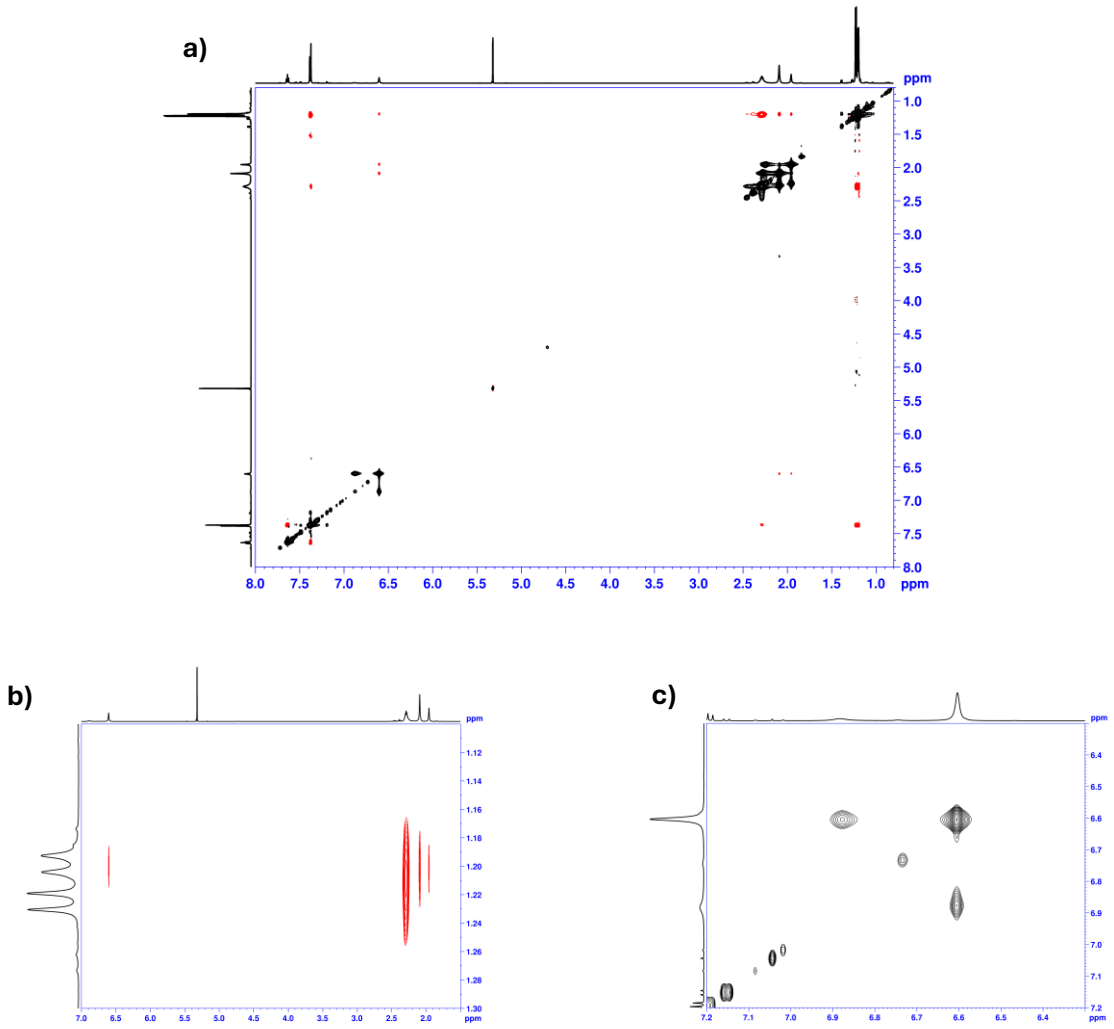

Figure 4.34 *– **a)** NOESY (600MHz, DCM–d_2) spectrum of [IPrAu(Mes–NCO)]SbF_6; **b)** zoom on the cross–peaks between the mesityl moiety and the iPr group at the NHC ligand; **c)** evidence for exchange between coordinated and non–coordinated Mes–NCO.*

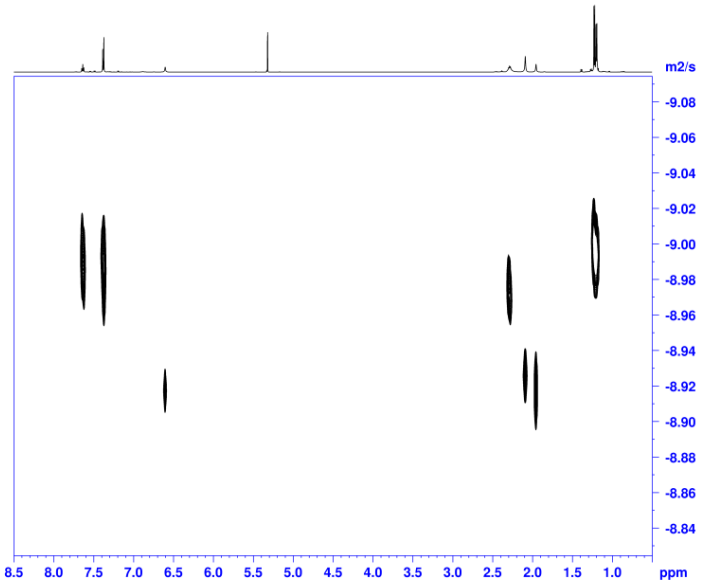

Figure 4.35 *– DOSY (600MHz, DCM–d_2) spectrum of [IPrAu(Mes–NCO)]SbF_6.*

Diffusion coefficient values are obtained by exponential fit of the datasets collected from the following peaks intensities (fitted at 95% of confidence level). The error is reported as maximum semi–dispersion of the obtained values.

- **δ_H (IPrAu$^+$):** 7.65, 7.64, 7.62 (t, Dipp, CH_{para}), 7.39, 7.37 (d, Dipp, CH_{meta}), 1.23, 1.22 (d, iPr, CH_3), 1.20, 1.19 (d, iPr, CH_3) ppm → $D_{Au–complex} = (9.8 \pm 0.3) \cdot 10^{-10}\ m^2/s$
- **δ_H (Mes–NCO, coord.):** 6.60 (brs, Mes, CH_{meta}), 2.09 (brs, Mes, $^{ortho}CH_3$), 1.96 (brs, Mes, $^{ortho}CH_3$) ppm → $D_{Mes–NCO,\ coord} = (1.17 \pm 0.02) \cdot 10^{-9}\ m^2/s$

The diffusion coefficient of Mes–NCO was separately determined by DOSY analysis of the pure compound in DCM–d_2:

δ_H (Mes–NCO, coord.): 6.86 (s, 2H, C_{Ar}–H), 2.28 (s, 6H, $^{meta}CH_3$), 2.25 (s, 3H, $^{para}CH_3$) ppm → $D_{Mes–NCO,\ free} = (2.20 \pm 0.11) \cdot 10^{-9}\ m^2/s$

C.2 – [IPrAu(Mes–^{15}NCO)]SbF_6

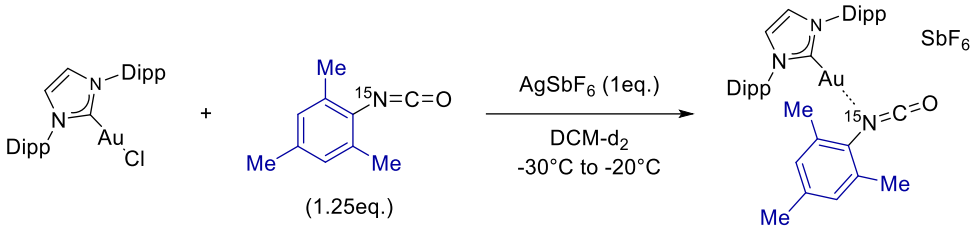

^{1}H NMR (600MHz, DCM–d_2, 253K): δ 7.62 (t, $^3J_{ortho}$ = 7.8Hz, 2H, Dipp, CH_{para}), 7.37 (s, 2H, CH_{indole}), 7.36 (d, $^3J_{ortho}$ = 7.8Hz, 4H, Dipp, CH_{meta}), 6.58 (s, 2H, Mes, CH_{meta}), 2.22 (hept, ^3J = 6.8Hz, 4H, iPr, CH), 2.05 (s, 6H, Mes, $^{ortho}CH_3$), 1.92 (s, 3H, Mes, $^{para}CH_3$), 1.20 (d, ^3J = 6.8Hz, 12H, iPr, CH_3), 1.15 (d, ^3J = 6.8Hz, 12H, iPr, CH_3) ppm; **^{13}C{^{1}H} NMR (150.9MHz, DCM–d_2, 253K): δ** 168.7 (s, 1C, C–Au), 145.7 (s, 4C, Dipp, C_{ortho}–iPr), 139.8 (s, $^2J_{CN}$ = 2.8Hz, 2C, Mes, C_{ortho}), 135.0 (s, 1C, Mes, C_{para}), 133.0 (s, 2C, Dipp, C_{ipso}–N), 132.0 (d, $^1J_{CN}$ = 20.0Hz, 1C, Mes, C_{ipso}–N), 131.3 (s, 2C, Dipp, C_{para}), 125.2 (d, $^1J_{CN}$ = 50.9Hz, 1C, N=C=O), 124.4 (s, 4C, Dipp, C_{meta}), 124.3 (s, 2C, $CH_{imidazol}$) 115.8 (d, $^3J_{CN}$ = 1.9Hz, 2C, Mes, C_{meta}), 28.7 (s, 4C, iPr, CH), 24.5 (s, 4C, iPr, CH_3), 23.7 (s, 4C, iPr, CH_3), 21.4 (s, 1C, Mes, $^{para}CH_3$), 19.3 (d, $^3J_{CN}$ = 1.4Hz, 2C, Mes, $^{ortho}CH_3$) ppm; **^{15}N NMR (60.8MHz, DCM–d_2, 253K): δ** 45.2 ppm.

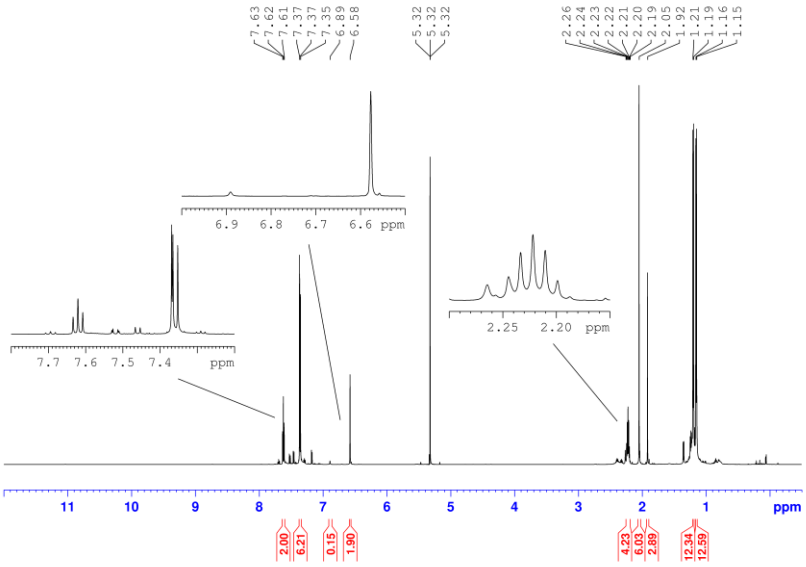

***Figure 4.36** – ^{1}H NMR (600MHz, DCM–d_2, 253K) spectrum of [IPerAu(Mes–^{15}NCO)]SbF_6.*

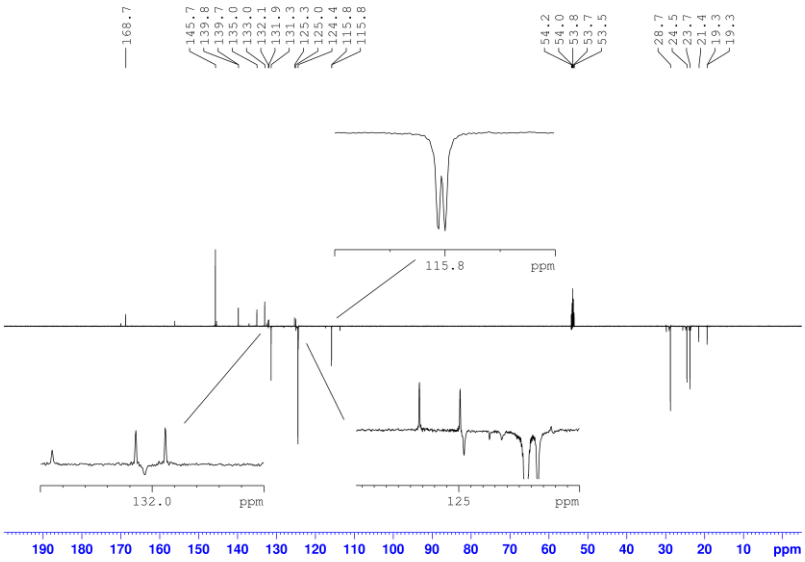

Figure 4.37 *– J–mod (600MHz, DCM–d_2, 253K) spectrum of [IPrAu(Mes–NCO)]SbF_6.*

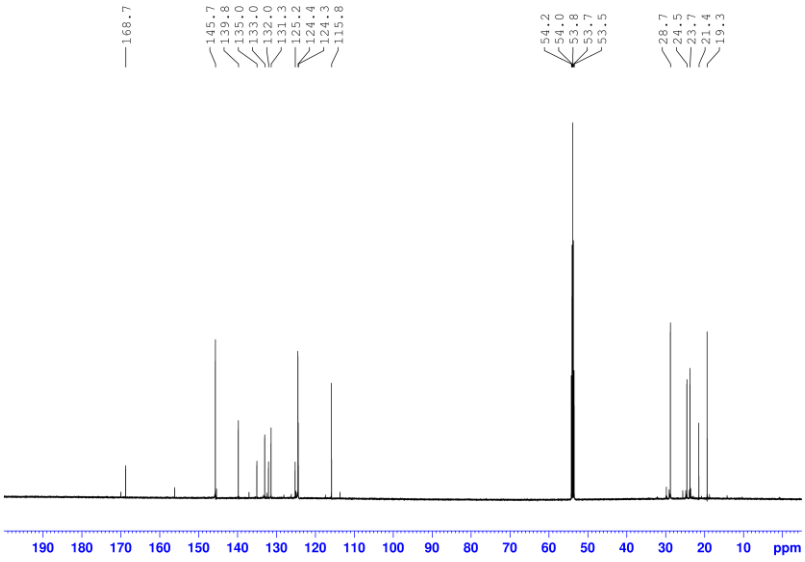

Figure 4.38 *– $^{13}C\{^1H,^{15}N\}$ NMR (600MHz, DCM–d_2, 253K) spectrum of [IPrAu(Mes–^{15}NCO)]SbF_6.*

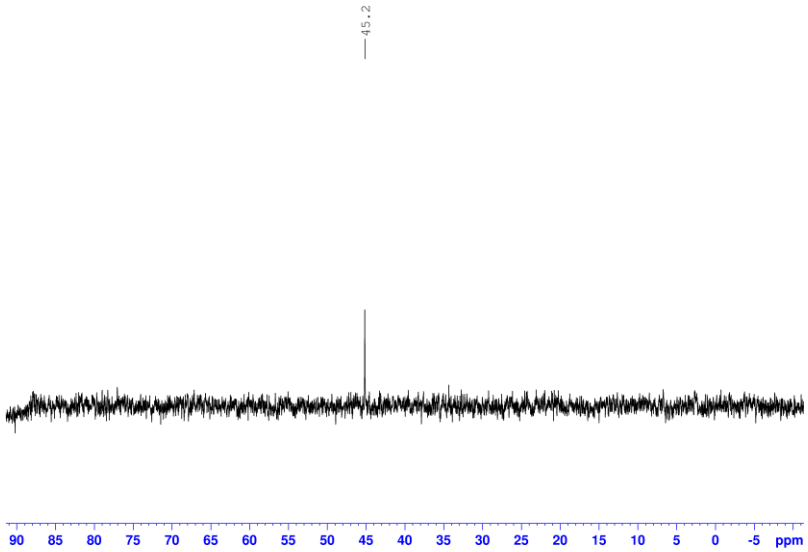

Figure 4.39 *– ^{15}N NMR (600MHz, DCM–d_2, 253K) spectrum of [IPrAu(Mes–^{15}NCO)]SbF_6.*

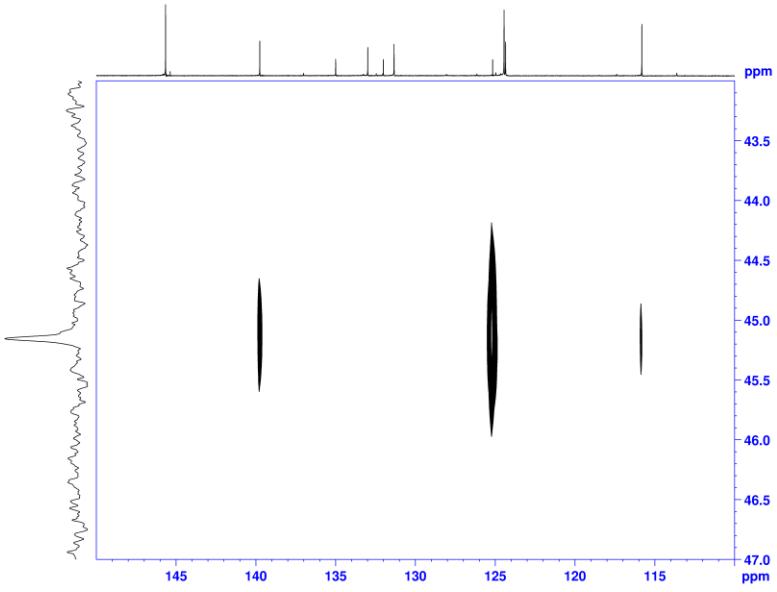

Figure 4.40 *– ^{13}C–^{15}N HMBC (600MHz, DCM–d_2, 253K) spectrum of [IPrAu(Mes–^{15}NCO)]SbF_6 (J_{CN}=10Hz).*

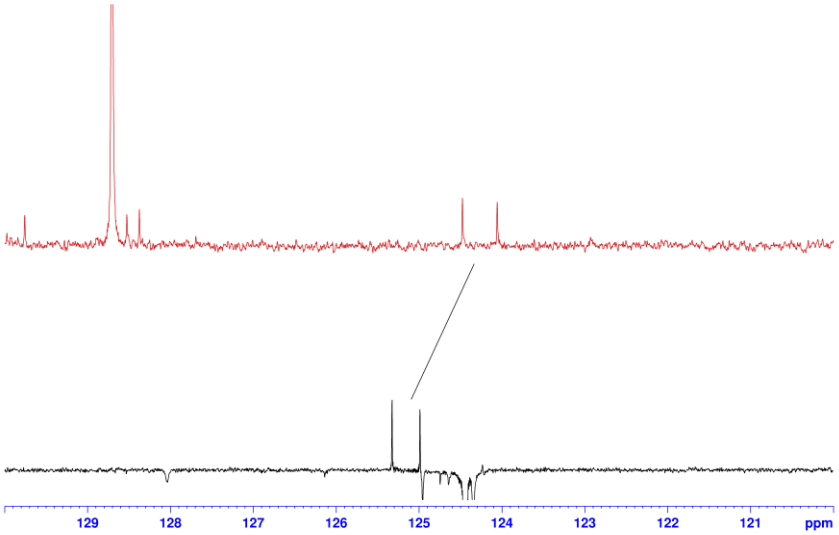

Figure 4.41 *– Staked $^{13}C\{^{1}H\}$ NMR spectra of [IPrAu(Mes–^{15}NCO)]SbF_6 (600MHz, DCM–d_2, 253K) and Mes–^{15}NCO (500MHz, DCM–d_2, 253K); zoom over the N=C=O carbon atom.*

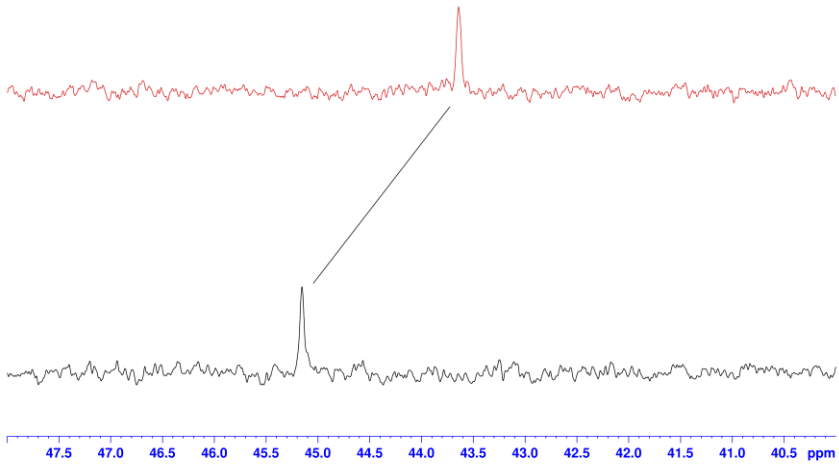

Figure 4.42 *– Staked ^{15}N NMR spectra of [IPrAu(Mes–^{15}NCO)]SbF_6 (600MHz, DCM–d_2, 253K) and Mes–^{15}NCO (500MHz, DCM–d_2, 253K).*

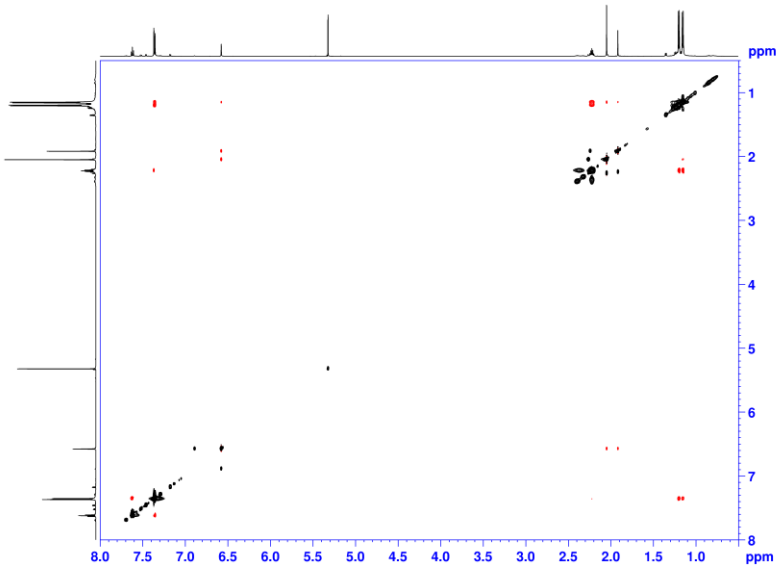

Figure 4.43 *– NOESY (600MHz, DCM–d_2, 253K) spectrum of [IPrAu(Mes–NCO)]SbF_6.*

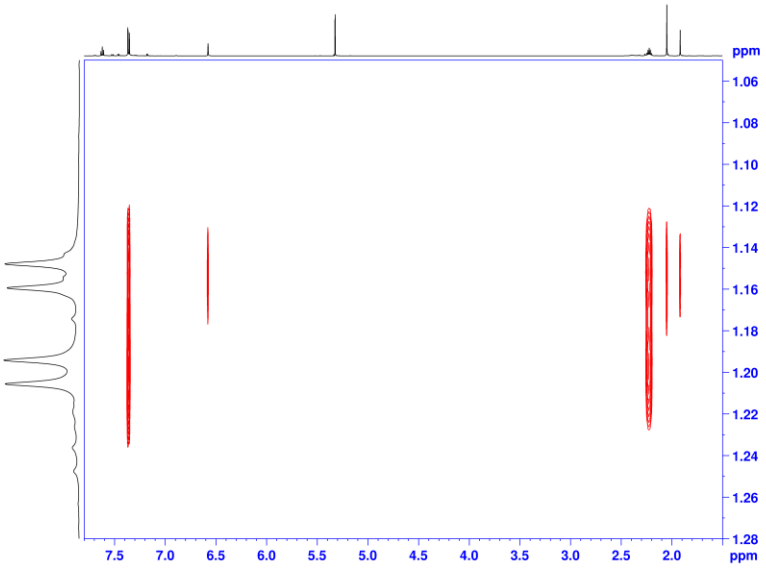

Figure 4.44 *– NOESY (600MHz, DCM–d_2, 253K) spectrum of [IPrAu(Mes–NCO)]SbF_6; zoom on the cross–peaks between the mesityl moiety and the iPr group at the NHC ligand.*

C.3 – [IPrAu(Ph–NCO)]SbF_6

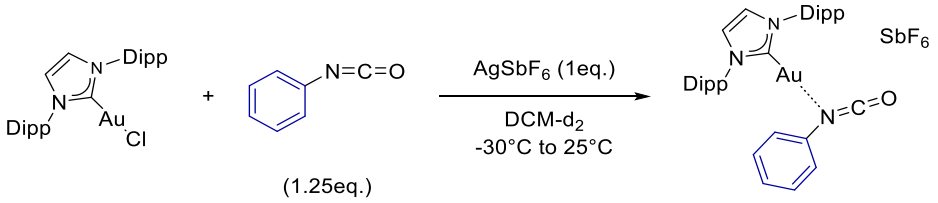

Only partial coordination of Ph–NCO was detected. Fast decomposition was also recorded, with formation of the homoleptic $[(IPr)_2Au]SbF_6$ complex. This species was also found in the case of [IPrAu(Mes–NCO)][SbF_6] but in minor quantities.

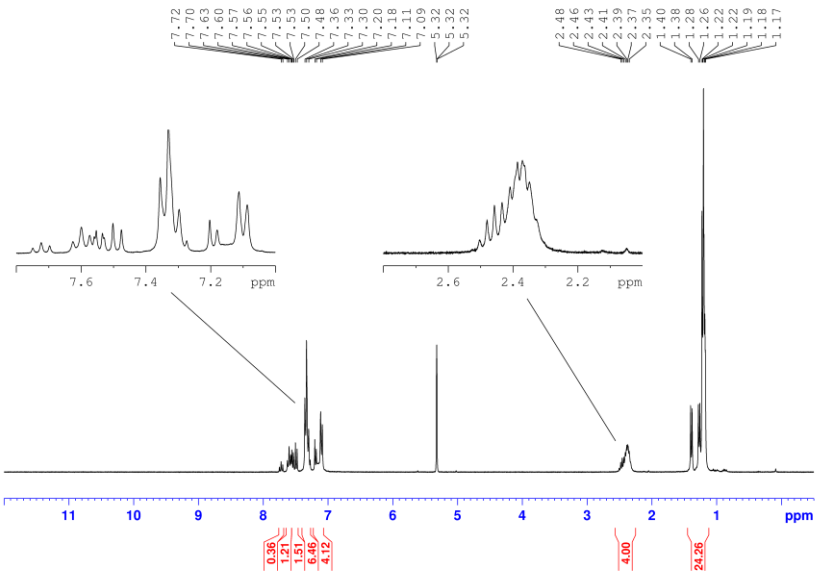

Figure 4.45 *– ^1H NMR (300MHz, DCM-d_2) spectrum of the reaction mixture.*

The species $[(IPr)_2Au]SbF_6$ is forming from the cationic complex $IPrAuSbF_6$, consistently with the reduction of part of the complex to Au^0. This last species, $IPrAuSbF_6$ was formed and revealed unstable at 25°C in DCM–d_2.

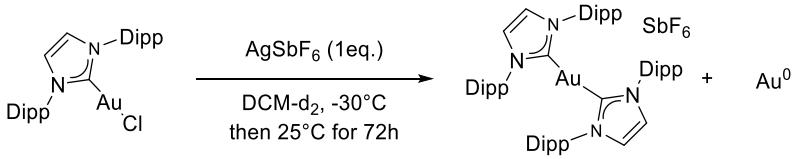

For the control test, the same procedure for the synthesis of [IPrAu(Ph–NCO)]SbF_6 was followed, but

in absence of phenylisocyanate. The reaction was monitored by ^{1}H NMR spectroscopy at different times. After 72h, the crude was filtered through celite, the solution was concentrated and cold pentane added. The obtained white solid was filtered from the supernatant, washed with pentane (2x5ml) and dried under vacuum. The characterization data are in agreement with the ones previously reported for the $[(IPr)_2Au]^+$ fragment.

^{1}H NMR (300MHz, DCM–d_2): δ 7.48 (t, J = 7.8Hz, 4H, Dipp, CH_{para}), 7.14 (d, J = 7.8Hz, 8H, Dipp, CH_{meta}), 7.04 (s, 4H, $CH_{imidazol}$), 2.27 (hept, J = 6.9Hz, 8H, iPr, CH), 1.04 (d, J = 6.9Hz, 24H, iPr, CH_3), 0.85 (d, J = 6.9Hz, 24H, iPr, CH_3) ppm; **^{13}C{^{1}H} NMR (75.5MHz, DCM–d_2): δ** 184.9 (s, 2C), 145.5 (s, 8C), 134.3 (s, 4C), 131.2 (s, 4C), 125.4 (s, 4C), 124.8 (s, 8C), 29.0 (s, 8C), 24.5 (s, 8C), 24.2 (s, 8C) ppm.

The spectrum of $IPrAuSbF_6$ is of difficult interpretation. Signals belonging to two different species are present after activation of the corresponding chlorido complex. This pattern of signals is as well found in the coordination attempt with Ph–NCO, confirming that only part of the cationize complex is effectively coordinated by the isocyanate.

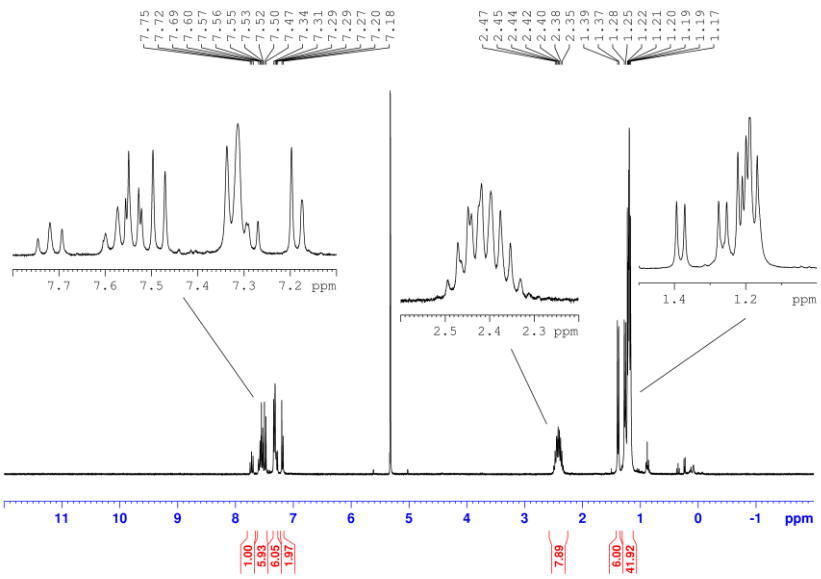

Figure 4.46 - *^{1}H NMR spectrum of IPrAuCl in presence of 1 equivalent of $AgSbF_6$.*

C.4 – [IPrAu(Bn–NCO)]SbF_6

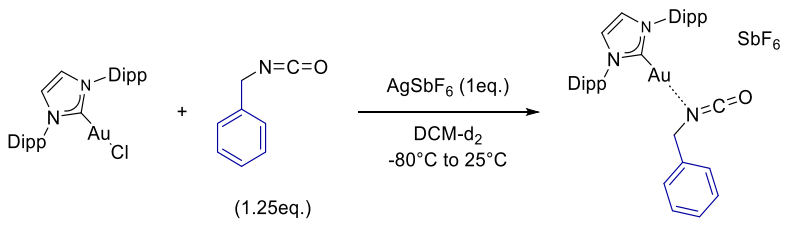

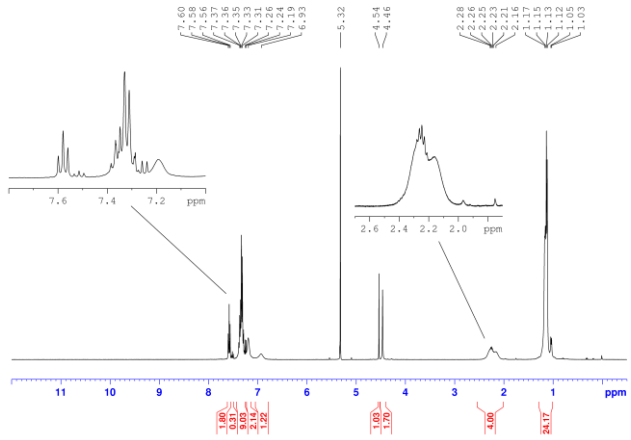

Figure 4.47 *– ^{1}H NMR (400MHz, DCM-d_2, -80C°) spectrum of the adduct with Bn-NCO.*

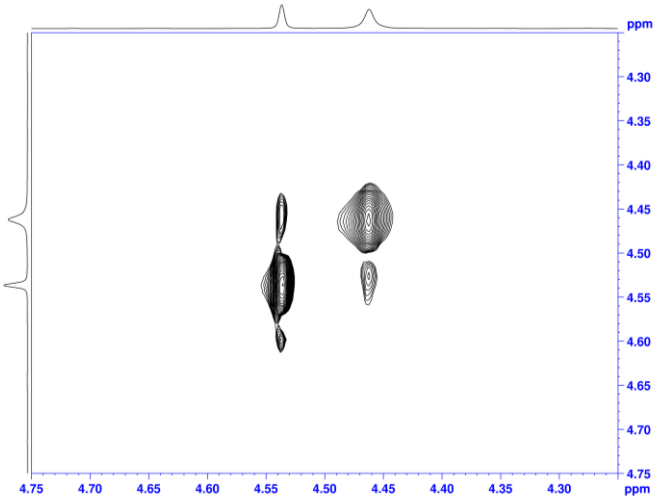

Figure 4.48 *– NOESY (400MHz, DCM-d_2, -80C°) spectrum of the adduct with Bn-NCO, zoom on the CH_2 groups.*

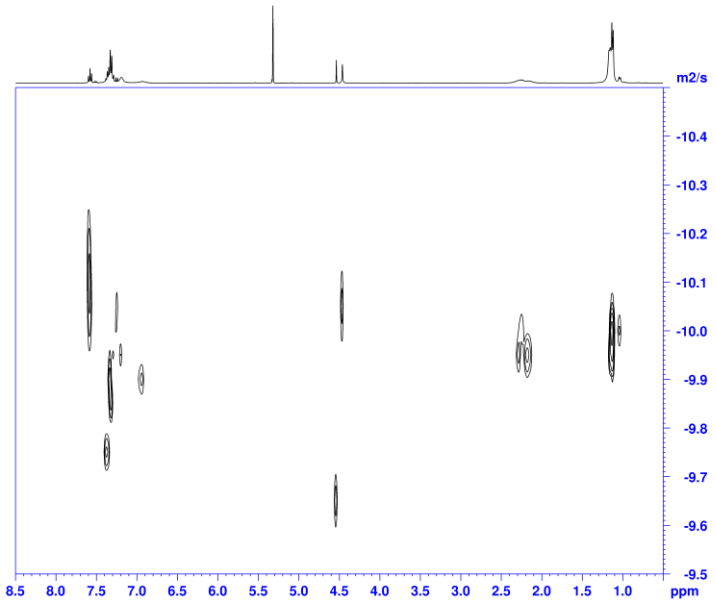

Figure 4.49 *– DOSY (400MHz, DCM-d_2, -80C°) spectrum of the adduct with Bn-NCO*

Diffusion coefficient values are obtained by exponential fit of the datasets collected from the following peaks intensities (fitted at 95% of confidence level). The error is reported as mean value of the given uncertanty over each measurement.

- **δ_H (IPrAu$^+$):** 7.60, 7.68, 7.56 (t, Dipp, 2H, CH_{para}), 2.26, 2.25 (m, iPr, CH), 1.13, 1.12 (m, iPr, CH_3) ppm → $D_{Au-complex} = (7.8 \pm 0.8) \cdot 10^{-11}\ m^2/s$

- **δ_H (Bn–NCO, coord.):** 4.46 (brs, 2H, Bn, CH_2) ppm → $D_{Mes-NCO,\ coord} = (7.5 \pm 1.3) \cdot 10^{-11}\ m^2/s$

- **δ_H (Bn–NCO, free):** 4.53 (s, 2H, Bn, CH_2) ppm → $D_{Mes-NCO,\ free} = (2.02 \pm 0.25) \cdot 10^{-10}\ m^2/s$

C.5 – [IPrAu(Cy–NCO)]SbF_6

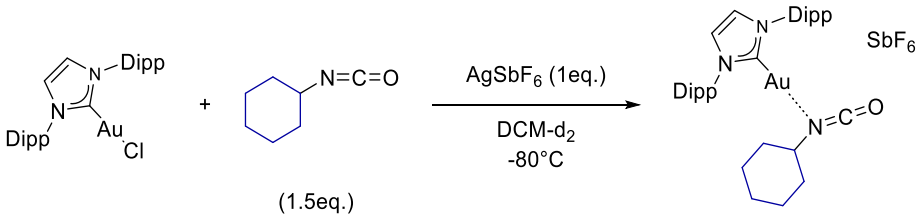

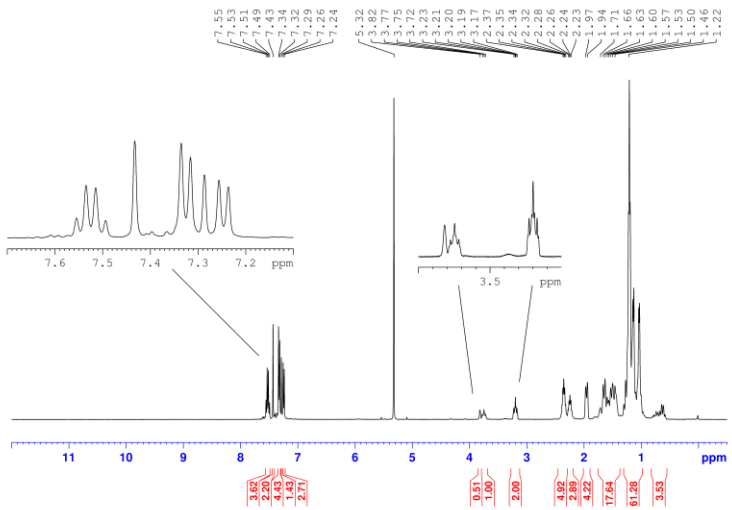

Figure 4.50 *– ^{1}H NMR (400MHz, DCM-d_2, -80C°) spectrum of the adduct with Cy-NCO.*

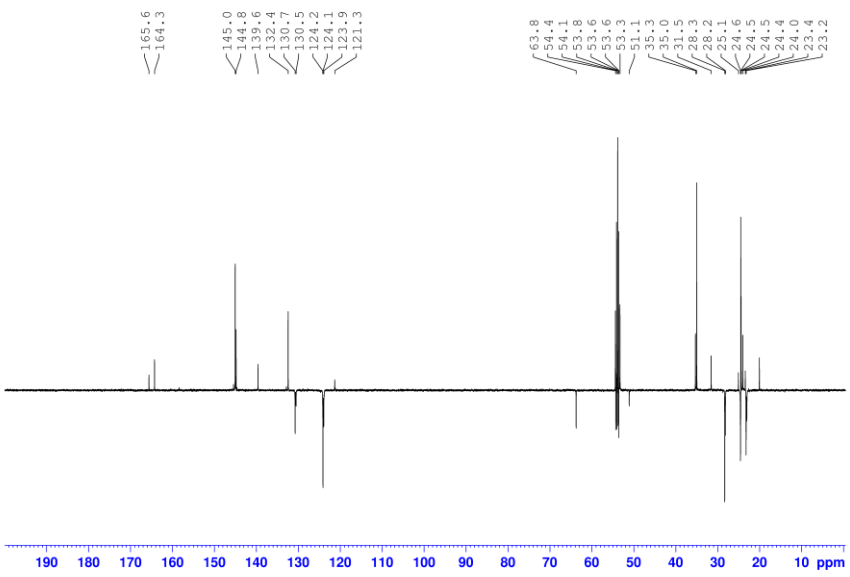

Figure 4.51 *– $^{13}C\{^{1}H\}$ NMR (400MHz, DCM-d_2, -80C°) spectrum of the adduct with Cy-NCO.*

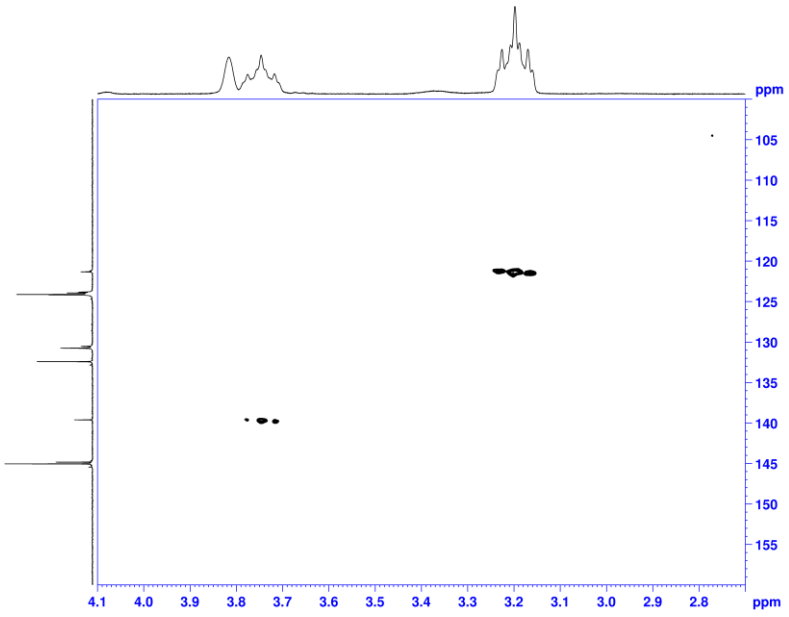

Figure 4.52 *– ^{1}H-^{13}C HMBC (400MHz, DCM-d_2, -80C°) spectrum of the adduct with Cy-NCO.*

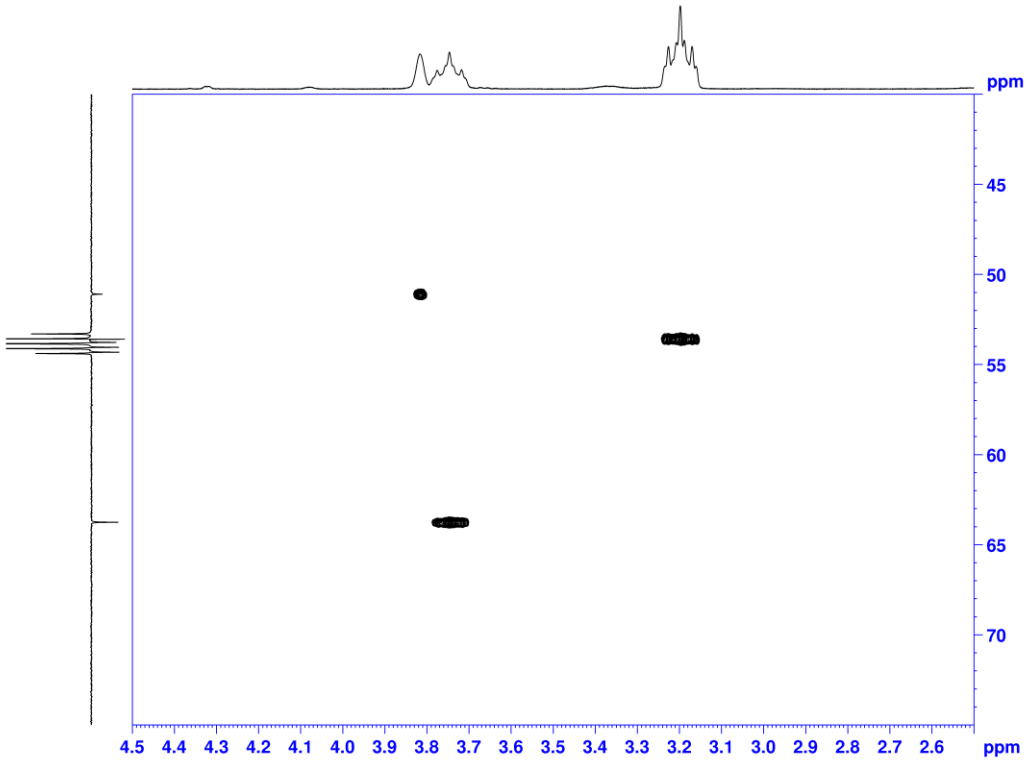

Figure 4.53 *– ^{1}H-^{13}C HSQC (400MHz, DCM-d_2, -80C°) spectrum of the adduct with Cy-NCO.*

^{1}H and ^{13}C NMR data relative to Cy–NCO are reported for clarity:

^{1}H NMR (500MHz, DCM–d_2): δ 3.44 (tt, J = 9.,1, 3.7 Hz, 1H, CH), 1.93–1.85 (m, 2H, CH_2) 1.75–1.67 (m, 2H, CH_2), 1.55–1.42 (m, 3H, CH_2), 1.38–1.26 (m, 3H, CH_2) ppm; **$^{13}C\{^{1}H\}$ NMR (125.8MHz, DCM–d_2): δ** 122.8 (s, 1C, N=C=O), 53.9 (s, 1C, CH), 35.2 (s, 2C, CH_2), 25.6 (s, 1C, CH_2), 24.2 (s, 2C, CH_2) ppm.

Characterization of the IPrAu-(N-methylpyrrole) π-complex

Inside a glovebox, a screw–cap NMR tube was loaded with $AgSbF_6$ (10.3mg, 0.03mmol, 1eq.) and 0.2ml of DCM–d_2. In separate vial, a solution of IPrAuCl (18.6mg, 0.03mmol, 1eq.) and N-methylpyrrole (3.4µl, 0.038mmol, 1.25eq.) in DCM–d_2 (0.5ml) was prepared, loaded in a syringe and the needle capped with a septum. Out of the glovebox, the NMR tube was cooled at -30°C and the solution was slowly added along the walls to ensure the liquid could properly cool down before reaching the second reagent. After 2 minutes from the addition, the tube was taken and gently shaken while keeping the low temperature. Immediate formation of AgCl was observed. The tube was then moved inside a NMR machine at 25°C for routine characterizations.

^{1}H NMR (300MHz, $CDCl_3$): δ 7.60 (t, ^3J = 7.8 Hz, 2H, Dipp, CH_{para}), 7.36 (d, ^3J = 7.8 Hz, 2H, Dipp, CH_{meta}), 7.32 (s, 2H, vinyl, CH), 6.87 (pt, J = 1.7Hz, 2H, N-CH_{pyrr}), 5.91 (pt, J = 1.7Hz, 2H, CH_{pyrr}), 3.39 (s, 3H, $CH_{3,pyrr}$), 2.37 (hept, ^3J = 6.9Hz, 4H, iPr, CH), 1.23 (d, ^3J = 6.9Hz, 6H, iPr, CH_3), 1.22 (d, ^3J = 6.9Hz, 6H, iPr, CH_3) ppm; **^{13}C{^{1}H} NMR (300MHz, $CDCl_3$): δ** 175.5 (s, 1C, C-Au), 146.1 (s, 4C, Dipp, C_{ortho}), 133.7 (s, 2C, Dipp, C_{ipso}), 131.4 (s, 2C, Dipp, CH_{para}), 128.9 (s, 2C, N-CH_{pyrr}), 124.7 (s, 4C, Dipp, CH_{meta}), 124.5 (s, 2C, IPr, $CH_{imidazol}$), 98.1 (s, 2C, CH_{pyrr}), 37.1 (s, 1C, $CH_{3,pyrr}$), 29.1 (s, 4C, iPr, CH), 24.8 (s, 4C, iPr, CH_3), 24.0 (s, 4C, iPr, CH_3) ppm.

4.8 References

[1] C. Lamberth, "Organic Isocyanates and Isothiocyanates: Versatile Intermediates in Agrochemistry" *Synthesis (Germany)* **2022**, *54*, 1250–1260.

[2] Z. Guo, X. Ding, Y. Wang, "How To Get Isocyanate?" *ACS Omega* **2024**, *9*, 11168–11180.

[3] A. K. Ghosh, A. Sarkar, M. Brindisi, "The Curtius rearrangement: mechanistic insight and recent applications in natural product syntheses" *Org. Biomol. Chem.* **2018**, *16*, 2006–2027.

[4] A. K. Ghosh, M. Brindisi, A. Sarkar, "The Curtius Rearrangement: Applications in Modern Drug Discovery and Medicinal Chemistry" *ChemMedChem* **2018**, *13*, 2351–2373.

[5] E. Delebecq, J.-P. Pascault, B. Boutevin, F. Ganachaud, "On the Versatility of Urethane/Urea Bonds: Reversibility, Blocked Isocyanate, and Non-isocyanate Polyurethane" *Chem. Rev.* **2013**, *113*, 80–118.

[6] A. Basu, S. Farah, K. R. Kunduru, S. Doppalapudi, W. Khan, A. J. Domb in *Advances in Polyurethane Biomaterials*, Elsevier, **2016**, pp. 217–246.

[7] P. Braunstein, D. Nobel, "Transition-metal-mediated reactions of organic isocyanates" *Chem. Rev.* **1989**, *89*, 1927–1945.

[8] a) J. Li, L. Ackermann, "Cobalt(III)-katalysierte C-H-Aminocarbonylierung von Arenen und Alkenen mit Isocyanaten und Acylaziden" *Angewandte Chemie* **2015**, *127*, 8671–8674. b) J. R. Hummel, J. A. Ellman, "Cobalt(III)-Catalyzed C–H Bond Amidation with Isocyanates" *Org. Lett.* **2015**, *17*, 2400–2403.

[9] K. D. Hesp, R. G. Bergman, J. A. Ellman, "Expedient Synthesis of *N* -Acyl Anthranilamides and β-Enamine Amides by the Rh(III)-Catalyzed Amidation of Aryl and Vinyl C–H Bonds with Isocyanates" *J. Am. Chem. Soc.* **2011**, *133*, 11430–11433.

[10] S. De Sarkar, L. Ackermann, "Ruthenium(II)-Catalyzed C□H Activation with Isocyanates: A Versatile Route to Phthalimides" *Chemistry A European J* **2014**, *20*, 13932–13936.

[11] J. Han, N. Wang, Z.-B. Huang, Y. Zhao, D.-Q. Shi, "Ruthenium-Catalyzed Carbonylation of Oxalyl Amide-Protected Benzylamines with Isocyanate as the Carbonyl Source" *J. Org. Chem.* **2017**, *82*, 6831–6839.

[12] S. Sueki, Y. Guo, M. Kanai, Y. Kuninobu, "Rhenium-Catalyzed Synthesis of 3-Imino-1-isoindolinones by C□H Bond Activation: Application to the Synthesis of Polyimide Derivatives" *Angew Chem Int Ed* **2013**, *52*, 11879–11883.

[13] W. Hou, B. Zhou, Y. Yang, H. Feng, Y. Li, "Rh(III)-Catalyzed Addition of Alkenyl C–H Bond to Isocyanates and Intramolecular Cyclization: Direct Synthesis 5-Ylidenepyrrol-2(5 *H*)-ones" *Org. Lett.* **2013**, *15*, 1814–1817.

[14] R. Zeng, P. Chen, G. Dong, "Efficient Benzimidazolidinone Synthesis via Rhodium-Catalyzed Double-Decarbonylative C–C Activation/Cycloaddition between Isatins and Isocyanates" *ACS Catal.* **2016**, *6*, 969–973.

[15] M. Rajesh, S. Puri, R. Kant, M. Sridhar Reddy, “Synthesis of Substituted Furan/Pyrrole-3-carboxamides through a Tandem Nucleopalladation and Isocyanate Insertion” *Org. Lett.* **2016**, *18*, 4332–4335.

[16] Y. Wu, B. Tian, S. Witzel, H. Jin, X. Tian, M. Rudolph, F. Rominger, A. S. K. Hashmi, “$AuBr_3$ -Catalyzed Chemoselective Annulation of Isocyanates with 2 *H* -Azirine” *Chemistry A European J* **2019**, *25*, 4093–4099.

[17] A. Dasgupta, M. G. Guerzoni, N. Alotaibi, Y. Van Ingen, K. Farshadfar, E. Richards, A. Ariafard, R. L. Melen, “Chemo- and regio-selective amidation of indoles with isocyanates using borane Lewis acids” *Catal. Sci. Technol.* **2022**, *12*, 5982–5990.

[18] J. Schießl, J. Schulmeister, A. Doppiu, E. Wörner, M. Rudolph, R. Karch, A. S. K. Hashmi, “An Industrial Perspective on Counter Anions in Gold Catalysis: Underestimated with Respect to ‘Ligand Effects’” *Adv. Synth. Catal.* **2018**, *360*, 2493–2502.

[19] M. Jia, M. Bandini, “Counterion Effects in Homogeneous Gold Catalysis” *ACS Catal.* **2015**, *5*, 1638–1652.

[20] P. La Manna, C. Talotta, M. De Rosa, A. Soriente, C. Gaeta, P. Neri, “An Atom-Economical Method for the Formation of Amidopyrroles Exploiting the Self-Assembled Resorcinarene Capsule” *Org. Lett.* **2020**, *22*, 2590–2594.

[21] L. Chen, C. Li, H. Wang, J. Li, S. Song, “HFIP-Promoted Aromatic Electrophilic Amidation of Indoles and Pyrroles with Isocyanates” *J. Org. Chem.* **2025**, *90*, 4271–4276.

[22] K. E. Roth, S. A. Blum, “Relative Kinetic Basicities of Organogold Compounds” *Organometallics* **2010**, *29*, 1712–1716.

[23] M. S. M. Holmsen, C. Blons, A. Amgoune, M. Regnacq, D. Lesage, E. D. Sosa Carrizo, P. Lavedan, Y. Gimbert, K. Miqueu, D. Bourissou, “Mechanism of Alkyne Hydroarylation Catalyzed by (P,C)-Cyclometalated Au(III) Complexes” *J. Am. Chem. Soc.* **2022**, *144*, 22722–22733.

[24] a) M. Navarro, A. Toledo, M. Joost, A. Amgoune, S. Mallet-Ladeira, D. Bourissou, “π Complexes of P^P and P^N chelated gold(I)” *Chem. Commun.* **2019**, *55*, 7974–7977. b) E. Herrero-Gómez, C. Nieto-Oberhuber, S. López, J. Benet-Buchholz, A. M. Echavarren, “Cationic η1/η2-Gold(I) Complexes of Simple Arenes” *Angew. Chem. Int. Ed.* **2006**, *45*, 5455–5459. c) V. Lavallo, G. D. Frey, S. Kousar, B. Donnadieu, G. Bertrand, “Allene formation by gold catalyzed cross-coupling of masked carbenes and vinylidenes” *Proc. Natl. Acad. Sci.* **2007**, *104*, 13569–13573.

[25] P. Milcendeau, M. Ramdani, E. van Elslande, X. Guinchard, “Cationic Au(I) Complexes of Indoles” *ACS Org. Inorg. Au* **2025**, DOI 10.1021/acsorginorgau.5c00075.

[26] L. Ricard, F. Gagosz, “Synthesis and Reactivity of Air-Stable N-Heterocyclic Carbene Gold(I) Bis(trifluoromethanesulfonyl)imidate Complexes” *Organometallics* **2007**, *26*, 4704–4707.

[27] A. Collado, A. Gómez-Suárez, A. R. Martin, A. M. Z. Slawin, S. P. Nolan, “Straightforward synthesis of [Au(NHC)X] (NHC = N-heterocyclic carbene, X = Cl, Br, I) complexes” *Chem. Commun.* **2013**, *49*, 5541–5543.

[28] P. García-Domínguez, “Synthesis of L–Au(I)–CF_2 H Complexes and Their Application as Transmetalation Shuttles to the Difluoromethylation of Aryl Iodides” *Organometallics* **2021**, *40*, 2923–2928.

[29] S. C. Scott, J. A. Cadge, G. K. Boden, J. F. Bower, C. A. Russell, “A Hemilabile NHC-Gold Complex and its Application to the Redox Neutral 1,2-Oxyarylation of Feedstock Alkenes” *Angew Chem Int Ed* **2023**, *62*, e202301526.

[30] R. Pedrazzani, S. Kiriakidi, M. Monari, I. Lazzarini, G. Bertuzzi, C. S. López, M. Bandini, “Fluorinated Biphenyl Phosphine Ligands for Accelerated [Au(I)]-Catalysis” *ACS Catal.* **2024**, *14*, 6128–6136.

[31] F. Ravera, M. S. Martinsen Holmsen, P. Sgarbossa, D. Bourissou, A. Biffis, “Gold(III) Catalysis in Ionic Liquids: The Case Study of Coumarin Synthesis” *Adv Synth Catal* **2025**, *367*, e202400706.

[32] R. Wei, L. Ma, S. Mallet-Ladeira, D. Bourissou, “Diazo Decomposition and Carbene Transfer Mediated by a Pincer Gold(III) Complex” *Organometallics* **2024**, *43*, 1775–1779.

[33] G. R. Fulmer, A. J. M. Miller, N. H. Sherden, H. E. Gottlieb, A. Nudelman, B. M. Stoltz, J. E. Bercaw, K. I. Goldberg, “NMR Chemical Shifts of Trace Impurities: Common Laboratory Solvents, Organics, and Gases in Deuterated Solvents Relevant to the Organometallic Chemist” *Organometallics* **2010**, *29*, 2176–2179.

[34] N. R. Babij, E. O. McCusker, G. T. Whiteker, B. Canturk, N. Choy, L. C. Creemer, C. V. D. Amicis, N. M. Hewlett, P. L. Johnson, J. A. Knobelsdorf, F. Li, B. A. Lorsbach, B. M. Nugent, S. J. Ryan, M. R. Smith, Q. Yang, “NMR Chemical Shifts of Trace Impurities: Industrially Preferred Solvents Used in Process and Green Chemistry” *Org. Process Res. Dev.* **2016**, *20*, 661–667.

[35] R. K. Harris, E. D. Becker, R. Goodfellow, P. Granger, “(IUPAC Recommendations 2001)” *Pure and Applied Chemistry* **2001**.

[36] S.-T. Liu, C.-I. Lee, C.-F. Fu, C.-H. Chen, Y.-H. Liu, C. J. Elsevier, S.-M. Peng, J.-T. Chen, “N-Heterocyclic Carbene Transfer from Gold(I) to Palladium(II)” *Organometallics* **2009**, *28*, 6957–6962.

[37] C. Yu, A. Kütt, G. Röschenthaler, T. Lebl, D. B. Cordes, A. M. Z. Slawin, M. Bühl, D. O’Hagan, “Janus Face All- *cis* 1,2,4,5-tetrakis(trifluoromethyl)- and All- *cis* 1,2,3,4,5,6-hexakis(trifluoromethyl)- Cyclohexanes” *Angew Chem Int Ed* **2020**, *59*, 19905–19909.

[38] S. Chakraborty, A. Gorski, O. Danylyuk, K. Niemirowicz-Laskowska, H. Car, M. Michalak, “NHC–Au–xanthate complexes” *Chem. Commun.* **2025**, *61*, 1697–1700.

[39] F. D. MEDINA, J. E. E. Weerts, W. M. MATON, *Amide Coupling Process*, **2022**, WO2022038166A1.

[40] B. Merla, C. Sundermann, U.-P. Jagusch, W. Englberger, H.-H. Hennies, B.-Y. Kögel, *Substituierte 5-Aminomethyl-1h-Pyrrol-2-Carbonsäureamide*, **2004**, WO2004058707A1.

[41] A. J. Carpenter, D. J. Chadwick, “The scope and limitations of carboxamide-induced .beta.-directed metalation of 2-substituted furan, thiophene, and 1-methylpyrrole derivatives. Application of the method to syntheses of 2,3-disubstituted thiophenes and furans” *J. Org. Chem.* **1985**, *50*, 4362–4368.

[42] 陈新, **凌倩**, **郭雪**, **金**洁, **景晨辰**, **王**竞冉, **桑吉达·拉赫曼**, 钱明成, **侯**亚男, 赵帅, *一种吡咯酰胺类衍生物及其制备方法和作为β2-肾上腺素受体别构拮抗剂的应用*, **2025**, CN119330867A.

[43] Z. Liu, S. Mao, H. Li, W. Liu, J. Tao, Y. Lu, H. Dong, J. Zhang, C. Song, Y. Duan, Y. Yao, "Discovery of novel amide derivatives against VEGFR-2/tubulin with potent antitumor and antiangiogenic activity" *Bioorganic Chemistry* **2024**, *151*, 107679.

[44] H. Jiang, K. Li, M. Zeng, C. Tan, Z. Chen, G. Yin, "Pd(II)/Lewis Acid Catalyzed Intramolecular Annulation of Indolecarboxamides with Dioxygen through Dual C–H Activation" *J. Org. Chem.* **2022**, *87*, 13919–13934.

[45] P. Sharma, R.-S. Liu, "[3 + 2]-Annulations of N-Hydroxy Allenylamines with Nitrosoarenes: One-Pot Synthesis of Substituted Indole Products" *Org. Lett.* **2016**, *18*, 412–415.

[46] D. Saylik, M. J. Horvath, P. S. Elmes, W. R. Jackson, C. G. Lovel, K. Moody, "Preparation of Isocyanates from Primary Amines and Carbon Dioxide Using Mitsunobu Chemistry1" *J. Org. Chem.* **1999**, *64*, 3940–3946.

[47] J. Du, L. Wang, M. Xie, L. Deng, "A Two-Coordinate Cobalt(II) Imido Complex with NHC Ligation: Synthesis, Structure, and Reactivity" *Angewandte Chemie International Edition* **2015**, *54*, 12640–12644.

[48] F. Reiß, A. Schulz, A. Villinger, N. Weding, "Synthesis of sterically encumbered 2,4-bis-m-terphenyl-1,3-dichloro-2,4-cyclo-dipnictadiazanes [m-TerNPnCl]2, (Pn = P, As)" *Dalton Trans.* **2010**, *39*, 9962–9972.

[49] J. E. Borger, A. W. Ehlers, M. Lutz, J. C. Slootweg, K. Lammertsma, "Functionalization of P4 Using a Lewis Acid Stabilized Bicyclo[1.1.0]tetraphosphabutane Anion" *Angewandte Chemie International Edition* **2014**, *53*, 12836–12839.

[50] D. Bélanger, X. Tong, S. Soumaré, Y. L. Dory, Y. Zhao, "Cyclic Peptide–Polymer Complexes and Their Self-Assembly" *Chemistry – A European Journal* **2009**, *15*, 4428–4436.

[51] L. P. Miller, J. A. Vogel, S. Harel, J. M. Krussman, P. R. Melvin, "Rapid Generation of P(V)–F Bonds Through the Use of Sulfone Iminium Fluoride Reagents" *Org. Lett.* **2023**, *25*, 1834–1838.

[52] H. Rao, H. Fu, Y. Jiang, Y. Zhao, "Easy Copper-Catalyzed Synthesis of Primary Aromatic Amines by Couplings Aromatic Boronic Acids with Aqueous Ammonia at Room Temperature" *Angew Chem Int Ed* **2009**, *48*, 1114–1116.